

SANTOS – AWE- MITSUI

COMPILED FOR
SANTOS LIMITED
(A.B.N. 80 007 550 923)

CASINO-3
INTERPRETED DATA REPORT

PREPARED BY:
R. Subramanian
(Consultant)
March 2004

CASINO-3

TABLE OF CONTENTS

LOCATION MAP

PAGE

WELL CARD	1
1 GEOLOGY	4
1.1 Introduction and Pre-drilling Summary	4
1.2 Field Description	4
1.3 Well Location	8
2 RESULTS OF DRILLING	8
2.1 Stratigraphic & Geophysical Prognosis	8
2.2 Stratigraphy and Depositional Environment	9
2.3 Hydrocarbon Summary	12
2.4 Summary	13
3 REFERENCES	15

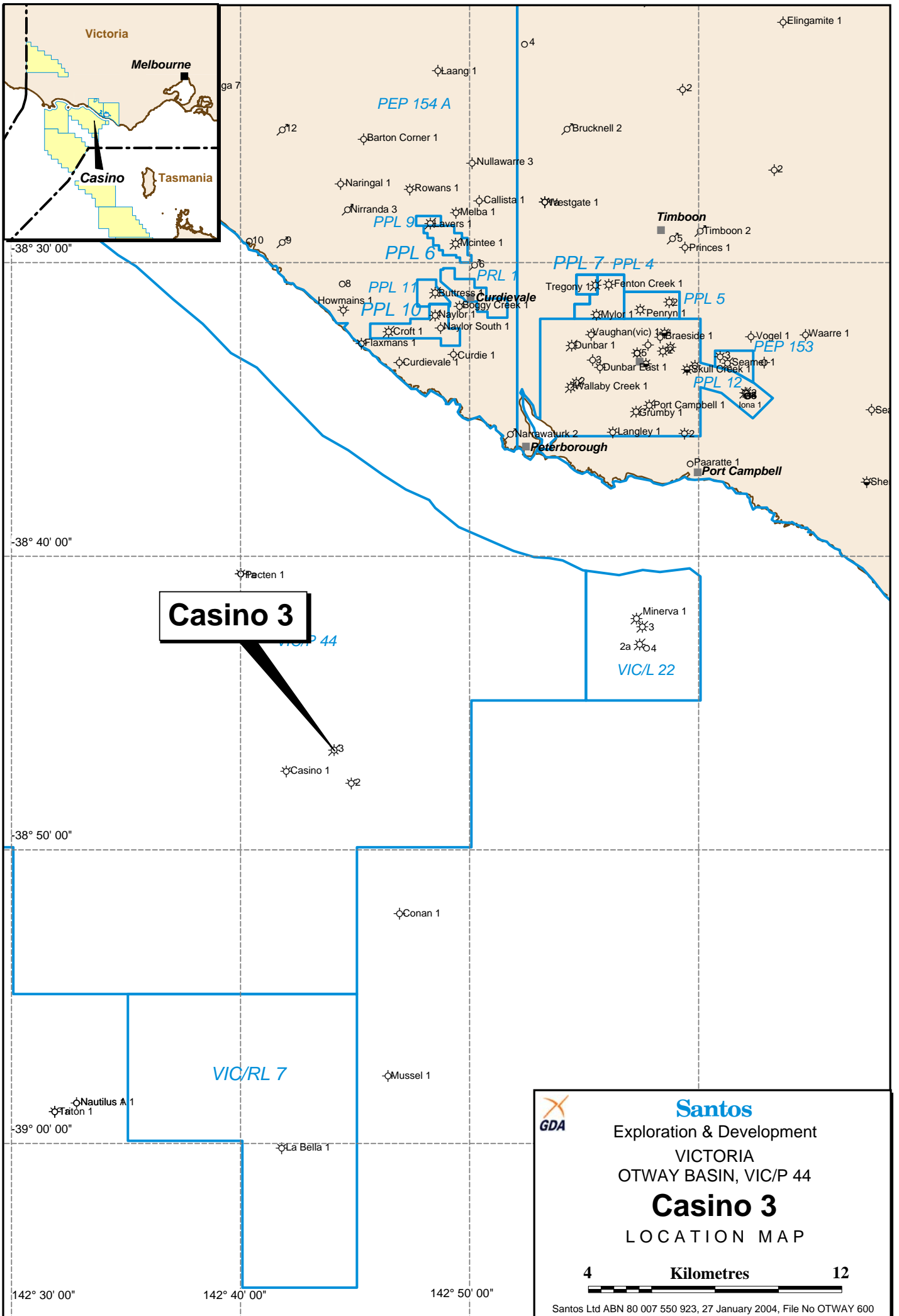
APPENDICES

I Electric Log Evaluation Results
II MDT Pressure Survey Report and Data
III Hydrocarbon Show Report
IV Geothermal Gradient
V Petrology Report
VI Palynology Report
VII Drill Stem Test Analysis Report

ENCLOSURES:

I Composite Log (1:500 Scale)
II Depth Structure Map
III Stratigraphic Cross Section
IV Log Interpretation Analogue Plot

LOCATION MAP



Victoria

Melbourne

Casino

Tasmania

-38° 30' 00"

-38° 40' 00"

-38° 50' 00"

-39° 00' 00"

142° 30' 00"

142° 40' 00"

142° 50' 00"

Casino 3

Minerva 1
3
2a
4
VIC/L 22

VIC/RL 7



Santos

Exploration & Development
VICTORIA
OTWAY BASIN, VIC/P 44

Casino 3

LOCATION MAP

4 Kilometres 12

Santos Ltd ABN 80 007 550 923, 27 January 2004, File No OTWAY 600

WELL CARD

WELL: CASINO-3	WELL CATEGORY: OFFSHORE GAS APP	SPUD: 14-10-03 TD REACHED: 30-10-03			
	WELL INTENT: GAS	RIG RELEASED: 13-11-03 CMPLT:			
		RIG: OCEAN EPOCH			
SURFACE LOCATION: LAT: 38° 46' 34.558" S LONG: 142° 44' 05.437" E (GDA94) NORTHING: 5706621.82M EASTING: 650700.11M		STATUS: GAS WELL ABANDONED – NO PRODUCTION (GAB)			
SEISMIC STATION: 2001 CASINO-3D, INLINE 6260, CDP 2546		REMARKS:			
ELEVATION SEA FLOOR: -66.7M LAT RT +22.4M LAT					
BLOCK/LICENCE: OTWAY BASIN - VIC / P 44					
TD 2135 M (LOGR EXTRAP) 2135 M (DRLR)					
PBTD M (LOGR) M (DRLR)		HOLE SIZE	CASING SIZE	SHOE DEPTH	TYPE
TYPE STRUCTURE: TILTED FAULT BLOCK CLOSURE		914MM	762MM	121.3M	461 KG/M X52
TYPE COMPLETION: NIL		445MM	340MM	635.8M	101 KG/M BTC L80
ZONE(S):		311MM	244MM	2113M	70 KG/M BTC L80

AGE	FORMATION OR ZONE TOPS	DEPTH (M)		THICK-NESS (m)	HIGH (H) LOW (L)
		LOGGERS RT (M)	SUBSEA (M)		
MID-LATE MIOCENE	SEABED (TOP HEYTESBURY GROUP)	89.1	66.7	507.9	1.3M H
EOCENE – OLIGOCENE	NIRRANDA GROUP: NARRAWATURK MARL	597.0	574.6	75.0	-
EOCENE	NIRRANDA GROUP: MEPUNGA FM	672.0	649.6	133.5	7.6M L
EOCENE	WANGERRIP GROUP: DILWYN FM	805.5	783.1	169.5	25.1M L
EOCENE	PEMBER MUDSTONE	975.0	952.6	63.0	-
PALAEOCENE	PEBBLE POINT FORMATION	1038.0	1015.6	86.0	-
PALAEOCENE	MASSACRE SHALE	1124.0	1101.6	12.0	-
LATE CRETACEOUS	TIMBOON SANDSTONE	1136.0	1113.6	112.0	49.4M H
LATE CRETACEOUS	PAARATE	1248.0	1225.6	368.5	-
LATE CRETACEOUS	SKULL CREEK	1616.5	1594.1	327.5	360.1M L
LATE CRETACEOUS	FLAXMAN	1944.0	1921.6	38.0	6.6M L
EARLY - LATE CRETACEOUS	WAARRE "C"	1982.0	1959.6	153.0	19.4M H
EARLY - LATE CRETACEOUS	WAARRE "B"	2035.0	2012.5	16.5	-
EARLY - LATE CRETACEOUS	WAARRE "A"	2051.5	2029.1	70.5	-
	TOTAL DEPTH (LOGGER EXTRAP)	2135.0	2112.6		

LOG	SUITE/ RUN	INTERVAL (M)	BHT/TIME COMMENTS
<u>PEX-DSI-HALS</u> GR MCFL HLLD HLLS HCAL SP DSI	1 / 1	2115 TO SURFACE 2118 TO 635.8 2120 TO 635.8 2120 TO 635.8 2118 TO 635.8 2095 TO 635.8 2108 TO 100	83C, 182F / 15:30 HRS NO REPEAT SECTION
<u>MDT-GR</u> (TOTAL : 24, 15 NORMAL, 2 LOST SEALS, 7CURTAILED, SAMPLES @ 2006.8M, 2 X 450CC, 1 GAL, 2 ¾ GAL. SAMPLE @ 1985.2M 1 X 450CC)	1 / 2	1611.2 TO 2063	85.5C, 185.9F / 33:30 HRS
<u>PEX-CMR-HNGS</u> GR (SPECTRAL GR) TNPH RHOZ CMR	1 / 3	2111 TO 635.8 2111 TO 635.8 2113 TO 635.8 2116 TO 1930	83C, 182F / 40:00HRS
<u>MCST</u>	1 / 4		UNABLE TO PASS 1870M PULL OUT FOR A WIPER TRIP
<u>MCST</u>	1 / 4A	2102.5 TO 1970.5	13 MCST CORES ATTEMPTED 13 CORES RECOVERED
<u>CST-GR</u>	1 / 5		MISRUN. NO BULLETS FIRED
<u>CST-GR</u>	1 / 6	2077.7 TO 1162.7	30 CORES ATTEMPTED. 20 BOUGHT, 1 LOST BULLET, 2 EMPTY, 7 MISFIRES.

LOG INTERPRETATION						PERFORATIONS				
INTERVAL(M)	Ø %	SW %	INTERVAL(M)	Ø %	SW %	FORMATION	INTERVAL			
WAARRE Cb:			TOP WAARRE CB(MAIN):			NIL				
NET PAY: 5.6M	14.4	25	NET PAY: 13.1M	18.7	15	CORES				
WAARRE Ca:						FORM	NO.	INTERVAL	CUT	REC
NET PAY: 8.1m	17.8	30				Waarre	1	2004-2031m	27m	24.7m (91.5 %)

PRODUCTION TEST RESULTS

A CASED HOLE DST OVER THE INTERVAL 2002-2011M RT FLOWED GAS AT 44.3MMSCF/D ON 64/64" CHOKE.

SUMMARY:

Casino-3 was drilled as an Otway Basin gas exploration well in the Victoria Offshore VIC/P44 licence. The Surface Location is Latitude: 38° 46' 34.558" S Longitude: 142° 44' 05.437" E (GDA94), Northing: 5706621.82m Easting: 650700.11m (MGA-94), with a seismic reference of Inline 6260, CDP 2546, Casino 3D Survey 2001. The location lies approximately 29 km south west of the town of Port Campbell, 24 km WSW of the Minerva gas field and 22 km North of the LaBella gas field. The Casino field is situated towards the western limit of the productive Waarre Sandstone play fairway of the Port Campbell Embayment. With reference to the earlier Casino wells, Casino-3 is approximately 3.3km NE of Casino-1 and approximately 2.4 km NW of Casino-2 (see Location Map). The water depth at the well location was 66.7m LAT.

The Casino structure is a tilted fault block with three way dip closure and up dip fault closure. Casino-1 and Casino-2 were drilled crestally on this fault block whereas Casino-3 was proposed in a down-dip location near the structural closure limit. Casino-1 and Casino-2 have established the presence of gas in the "Younger" and "Older" sands of the Waarre Sandstone.

The objectives of Casino-3 were to :

- Establish a GWC/LKG in the "Younger" Waarre sand. Approximately 28m gross gas column for 15-20m of net pay is predicted in this sand. Cut a full-hole core and DST this sand to establish productivity.
- Establish pressure regimes in the "Younger" Waarre sand to determine if normally pressured, over-pressured or compartmentalised.
- Establish reservoir characteristics in the "Older" Waarre sand in a water leg.
- Allow confirmation of the OGIP and Recoverable of the Casino Gas Field.

Casino-3 was spudded at 22:00 hrs on 14/10/03. A 914mm (36") hole was drilled from the seabed at 89.5m to 121.3m. The 760mm (30") casing was then run and set at 121.3m. A 445mm (17.5") hole was drilled from 121.3m to 645m with returns to the seafloor and 340mm (13-3/8") casing run and set at 635.8m. The blow out preventers was installed and pressure tested. Adverse weather conditions then resulted in the suspension of drilling operations. A 311mm (12-1/4") hole was drilled using 2 bits, from 645m to the core point of 2004m. MWD/LWD data (gamma ray, resistivity, sonic data and surveys) was acquired in this drilling phase from 1226.5m to 2004m. A coring assembly was run in and a 27m core was cut from 2004m to 2031m with a recovery of 24.7m (91.5%). Drilling of the 311 mm (12.25") phase continued from 2031m to the Total Depth of 2135m (D) which was reached at 08:00 hrs on 30/10/03.

At Total Depth, the hole was circulated clean and the drillstring was pulled out of hole to run wireline logs. Schlumberger was rigged up and the following wireline logs were run. Run 1: DSI-PEX-HALS, Run 2: MDT-GR, Run 3: PEX-CMR-HNGS, Run 4: MCST-GR and Run 5: SWC-GR. After rigging down Schlumberger, a string of 244mm (9 5/8") casing was run and cemented at 2113m. The well was then production tested and thereafter abandonment plugs were set as per program, Plug 1: 2013m to 1970m, Plug 2: 2170m to 2120m and Plug 3: 175m to 135m. The rig was released at 19:00 hours on 13/11/03.

The penetrated depths of most formations in Casino-3 were within 50m of their respective prognosed depths as can be seen in the table above. The notable exception was the Skull Creek Formation which was intersected 360m low to prognosis due to a thickening of the overlying Paarate Formation and the Timboon Sandstone. The Belfast Mudstone nor the Eumeralla Formation were intersected.

Casino-3 encountered the top of the Waarre Formation at 1982m RT (-1959.6m SS) which was 19.4m high to prognosis. The well penetrated 153m (using logger extrapolated depth) of Waarre Formation terminating in the Waarre A unit. The Waarre Formation was as predicted, with Unit Ca/Cb (53m thick), Unit B (16.5m thick) and Unit A (70.5m+ thick) present.

Log evaluation of the Waarre Formation indicates a total 26.8m of gas pay (Av Porosity 17.5% Av Sw 21.6%) versus prognosed gas pay of 15-20m. Of this total, 4m of gas pay was in the Waarre Cb unit, 12.2m in the Top Porosity Main CB unit and 7.9m in the Waarre Ca unit. The well encountered a gas water contact in Unit C at 2021.4m RT (-1999mSS) which is 8m above the prognosed gas water contact. The unit C reservoir sand was confirmed to be normally pressured. A cased hole DST over the interval 2002-2011m RT flowed gas at 44.3MMscf/d on 64/64" choke. Unit A reservoir sand was water wet at Casino-3 as prognosed with average porosity of 16%.

Casino-3 achieved its key objectives in that:

- The well encountered the Waarre Formation close to prognosis thereby conforming the pre-drill structural interpretation.
- The Waarre Formation was developed as predicted
- The well encountered 20m of gas pay in Unit C as predicted.
- A gas water contact was established at -1999mSS in Unit C and this sand was confirmed to be normally pressured.
- Unit C was successfully tested with a cased hole DST to establish flow capacity.

AUTHOR: R. SUBRAMANIAN

DATE: March 2004

1. GEOLOGY

1.1 INTRODUCTION

Casino-3 was drilled as an Otway Basin gas exploration well in the Victoria Offshore VIC/P44 licence. The Surface Location is Latitude: 38° 46' 34.558" S Longitude: 142° 44' 05.437" E (GDA94), Northing: 5706621.82m Easting: 650700.11m (MGA-94), with a seismic reference of Inline 6260, CDP 2546, Casino 3D Survey 2001. The location lies approximately 29 km south west of the town of Port Campbell, 24 km WSW of the Minerva gas field and 22 km North of the LaBella gas field. The Casino field is situated towards the western limit of the productive Waarre Sandstone play fairway of the Port Campbell Embayment. With reference to the earlier Casino wells, Casino-3 is approximately 3.3km NE of Casino-1 and approximately 2.4 km NW of Casino-2 (see Location Map). The water depth at the well location was 66.7m LAT.

The Casino structure is a tilted fault block with three way dip closure and up dip fault closure. Casino-1 and Casino-2 were drilled crestally on this fault block whereas Casino-3 is proposed in a down-dip location near the structural closure limit. Casino-1 and Casino-2 have established the presence of gas in the "Younger" and "Older" sands of the Waarre Sandstone.

The objectives of Casino-3 were to:

- Establish a GWC/LKG in the "Younger" Waarre sand. Approximately 28m gross gas column for 15-20m of net pay is predicted in this sand. Cut a full-hole core and DST this sand to establish productivity.
- Establish pressure regimes in the "Younger" Waarre sand to determine if normally pressured, over-pressured or compartmentalised.
- Establish reservoir characteristics in the "Older" Waarre sand in a water leg.
- Allow confirmation of the OGIP and Recoverable of the Casino Gas Field.

The risks on Casino-3 were:

- Depth conversion could be inaccurate and consequently the structure was not as prognosed.
- The amplitude anomaly observed in the "Younger" sand was a function of low gas saturation.
- The "Younger" sand was over-pressured as was the case with the "Older" sand.
- Fault compartmentalisation of the down dip sector of the structure.
- "Younger" sand thickness and reservoir character have diminished in this area of the field.
- A contingent plan to deviate up dip on the structure if needed had been factored into the project.

Casino-3 was drilled by the semi-submersible drilling rig "Diamond Offshore Ocean Epoch".

1.2 FIELD DESCRIPTION

General Background

The Casino gas field was discovered in September-October 2002. The field contains gas in two separate Waarre Sandstone reservoir units designated the "Older" and "Younger" sands in a tilted fault block with three way dip closure structure. Top and side seal are provided by the Belfast Mudstone. The gas at Casino has minimal CO₂ (<1%) and is low in liquids (approx. 2 bbl/mmcft). The geology, geophysical mapping and exploration history of the field are extensively discussed in the Casino-1, Casino-2 and Casino-3 Well Proposals, Interpreted Data Reports, Post Well Audits and Casino Reservoir Modeling Report.

While Casino-1 and Casino-2 are crestal on the Casino structure, Casino-3 was proposed as a down-dip appraisal well near the limit of structural closure. It is located approximately 3.3km NE of Casino-1 and 2.4km NW of Casino-2. The location is regarded as carrying a low to moderate risk and has been selected following integration of geological, geophysical and dynamic simulation studies. Critical risks were seen as in accuracy of depth conversion, overpressure in the “Younger” sand, under estimation of gas saturations, unpredicted reservoir thickness/character variations and fault compartmentalisation of the reservoir. As a further step in risk mitigation the contingency of sidetracking to an up-dip location on the “Younger” sand was factored into the drilling program.

The primary objective of the Casino-3 gas appraisal well was to establish the OGIP, productivity and reserves of the “Younger” sand. The well has been located near the proposed GWC for this unit and should therefore unambiguously delineate the maximum resource in the unit. The secondary objective was to obtain critical data to assist in definition of the gas resource in the “Older” sand.

Objectives

Casino-3 is a gas appraisal well located down-dip on the Casino structure. It was proposed to drill the well to a total depth of 2147mRT, approximately 143m into the Waarre Formation. The well was to be plugged and abandoned.

The overall objective was that post Casino-3, an OGIP and recoverable resource above the economic threshold would be identified on the Casino field such that a development project could commence with a first gas production in early 2006.

To achieve this outcome specific objectives were:

- The primary objective is to define fluid limits in the “Younger” sand by defining a GWC at – 2007mSS. This sand would be cored. Production testing was to be performed to evaluate productivity and define pressure regimes.
- A secondary objective of the well was to encounter the “Older” sand in a water leg thereby providing information on reservoir character; which would be applied for more accurate OGIP estimates.
- The well would penetrate the Flaxman Formation allowing assessment of the petroleum potential of this unit. The Flaxman Formation had about 5m of gas pay at the Minerva Field (20km to ENE).
- The contingency of sidetracking to an up-dip location (70m vertical in 440m horizontal offset for the “Younger” sand) has been incorporated as an option if warranted.

Reservoir/Fluid Limits.

“Older” Sand

The “Older” sand contains 24m of gas pay (Av Por 14.7% and Av Sw 40%) at the top of the Waarre Unit B and Unit A in Casino-1 (primarily Unit A). The well encountered an LKG at -1764mSS. In Casino-2 the unit was encountered in a transition zone approximately 35m thick in which Sw is in the order of 70%. 6.6m of gas pay (Av Por 14.7% and Av Sw 54%) are defined in this zone. MDT readings indicate the sand to be over-pressured and a FWL has been established at -1838mSS. A gross gas column height to 206m is defined in this sand. Since the fluid limits are well established in this sand further appraisal is related to better understanding of reservoir character and petrophysical control, and this would be achieved by a proposed MSCT coring program in the unit in the well. Casino-3 was proposed to encounter the “Older” sand in the water leg at about -2040mSS with about 32m of good porosity section prognosed.

“Younger” Sand

The “Younger” sand is absent at Casino-1. In Casino-2 the sand contains 22.3m of gas pay (Av Por 21.3% and Av Sw 23%) in Units Ca and Cb of the Waarre Sandstone. (Figure 6) The well encountered an LKG at -1760mSS. A FWL has not been established in this sand from MDT pressures. The range is from -1850mSS applying the “Older” sand water gradient to about -2007mSS using a normally pressured aquifer. This lower limit is near the down-dip limit of structural closure on the sand. The “Older and “Younger” sands are not in communication; being separated by a shale barrier in the Waarre B unit. The primary objective in Casino-3 is to establish a gas water contact in the “Younger” sand. The prognosis has the well intersecting a gross 33m of “Younger” sand with the base at -2012mSS i.e. approx. 5m below the predicted GWC in the sand. It was proposed to take a 27m full hole core in the “Younger” sand (if gas bearing) and also run a Drill Stem Test, to establish productivity. If the outcome was as prognosed the penetration of 28m of gross gas column (predicted top 8m non-net pay, 15-20m net pay, then 5m water) would provide an ideal interval for DST.

The outcome in the “Younger” sand as prognosed, would confirm OGIP models above the economic threshold to commence development of the Casino gas field.

The likelihood of the Casino-3 well encountering a gas/water contact as prognosed in the “Younger” sand was considered to be high in that an amplitude anomaly is present in the sand out to the structural limit. To date, amplitude anomalies on the Casino field have proven to be highly reliable and effective in prediction of gas charged reservoirs.

Structure

The pre-drill depth structure on the “Younger” sand is shown in Figure 4 of the Well proposal. Depth conversion for this has taken into account the results of Casino-1 and Casino-2. Despite the proximity of these wells to Casino-3, the Casino-3 location being down-dip, has a substantially thicker Belfast Mudstone section which raised velocity problems. The geophysical depth prognosis for the Casino-3 location is contained in Attachment 1 of the Well Proposal. RMS impedance of the “Younger” sand was used to identify areas of better gas charged sand development on the field.

Extensive assessment of the nature and magnitude of the faulting in the down-dip area of the structure in the vicinity of the Casino-3 location had raised the concern was that this NW-SE aligned faulting may connect over the structure and result in compartmentalisation of the reservoir. It was concluded that the faults are probably not extensively connected, have minimal throws and as a result reservoir segregation was unlikely

Risks

Overall Casino-3 is rated as a low to moderate risk well. Key risks and influencing factors are reviewed below.

- Depth conversion is inaccurate resulting in the Waarre top being substantially high or low. This was regarded as carrying a moderate risk due to velocity data from the nearby Casino-1 and Casino-2 wells and application of seismic interval velocities. However the down-dip location of Casino-3 has a substantial thickening of the Belfast Mudstone section and this could provide velocity errors. Pre-drill depth prognoses at Casino-1 and Casino-2 were within 10m of the actual.
- The “Younger” sand was over-pressured similar to the “Older” sand i.e. FWL is at approx. -1850mSS rather than the predicted FWL at -2007mSS. Lowering this risk on this, was the observation that the amplitude anomaly extends out to the -2007mSS contour area (which is in near structural closure) and to date amplitude anomalies have proven to be reliable and effective in defining gas pools.
- The “Younger” sand amplitude anomaly is a function of low gas saturation sand. To date this had not been in case on the Casino structure.
- Fault compartmentalisation had occurred in the down-dip area of the Casino structure where a series of NW-SE aligned faults are mapped. Extensive geophysical review favours a model where these faults form part of a relay ramp system and were not substantive enough to prevent sand on sand contact. Hence the risk on compartmentalisation is regarded as low.
- There was a risk that in the “Younger” sand the sand thickness and reservoir quality are not as currently modeled over the whole field. This was because there is only one reservoir intersection (Casino-2) in an up-dip area of the field. If the sand was thinner, poorer porosity or has lower net to gross than modeled, the field resource would be lowered.
- A contingency option to sidetrack to an up-dip location on the “Younger” sand (70 m vertical in 440m horizontal section) had been identified. This option would be applied if the results of the vertical Casino-3 warranted it.

1.3 WELL LOCATION

Casino-3 is located in the Otway Basin, Victoria Offshore VIC/P44 license. The Surface Location details are given below. The location lies approximately 29 km south west of the town of Port Campbell, 24 km WSW of the Minerva gas field and 22 km North of the LaBella gas field. With reference to the earlier Casino wells, Casino-3 is approximately 3.3km NE of Casino-1 and approximately 2.4 km NW of Casino-2. The water depth at the well location was 66.7m LAT.

The Surface Surveyed Location for Casino-3 is :

Latitude: 38° 46' 34.558" South
Longitude: 142° 44' 05.437" East (GDA-94).
Easting: 650 700.11 m
Northing: 5706 621.82 m (MGA-94)
Rig Diamond Offshore - Ocean Epoch

The Seismic Location for Casino-3 is:

Inline 6260, CDP 2546.
2001 Casino 3D seismic dataset.

2. RESULTS OF DRILLING

2.1 STRATIGRAPHY & GEOPHYSICAL PROGNOSIS

While drilling Casino-3, the penetrated depths of most formations in Casino-3 were within 50m of their respective prognosed depths as can be seen in the table above. The notable exception was the Skull Creek Formation which was intersected 360m low to prognosis. The Belfast Mudstone was not intersected and neither was the Eumeralla Formation.

The Waarre Formation, which constitutes the main reservoir, is a prominent and generally reliable seismic reflector. However due to the extremely complex post-depositional faulting in the area, the reflector is very broken-up in a regional sense. During the drilling of Casino-3 the primary objective Waarre Formation was penetrated 19.4m high to the prognosed depth. The depth prognosis was reasonably accurate. Depth conversion was not considered an issue. The gas sand has a strong amplitude anomaly confirming the effectiveness of the prognosis.

The well penetrated 153m (using logger extrapolated total depth) of Waarre Formation terminating in the Waarre A unit. The Waarre Formation was as predicted, with Unit Ca/Cb (53m thick), Unit B (16.5m thick) and Unit A (70.5m+ thick) present.

2.2 STRATIGRAPHY & DEPOSITIONAL ENVIRONMENT (Drillers MDRT Depths)

The well card at the front of this report tables the subsea elevations and thickness of formations penetrated in Casino-3. A brief description of lithology and interpreted environments of deposition follows. More detailed descriptions can be found in Section 2.1 of the Basic Data Report.

Total depth for Casino-3 was reached at 2135m (D), in the Late Cretaceous **Sherbrook Group** which overlies the Early Cretaceous Eumeralla in the Otway Basin. The Eumeralla Formation was not penetrated in Casino-3.

The Waarre Formation makes up the oldest formation of the Sherbrook Group and is dated to be Turonian in age (Partridge, 1997). The Waarre Formation which was intersected at 1982m, was deposited as the initial post-rift sequence at the commencement of Turonian time. Microplankton at the base of the Waarre formation record the first evidence of wholesale marine incursion into the Otway Basin. The section is sub-divided into three sub-units – Waarre “A”, “B” & “C”.

Casino-3 penetrated 83.5m of “A” unit which represents a basal transgressive systems tract (TST) characterised by flooding of an incised valley with sediments deposited under marginal marine/estuarine conditions. Lithologically, the unit is similar to the underlying Eumeralla Formation from which it is sourced. The unit is comprised of fine to coarse grained lithic sandstone, interbedded with thin beds of silty carbonaceous mudstone. Onshore the sandstones are dominantly fluvial, but offshore marine conditions are indicated by coarsening upward beds.

Unit “B” which was 11.5m thick was deposited under estuarine conditions. Onshore, Unit “B” is comprised of carbonaceous mudstone with thin interbeds of coal. Glauconitic mudstone and siltstone, with thin interbeds of dolomitic and calcareous sandstone, is common. Offshore wells show greater marine influence with increasing glauconitic content and common occurrence of dinoflagellates and microplankton.

Unit “C” is characterised by initial estuarine/deltaic conditions succeeded by high-energy sands. The 58m thick unit consists of fine to very coarse grained quartzose sandstone deposited in thick, blocky to fining upwards beds. The sandstone is carbonaceous and thin coals are occasionally developed. Towards the basin, the sandstone becomes finer grained with fining upwards beds developed in Mussel-1 and LaBella-1.

The sandstone is off-white to light brownish-grey to light grey, very fine to very coarse, but dominantly fine to medium in size, though dominantly medium grained towards the base. The grains are angular to subrounded, poorly to moderately sorted, generally contain a weak to moderate silica cement. There is trace to common white to light grey argillaceous matrix throughout, clear to opaque quartz grains, and minor black coaly detritus. The sandstone is friable to moderately hard, has poor to fair visible porosity without any hydrocarbon fluorescence. The sandstone packages are generally blocky in shape. The basal Waarre is interpreted to be shallow marine to marginal marine. After the transgression in the lower part of the Waarre, the formation became more regressive, depositing the best reservoir sands in the lower coastal and delta areas.

In the Otway Basin, the Waarre Formation was transgressed by another flooding event (conformably overlain) by the **Flaxmans Formation** which is the seal for the Waarre reservoir at Casino-3. In the Casino-3 well the Flaxmans Formation was 38m thick and consists of interbedded Sandstone and Siltstone. The Siltstone is generally coloured very pale to pale brown or medium brown grey, it is argillaceous and arenaceous, with common glauconite grains. The siltstone grades to very fine SANDSTONE, is moderately hard to hard and is blocky to subblocky. The Sandstone is coloured off white, milky, pale to medium yellow. The grain size is coarse to very coarse, occasionally very fine to medium grained. The sandstone is poorly sorted, angular to occasional subrounded and has moderate calcareous cement with common kaolinitic matrix. There are occasional glauconitic grains. The sandstone is moderately hard to hard with poor visual and inferred porosity and has no fluorescence.

The **Skull Creek Mudstone**, (sometimes considered part of the Paaratte Formation), unconformably overlies the Flaxmans Formation. The Belfast Mudstone and Nullawarre Greensand were not evidenced at Casino-3. The top of the Skull Creek Mudstone was encountered at 1616.5m and is 337.5m thick. The formation was penetrated 360m low to prognosis due to a thickening of the overlying Paarate Formation and the Timboon Sandstone. It comprises a medium to dark brownish-grey, grading to brown black siltstone which is argillaceous and grades to a silty claystone. The Skull Creek Mudstone commonly has dispersed fine to medium quartz grains, trace glauconite and trace disseminated pyrite. It is soft to firm and generally amorphous to subblocky. A pro-delta environment of deposition is interpreted for the Skull Creek and an age of Santonian has been attributed to the Skull Creek Mudstone.

The top of the youngest formation of the Sherbrook Group, the **Timboon Sandstone** was intersected at 1136m. The formation is 112m thick and is made up of thin to fairly thick sandstone packages, interbedded with siltstone. The sandstone is pale grey to grey, clear to translucent, predominantly medium grained to minor coarse grained. The sandstone is moderately well sorted and the grains are subrounded to subangular in part. The sandstone has a weak siliceous cement, has trace lithic fragments and traces of disseminated pyrite. The sandstone is friable to loose, and occasionally in moderately hard aggregates. No hydrocarbon fluorescence was observed. The interbedded siltstone is light to medium brown to brown grey, arenaceous, slightly calcareous with minor disseminated pyrite. The siltstone is firm to moderately hard and subblocky. The Timboon Sandstone was deposited in a deltaic environment, in this case, presumably delta plain, and has been dated to be Campanian to Maastrichtian in age in the Otway Basin.

The **Massacre Shale** overlies the Timboon Sandstone. It was penetrated at 1124m and is 12m thick. The formation consists of siltstone interbedded with minor sandstone. The siltstone is medium grey, medium to dark brown, arenaceous and grades to silty sandstone, carbonaceous in part, has rare white argillaceous laminations, has common disseminated pyrite and is moderately hard to occasionally very hard and generally subblocky. The interbedded sandstone are pale to medium grey, clear to translucent to off white, medium to coarse grained. There are occasional very coarse subrounded polished bit-fractured quartz fragments. The sandstone is moderately poorly sorted with subangular to minor angular grains. The sandstone has common moderate strong calcareous and dolomitic cement, minor white argillaceous matrix and occasional medium grey silty matrix. Disseminated pyrite is common and the aggregates are hard to occasionally very hard aggregates. There are loose grains in part and no hydrocarbon fluorescence was observed. The Massacre Shale forms the boundary between the Cretaceous and the Tertiary.

Overlying the Massacre Shale is the oldest unit in the **Wangerrip Group**, the **Pebble Point Formation**. At Casino-3, the Pebble Point is 86 thick and was intersected at 1038m. The formation is composed of interbedded claystone and sandstone. Sandstone is pale grey, clear to translucent, predominantly medium grained with minor coarse grained, becoming coarser with depth, moderately well sorted, with subangular to minor angular grains and occasionally subrounded grains. The sandstone has trace weak to moderately hard siliceous cement. It is partly friable to moderately hard, generally loose and has fair inferred porosity but no hydrocarbon fluorescence. The interbedded claystone is medium grey and medium to dark brown, slightly arenaceous, siliceous in part, partly silty, soft to firm, occasionally very hard, dispersive, amorphous to subblocky. The environment of deposition for the Pebble Point is interpreted to be shallow water, nearshore, restricted marine with periodic influxes of coarse detrital material. Various megafossils and microfossils have been identified in the formation that indicate an age ranging from Maastrichtian for the oldest strata, to Palaeocene, and even Late Palaeocene (Abele *et al*, 1995).

Conformably overlying the Pebble Point is the **Pember Mudstone**, which was penetrated at 975m and is 63m thick. The formation consists mainly of claystone which is medium to dark brown, slightly arenaceous, silty, predominantly soft and minor firm, dispersive and amorphous to subblocky. The claystones are interbedded with minor sandstones which are pale brown, translucent, predominantly coarse grained, well sorted and with subrounded grains, with trace moderately strong to strong siliceous cement, with trace silty matrix. The aggregates are moderately hard to hard and loose in part with generally poor visual porosity and no hydrocarbon fluorescence. The Pember Mudstone was deposited in a marine environment where there was restricted circulation and low energy conditions, probably below or close to storm wave base. It has been given an age of Late Palaeocene to Early Eocene (Abele *et al*, 1995) based on a study of associated palynomorphs.

The **Dilwyn Formation** conformably overlies the Pember Mudstone at Casino-3 and was penetrated at 805.5m and is 169.5m thick. The section consists predominantly of sandstone with minor interbedded silty claystone. The sandstone is pale to medium grey, also minor pale yellow, is medium to coarse grained, moderately well sorted, with predominantly subrounded to rounded grains and partly subangular grains, with trace pyrite cement, with trace lithic fragments and commonly loose. The sandstone has a fair inferred porosity but no hydrocarbon fluorescence. The claystone is medium to dark grey and dark brown, soft to firm, occasionally hard, with trace pyrite and is very soft, very dispersive and non fissile.

Both macrofossils and microfossils from the Dilwyn have been dated to be Early Eocene. The environment of deposition is interpreted to be shallow marine, with the cleaner sandy portions representing shoreface deposits of a coastal barrier system and the interbedded section possibly back beach lagoon sediments, with some breaching occurring. Another interpretation is that the Dilwyn could have formed in a lower delta plain area with the sands, distributary channels and mouth bars, and the clays, the interdistributary bay fills (Abele *et al.*, 1995).

The Dilwyn Formation is the youngest unit of the Wangerrip Group, and is unconformably overlain by the **Mepunga Formation**, the oldest formation of the **Nirranda Group**. In the Casino-3 well the Mepunga was intersected at 672m and is 133.5m thick. The massive sandstone is medium brown to occasionally dark brown, partly medium yellow brown, coarse to very coarse grained and minor medium grained, moderately well sorted, with grains that are subrounded to occasionally rounded and minor subangular. The sandstone has a weak siliceous cement and common Fe-staining. There are traces of glauconite and trace pyrite. The sandstone is poorly consolidated and loose in part and partly friable to moderately hard. The porosity is inferred to be fair with no hydrocarbon fluorescence being observed. There are trace of claystone which is medium brown, slightly to very silty in part, with abundant dispersed very fine to grit-sized brown-stained quartz grains in places. It is slightly calcareous in part, with a trace of glauconite, trace to common pyrite and is very soft, very dispersive and non fissile. According to dating of forams, molluscs and palynomorphs discovered within the Mepunga, an age of Middle Eocene to Early Oligocene has been given. The sandstones have been interpreted as being deposited in beach and nearshore locations as barrier islands, whereas the claystones regarded as estuarine and some as deep lagoonal in origin (Abele *et al*, 1995).

The **Narrawaturk Marl** overlies the Mepunga Formation with a conformable contact. The marl was encountered behind the casing shoe at 597m (GR pick). No cuttings of the Narrawaturk Marl were studied in the Casino-3 well since drilling was riserless. Based on offset well information, the formation is generally made up of a calcareous claystone which is intergraded with and intergrading to marl and commonly has fossil fragments of echinoid spines and bryozoa. The fossil fragments have been dated to be Late Eocene to Early Oligocene, but no older than Oligocene in age. The marl was deposited in an open marine environment, mostly below storm wave base.

Formations younger than the Narrawaturk Marl are behind casing and were not studied. These include formations (typically limestones) of the **Heytesbury Group** like the Clifton Formation which grades into the **Gellibrand Marl** which is overlain, with a transitional contact, by the **Port Campbell Limestone**, the topmost formation of the Heytesbury Group. The Port Campbell Limestone is Middle to Late Miocene in age and was deposited in a moderate-energy, continental shelf environment, above fair weather wave base. It is uncertain if all these formations were penetrated Casino-3 prior to installing the marine riser when all returns were to the seafloor.

2.3 HYDROCARBON SUMMARY (Logger's MDRT Depths)

Ditch gas values were monitored and recorded in units (U) by F.I.D (flame ionisation detector) Total Gas detector, where one unit is equivalent to 200 ppm (parts per million) of methane gas in air. The ditch gas was also monitored for hydrocarbon gas composition by a F.I.D. chromatograph. Gas composition refers to percent components of the hydrocarbon alkane series: (methane, ethane, propane, butane and pentane). Gas compositions are quoted as the percentage ratios of these five gases (i.e. 94/2/1/1/1 denotes 94% C1, 2% C2, 1% C3, 1% C4 and 1% C5). Ditch cuttings were tested for hydrocarbon fluorescence by using an ultra-violet fluoroscope.

Since returns were to the seafloor in the 914mm (36") and 445mm (17.5") sections, gas readings are not available. After drilling out the 340mm (13-3/8") casing shoe at 635m returns were to the surface and realtime gas monitoring was possible. From the casing shoe at 635m to 1030m, Total Gas in trace quantities was recorded and consisted of 100% C1. From 1030m to 1475m (middle of the Paarate Formation), background gas ranging from traces to 20 units was recorded and consisted of 100% C1. From 1475m to 1965m (in the upper part of the Flaxmans Formation), the background gas increased marginally to range generally between 10 and 20 units and comprised of 99/1/trace %. An increase to 100 units was observed from a slightly sandy section at 1965m.

In the upper Unit "C" of the Waarre Formation, the primary target for the well, background gas ranged increased significantly to 490 units over a general background of 30 units. The composition of the gas was 97/2/1/tr %. Log analysis of the Waarre Formation indicates a total 24.1m of gas pay (Average porosity 18.2% Average Sw 22%) versus prognosed gas pay of 15 to 20m. Of this total, 4m of gas pay was in the Waarre Cb unit, 12.2m in the Top Porosity Main CB unit and 7.9m in the Waarre Ca unit

The gas levels dropped off in the underlying Unit "B" and Unit "A" to range between 4 and 20 units with a composition of 98/2/tr/tr %. No pay was identified by log analysis in these two units of the Waarre Formation.

2.4 SUMMARY

Casino-3 was drilled as an Otway Basin gas exploration well in the Victoria Offshore VIC/P44 licence. The Surface Location is Latitude: 38° 46' 34.558" S Longitude: 142° 44' 05.437" E (GDA94), Northing: 5706621.82m Easting: 650700.11m (MGA-94), with a seismic reference of Inline 6260, CDP 2546, Casino 3D Survey 2001. The location lies approximately 29 km south west of the town of Port Campbell, 24 km WSW of the Minerva gas field and 22 km North of the LaBella gas field. The Casino field is situated towards the western limit of the productive Waarre Sandstone play fairway of the Port Campbell Embayment. With reference to the earlier Casino wells, Casino-3 is approximately 3.3km NE of Casino-1 and approximately 2.4 km NW of Casino-2 (see Location Map). The water depth at the well location was 66.7m LAT.

The Casino structure is a tilted fault block with three way dip closure and up dip fault closure. Casino-1 and Casino-2 were drilled crestally on this fault block whereas Casino-3 is proposed in a down-dip location near the structural closure limit. Casino-1 and Casino-2 have established the presence of gas in the "Younger" and "Older" sands of the Waarre Sandstone.

The objectives of Casino-3 were to:

- Establish a GWC/LKG in the "Younger" Waarre sand. Approximately 28m gross gas column for 15-20m of net pay was predicted in this sand. Cut a full-hole core and DST this sand to establish productivity.
- Establish pressure regimes in the "Younger" Waarre sand to determine if normally pressured, over-pressured or compartmentalised.
- Establish reservoir characteristics in the "Older" Waarre sand in a water leg.
- Allow confirmation of the OGIP and Recoverable of the Casino Gas Field.

Casino-3 was spudded at 22:00 hrs on 14/10/03. A 914mm (36") hole was drilled from the seabed at 89.5m to 121.3m. The 760mm (30") casing was then run and set at 121.3m. A 445mm (17.5") hole was drilled from 121.3m to 645m with returns to the seafloor and 340mm (13-3/8") casing run and set at 635.8m. The blow out preventers was installed and pressure tested. Adverse weather conditions then resulted in the suspension of drilling operations. A 311mm (12-1/4") hole was drilled using 2 bits, from 645m to the core point of 2004m. MWD/LWD data (gamma ray, resistivity, sonic data and surveys) was acquired in this drilling phase from 1226.5m to 2004m. A coring assembly was run in and a 27m core was cut from 2004m to 2031m with a recovery of 24.7m (91.5%). Drilling of the 311 mm (12.25") phase continued from 2031m to the Total Depth of 2135m (D) which was reached at 08:00 hrs on 30/10/03.

At Total Depth, the hole was circulated clean and the drillstring was pulled out of hole to run wireline logs. Schlumberger was rigged up and the following wireline logs were run. Run 1: DSI-PEX-HALS, Run 2: MDT-GR, Run 3: PEX-CMR-HNGS, Run 4: MCST-GR and Run 5: SWC-GR. After rigging down Schlumberger, a string of 244mm (9 5/8") casing was run and cemented at 2113m. The well was then production tested and thereafter abandonment plugs were set as per program, Plug 1: 2013m to 1970m, Plug 2: 2170m to 2120m and Plug 3: 175m to 135m. The rig was released at 19:00 hours on 13/11/03.

The penetrated depths of most formations in Casino-3 were within 50m of their respective prognosed depths as can be seen in the table above. The notable exception was the Skull Creek Formation which was intersected 360m low to prognosis due to a thickening of the overlying Paarate Formation and the Timboon Sandstone. The Belfast Mudstone nor the Eumeralla Formation were intersected. Casino-3 was drilled as a vertical well with a maximum inclination of 2.9° close to total depth. At total depth the maximum calculated displacement is 7m towards the SSW direction.

Casino-3 encountered the top of the Waarre Formation at 1982m RT (-1959.6m SS) which was 19.4m high to prognosis. The well penetrated 140m of Waarre Formation terminating in the Waarre A unit. The Waarre Formation was as predicted, with Unit Ca/Cb (53m thick), Unit B (16.5m thick) and Unit A (70.5m+ thick) present.

Log evaluation of the Waarre Formation indicates a total 24.1m of gas pay (Av Porosity 18.2% Av Sw 22%) versus prognosed gas pay of 15-20m. Of this total, 4m of gas pay was in the Waarre Cb unit, 12.2m in the Top Porosity Main CB unit and 7.9m in the Waarre Ca unit. The well encountered a gas water contact in Unit C at 2021.4m RT (-1999mSS) which is 8m above the prognosed gas water contact. The unit C reservoir sand was confirmed to be normally pressured. A cased hole DST over the interval 2002-2011m RT flowed gas at 44.3MMscf/d on 64/64" choke. Unit A reservoir sand was water wet at Casino-3 as prognosed with average porosity of 16%.

Casino-3 achieved its key objectives in that:

- The well encountered the Waarre Formation close to prognosis thereby conforming the pre-drill structural interpretation.
- The Waarre Formation was developed as predicted
- The well encountered 20m of gas pay in Unit C as predicted.
- A gas water contact was established at -1999mSS in Unit C and this sand was confirmed to be normally pressured.
- Unit C was successfully tested with a cased hole DST to establish flow capacity.

3. REFERENCES

- Santos, 2003 Casino-3 Well Proposal, Prepared for Santos Ltd, (unpublished).
- Subramanian, R., 2003 Casino-3 Basic Data Report, Prepared for Santos Limited, (unpublished).
- Subramanian, R., 2002 Casino-1 Interpreted Data Report, Prepared for Santos Limited, (unpublished).
- Subramanian, R., 2002 Casino-2 Interpreted Data Report, Prepared for Santos Limited, (unpublished).
- Santos, 2001 Penryn-1 Well Completion Report, Prepared for Santos Limited, (unpublished).
- Abele, C., Pettifer, G., Tabassi, A. 1995 The Stratigraphy, Structure, Geophysics, and Hydrocarbon Potential of The Eastern Otway Basin. Department of Agriculture, Energy And Minerals of Victoria. Geological Survey Of Victoria, Geological Survey Report 103.
- Partridge, A., 1997 New Upper Cretaceous Palynology of The Sherbrook Group Otway Basin. Biostrata Pty. Ltd. In PESA News, April/May.

APPENDIX I : ELECTRIC LOG EVALUATION RESULTS

Log analysis of the Waarre Formation indicates a total 24.1m of gas pay (Av porosity 18.2% Av Sw 22%) versus prognosed gas pay of 15 to 20m. Of this total, 4m of gas pay was in the Waarre Cb unit, 12.2m in the Top Porosity Main CB unit and 7.9m in the Waarre Ca unit.

A summary of the Log analysis is presented overleaf.

CASINO-3 LOG ANALYSIS SUMMARY

Net Pay; Por >4, Vsh<45 & Sw <70

(Depth in metres)

FORMATION	SAND INTERVAL	GROSS SAND (m)	LDG SAND (m)	AVG PHIs (%)	Kh _s (MD)	LDG PAY (m)	AVG PHIp (%)	WT.AVG SW (%)	Kh _p (MD)
WAARRE Cb	1982-1995	5.9	5.8	14.2	3606.9	5.6	14.4	25	3606.9
TOP WAARRE MAIN CB PAY	1996-2010	13.1	13.1	18.7	29589	13.1	18.7	15	29589
WAARRE Ca	2011-2035	13.4	13.3	16.2	4598.3	8.1	17.8	30	4311
WAARRE B	2035-2051	0.2	0.2	10.7	0.2	0	-	-	0
WAARRE A	2052-2099	34	33.2	9.7	358.9	0	-	-	0

CASINO_3
Sand Summary

Net Pay; Por >10 ,Vsh<4 5 & Sw <70
Depth in metres

FORMATION	SAND INTERVAL	GROSS SAND (m)	NET SAND (m)	AVG PHIs (%)	Kh_s (MD)	NET PAY (m)	AVG PHIp (%)	WT.AVG SW (%)	Kh_p (MD)
WAARRE Cb	1982-1995	5.9	4	17.2	3606.9	4	17.2	22	3606.9
TOP WAARRE MAIN CB PAY	1996-2010	13.1	12.2	19.5	29589	12.2	19.5	14	29589
WAARRE Ca	2011-2035	13.4	12.5	16.8	4598.3	7.9	18	30	4311
WAARRE B	2035-2051	0.2	0.2	10.7	0.2	0	-	-	0
WAARRE A	2052-2099	34	15.4	12.5	358.9	0	-	-	0

APPENDIX II : MDT PRESSURE SURVEY REPORT AND DATA

SUMMARY

A summary of the Free Water Levels (FWLs) based on interpretation of the available pressure data for the Casino Field is presented in Table 1. Wireline pressure data indicates that the gas accumulations of the Waarre C and Waarre A reservoirs are isolated with separate FWLs. Review of regional pressure data indicates that the aquifers of both the Waarre A and Waarre C are overpressured compared to the regional aquifer of the Waarre C.

The range in FWL for each reservoir reflects the uncertainty in measurement, gauge accuracy and pretest pressure validity.

TABLE 1: SUMMARY OF INTERPRETED FWLS FOR THE WAARRE C AND WAARRE A, CASINO FIELD

Reservoir	Most Likely FWL (TVD mSS)	Maximum FWL (TVD mSS)	Minimum FWL (TVD mSS)
Waarre C	1999	2000	1994
Waarre A	1839	1840	1836

Pressure Interpretation Methodology

The most commonly used wireline pressure interpretation technique, and the one adopted for this study, is the pressure-depth diagram. This technique involves plotting stabilised formation pressure against true vertical depth. The intersection of hydrocarbon and water pressure gradient provides a free water level for the reservoir. Several authors have proposed an alternative technique, referred to as the 'Excess Pressure Plot' (Brown, 2003). This technique enhances the measurement of fluid densities and resolves small density changes and pressure barriers that are not likely to be recognised by standard analysis. Given the significant density contrast between the reservoir and aquifer fluids in Casino Field, the traditional technique of pressure versus true vertical depth was considered appropriate for this study.

Data Quality Control

Wireline Pressure data was acquired in Casino 1, 2 and 3 with Schlumberger's Modular Dynamic Tester (MDT) tool. The tool was run in openhole and pressures were measured with Compensated Quartz Gauge (CQG). Overall data quality was excellent enabling fluid limits to be determined for each reservoir. However, several data quality issues were observed. Gauge accuracy, supercharging and depth measurement issues resulted in uncertainty in FWL interpretations. This uncertainty is reflected in the range in FWL interpretations for the Waarre C & A reservoirs.

Pressure Stability

Only MDT pre-tests that achieved a stable build-up pressure were included in the interpretation. The temperature compensated quartz gauge (CQG) used in the MDT tool has a reported resolution of 0.001 psi (Economides et al 1994). A pre-test build up was generally considered to have stabilised when the change in gauge pressure was less than 0.01 psi. For a number of pretests the pressure build-up was very slow due to low permeability rock. In order to save rig time and prevent tool sticking several of these tests were terminated prematurely. The final pressures from these tests had not stabilised and therefore are not representative of formation pressure. These pretests were excluded from the interpretation.

Another cause of unrepresentative formation pressures was tool plugging or unseating of the probe packer during the pretest. These tests are usually characterised by a major difference in expected formation pressure and typically aborted. These tests were also excluded from the interpretation.

Supercharging

Supercharging results from leakage of mud filtrate through the filter cake, which increases sandface pressure above formation pressure. The MDT probe measures pressure near the borehole wall, thus supercharged tests have high pressures unrepresentative of the formation pressure. Where supercharging is tens to hundreds of psi in excess of formation pressure, supercharging can be identifiable solely on the basis of high pressure. Those pretest pressures that were identified as supercharged were excluded from the interpretation. Figures 1 and 2 are an illustration of pretests for the Waarre C and A. All pressures included in the plot are interpreted to have stabilised (as discussed in the section above). Those pressures in excess of the expected formation pressure are readily identifiable and excluded from the fluid limit interpretation. An exception to this, is the pretests of the Waarre C aquifer in Casino 3, which is discussed in the Fluid Limit Interpretation section.

Depth Control

MDT pretest depths are based on wireline depth measurement. In all three wells a gamma ray (GR) was run with the MDT tool. The GR was used as a correlation log to the first GR run in the hole. In all wells, Measurement While Drilling (MWD) was acquired. The MWD suite comprised a directional survey, gamma ray and resistivity. A comparison of MWD depth (equivalent to Driller's depth) against Loggers depth indicates that there is a depth discrepancy at the top of the Waarre Sandstone. Wireline logging measures depth via measuring cable length as it passes through a wheel. This measurement corrects for cable stretch to provide a true depth. However, the accuracy of the measurement is dependent on the cable stretch correction which varies based on cable type and history, therefore is prone to inaccuracy. Provided that the pipe tally is correct, Driller's depth (and MWD) should be an accurate measurement of true depth. A comparison of driller's and loggers depth at top Waarre Sandstone is presented in Table 2. Except in very shallow wells, wireline depths are usually deeper than driller's depth by approximately 1m for every 1000m. This is the case for Casino 1 and 2, however there is a significant depth discrepancy in Casino 3. This is evident when the pretest pressures from the Waarre C gas reservoir in Casino 2 and Casino 3 are compared. There is a significant offset in gas pressure gradient between Casino 2 and 3 when formation pressure is plotted against loggers depth (Figure 3). When pressure is plotted against Drillers Depth (TVD SS) this offset is reduced (Figure 4).

TABLE 2: DIFFERENCE BETWEEN LOGGERS AND DRILLERS DEPTH AT TOP WAARRE C.

	Drillers Depth (mRT)	Loggers Depth (mRT)	Difference
Casino 1	1761	1763	2
Casino 2	1758	1760	2
Casino 3	2002	2005.7	3.7

Gauge Accuracy

Absolute-gauge and depth accuracy limits the interpretation of data from multiple wells, even where the tool type and service company are the same. Accuracy for the CQG is reported as +/- 0.01% of reading + 2 psi (Economides et al, 1994). This equates to a gauge accuracy of +/- 2.287 psi for the Casino wells. The observed offset in gas gradient in Figure 4 may also be explained by gauge inaccuracy.

Fluid Limit Interpretation

Figure 5 is a plot of pressure versus true vertical depth (sub sea above MSL) for Casino 1, 2 and 3. Pressures were obtained from both the gas reservoir and aquifer for the Waarre C and Waarre A sandstones. Consequently, a well defined FWL was evident for each reservoir.

The Waarre C and A gas reservoirs are isolated with separate FWLs. The Waarre A aquifer is significantly overpressured with respect to the regional aquifer for the Waarre while the Waarre C aquifer may be slightly overpressured. The following is a discussion of the interpretation of fluid limits for each reservoir.

Waarre A

A gas column for the Waarre A was intersected in Casino 1 and pressures from MDT pretests from this well define the gas gradient for the Waarre A. Gas samples were also acquired from Casino 1 with the MDT tool. Compositional analysis of the gas indicates that the reservoir fluid has a Specific Gravity of 0.6 (air=1), which is consistent with the gas pressure gradient of 0.17753 psi/m (0.05411 psi/ft).

The water gradient for the Waarre A reservoir in Casino was determined from valid pretests in Casino 2 and 3. Apparent formation water salinity calculations (based on Pickett Plots) indicate that the aquifer of the Waarre A comprises a brine salinity of 15 000 ppm (Total Dissolved Solids of 1.5%). This salinity is equivalent to a brine density of 63 lb/ft (at standard conditions) which is consistent with the water gradient from pretests of 1.388 psi/m (0.423 psi/ft).

As discussed under Data Quality Control, there is a difference between depth measured by Drillers and the Logging contractor. This discrepancy raises uncertainty about the true measured depth and therefore FWL interpretation. The 'Minimum' and 'Most Likely' FWL interpretations for the Waarre A reflect this uncertainty. The 'Minimum' FWL is based on Driller's Depth (Figure 7) and 'Most Likely' based on Logger's Depth (Figure 6). As mentioned previously, Driller's depth is considered the more accurate measurement of depth. However, the major horizons within the subsurface static model are tied to Logger's depth at each of the wells. Therefore, for consistency, the 'Most Likely' FWL interpretation is considered to be based on Logger's Depth.

The 'Maximum' FWL interpretation for the Waarre A incorporates gauge inaccuracy. If the Casino 1 pretests are shifted +2 psi (the maximum gauge inaccuracy) the FWL interpretation is 1840 mSS.

Waarre C

The Waarre C gas reservoir was encountered in Casino 2 and 3. Valid pretest formation pressures from these wells define the gas gradient for the Waarre C. Gas samples were also acquired from Casino 2 and 3 with the MDT tool. Compositional analysis of the gas indicates that the reservoir fluid has a Specific Gravity (air=1) of 0.59, which is equivalent to a gas pressure gradient of 0.177 psi/m (0.054 psi/ft).

As discussed in the section above (Data Quality Control), Figure 8 illustrates two gas pressure gradients for the Waarre C. These gas gradients represent the range of uncertainty of the position of the gas gradient for the Waarre C. The intersection of these gradients and the water gradient represents the 'Minimum' and 'Most Likely' FWL interpretations.

The minimum gas line is based on gas gradient from Casino 3 PVT fitted to the Casino 3 pretests of the Waarre C, plotted against Driller's depth (Figure 8) The 'Most Likely' gas line is based on the gas gradient from Casino 2 PVT, fitted to the Casino 2 pretests of the Waarre C, plotted against Logger's Depth (Figure 9).

The 'Minimum' and 'Most Likely' FWL interpretations are based on the respective gas gradients intersecting a water gradient. The water gradient is the same as the Waarre A (1.388 psi/m) fitted to the only valid pretest of the Waarre C aquifer (at 2001.5 mSS). However, it cannot be certain if this pretest is not supercharged. Consequently the maximum FWL interpretation is based on the interpreted 'Water Up Too' based on wireline log interpretation of Casino 3 i.e. 2000 m TVDSS.

Regional Interpretation

Casino pressure data was also reviewed in a regional context. Presented in Figure 10 is pressure data for the Waarre Sandstone of the Otway Basin. A well defined regional pressure gradient is evident for the Waarre C aquifer. The aquifer is normally pressured Slight deviations from the regional gradient is interpreted to be a result of variation in formation water salinity, gauge inaccuracies, possible supercharging and depth control uncertainties. Highlighted in Figure 10 is the aquifer pressure data of the Waarre C in the Minerva Field which falls on the regional aquifer gradient. Illustrated in Figure 11 is the Casino & Minerva pressure data. The aquifer gradient for Minerva defines the regional pressure gradient for the Waarre aquifer. Evident from the plot is the overpressured aquifers of the Waarre C and A in the Casino Field. The Waarre A aquifer is significantly overpressured by approximately 190 psi while the Waarre C appears to be slightly overpressured by 14 psi.

References

Brown, A. 2003, Improved Interpretation of Wireline Pressure Data. AAPG Bulletin, v. 87, No. 2, p. 295-311.

Economides, MJ. Daniel Hill, A & Ehlig-Economides, C. 1994, Petroleum Production Systems. Prentice Hall Petroleum Engineering Series, p. 285-288.

Figure 1: Waarre C MDT data including supercharged pretests.

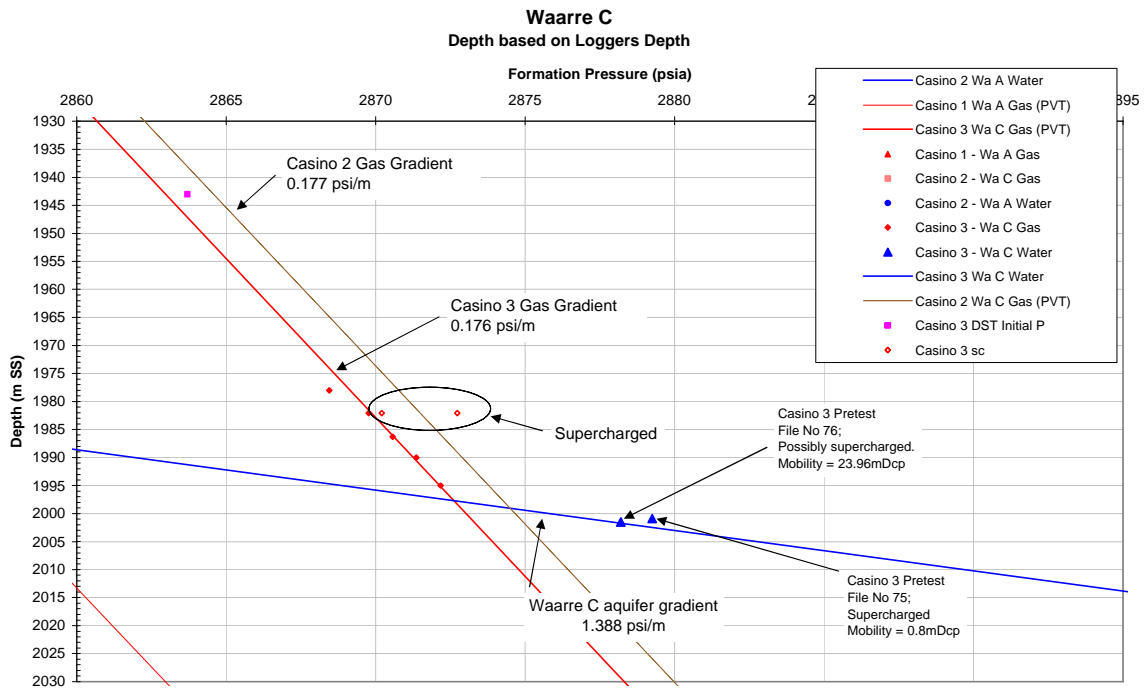


Figure 2: Waarre A MDT data including supercharged pretests

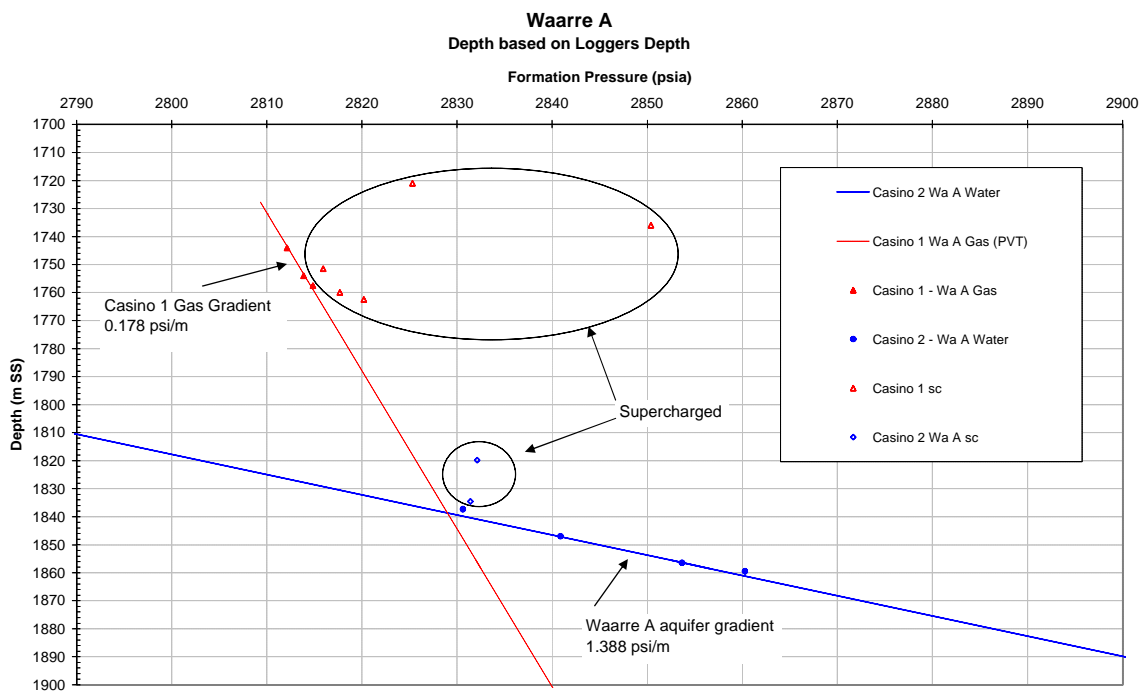


Figure 3: Waarre C pretest data illustrating gas gradient offset. Depth is based on Logger's measurement

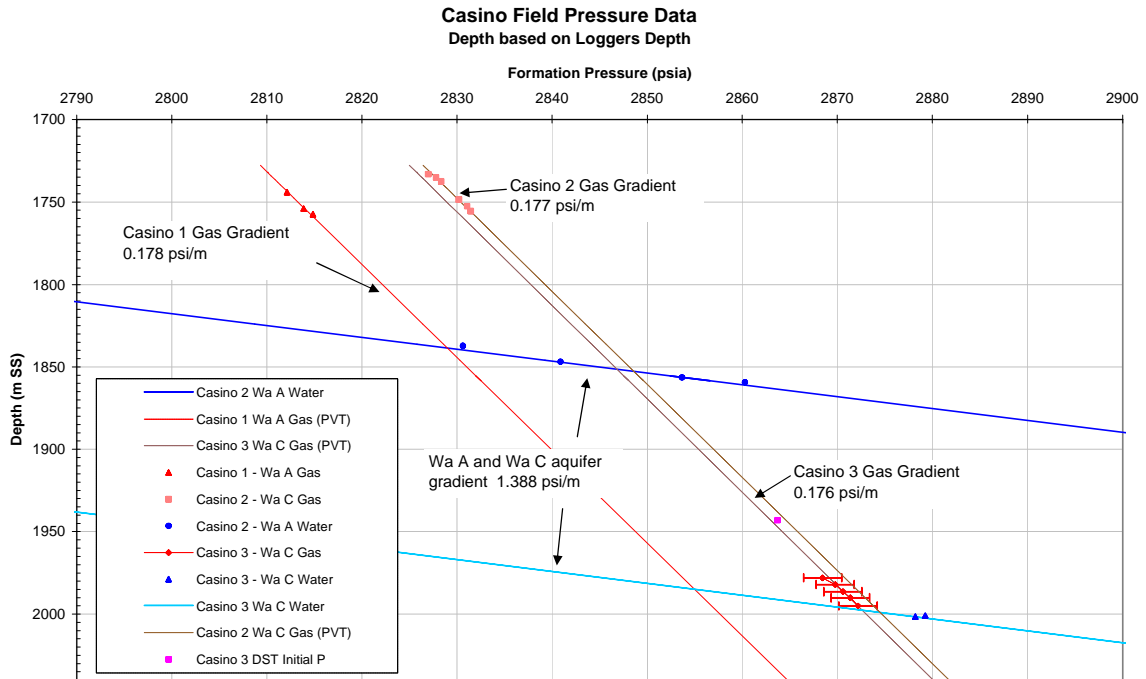


Figure 4: Waarre C pretest data illustrating gas gradient offset. Depth is based on Driller's measurement

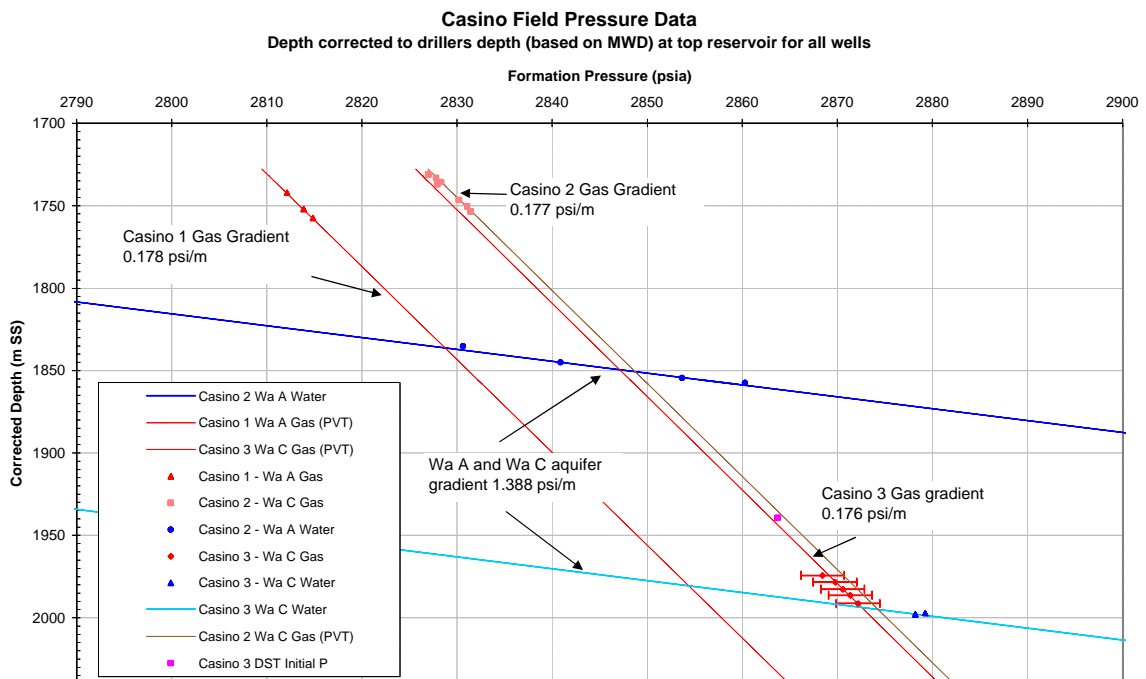


Figure 5: FWL interpretation for the Waarre C and A reservoirs.

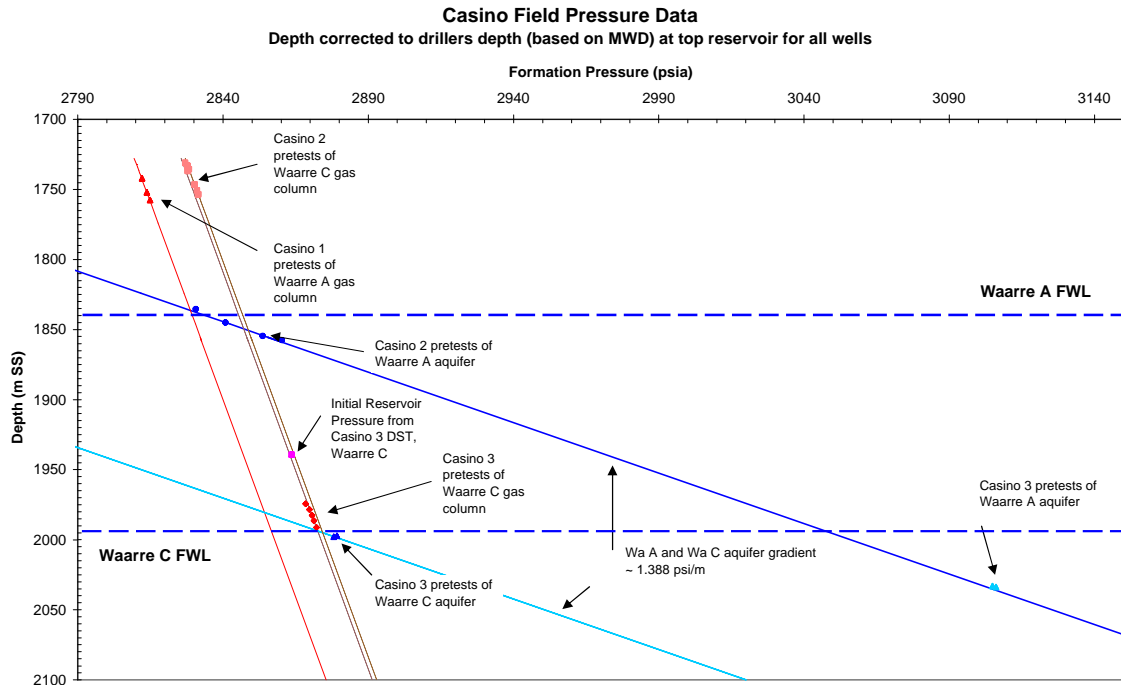


Figure 6: 'Most Likely' FWL interpretation for the Waarre A

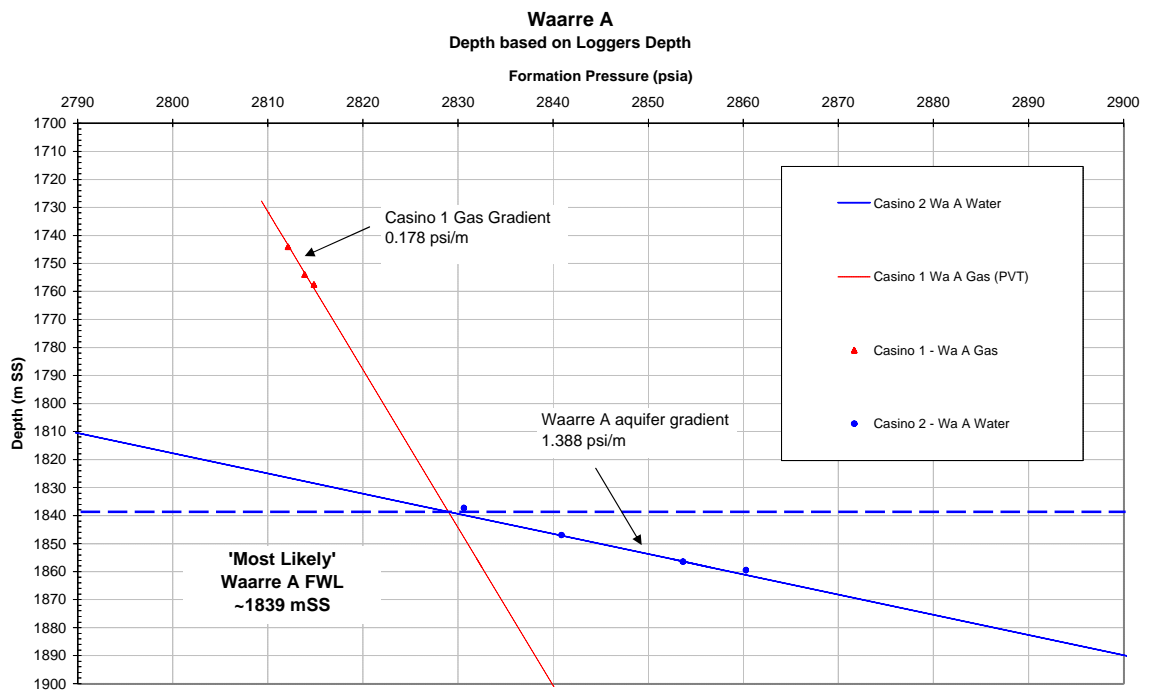


Figure 7: 'Minimum' FWL interpretation for the Waarre A

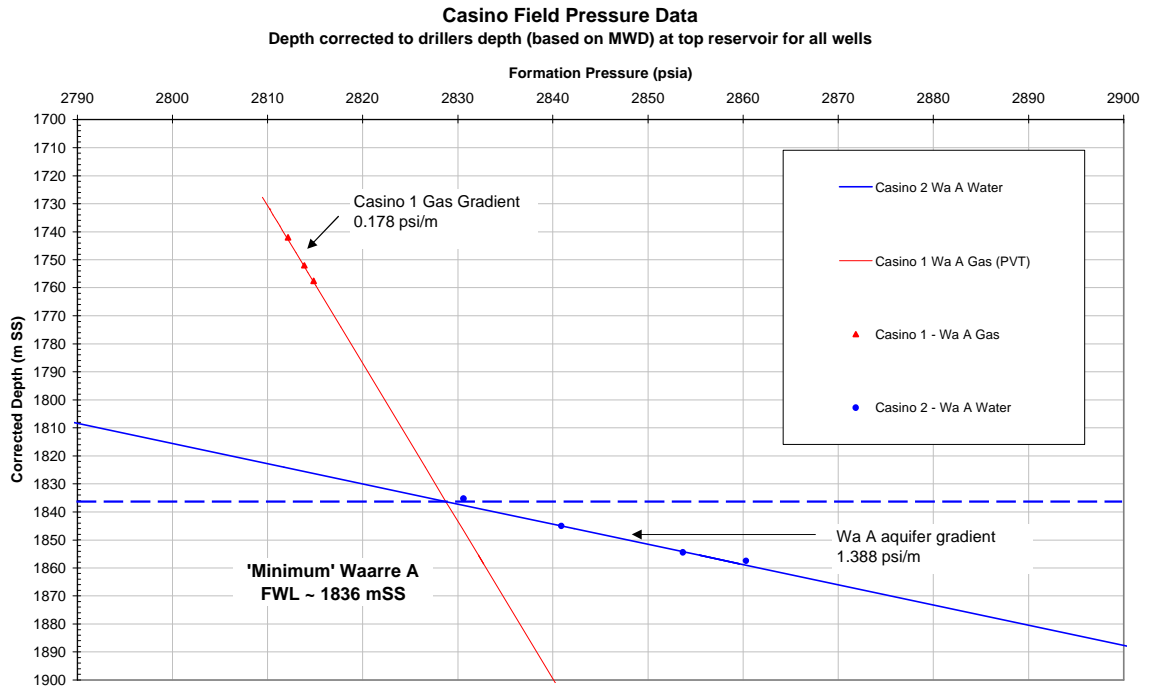


Figure 8: Minimum FWL interpretation for the Waarre C

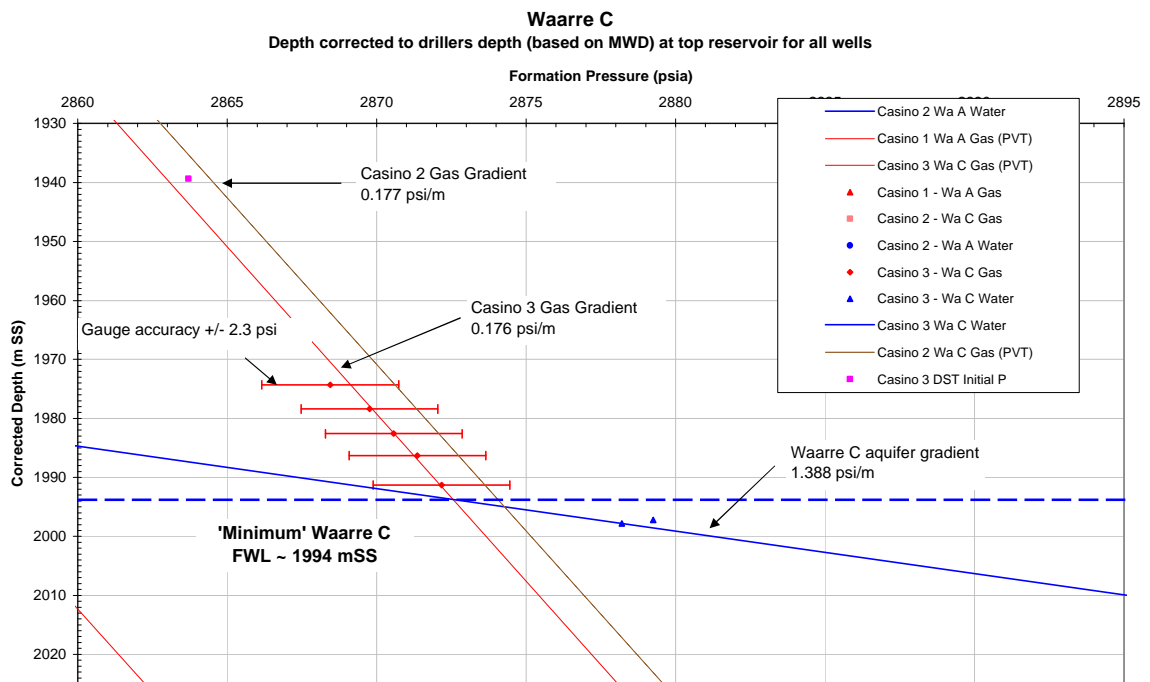


Figure 9: 'Most Likely' FWL interpretation for the Waarre C

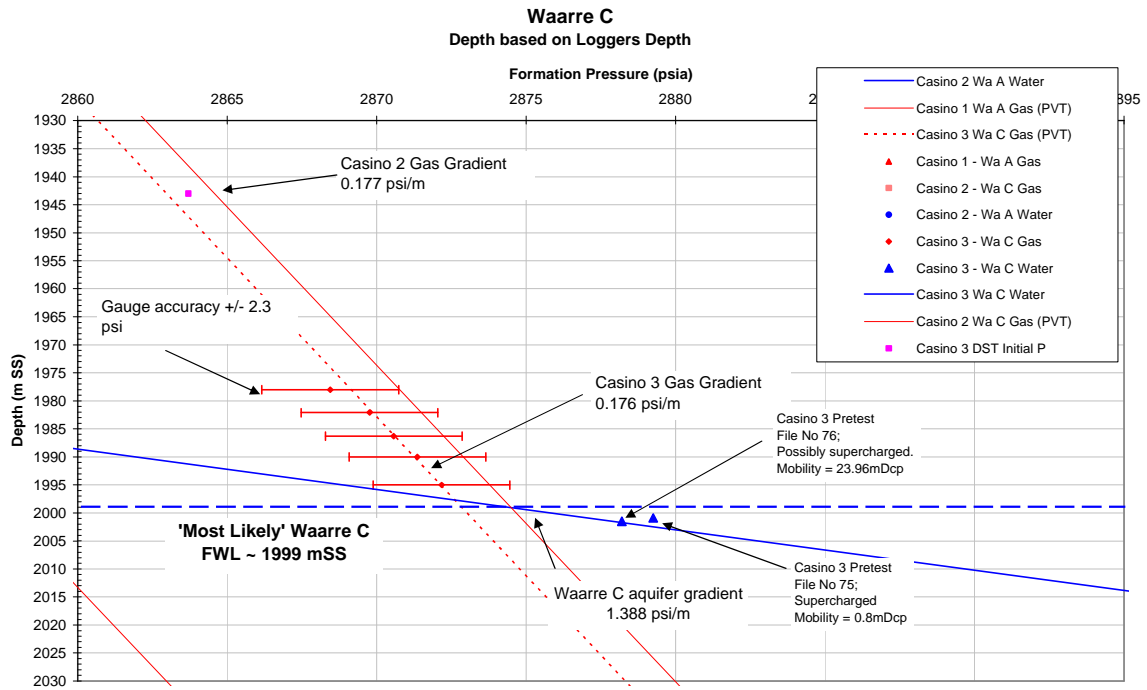


Figure 10: Regional aquifer gradient for the Waarre Sandstone

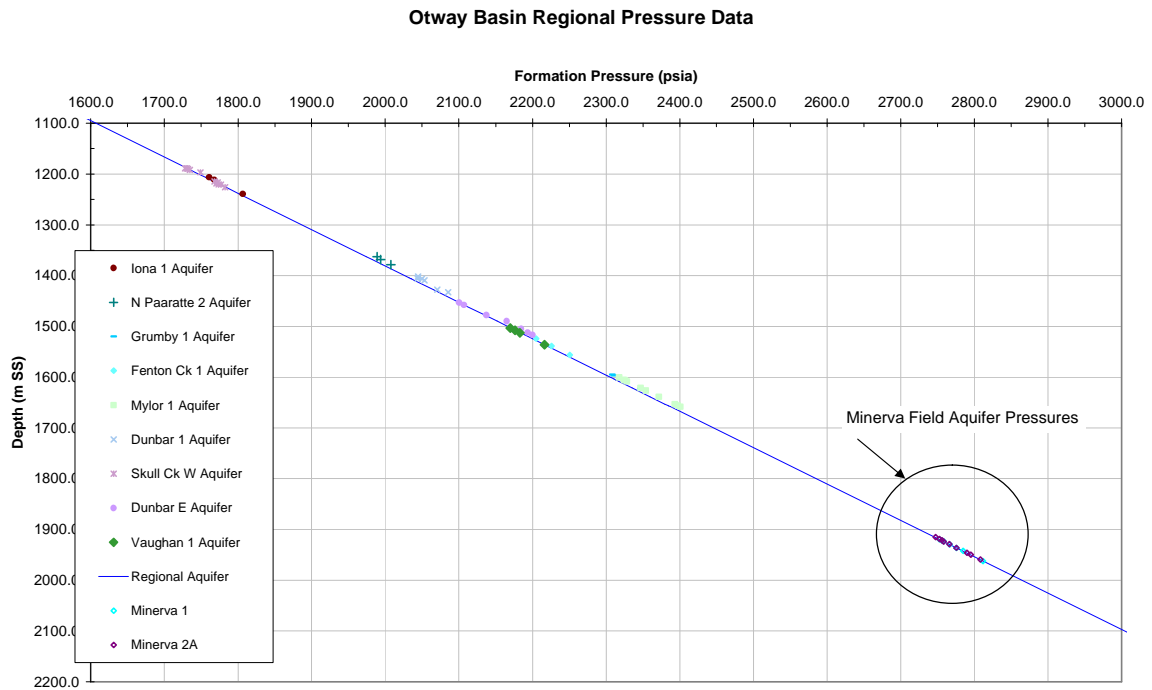
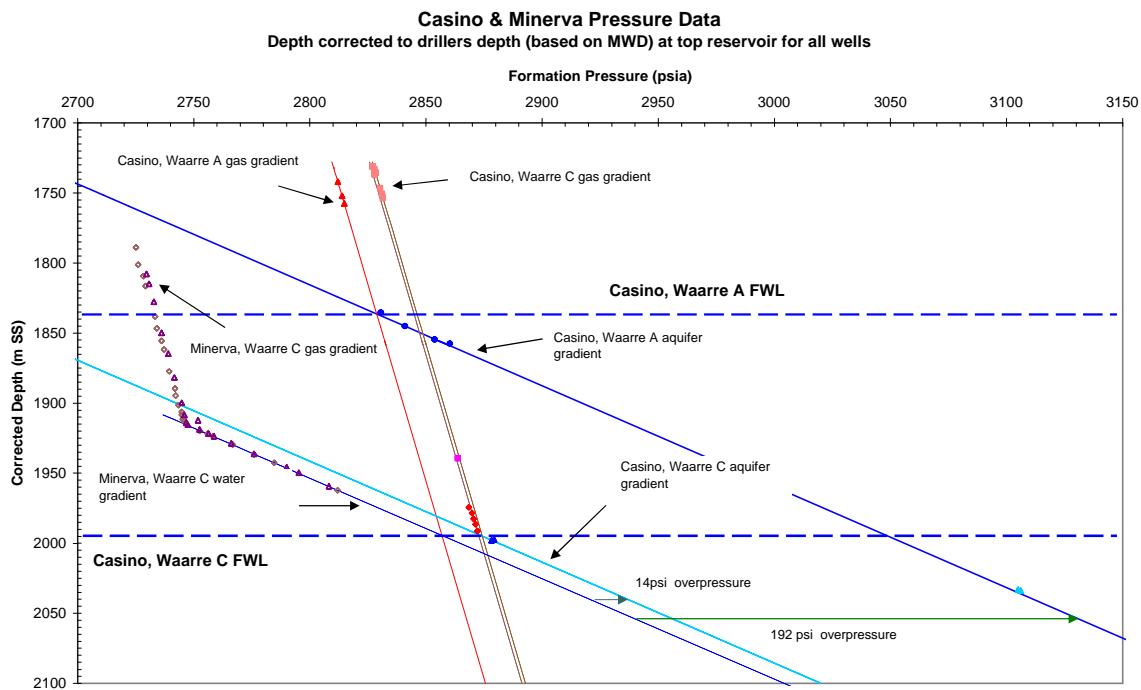


Figure 11: Casino and Minerva pressure data, illustrating overpressured aquifers of the Waarre C & A,



Santos

MDT PRESSURE SURVEY (RUN 2)

WELL: Casino 3

RT:22.4 metres

Gauge Type :CQG

Page :1 OF 2

WITNESS: M. Lahiff/ J Pitman

Time since last circ :10:00 hrs on 30/10/03

Probe/Packer Type :Standard

Date :31/10/2003

	FORMATION	DEPTH RT MD m	DEPTH SUBSEA m	FILE NO	TEST RESULTS			TEMP deg F	D/D MOB MD/CP	TYPE D/D	INTERPRETATION TYPE BUILD	Super Charged	COMMENTS
					HYDRO BEFORE PSIA	FORM PRESS PSIA	HYDRO AFTER PSIA						
				65									CORRELATION
1	Waarre C	2000.4	1978.0	66	3360.40	2868.45	3358.80	180.0	29.3	N	Stable		
2	Waarre C	2004.5	1982.1	67	3367.70	2872.73	3367.50	177.5	643.2	N	Stable	Possibly SC	
3	Waarre C	2004.5	1982.1	68	3367.90	2869.76	3368.45	178.3	6682.8	N	Stable		
4	Waarre C	2008.7	1986.3	69	3374.86	2870.57	3374.60	179.3	5814.0	N	Stable		
5	Waarre C	2009.7	1987.3	70	3376.12		3376.56	179.8	0.9	N	Unstable - pretest curtailed		
6	Waarre C	2012.2	1989.8	71	3380.43	2874.20	3380.60	180.7	66.2	N	Unstable - pretest curtailed	Possibly SC	
7	Waarre C	2012.4	1990.0	72	3380.72	2871.36	3381.08	181.1	3696.40	N	Stable		
8	Waarre C	2017.4	1995.0	73	3389.00	2872.17	3377.30	182.0	1090.90	N	Stable		
9	Waarre C	2023.2	2000.8	74	3399.50								Lost seat
10	Waarre C	2023.3	2000.9	75	3399.62	2879.25	3398.92	182.9	0.80	N	Stable	Possibly SC	Very slow BU. Tight
11	Waarre C	2023.9	2001.5	76	3400.26	2878.20	3400.14	183.0	23.96	N	Stable		Valid Aquifer Pressure for Younger Sand
12	Waarre C	2025.2	2002.8	77	3402.03		3402.98	183.9		N	Unstable - pretest curtailed		Very slow BU. Tight
13	Waarre C	2025.1	2002.7	78	3401.94	2944.00	3402.11	184.2	0.27	N	Unstable - pretest curtailed	SC	
14	Waarre C	2025.3	2002.9	79	3402.43	2910.00	3402.98	184.3	0.64	N	Unstable - pretest curtailed	SC	
15	Waarre A	2059.9	2037.5	80	3459.61	3106.08	3459.77	184.8	12.73	N	Stable		Valid Aquifer Pressure for Older Sand
16	Waarre A	2060.7	2038.3	81	3460.22	3120.80	3461.03	185.6	0.71	N	Stable	Possibly SC	
17	Waarre A	2059.2	2036.8	82	3458.45	3104.92	3458.56	185.9	9.98	N	Stable		Valid Aquifer Pressure for Older Sand
													CORRELATION
													MRSC Samples (1 & 2 3/4 gallon) &
18	Waarre C	2004.5	1982.1	86	3368.06	2870.20	3367.18		3040.90	N			MRMS Sam ples (2 X 450cc bottles)
19	Flaxmans	1985.5	1963.1	87	3336.50	2083.33	3336.22	183.9	5.70	N	Unstable - pretest curtailed		Very slow BU. Tight
20	Flaxmans	1984.3	1961.9	88	3333.93	2868.86	3334.40	183.0	191.80	N	Stable	Possibly SC	Slow BU
21	Flaxmans	1982.9	1960.5	89									Lost seat

Expected Water Gradient: 0.433 psi/ft

Mud Weight : 9.6ppg

Santos

MDT PRESSURE SURVEY (RUN 2)

WELL: Casino 3

RT:22.4 metres

Gauge Type :CQG

Page :2 OF 2

WITNESS: M. Lahiff/ J Pitman

Time since last circ :10:00 hrs on 30/10/03

Probe/Packer Type :Standard

Date :31/10/2003

	FORMATION	DEPTH	DEPTH	FILE	HYDRO	TEST RESULTS		TEMP	D/D	TYPE	INTERPRETATION	Super Charged	COMMENTS
		RT	SUBSEA			NO	BEFORE						
		MD	m		PSIA	PRESS	AFTER		MD/CP				
		m	m			PSIA	PSIA						
22	Flaxmans	1982.9	1960.5	90	3332.06	2866.91	3330.93		48.20	N			MRMS Sample (1 x 450cc)
				91									CORRELATION
23	Belfast Greensand	1616.2	1593.8	92	2724.56	2321.33	2724.52	169.30	16.70	N			Stable
24	Belfast Greensand	1609.1	1586.7	93	2712.55	1874.14	2712.59	167.40	2.20	N			Unstable - pretest curtailed Very slow BU. Tight

24 PRE-TESTS: 15 Normal, 2 Lost Seals, 7 curtailed

SAMPLES: 2004.5m; 1& 2 3/4 gallon and 2 X 450cc bottles

1982.9m; 1 X 450 cc bottle

* Note: Above readings noted real-time.

Expected Water Gradient: 0.433 psi/ft

Mud Weight : 9.6ppg

The 1 gallon and 2 3/4 gallon samples were opened on surface and contained:

2 3/4 gallon: Surface pressure 3350 psi
 Ambient Temperature 11 deg C
 Gas volume: 1752 cu. ft.
 Breakdown: C1: 97.6296%, C2 1.7746%, C3 0.4398%, iC4 0.0677%, nC4 0.0703%,
 iC5 0.0118% nC5 0.0062% CO2 0.0%

1 gallon: Surface pressure 3600 psi
 Ambient Temperature 11 deg C
 Gas volume 1054 cu.ft.
 Breakdown: C1 97.5572% C2 1.7809% C3 0.4734% iC4 0.0724% nC4 0.0873%
 iC5 0.0173% nC5 0.0116% CO2 0.07%

APPENDIX III: HYDROCARBON SHOW REPORT

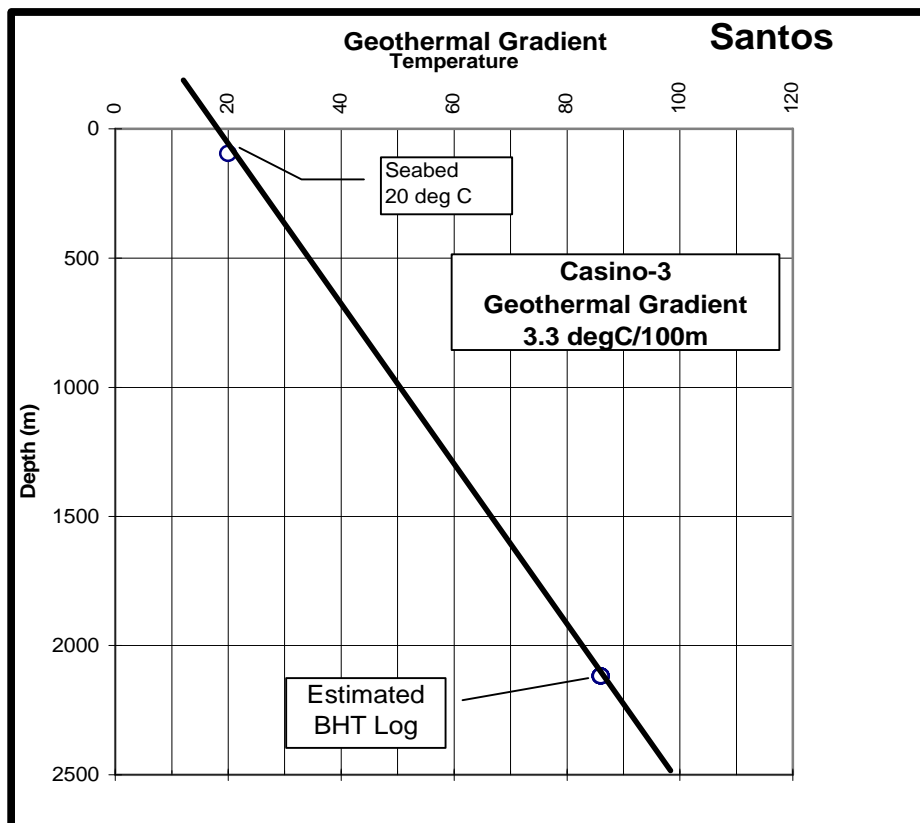
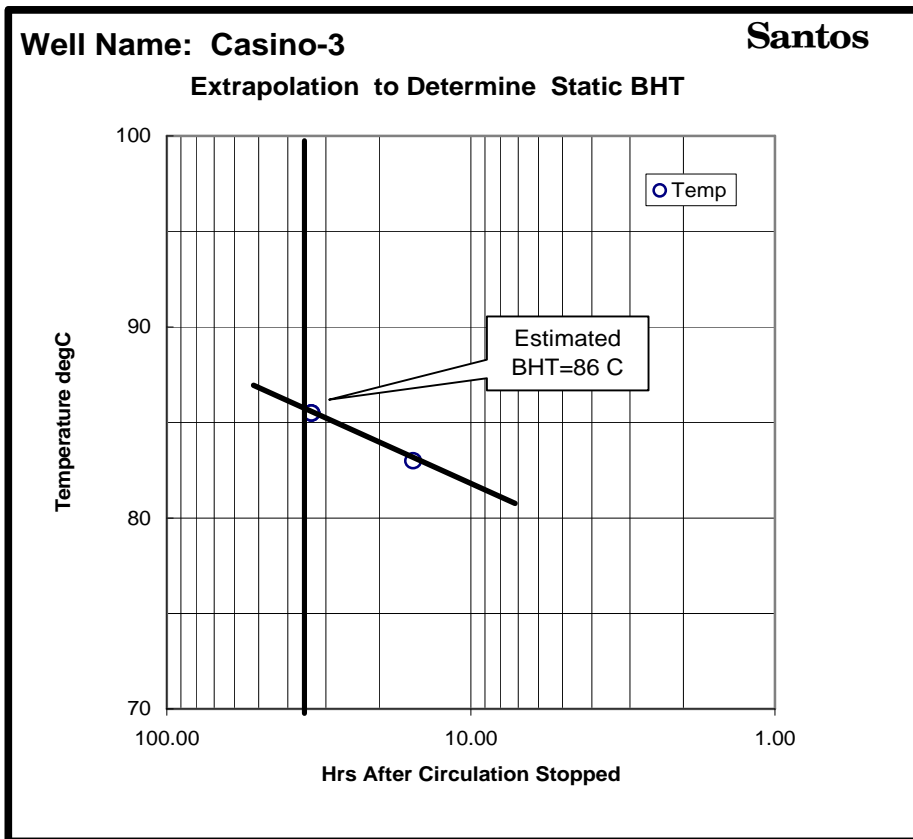
No Fluorescence was observed in Casino-3.

APPENDIX IV : GEOTHERMAL GRADIENT

Data from Wireline Logs were used to estimate a Geothermal Gradient. An extrapolated static bottom hole temperature of 86°C at 2118' (logging depth) and a geothermal gradient of 3.3°C/100m were calculated from downhole temperatures recorded during logging operations.

LOG	TEMP	DEPTH	TIME SINCE LAST CIRCULATION
PEX-HALS-DSI-HNGS	83°C	2118m	15.50 hrs
MDT	85.5°C	2063m	33.50 hrs
SEABED	20°C	93m	

The results are depicted graphically overleaf.



APPENDIX V : PETROLOGY REPORT

Report prepared for:

SANTOS Ltd
91 King William St
Adelaide
SA 5000

PETROLOGY REPORT

CASINO-3

OTWAY BASIN (VIC/P 44)

Report prepared by:

Dr S E PHILLIPS
PGPC
1c Short Crescent
Beaumont SA 5066
January 2004

In requesting the services of Phillips-Gerrard Petrology Consultants (PGPC) the client agrees that PGPC is acting in an advisory capacity and shall not be liable or responsible for any loss, damages or expenses incurred by the client, or any other person or company, resulting from any data or interpretation presented in this report.

CONTENTS

	<i>PAGE</i>
1. SUMMARY	2
2. INTRODUCTION	4
TABLE 1. SUMMARY OF SAMPLES & SERVICES	
3. METHODS	5
4. PETROLOGY	6
TABLE 2. POINT COUNT DATA	
4.1 Casino-3, MSCT 6, depth 2102.5m (loggers)	10
4.2 Casino-3, MSCT 5, depth 2093.5m (loggers)	12
4.3 Casino-3, MSCT 4, depth 2082.5m (loggers)	14
4.4 Casino-3, MSCT 7, depth 2070.5m (loggers)	16
4.5 Casino-3, MSCT 13, depth 2061.5m (loggers)	18
4.6 Casino-3, Core chip, depth 2028.5m (drillers)	20
4.7 Casino-3, Core plug 75, depth 2026.49m (drillers)	22
4.8 Casino-3, Core plug 73, depth 2025.90m (drillers)	24
4.9 Casino-3, Core plug 62, depth 2022.60m (drillers)	26
4.10 Casino-3, Core plug 59, depth 2021.76m (drillers)	28
4.11 Casino-3, Core plug 52, depth 2019.60m (drillers)	30
4.12 Casino-3, Core plug 41, depth 2016.39m (drillers)	32
4.13 Casino-3, Core plug 31, depth 2013.30m (drillers)	34
4.14 Casino-3, Core plug 20, depth 2009.94m (drillers)	36
4.15 Casino-3, Core plug 12, depth 2007.59m (drillers)	38
4.16 Casino-3, Core plug 9, depth 2006.70m (drillers)	40
4.17 Casino-3, Core plug 5, depth 2005.46m (drillers)	44
4.18 Casino-3, MSCT 3, depth 2005.5m (loggers)	46
4.19 Casino-3, MSCT 2, depth 2002.5m (loggers)	48
4.20 Casino-3, MSCT 1, depth 1987.0m (loggers)	50
4.21 Casino-3, MSCT 11, depth 1970.5m (loggers)	52
5. GRAIN SIZE ANALYSES	54
TABLE 3. GRAIN SIZE DATA	
6. X-RAY DIFFRACTION	60
TABLE 4. BULK XRD RESULTS	
TABLE 5. CLAY XRD RESULTS	
7. SCANNING ELECTRON MICROSCOPY	62
8. DISCUSSION	85
9. CONCLUSIONS	104
10. GLOSSARY	105
11. REFERENCES	106
12. APPENDIX A (XRD traces)	108

Front cover

Thin section photomicrograph of Casino-3, MSCT 3, 2005.5m (loggers). Plane light. Horizontal field of view 3.25mm.

1. SUMMARY

Santos Ltd submitted eleven core plug offcuts, nine MSCT and one core chip to PGPC from the Late Cretaceous Waarre and Flaxman Formations in the well Casino-3 from the Otway Basin (VIC/P 44). The study was designed to ascertain sediment provenance, depositional environments, diagenetic alteration and factors controlling reservoir quality, and to compare this data with results from Casino-1 and Casino-2 (Phillips, 2003). All samples were described in thin section; point counted and analysed for grain size. Selected samples were further studied by X-ray diffraction and Scanning electron microscopy.

Waarre Unit A at Casino-3 is comprised of medium to coarse grained, poor to moderately well sorted feldspathic litharenites and carbonate cemented sublitharenites. These sandstones are slightly coarser grained, they contain less lithics, and grains are more angular than Unit A sediments in Casino-2 and -1. Throughout Unit A sediment was dominantly derived from both a metamorphic and igneous (volcanic and plutonic) terrane. There are a higher percentage of volcanic lithics at Casino-2. Based on the presence of glaucony and framboidal pyrite, deposition probably occurred in a marginal marine setting. Grain size distributions are unimodal and slightly positively skewed reflecting a fluvial influence, possibly in an estuary. Casino-3 may have been located closer to the channel axis than Casino-2, and Casino-1 may be juxtaposed to a marsh. Oxidation due to exposure is only apparent in sediments from the base of Casino-2.

At Casino-3 Waarre Unit Ca sandstones are composed of very fine to medium grained, poor to well sorted sublitharenites and subarkoses. A significant change in sediment provenance and depositional environments is apparent in this regressive sequence compared to Unit A. Sandstones from Unit Ca at Casino-2 are coarser grained and more quartz rich but this may be an artifact of sampling. Throughout Unit Ca volcanic lithics are absent and there is a decline in the number of both feldspars (particularly plagioclase) and total lithics. Sediment continued to be supplied from a metamorphic/igneous terrane but the volcanic source had been cut-off. Greywackes at the base of Unit Ca contain relatively high percentages of glaucony, they have bimodal grain size distributions and sedimentary structures which might reflect deposition in a prodelta setting. Overlying fine grained laminated storm deposits have been bioturbated. Cleaner and coarser grained stacked tidal channels display evidence of cross bedding. Lagoonal or tidal flat muddy sediments near the top of the sequence are probably not laterally continuous across the field. Migrating tidal channels may have intermittently eroded into this unit. There are indications from grain size distributions that Casino-3 was located closer to the marine influence than Casino-2 at this time.

Medium to coarse grained, moderately to well sorted, texturally mature subarkoses and quartzarenites from Waarre Unit Cb have less feldspars and lithics than Unit Ca. Lithics of volcanic origin and chalcedony are absent, but the sediment continued to have a metamorphic/igneous (possibly granitic) provenance. A positively skewed grain size distribution at Casino-2 is consistent with a fluvial depositional environment. Negatively skewed grain size at Casino-3 and a possible beach facies at the top of the sequence indicate a stronger marine influence. Micritic rims followed by an equant circumgranular carbonate cement in MSCT 1 could reflect a change from marine to meteoric phreatic regimes.

Diagenetic alteration in the Waarre Formation was typically consistent across the Casino Field. Most of the dissolution and precipitation of authigenic minerals was early diagenetic being related to depositional environments and flushing by meteoric waters. Glaucony and framboidal pyrite reflect marine settings with high Fe and dissolved sulphate available. Early siderite cements and nodules precipitated from meteoric waters low in dissolved sulphate. In marine settings the siderite may reflect temporary exposure or flushing in burrows and palaeoaquifers after burial. Grain replacing and pore filling kaolinite formed before at least one phase of siderite and possibly before the precipitation of quartz overgrowths. Mechanical compaction ceased when these overgrowths had developed. K-feldspar overgrowths are restricted to Unit A where alteration of volcanic lithics may have provided the necessary K, Si and Al. The origin of barite cement at the base of Unit A in Casino-3 is ambiguous. It could represent either a contaminant from the drilling

mud, or a late diagenetic cement related to the migration of saline brines. Localised late diagenetic ferroan calcite cements with minor ankerite and dolomite, concentrate at the base of Unit A in both Casino-2 and Casino-3, and at the base of Unit Ca in Casino-3. Distribution of the calcite cements may be related to detrital plagioclase which provided a source of calcium and CO₂ derived from the alteration of organic matter. These carbonate cements may not be laterally continuous across the field. Dissolution to produce secondary pores occurred in response to early meteoric flushing and then again later when hydrocarbons migrated.

Assessment of the factors controlling porosity and permeability in the Waarre Formation were undertaken using linear regressions of a number of parameters. Depth (representing changes in pressure, temperature and time) and rock composition (grain size, sorting, detrital and authigenic mineralogy) were tested as controls of porosity. Rock composition and porosity were used to identify what had influenced permeability. A strong correlation was found between permeability and primary intergranular porosity. Intergranular pores are preserved where early development of quartz and feldspar overgrowths (or circumgranular cement in the beach facies) provided a rigid framework to minimise mechanical compaction. Quartz overgrowths are better developed in the cleaner sands where there are less lithics in Units Ca and Cb. Therefore detrital mineralogy determined the distribution of authigenic minerals that were the prime control of porosity, and porosity controlled permeability. Late ferroan calcite cements had a detrimental but localised influence on reservoir quality. Reactive clay minerals that are confined to altered lithics and grains of glaucony do not appear to have a significant influence on permeability.

The medium grained, very poorly sorted sublitharenite studied from the Flaxman Formation at Casino-3 contains glaucony that is up to coarse sand in size indicating formation *in situ*. Deposition in this marine setting was rapid but very intermittent, possibly from turbidity currents or as slumps on a delta front. Sediment provenance was very similar to that in MSCT 1 from Waarre Unit Cb. Reservoir quality is restricted by the abundance of detrital clay and siderite cement in the sublitharenite.



2. INTRODUCTION

Santos Ltd submitted eleven core plug offcuts, nine MSCT and one core chip to PGPC from the well Casino-3 in the Otway Basin (VIC/P 44). Samples were selected from the Flaxman and Waarre Formations for detailed petrological description. The aims of the study were to ascertain the lithology, mineralogy, sediment provenance, diagenetic alteration and factors controlling reservoir quality. This information was designed to provide a basis for comparison with data previously obtained from Casino-1 and Casino-2 (Phillips, 2003).

The client supplied a sedimentological core log and interpretation from Casino-3 (Lemon, 2003), stratigraphic column (dated 13.1.04), corrected depths, log of the relevant depths in Casino-3 and a cross section of wireline logs from Casino-1, -2 & -3 to aid the petrology study. Depths were corrected by the addition of 4m to all core samples and the subtraction of 2.3m from all MSCT samples to give a correct log depth. After a preliminary description of the thin sections the services listed below (Table 1) were provided by PGPC.

TABLE 1. SUMMARY OF SAMPLES & SERVICES

Sample Type/No.	Depth (m) Log/driller	Corrected Log Depth (m)	Unit	TS description	Grain size analysis	Point count	XRD (Bulk/clay)	SEM
MSCT 6	2102.5 (L)	2100.2	Waarre A	*	*	*	*	-
MSCT 5	2093.5 (L)	2091.2		*	*	*	-	-
MSCT 4	2082.5 (L)	2080.2		*	*	*	-	-
MSCT 7	2070.5 (L)	2068.2		*	*	*	-	-
MSCT 13	2061.5 (L)	2059.2		*	*	*	*	*
Core chip	2028.5 (D)	2032.5	Waarre Ca	*	*	*	*	-
Core plug 75	2026.49 (D)	2030.49		*	*	*	*	*
Core plug 73	2025.90 (D)	2029.9		*	*	*	-	-
Core plug 62	2022.60 (D)	2026.6		*	*	*	*	-
Core plug 59	2021.76 (D)	2025.76		*	*	*	*	-
Core plug 52	2019.60 (D)	2023.6		*	*	*		*
Core plug 41	2016.39 (D)	2020.39		*	*	*	*	*
Core plug 31	2013.30 (D)	2017.3		*	*	*	-	-
Core plug 20	2009.94 (D)	2013.94		*	*	*	-	-
Core plug 12	2007.59 (D)	2011.59		*	*	*	-	-
Core plug 9	2006.70 (D)	2010.7		*	*	*	*	*
Core plug 5	2005.46 (D)	2009.46	Waarre Cb	*	*	*	-	*
MSCT 3	2005.5 (L)	2003.2		*	*	*	-	-
MSCT 2	2002.5 (L)	2000.2		*	*	*	-	-
MSCT 1	1987.0 (L)	1984.7		*	*	*	-	-
MSCT 11	1970.5 (L)	1968.2	Flaxman	*	*	*	*	-

3. METHODS

Thin section

Core plugs and MSCT were impregnated with araldite prior to thin section preparation. Blue dye was used in the araldite to facilitate description of porosity and permeability. Thin sections were prepared using standard techniques to produce a thickness of 30 microns (Adams *et al*, 1984). Those samples containing significant carbonate were half stained with alizarin red-S and potassium ferricyanide to differentiate the carbonate species (Adams *et al*, 1984). Thin sections were systematically scanned to determine lithology, composition, porosity and textural relationships. Siliciclastics have been classified according to guidelines by Folk (1974) and carbonates are classified using the nomenclature of Tucker (2001). Grain morphology (both sphericity and roundness) was estimated by comparison with charts in Pettijohn *et al* (1987), grain fabric (packing and texture) from the diagram in Tucker (2001) and sorting from diagrams by Harrell (1984). All percentages of composition given in Table 2 are counts of 500 points following the method of Stanton & Wilson (1994). The basic data for grain size analyses was collected by measuring the long axis of 100 representative grains in thin section. The graphic mean and inclusive graphic standard deviation (Folk, 1974) were then calculated.

X-ray diffraction (XRD)

To determine bulk mineralogy by XRD, samples were ground in a Siebtechnik mill and back mounted into aluminium holders. Continuous scans were run of these powder pressings from 3° to $75^{\circ} 2\theta$, at 1° /minute, using Co $K\alpha$ radiation, 50kV and 35mA, on a Philips PW1050 diffractometer. For detailed clay mineralogy a less than 5 micron size fraction was separated. This was obtained by hand crushing, addition of dispersion solution, mechanical shaking for 10 minutes and settling of the dispersed material in a water column according to Stokes' Law. The less than 5 micron fraction was pipetted off and prepared as an oriented sample on ceramic plates held under vacuum. Samples were saturated with Mg solution and treated with glycerol. Continuous scans of oriented clay samples were run from 3° to $45^{\circ} 2\theta$ at 1° /minute. Peaks were identified by comparison with JCPDS files stored in a computer program called XPLOT.

Scanning electron microscopy (SEM)

Scanning electron microscope studies were undertaken on broken segments of samples mounted with araldite on aluminium pin-type stubs. The samples were evaporatively coated with carbon (15nm) and gold/palladium (20nm) prior to viewing in a Philips XL30 FEG Scanning Electron Microscope at 20kV. The elemental composition of each mineral photographed was identified using an EDAX DX-4 energy dispersive spectrometer.

4. PETROLOGY

TABLE 3. POINT COUNT DATA

Sample No. Depth (m)	MSCT 6 2102.5 (L)	MSCT 5 2093.5 (L)	MSCT 4 2082.5 (L)	MSCT 7 2070.5 (L)	MSCT 13 2061.5 (L)
Stratigraphic Unit	A	A	A	A	A
Framework grains					
Quartz - mono	34.2	35.8	31.4	37.8	40.6
- poly	12.4	12.2	8.0	6.6	7.4
Feldspar - Kspar	3.2	5.2	6.2	6.8	6.2
- plagioclase	0.0	0.0	0.0	0.6	0.4
Lithics - sedimentary	2.2	2.8	3.2	3.2	4.0
- metamorphic	3.6	5.6	7.8	11.2	6.6
- igneous	2.4	2.0	1.2	2.8	1.2
- unknown	0.0	0.0	0.0	0.0	0.0
Mica - muscovite	0.4	0.4	0.2	0.2	0.4
- biotite	0.0	0.0	0.0	0.2	0.0
Accessory - zircon	0.0	0.0	0.0	0.2	0.2
- tourmaline	0.2	0.0	0.2	0.2	0.2
- rutile	0.0	0.0	0.0	0.0	0.2
- sphene	0.0	0.0	0.0	0.0	0.0
- others	0.0	0.0	0.0	0.2	0.0
Matrix					
Clay	0.0	0.0	0.0	2.4	0.4
Organic matter	0.6	0.0	0.4	0.6	0.2
Authigenic minerals					
Glaucony	0.0	0.0	0.0	0.4	0.0
Barite - replace	0.4	0.4	0.0	0.0	0.0
- fill pores	2.6	2.4	0.0	0.0	0.0
Fe carbonate - replace	1.6	1.4	6.0	6.0	4.4
- fill pores	0.4	0.4	3.0	4.0	4.6
Clear carbonate - replace	7.2	9.0	13.8	0.2	4.4
- fill pores	13.4	9.8	8.6	0.6	4.0
Quartz	1.2	2.4	0.4	1.0	0.4
Feldspar	0.2	0.4	0.6	0.6	0.4
Illite - replace	0.6	0.6	0.8	1.8	1.4
Kaolin - replace	3.4	1.4	2.0	2.6	2.4
- fill pores	0.8	0.8	0.4	0.4	0.2
Pyrite - replace	0.4	0.2	0.0	0.2	0.0
- fill pores	0.4	0.2	0.2	0.2	0.2
Porosity					
Intergranular	0.0	0.0	0.0	1.6	1.8
Dissolution	7.8	6.2	5.2	6.6	7.4
Fracture	0.0	0.0	0.0	0.2	0.0
Micropores	0.4	0.4	0.4	0.6	0.4
TOTAL	100.0	100.0	100.0	100.0	100.0

TABLE 3. POINT COUNT DATA (continued)

Sample No. Depth (m)	Core chip 2028.5 (D)	CP 75 2026.49 (D)	CP 73 2025.90 (D)	CP 62 2022.60 (D)	CP 59 2021.76 (D)
Stratigraphic Unit	Ca	Ca	Ca	Ca	Ca
Framework grains					
Quartz - mono	33.2	34.8	56.8	47.8	50.8
- poly	3.2	3.6	4.0	3.2	3.6
Feldspar - Kspar	3.6	1.2	3.4	1.8	4.2
- plagioclase	0.6	0.0	0.2	0.0	0.4
Lithics - sedimentary	0.6	0.8	0.6	0.4	0.8
- metamorphic	2.4	4.4	4.6	4.0	8.0
- igneous	0.4	0.0	0.0	0.0	0.0
- unknown (oxidised)	0.2	0.6	0.0	0.6	0.6
Mica - muscovite	0.6	0.8	0.6	0.4	2.4
- biotite	0.4	0.6	0.2	0.2	0.4
Accessory - zircon	0.2	0.4	0.4	1.0	0.4
- tourmaline	0.2	0.2	0.4	0.4	0.2
- rutile	0.0	0.2	0.6	0.4	0.6
- sphene	0.0	0.2	0.0	0.0	0.2
- others	0.2	0.0	0.2	0.4	0.0
Matrix					
Clay	37.2	1.6	0.6	0.0	7.2
Organic matter	5.4	0.4	0.4	0.2	1.0
Authigenic minerals					
Glaucony - glauconite	4.2	0.8	0.0	0.0	0.4
- chlorite	2.0	3.0	3.8	1.8	6.6
Barite - replace	0.0	0.0	0.0	0.0	0.0
- fill pores	0.0	0.0	0.0	0.0	0.0
Fe carbonate - replace	0.0	2.0	1.2	1.2	2.8
- fill pores	0.0	0.6	0.4	0.6	0.6
Clear carbonate - replace	1.0	20.2	2.8	12.4	0.0
- fill pores	0.0	14.8	4.2	10.4	0.0
Quartz	0.0	0.0	1.0	0.8	0.2
Feldspar	0.0	0.0	0.0	0.0	0.0
Illite - replace	0.0	1.2	0.0	0.2	0.2
Kaolin - replace	0.4	1.8	1.0	1.2	2.0
- fill pores	0.0	0.0	0.0	0.0	0.0
Pyrite - replace	2.8	1.2	0.4	0.2	1.2
- fill pores	0.0	1.0	0.4	0.4	0.0
Porosity					
Intergranular	0.0	0.0	1.8	1.2	0.8
Dissolution	0.0	3.4	9.6	8.6	4.0
Fracture	1.2	0.0	0.0	0.0	0.0
Micropores	0.0	0.2	0.4	0.2	0.4
TOTAL	100.0	100.0	100.0	100.0	100.0

TABLE 3. POINT COUNT DATA (continued)

Sample No. Depth (m)	CP 52 2019.6 (D)	CP 41 2016.39 (D)	CP 31 2013.3 (D)	CP 20 2009.94 (D)	CP 12 2007.59 (D)
Stratigraphic Unit	Ca	Ca	Ca	Ca	Ca
Framework grains					
Quartz - mono	56.2	37.0	63.8	59.2	67.0
- poly	4.8	2.0	4.8	2.6	3.2
Feldspar - Kspar	4.6	1.6	3.0	3.6	3.4
- plagioclase	0.0	0.4	0.0	0.0	0.0
Lithics - sedimentary	1.4	0.0	0.8	0.8	0.6
- metamorphic	3.6	2.4	1.4	3.8	1.6
- igneous	0.2	0.0	0.4	0.0	0.2
- unknown (oxidised)	0.2	1.0	0.0	0.4	0.0
Mica - muscovite	0.8	1.6	0.2	0.8	0.2
- biotite	0.2	0.4	0.2	0.0	0.0
Accessory - zircon	0.4	0.6	0.2	0.4	0.2
- tourmaline	0.4	0.2	0.4	0.6	0.4
- rutile	0.6	0.6	0.2	0.2	0.2
- sphene	0.2	0.0	0.0	0.0	0.0
- others	0.4	0.2	0.0	0.0	0.2
Matrix					
Clay	0.6	0.8	0.0	0.4	0.0
Organic matter	0.6	0.6	0.2	0.2	0.0
Authigenic minerals					
Glaucony - glauconite	1.0	0.8	0.0	0.8	0.2
- chlorite	1.4	4.2	0.0	0.4	0.0
Barite - replace	0.0	0.0	0.0	0.0	0.0
- fill pores	0.0	0.0	0.0	0.0	0.0
Fe carbonate - replace	0.8	19.0	0.2	0.4	0.2
- fill pores	0.8	14.2	0.0	0.0	0.0
Clear carbonate - replace	0.0	0.0	0.2	0.2	0.0
- fill pores	0.0	0.0	0.0	0.0	0.0
Quartz	2.4	0.0	3.2	3.0	4.0
Feldspar	0.0	0.0	0.0	0.0	0.0
Illite - replace	0.4	0.0	0.0	0.0	0.2
Kaolin - replace	3.0	0.4	1.2	2.2	1.4
- fill pores	1.0	0.0	0.4	0.4	0.4
Pyrite - replace	0.4	3.0	0.2	1.4	0.0
- fill pores	0.4	1.0	0.4	2.4	0.4
Porosity					
Intergranular	2.0	0.4	15.8	11.8	12.4
Dissolution	10.8	7.4	2.6	3.6	3.4
Fracture	0.0	0.0	0.0	0.0	0.0
Micropores	0.4	0.2	0.2	0.4	0.2
TOTAL	100.0	100.0	100.0	100.0	100.0

4.1 Casino-3, MSCT 6, depth 2102.5m (Logger) Waarre A

<u>Rock classification:</u>	Carbonate Cemented Sublitharenite
<u>Texture:</u>	
Sedimentary structures:	very weakly defined bedding outlined by changes in grain size & associated concentration of lithics
Average grain size:	coarse sand (0.63mm)
Range in grain size:	fine sand to granules
Roundness / sphericity:	subangular/ low sphericity
Sorting:	moderately well (0.61 ϕ)
Texture:	grain supported
Packing / grain contacts:	moderately close packing/ dominantly tangential grain contacts
Pore types:	secondary porosity characterised by grain size dissolution pores, intragranular pores, honeycomb pores and micropores associated with kaolin
<u>Composition:</u>	
Framework grains:	monocrystalline quartz, polycrystalline quartz up to pebble size with straight crystal boundaries, fresh, fractured, sericitised & corroded K-feldspars with remnants of tartan twinning & others that lack twinning, lithics of illitic shale, micaceous schist, quartzite, chalcedony, dusty, oxidised & clear chert & ?devitrified volcanic glass, deformed & splayed muscovite flakes up to 0.6mm length, accessory angular very fine sand size tourmaline
Matrix:	one blocky fragment, very coarse sand in size of opaque material is probably organic matter
Authigenic minerals:	prismatic & rare rhombohedral quartz overgrowths prior to carbonate cement, pervasive pore filling & grain replacing poikilotopic, twinned clear carbonate spar, minor dusty grain replacing & pore filling scalenohedral spar, grain replacing & pore filling subhedral kaolin with highly variable diameters from 10-50 microns, minor blocky pyrite partially replacing lithics & rare clusters of pyrite framboids on grain margins, patchy cement of colourless, blocky ?barite appears to postdate quartz, replace kaolin, and ?predate carbonate, either zoning of K-feldspars or weakly developed feldspar overgrowths that lack twinning

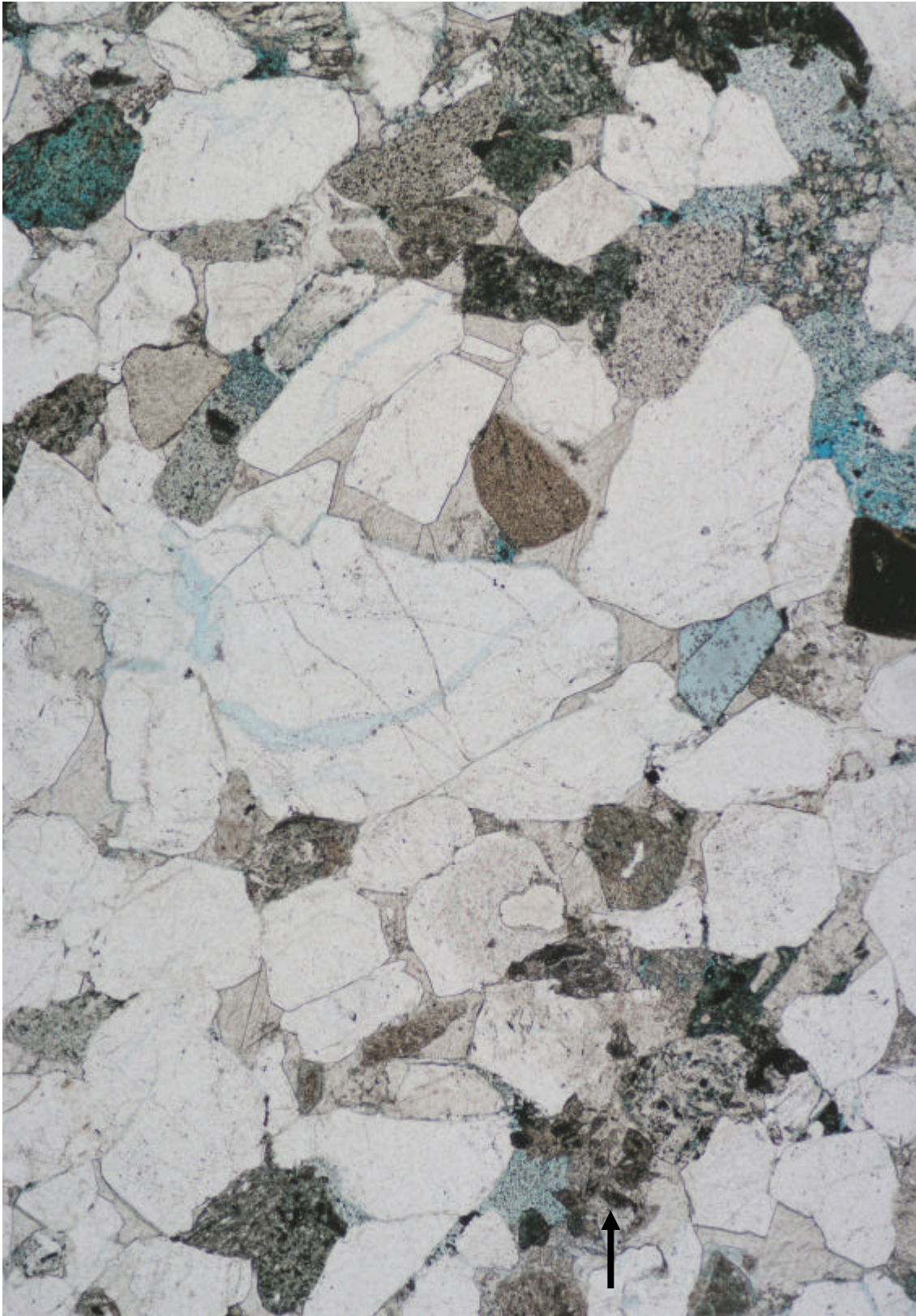


Figure 1 General field of view illustrating the irregular distribution of secondary pores (blue). Intergranular pores have been filled with blocky carbonate spar & there is minor scalenohedral spar (arrow) apparent. Note the abundance of lithics (brown). Casino-3, MSCT 6, depth 2102.5m (Logger). Plane light. Horizontal field of view 3.25mm.

4.2 Casino-3, MSCT 5, depth 2093.5m (Logger) Waarre A

<u>Rock classification:</u>	Carbonate Cemented Sublitharenite
<u>Texture:</u>	
Sedimentary structures:	weak grain alignment indicates the orientation of bedding
Average grain size:	coarse sand (0.57mm)
Range in grain size:	very fine to very coarse sand
Roundness / sphericity:	subangular with low to moderate sphericity
Sorting:	moderately well (0.67 ϕ)
Texture:	grain supported
Packing / grain contacts:	moderately open / point & tangential grain contacts
Pore types:	dominantly secondary porosity comprised of grain size pores, intragranular & honeycomb pores, with rare micropores associated with kaolin, fracturing is considered an artifact of sampling
<u>Composition:</u>	
Framework grains:	monocrystalline quartz rarely has highly strained extinction, polycrystalline quartz with straight crystal boundaries, corroded & sericitised K-feldspars that lack twinning, lithics of dusty & clear chert, chalcedony, metasediments (including shale, quartzite & schist), devitrified glass, ?granite & mudstone, muscovite flakes up to 0.6mm long are bent & partially replaced by carbonate,
Authigenic minerals:	pervasive pore filling & grain replacing clear poikilotopic twinned carbonate spar, minor colourless pore filling ?barite appears to be replaced by carbonate & has replaced kaolin, a minor phase of dissolution could postdate the barite, rare dusty single scalenohedra crystals occur within the clear spar, minor euhedral quartz overgrowths prior to carbonate spar & ?barite, grain replacing & pore filling kaolin booklets up to 20 microns in diameter, minute blocky pyrite has replaced a grain & rare pyrite framboids occur on grain margins, rare feldspar overgrowths lack twinning

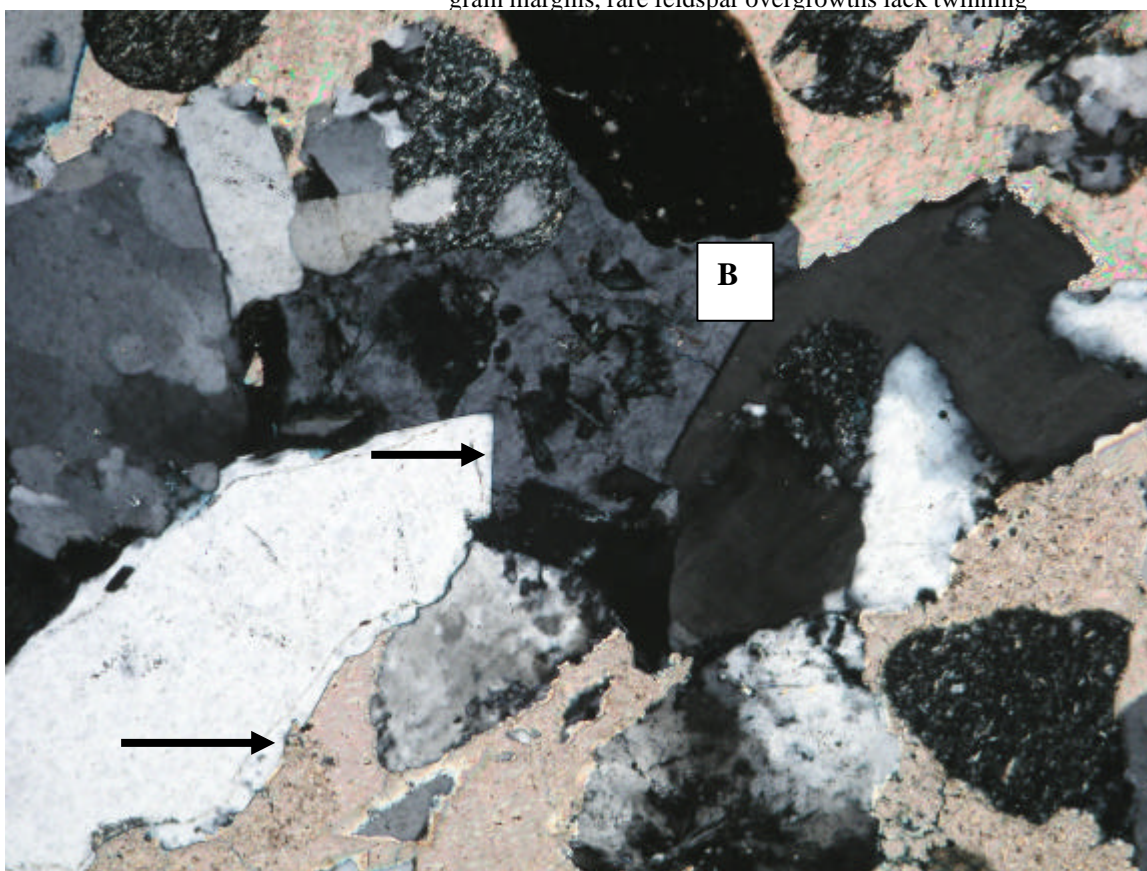


Figure 2a
 Quartz overgrowths (arrows) precipitated prior to the pore filling clear carbonate spar (pinkish) and the partially dissolved ?barite (B). Casino-3, MSCT 5, depth 2093.5m (Logger). Crossed nicols. Horizontal field of view 1.30mm.

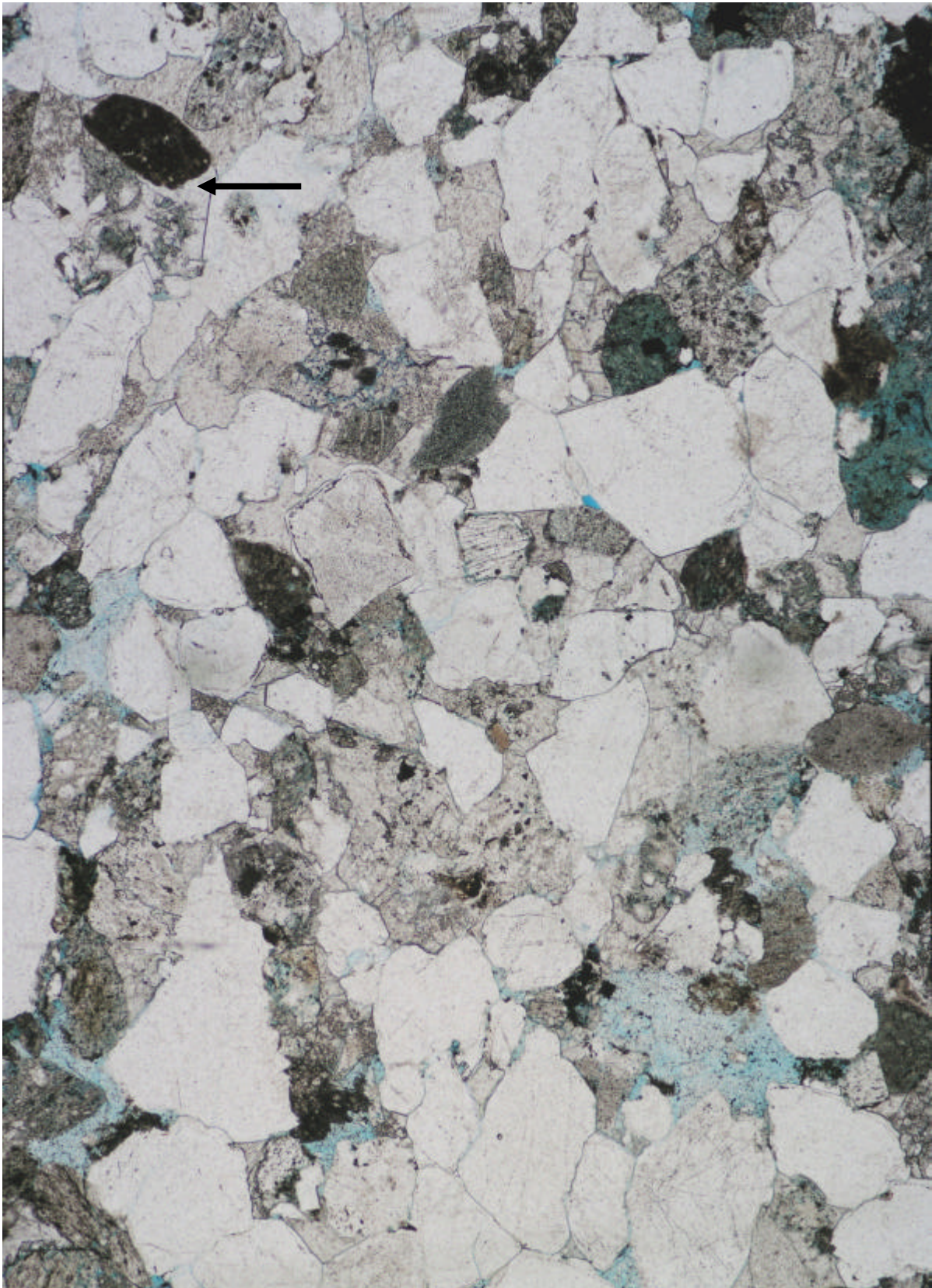


Figure 2b
General view illustrating the pervasive nature of the carbonate cement and hence lack of porosity. The location of the ?barite in Figure 5a is shown by the arrow. Casino-3, MSCT 5, depth 2093.5m (Logger). Plane light. Horizontal field of view 3.25mm.

4.3 Casino-3, MSCT 4, depth 2082.5m (Logger) Waarre A

<u>Rock classification:</u>	Carbonate Cemented Feldspathic Litharenite
<u>Texture:</u>	
Sedimentary structures:	weak grain alignment indicates the orientation of bedding which has been disrupted by a burrow approximately 2mm wide & filled with very poorly sorted sediment
Average grain size:	medium sand (0.32mm)
Range in grain size:	coarse silt to coarse sand
Roundness / sphericity:	angular to subangular with low sphericity
Sorting:	moderately sorted (0.80 ϕ)
Texture:	grain supported
Packing / grain contacts:	moderately close packing / tangential & minor concavo-convex contacts
Pore types:	secondary porosity of grain size, intragranular & honeycomb pores, micropores associated with kaolin
<u>Composition:</u>	
Framework grains:	monocrystalline quartz, polycrystalline quartz with either straight or sutured crystal boundaries, highly corroded & sericitised feldspars either lack twinning or have tartan twinning, remnants of feldspars with granophyric intergrowths, lithics of shale, deformed micaceous schist, quartzite, one grain of pyrophyllite (metamorphic), mudstone, volcanics, chert & chalcedony, bent & splayed muscovite, accessory silt size tourmaline
Matrix:	minute crenulated stringers of organic matter
Authigenic minerals:	prismatic quartz overgrowths are embayed by carbonate, poikilotopic, twinned carbonate spar fills pores & partially to completely replaces grains, the anhedral nature of much of the carbonate suggests a phase of dissolution, dusty anhedral micritic carbonate has partially replaced grains & stringers of organic matter & is interspersed with the clean spar, the micrite is more abundant in the burrow, isolated grains are replaced by subhedral kaolin booklets up to 30 microns in diameter, rare corroded feldspars with tartan twinning have overgrowths that lack twinning, rare pyrite on grain margins

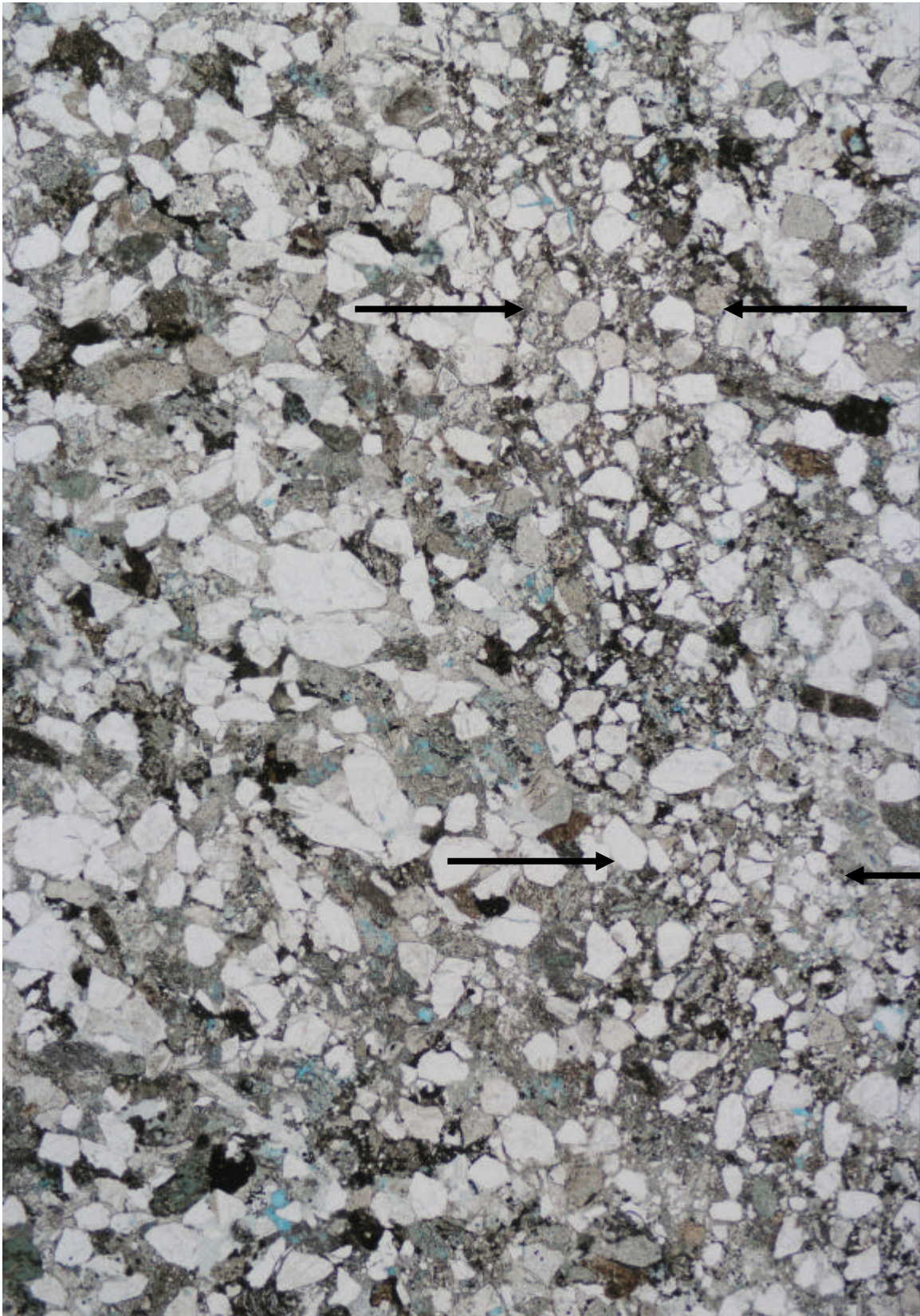


Figure 3
A burrow (arrows) filled with finer grained sediment has disrupted bedding in this sandstone. Porosity is restricted to isolated secondary pores (blue) due to the pervasive nature of carbonate cement (small arrow). Casino-3, MSCT 4, depth 2082.5m. Plane light. Horizontal field of view 6.5mm.

4.4 Casino-3, MSCT 7, depth 2070.5m (Logger) Waarre A

Rock classification:

Feldspathic Litharenite

Texture:

Sedimentary structures:	two crenulated thin (less than 0.6mm) clay rich laminae parallel bedding
Average grain size:	medium sand (0.30mm)
Range in grain size:	clay to coarse sand
Roundness / sphericity:	angular to subangular with low sphericity
Sorting:	poor (1.15 ϕ)
Texture:	grain supported
Packing / grain contacts:	moderately close / dominantly tangential grain contacts, concavo-convex contacts where ductile lithics have been deformed
Pore types:	grain size dissolution pores dominant, minor honeycomb pores, micropores, grain fracturing of feldspars & rare intragranular & primary intergranular pores

Composition:

Framework grains:	monocrystalline quartz, polycrystalline quartz with either straight or sutured crystal boundaries, K-feldspars which either lack twinning or have tartan & simple twins are corroded & sericitised, granophyric texture where grains of K-feldspar are intergrown with quartz, plagioclase with albite twinning is angular & fresh, lithics of shale, quartzite, one grain of pyrophyllite (metamorphic), ?granite, corroded ?rhyolite with spherulitic texture, ?devitrified glass, chert, chalcedony, siltstone & mudstone, bent & splayed biotite, fresh bent muscovite up to 0.75mm in length, accessory very fine to fine sand size zircon, tourmaline & ?monazite
Matrix:	dark brown anhedral clay, stringers of organic matter & minor silt to very fine sand size grains concentrate in the laminae, rare blocky opaque organic matter in the intervening beds
Authigenic minerals:	isolated grains have been replaced & pores filled by kaolin booklets which are 10-20 microns in diameter, rare quartz overgrowths outlined by dust rims on monocrystalline quartz, dusty anhedral to subhedral scalenohedral carbonate spar has partially filled pores & replaced grains including micas & shale lithics throughout the section, rare pore filling & grain replacing clear carbonate spar, bright green fine sand size grain with a wormy texture typical of glaucony (glauconite), other green grains have slightly more fibrous habit typical of chlorite, irregular feldspar overgrowths lack twinning, rare pyrite framboids replacing grains & concentrating in the detrital clay

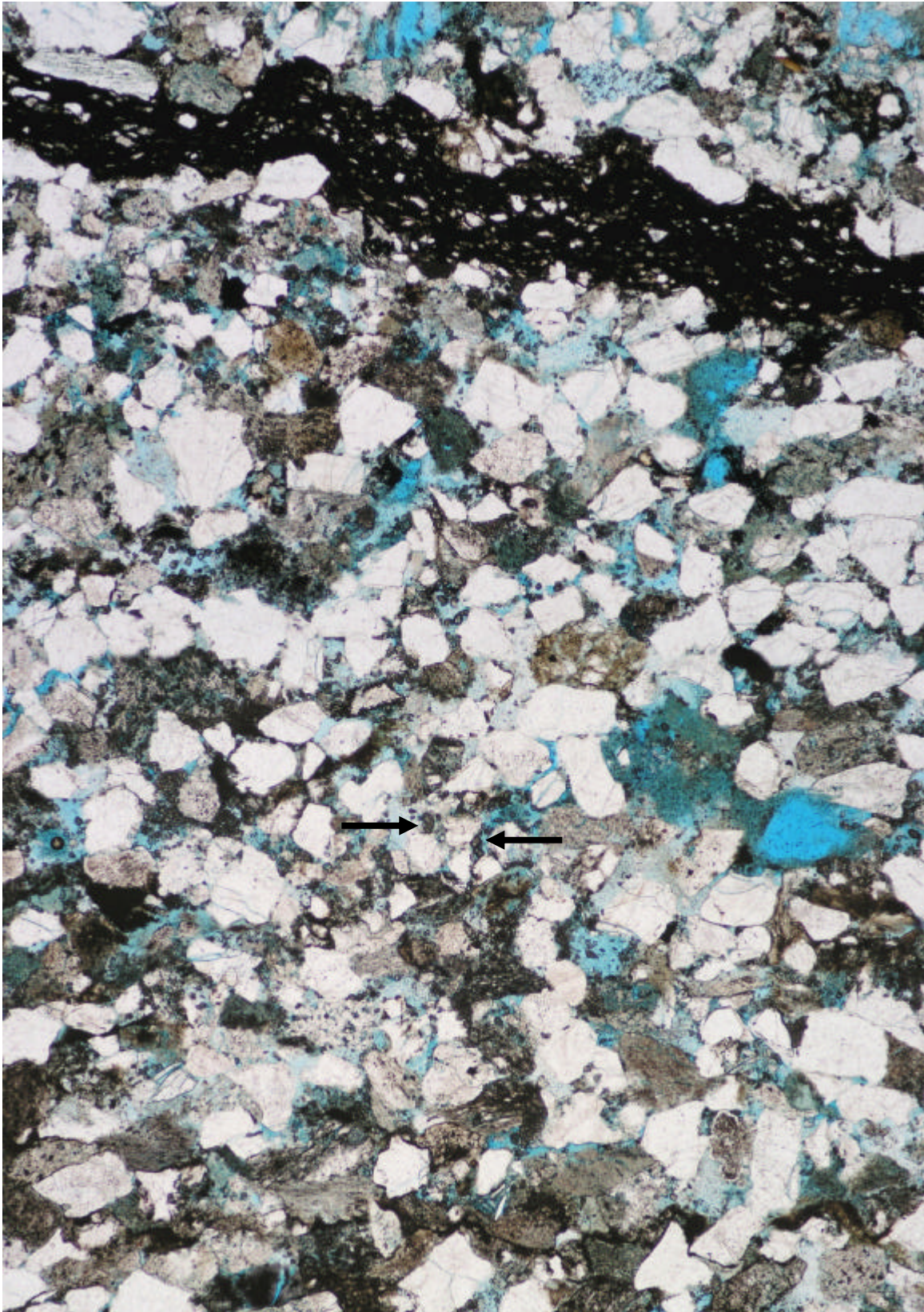
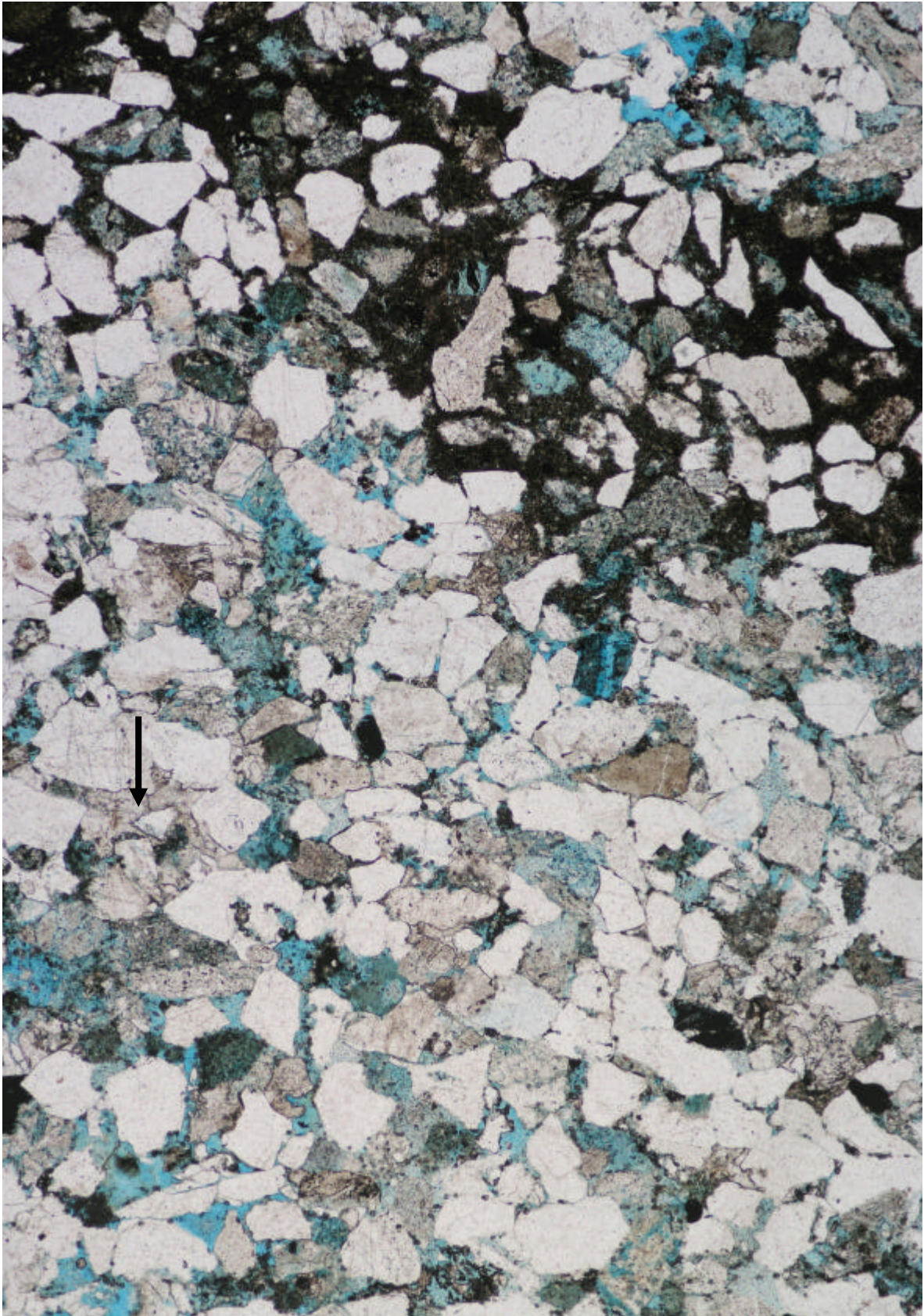


Figure 4 Clay rich laminae (dark brown) would limit vertical permeability in this sandstone. Note the grain size dissolution pores (blue) and minute crystals of dusty carbonate spar (arrows). Lithics & altered feldspars are commonly brownish in colour at this magnification. Casino-3, MSCT 7, depth 2070.5m (Logger). Plane light. Horizontal field of view 3.25mm.

4.5 Casino-3, MSCT 13, depth 2061.5m (Logger) Waarre A

<u>Rock classification:</u>	Feldspathic Litharenite
<u>Texture:</u>	
Sedimentary structures:	grain alignment & changes in grain size indicate the orientation of bedding, contact between beds is planar & sharp, incipient ?siderite nodule development approximately 1.5cm diameter cross cuts bedding
Average grain size:	medium sand (0.31mm)
Range in grain size:	very fine to coarse sand
Roundness / sphericity:	angular to subangular with low sphericity
Sorting:	moderately well (0.56 ϕ)
Texture:	grain supported
Packing / grain contacts:	moderately close / point & tangential, concavo-convex where lithics deformed
Pore types:	primary intergranular pores, secondary grain size dissolution pores, honeycomb pores, intragranular pores & micropores
<u>Composition:</u>	
Framework grains:	monocrystalline quartz, polycrystalline quartz with dominantly straight crystal boundaries but rare highly sutured examples exist, corroded & sericitised K-feldspars, relatively fresh plagioclase with albite twinning, lithics of chert, chalcedony, shale, micaceous schist, quartzite, mudstone, siltstone, devitrified glass & ?rhyolite, splayed & straight flakes of muscovite up to 0.35mm length, accessory medium sand size tourmaline & fine sand size zircon & ?rutile
Matrix:	dark brown anhedral clay concentrates in one section of the nodule rim, rare stringers of organic matter
Authigenic minerals:	euhedral terminations indicate the presence of quartz overgrowths, patchy pore filling & grain replacing cement of clear carbonate spar, rare pyrite framboids on grain margins, micritic ?siderite concentrates as a distinctive rim of variable thickness on the incipient nodule, there appears to be very minor grain displacement in the rim but not inside the nodule where grain alignment conforms to bedding, single crystals of dusty anhedral to subhedral scalenohedral spar are scattered throughout the section & locally cluster to form a pore filling cement, clear spar appears to postdate the dusty spar, isolated grains have been replaced by kaolin booklets up to 50 microns diameter & rarely does kaolin fill pores, discontinuous feldspar overgrowths that lack twinning on rare grains, authigenic anatase rimming a grain replaced by carbonate

**Figure 5**

Framework grains appear to have a floating texture within the dark rim of micritic siderite (opaque at this magnification) on the edge of the incipient nodule. Patches of clear spar (arrow) cement the surrounding sediment. Casino-3, MSCT 13, depth 2061.5m (Logger). Plane light. Horizontal field of view 3.25mm.

4.6 Casino-3, Core chip, depth 2028.5m (Driller) Waarre Ca

<u>Rock classification:</u>	Greywacke
<u>Texture:</u>	
Sedimentary structures:	laminae with variable concentrations of clay, organic matter & sand, disrupted due to bioturbation
Average grain size:	very fine sand (0.09mm)
Range in grain size:	clay to coarse sand
Roundness / sphericity:	angular to subangular with low sphericity
Sorting:	very poor (2.82 ϕ)
Texture:	matrix supported
Packing / grain contacts:	close packing / minor point & tangential contacts in the sandy laminae, crenulated stringers of organic matter & deformed ductile grains
Pore types:	minor open fractures cross cut bedding & grains
<u>Composition:</u>	
Framework grains:	monocrystalline quartz with examples that have embayed margins typical of a volcanic origin, polycrystalline quartz with straight crystal boundaries, fresh plagioclase & K-feldspar with either no twinning or tartan twinning & up to very coarse sand in size, lithics of chert (fresh & oxidised), chalcedony, quartzite, micaceous schist, ?granite & pyrophyllite, flakes of bent muscovite & biotite up to 0.15mm in length, accessory silt to very fine sand size zircon, opaques & silt to medium sand size tourmaline
Matrix:	anhedral dark brown clay with illitic laths, stringers of opaque organic matter (?vitrinite) & lesser orange coloured (?liptinite), silt size quartz
Authigenic minerals:	up to medium sand size bright green rounded grains with wormy texture typical of glaucony (?glauconite) are deformed due to compaction, in many instances it appears that micas have been replaced by glaucony (?chlorite), clusters of pyrite framboids in the clay rich laminae, blocky pyrite has replaced organic matter & glaucony & is scattered throughout the matrix, anhedral clear spar has replaced matrix & grains, mica replaced by kaolin has platelets 100 microns in diameter & other grains replaced by kaolin booklets which are up to 25 microns diameter



Figure 6
The highest concentration of glaucopy (greenish - arrow) occurs in a sandy bed which may suggest minor reworking. Note the open fracture (blue) and undulating contact between sandy and clay rich (brown) laminae. Opaques are either pyrite or organic matter. Casino-3, Core chip, depth 2028.5m (Driller). Plane light. Horizontal field of view 3.25mm.

4.7 Casino-3, Core plug 75, depth 2026.49m (Driller) Waarre Ca

<u>Rock classification:</u>	Carbonate Cemented Sublitharenite
<u>Texture:</u>	
Sedimentary structures:	thin planar laminae less than 2mm wide outlined by variations in the concentration of clay stringers, pyrite nodules
Average grain size:	very fine sand (0.08mm)
Range in grain size:	clay to fine sand
Roundness / sphericity:	subangular to subrounded with low sphericity
Sorting:	poor (1.01 ϕ)
Texture:	grain supported
Packing / grain contacts:	moderately close packing / tangential & suturing where clay stringers present
Pore types:	dominantly secondary dissolution pores which are grain sized, honeycomb & intragranular, rare micropores associated with kaolin
<u>Composition:</u>	
Framework grains:	monocrystalline quartz, polycrystalline quartz with straight crystal boundaries, fresh, corroded & sericitised K-feldspars rarely with tartan twinning, lithics of quartzite, shale, micaceous schist, mudstone, chalcedony & chert, isolated oxidised grains of unknown origin, straight & splayed muscovite & biotite flakes up to 0.2mm in length, accessory very fine sand size tourmaline, sphene, rutile & silt size zircon stringers & patches of anhedral pale to dark brown clay concentrated in selected laminae, blocky opaque organic matter
Matrix:	
Authigenic minerals:	rounded grains & ?micas replaced by glaucony (?chlorite), rare oxidised grains of glaucony, pervasive pore filling & grain replacing clear poikilotopic carbonate spar, minor Fe rich anhedral spar possibly replacing clay stringers or micas, grain replacing kaolin booklets up to 25 microns in diameter & much larger platelets where micas have been replaced, blocky pyrite forms a massive cement in the rounded nodules which are up to 0.6mm diameter



Figure 7 General view illustrating the diffuse contact between laminae with clay stringers (upper portion of photo) and those that lack stringers. Note the secondary nature of pores (pale blue) and the edge of a pyrite nodule (opaque - Lower LHS). Casino-3, Core plug 75, depth 2026.49m (Driller). Plane light. Horizontal field of view 1.30mm.

4.8 Casino-3, Core plug 73, depth 2025.90m (Driller) Waarre Ca

Rock classification:

Sublitharenite

Texture:

Sedimentary structures:	weakly defined thin laminae are cross cut by a burrow which is partially filled with clay
Average grain size:	very fine sand (0.10mm)
Range in grain size:	clay to fine sand
Roundness / sphericity:	subangular to subrounded with low sphericity
Sorting:	moderately well (0.69 ϕ)
Texture:	grain supported
Packing / grain contacts:	close packing / tangential & concavo-convex contacts
Pore types:	grain size dissolution pores, honeycomb pores, micropores associated with kaolin, rare primary intergranular pores

Composition:

Framework grains:	monocrystalline quartz, polycrystalline quartz with straight crystal boundaries, corroded & fresh K-feldspars, fresh plagioclase with albite twinning, lithics of shale, chert, micaceous schist & quartzite, fresh, straight muscovite & altered biotite flakes up to 0.18mm, accessory silt size tourmaline, zircon, rutile & opaques
Matrix:	anhedral dark brown clay in laminae & the burrow, minor opaque organic matter
Authigenic minerals:	patchy pore filling & grain replacing clear & Fe rich anhedral carbonate spar, the latter is most abundant replacing detrital clays, dusty green deformed grains with a wormy texture typical of glaucony, straight grain contacts & euhedral terminations indicate the presence of quartz overgrowths, micas replaced by kaolin have booklets up to 60 microns in diameter, rare patches of blocky pyrite

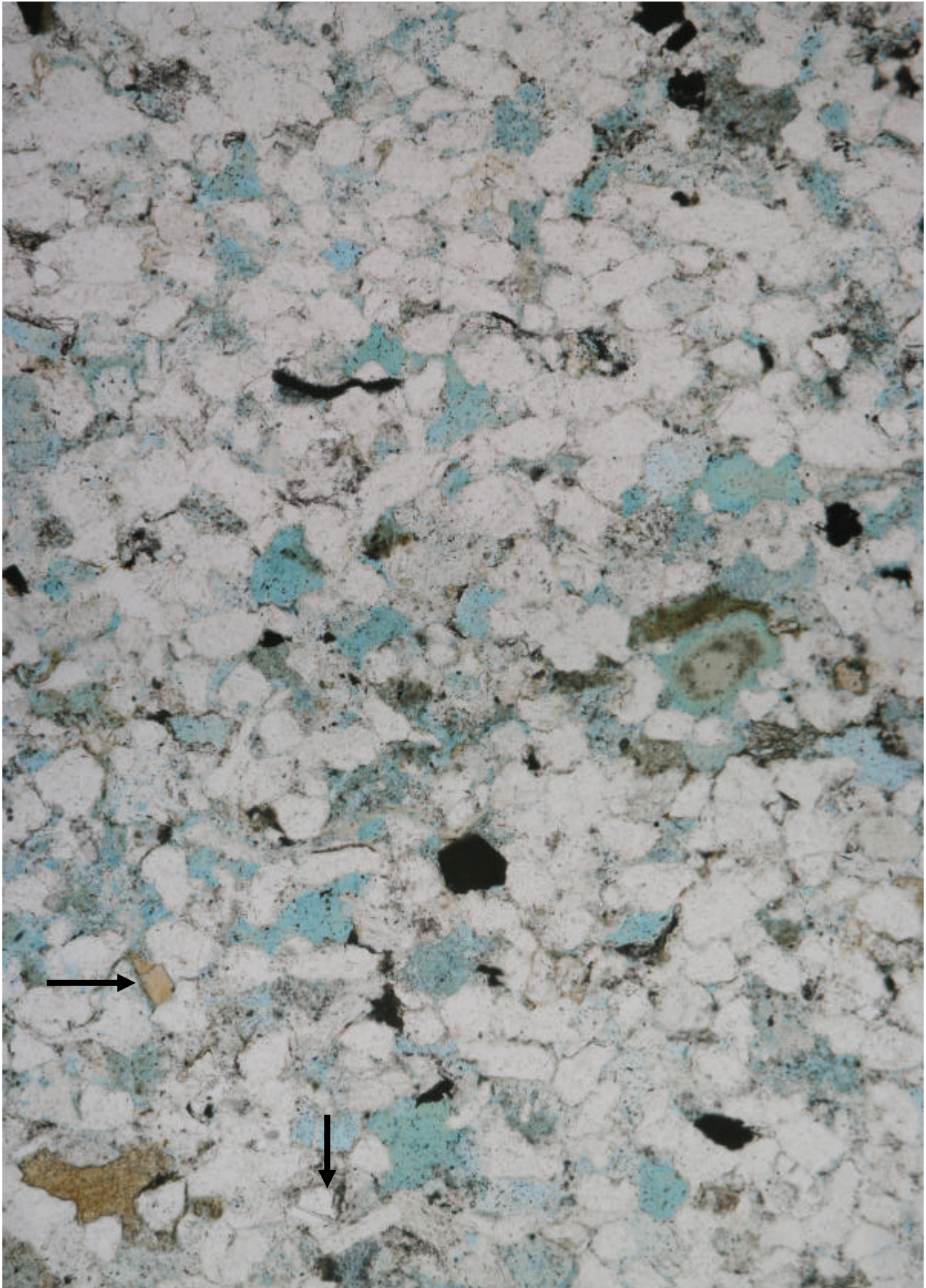


Figure 8
General field of view illustrating the fine grained nature of this sandstone & the dominance of secondary porosity (blue). Fe rich anhedral spar (orange) & various accessory minerals (arrows) are apparent. Much of the dusty material in this section is probably grinding paste from thin section preparation. Casino-3, Core plug 73, depth 2025.90m (Drillers). Plane light. Horizontal field of view 1.30mm.

4.9 Casino-3, Core plug 62, depth 2022.60m (Driller) Waarre Ca

<u>Rock classification:</u>	Carbonate Cemented Sublitharenite
<u>Texture:</u>	
Sedimentary structures:	possible thin laminae highlighted by variations in the degree of cementation
Average grain size:	very fine sand (0.10mm)
Range in grain size:	coarse silt to medium sand
Roundness / sphericity:	subangular to subrounded with low to moderate sphericity
Sorting:	well sorted (0.41 ϕ)
Texture:	grain supported
Packing / grain contacts:	moderately open / point & tangential contacts
Pore types:	secondary dissolution pores are dominantly grain size with minor intragranular pores & micropores
<u>Composition:</u>	
Framework grains:	monocrystalline quartz, polycrystalline quartz with either sutured or straight crystal boundaries, partially corroded & sericitised K-feldspars, lithics of chert, quartzite & micaceous schist, rare oxidised grains of unknown origin, straight flakes of fresh muscovite & altered biotite up to 0.35mm in length, silt to very fine sand size zircon, tourmaline, opaques & rutile
Matrix:	rare blocky opaque organic matter
Authigenic minerals:	deformed grains of green glaucony have a slightly fibrous texture, straight grain contacts & rare triple point junctions indicate the presence of quartz overgrowths prior to carbonate, pore filling twinned poikilotopic ferroan calcite spar appears to postdate an earlier phase of grain replacing calcite, minor pore filling & grain replacing spar did not respond to staining & therefore could be either ankerite or siderite, pyrite framboids on grain margins & replacing grains of glaucony, isolated patches of blocky pyrite cement, kaolin booklets up to 15 microns in diameter have replaced grains including micas

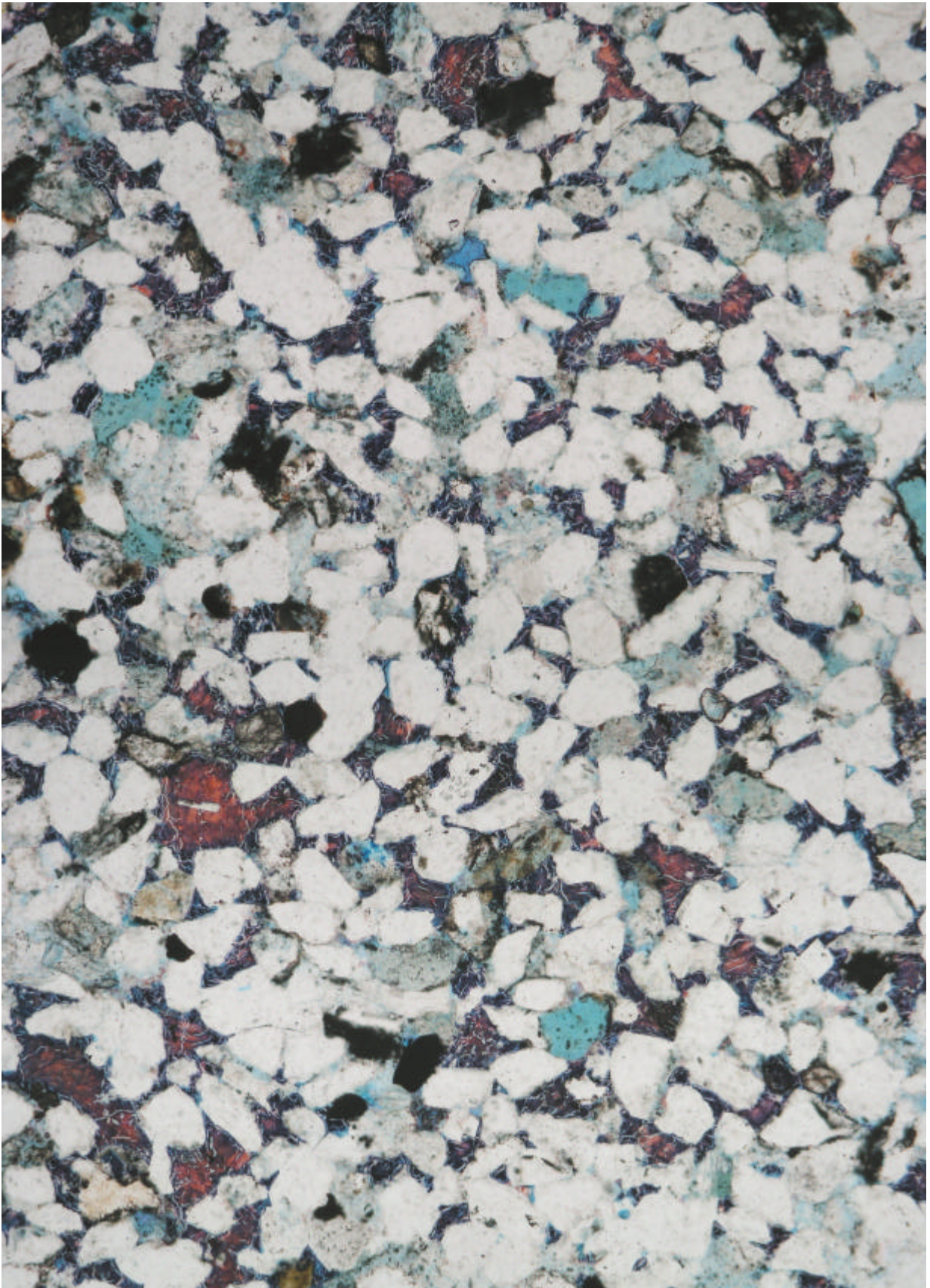


Figure 9

Pore filling ferroan calcite spar (very dark blue) postdates the grain replacing calcite (red) spar. Isolated secondary grain size pores (pale blue) are apparent. Casino-3, Core plug 62, depth 2022.60m (Driller). Plane light. Stained section. Horizontal field of view 1.30mm.

4.10 Casino-3, Core plug 59, depth 2021.76m (Driller) Waarre Ca

<u>Rock classification:</u>	Sublitharenite
<u>Texture:</u>	
Sedimentary structures:	thin laminae of variable thickness (~1-3mm) enriched in clay & mica alternate with cleaner laminae, contacts are planar & sharp
Average grain size:	very fine sand (0.09mm)
Range in grain size:	clay to medium sand
Roundness / sphericity:	subangular with low sphericity
Sorting:	poor (1.48 ϕ)
Texture:	grain supported
Packing / grain contacts:	close packing / tangential, concavo-convex & sutured contacts
Pore types:	secondary grain size dissolution pores & honeycomb pores, with rare intergranular pores restricted to the cleaner laminae & micropores associated with authigenic clays
<u>Composition:</u>	
Framework grains:	monocrystalline quartz, polycrystalline quartz with straight & sutured crystal boundaries, fresh, sericitised & corroded K-feldspars with no twinning or tartan twinning, rare fresh plagioclase, lithics of micaceous schist, quartzite, chert & chalcedony, rare oxidised grains of unknown origin, straight & bent muscovite & biotite flakes up to 0.35mm in length, accessory silt to very fine sand size rutile, zircon, sphene & tourmaline
Matrix:	anhedral dark brown clay forms thin discontinuous crenulated stringers in the clay rich laminae, minor associated opaque organic matter
Authigenic minerals:	micas within the clay rich laminae have been replaced by chlorite, rare more rounded green grains are composed of glaucony with a wormy texture, triple point junctions in the clean laminae indicate quartz overgrowths, framboidal & blocky pyrite concentrate in the clay rich laminae, patchy pore filling & grain replacing anhedral Fe rich spar, minor development of anhedral carbonate nodules up to 0.3mm diameter, large kaolin booklets where micas have been replaced



Figure 10

Sharp contacts between clay rich and clean laminae are apparent in this field of view. Porosity (pale blue) is better preserved in the clean laminae. Note the Fe rich carbonate (orange) & glaucony (green) in the clay laminae. A zircon with hydrocarbon envelope (arrow) is also evident. Casino-3, Core plug 59, depth 2021.76m (Driller). Plane light. Horizontal field of view 1.30mm.

4.11 Casino-3, Core plug 52, depth 2019.60m (Driller) Waarre Ca

<u>Rock classification:</u>	Sublitharenite
<u>Texture:</u>	
Sedimentary structures:	discontinuous crenulated clay rich laminae, disruption of grain alignment could be due to bioturbation
Average grain size:	fine sand (0.14mm)
Range in grain size:	clay to coarse sand
Roundness / sphericity:	subangular with low sphericity
Sorting:	moderately (0.75 ϕ)
Texture:	grain supported
Packing / grain contacts:	moderately open / point & tangential grain contacts
Pore types:	primary intergranular pores, secondary dissolution pores are grain size, intragranular & honeycomb, micropores
<u>Composition:</u>	
Framework grains:	monocrystalline quartz, polycrystalline quartz with either straight or sutured crystal boundaries, fresh, corroded & sericitised K-feldspars lack twinning, or have tartan & simple twinning, rare remnants of granophyric texture, lithics of chert (fresh & oxidised), chalcedony, quartzite & micaceous schist, grains replaced by hematite in the clay laminae, straight & splayed altered muscovite & biotite flakes up to 0.15mm, accessory very fine sand size zircon, opaques, sphene, rutile & tourmaline
Matrix:	dark brown anhedral clay forms crenulated stringers around grains in the discontinuous laminae, blocky opaque organic matter with cellular structure (?inertinite) in the cleaner sand
Authigenic minerals:	grain replacing & pore filling anhedral Fe rich carbonate spar, euhedral terminations & straight grain contacts indicate the presence of quartz overgrowths, grain replacing & pore filling kaolin booklets up to 25 microns diameter, traces of illite associated with the kaolin, deformed grains replaced by chlorite & other green grains with a wormy texture typical of glaucony, blocky & framboidal pyrite on grain margins & partially replacing grains & clay

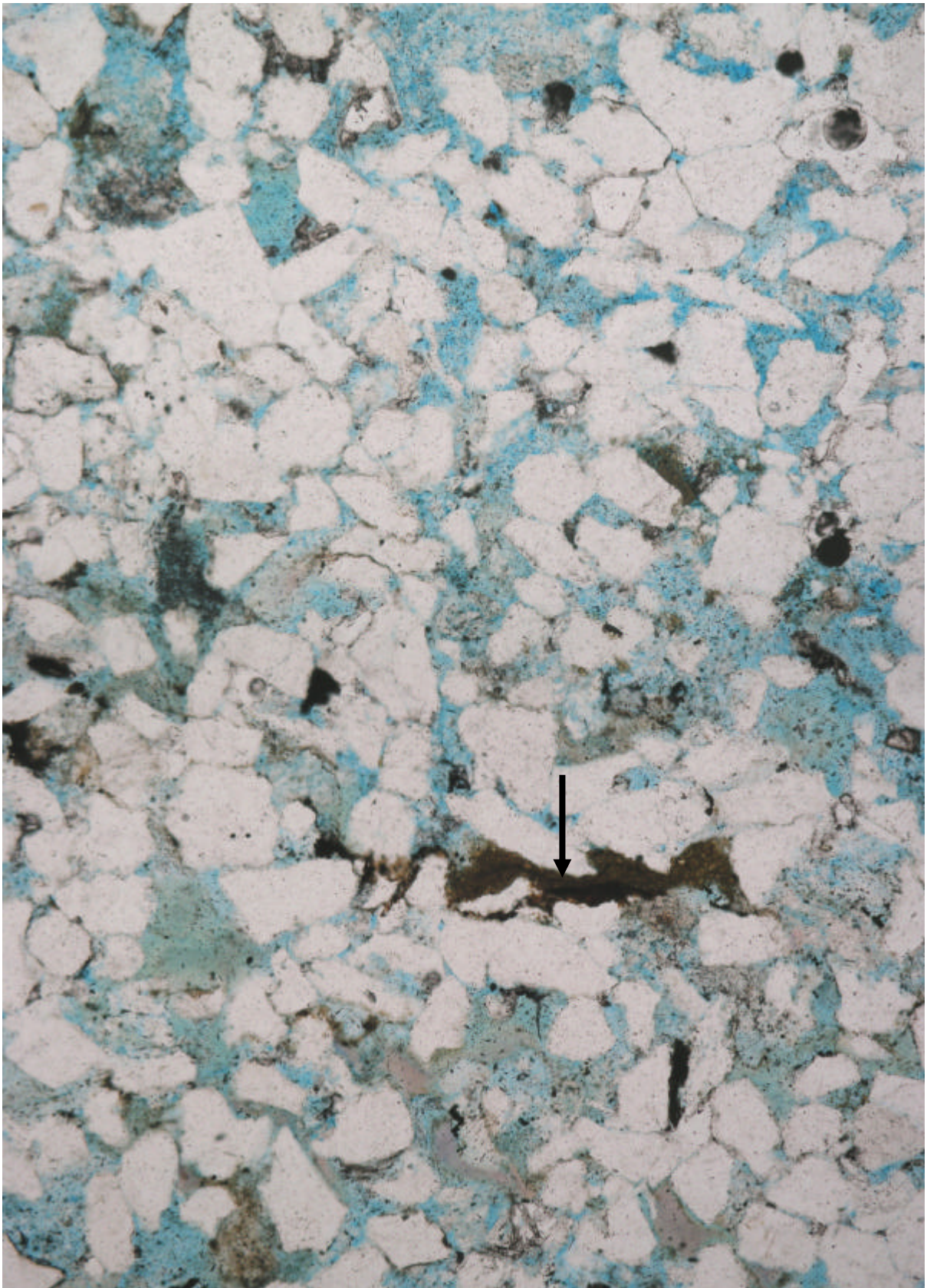


Figure 11 General field of view illustrating the moderately open packing in this sandstone. Porosity (blue) is a combination of primary intergranular pores, secondary pores & micropores. Note the Fe rich carbonate (arrow) that has probably replaced a clay stringer. Casino-3, Core plug 52, depth 2019.60m (Driller). Plane light. Horizontal field of view 1.30mm.

4.12 Casino-3, Core plug 41, depth 2016.39m (Driller) Waarre Ca

<u>Rock classification:</u>	Carbonate Cemented Sublitharenite
<u>Texture:</u>	
Sedimentary structures:	thin planar laminae between 1 and 3 mm thick are cross cut by a carbonate cemented structure which could be a burrow
Average grain size:	very fine sand (0.07mm)
Range in grain size:	clay to fine sand
Roundness / sphericity:	angular to subangular with low to moderate sphericity
Sorting:	moderately well (0.70 ϕ)
Texture:	grain supported
Packing / grain contacts:	very open / point & tangential contacts
Pore types:	dominantly secondary grain size pores with rare honeycomb & intragranular pores, isolated primary intergranular pores, micropores
<u>Composition:</u>	
Framework grains:	monocrystalline quartz, polycrystalline quartz with straight crystal boundaries, corroded & sericitised K-feldspars lack twinning & fresh feldspars have tartan twinning, fresh plagioclase with albite twinning, lithics of micaceous schist & quartzite, rare oxidised grains of unknown origin, straight flakes of muscovite & biotite up to 0.2mm length, accessory silt size zircon, tourmaline, opaques & rutile
Matrix:	pale brown clay rich stringers & opaque organic matter
Authigenic minerals:	pervasive anhedral to subhedral Fe rich carbonate spar has filled pores & replaced grains, the cement is not poikilotopic but comprised of interlocking single crystals up to 0.1 mm diameter with either scalenohedral or rhombic habits, nodules up to 0.5mm diameter of Fe rich micrite with rims of radiating spar concentrate in the ?burrow, blocky pyrite has replaced grains & filled adjacent pores as a localised cement, deformed grains have been replaced by glaucony, grain replacing kaolin booklets up to 20 microns in diameter

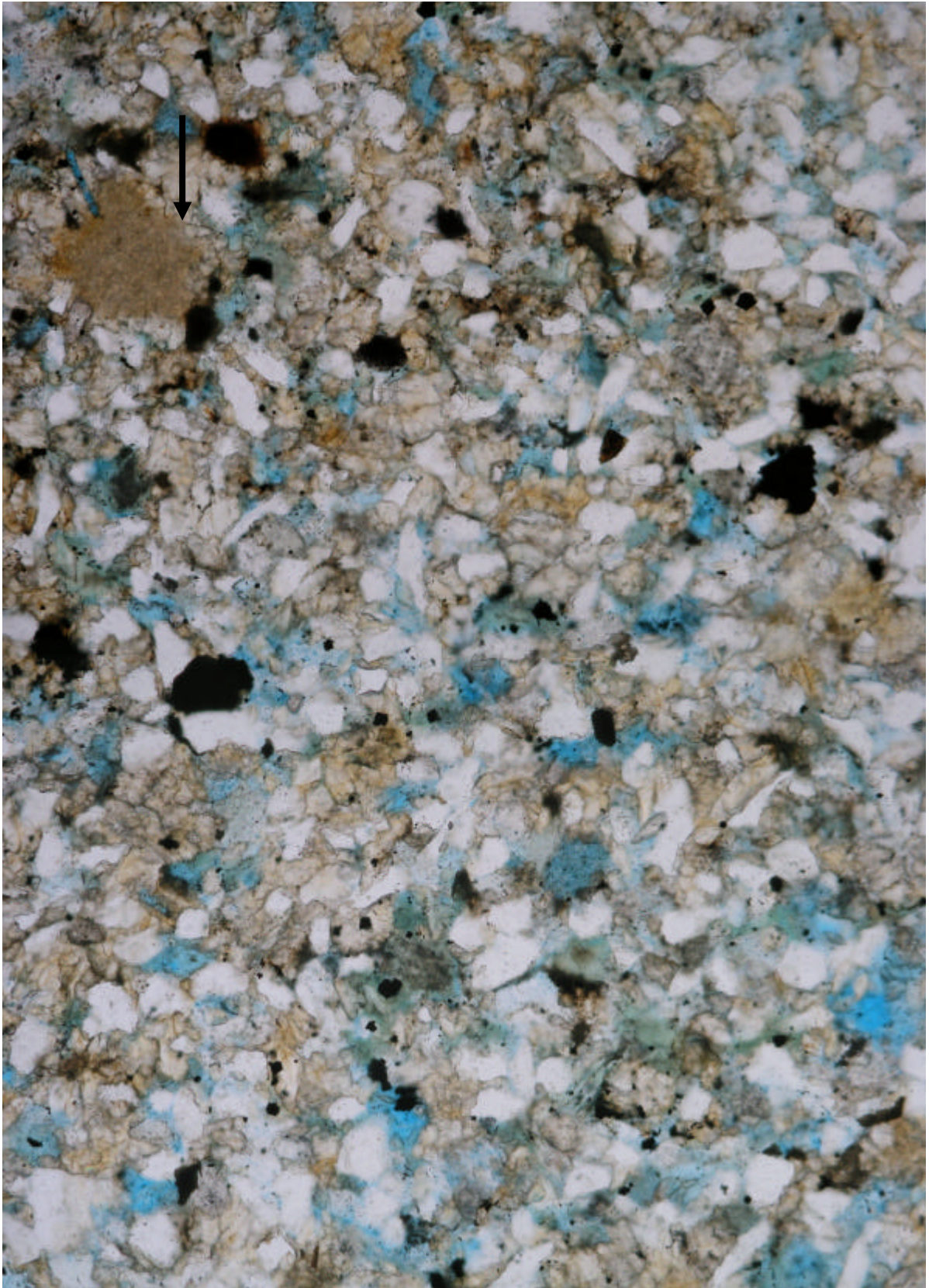


Figure 12 General view illustrating a small nodule with rim of spar (arrow) and dominance of secondary dissolution pores (blue). Blocky pyrite (opaque), oxidised grains & rutile are also apparent. Casino-3, Core plug 41, depth 2016.39m (Driller). Plane light. Horizontal field of view 1.30mm.

4.13 Casino-3, Core plug 31, depth 2013.30m (Driller) Waarre Ca

Rock classification:

Subarkose

Texture:

Sedimentary structures:	cross bedding indicated by changes in grain size
Average grain size:	medium sand (0.38mm)
Range in grain size:	fine to very coarse sand
Roundness / sphericity:	subangular to subrounded with low to moderate sphericity
Sorting:	moderately well (0.66 ϕ)
Texture:	grain supported
Packing / grain contacts:	open packing / point & tangential grain contacts
Pore types:	dominantly primary intergranular pores, rare grain size, intragranular & honeycomb dissolution pores, micropores

Composition:

Framework grains:	monocrystalline quartz, polycrystalline quartz with either sutured or straight crystal boundaries, corroded K-feldspars that lack twinning, fresh feldspars with tartan twinning, remnants of corroded granophyric texture, lithics of chert (fresh & dusty), shale, quartzite, mudstone & ?granite, splayed & altered muscovite & rare biotite flakes up to 0.35mm in length, accessory very fine to medium sand size tourmaline & rutile, silt to fine sand size zircon
Matrix:	rare blocky opaque organic matter
Authigenic minerals:	euhedral rhombohedral & prismatic quartz overgrowths, pore filling & grain replacing kaolin booklets up to 40 microns diameter, grain replacing & pore filling blocky pyrite, rare framboidal pyrite on grain margins, clusters of minute clear rhombs of spar where a grain has been removed by dissolution, anhedral Fe rich microspar has replaced one deformed grain

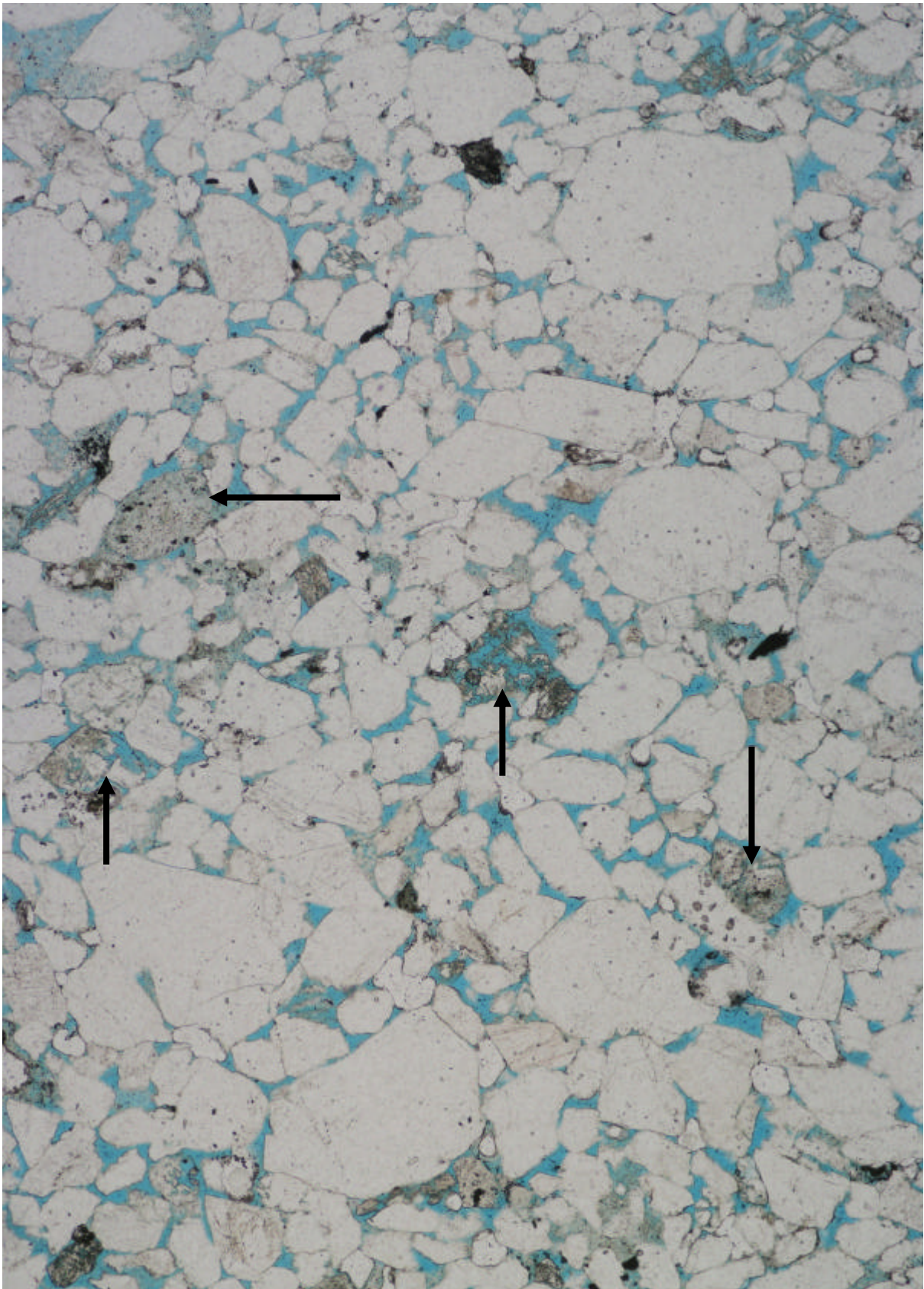


Figure 13 Elongate primary intergranular pores in this sandstone suggest good permeability. Note the variable grain size and number of highly corroded feldspars (arrows). Casino-3, Core plug 31, depth 2013.30m (Driller). Plane light. Horizontal field of view 3.25mm.

4.14 Casino-3, Core plug 20, depth 2009.94m (Driller) Waarre Ca

<u>Rock classification:</u>	Sublitharenite
<u>Texture:</u>	
Sedimentary structures:	crenulated clay rich stringer, disruption of grain alignment may indicate the presence of bioturbation, concentration of accessory minerals & pyrite in select laminae
Average grain size:	fine sand (0.19mm)
Range in grain size:	coarse silt to medium sand
Roundness / sphericity:	angular to subrounded with low to moderate sphericity
Sorting:	well (0.44 ϕ)
Texture:	grain supported
Packing / grain contacts:	moderately open packing/ point & tangential grain contacts
Pore types:	primary intergranular pores, secondary grain size & honeycomb pores, micropores
<u>Composition:</u>	
Framework grains:	monocrystalline quartz, polycrystalline quartz with straight crystal boundaries, corroded K-feldspars that lack twinning, lithics of chert (fresh & oxidised), micaceous schist & quartzite, bright orange grain of unknown origin & rare oxidised grains, splayed & altered muscovite flakes up to 0.45mm in length, accessory silt to fine sand size zircon, tourmaline & rutile
Matrix:	dark brown anhedral clay in the stringer & opaque to reddish organic matter
Authigenic minerals:	euhedral rhombohedral & prismatic quartz overgrowths, grain replacing & pore filling kaolin booklets & verms up to 20 microns in diameter, framboidal & blocky pyrite concentrates along grain margins, in pore throats & has replaced detrital clay, chlorite has replaced deformed elongate grains (?mica) & more rounded green grains are replaced by glaucony with a wormy texture, rare clusters of single rhombic minute clear spar appear to postdate grain dissolution, pore filling/grain replacing anhedral Fe rich microspar

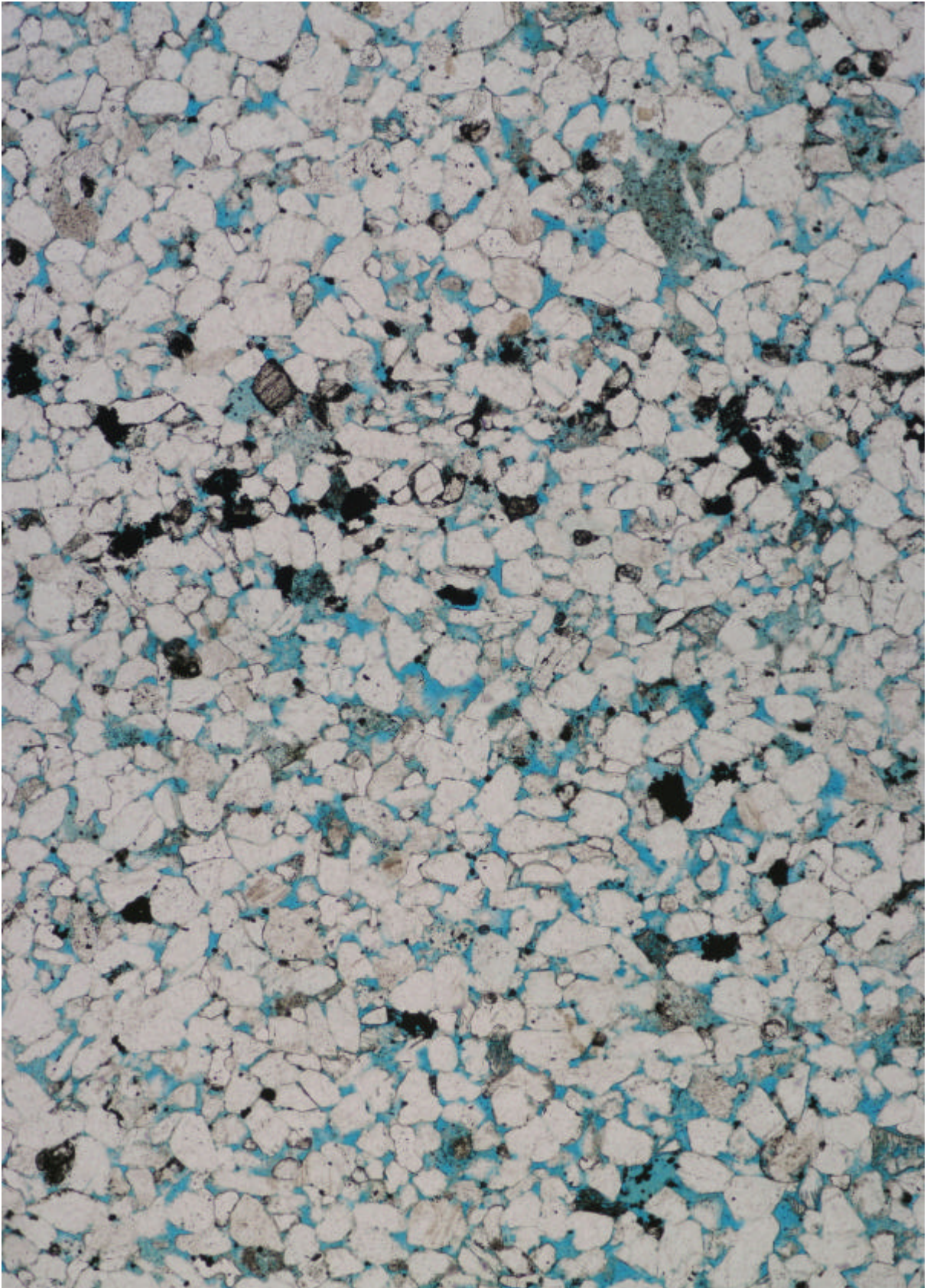


Figure 14 Laminae with high concentrations of accessory minerals and pore filling pyrite (opaque) may limit vertical permeability. Cleaner laminae have a high percentage of primary intergranular pores. Casino-3, Core plug 20, depth 2009.94m (Driller). Plane light. Horizontal field of view 3.25mm.

4.15 Casino-3, Core plug 12, depth 2007.59m (Driller) Waarre Ca

Rock classification:

Subarkose

Texture:

Sedimentary structures:	grain alignment suggests the presence of cross bedding
Average grain size:	medium sand (0.26mm)
Range in grain size:	very fine to coarse sand
Roundness / sphericity:	angular to subrounded with low to moderate sphericity
Sorting:	well (0.43 ϕ)
Texture:	grain supported
Packing / grain contacts:	open packing/ point & tangential grain contacts
Pore types:	dominantly primary intergranular pores, minor honeycomb & grain size dissolution pores, micropores

Composition:

Framework grains:	monocrystalline quartz, polycrystalline quartz with either straight or sutured crystal boundaries, highly corroded & sericitised K-feldspars that lack twinning or have tartan & simple twinning, lithics of chert, ?granite, micaceous schist & quartzite, splayed & altered muscovite flakes up to 0.25mm in length, accessory minerals of silt to fine sand size zircon, tourmaline, rutile & opaques
Authigenic minerals:	prismatic & rhombohedral quartz overgrowths, kaolin booklets & verms up to 50 microns in diameter have replaced grains (including micas) & filled adjacent pores, trace amounts of illite are associated with the kaolin, splayed micas replaced by micritic carbonate, rare framboidal pyrite on grain margins, slightly deformed very fine sand size green grains with a wormy texture similar to glaucony,

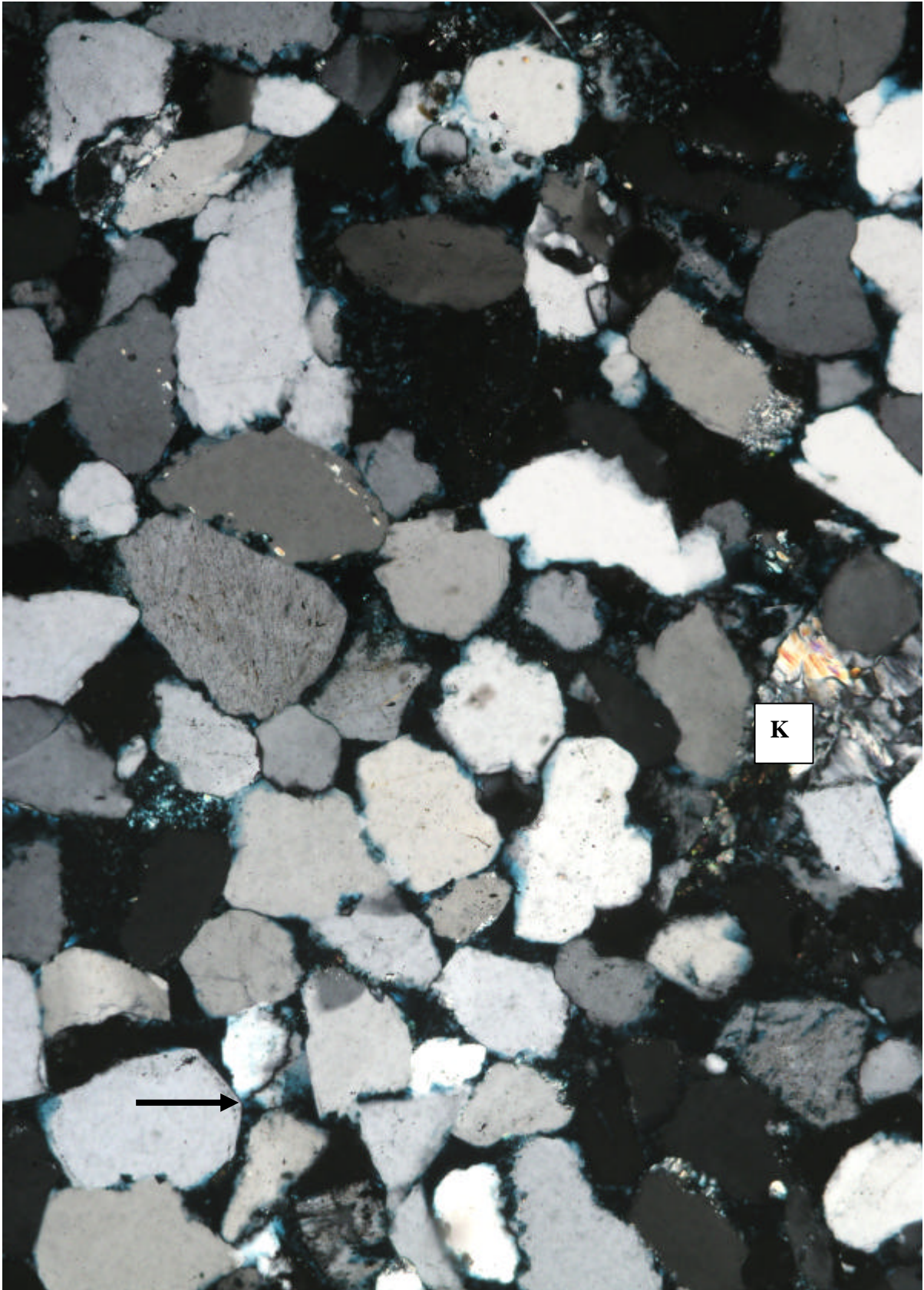


Figure 15
The high percentage of monocrystalline quartz with rhombohedral (arrow) and prismatic overgrowths is evident in this field of view. Note the mica partially altered to kaolin (K). Casino-3, Core plug 12, depth 2007.59m (Driller). Crossed nicols. Horizontal field of view 1.30mm.

4.16 Casino-3, Core plug 9, depth 2006.70m (Driller) Waarre Ca

<u>Rock classification:</u>	Laminated mudstone & fine sandstone
<u>Texture:</u>	
Sedimentary structures:	laminae of variable thickness from less than 1mm up to 5 mm of clean versus clay rich sediment, sharp erosional contacts & flame structures between laminae, sandy laminae grade upwards from clean sand to more clay rich, there are ripples, lenticular & flaser cross bedding, volcano shaped dewatering structures & a possible burrow apparent. The latter is approximately 1.5cm diameter, rounded in shape & filled with fine to coarse grained (average medium) sand cemented by kaolin.
Average grain size:	medium silt (0.07mm) but grain size distribution is bimodal & results from the burrow fill have been omitted
Range in grain size:	clay to fine sand
Roundness / sphericity:	angular to subrounded with low to moderate sphericity
Sorting:	very poor (2.47 ϕ)
Texture:	grain supported & matrix supported in alternating laminae
Packing / grain contacts:	moderately close / tangential grain contacts (open packing in the burrow with point contacts)
Pore types:	secondary pores include grain size dissolution pores, intragranular pores & honeycomb pores, micropores in the burrow, fracturing parallel to bedding is probably an artifact
<u>Composition filling the burrow:</u>	
Framework grains:	angular to subrounded, medium grained, embayed monocrystalline quartz, polycrystalline quartz with either straight or sutured crystal boundaries, partially corroded K-feldspars that lack twinning, feldspars with tartan twinning & granophyric texture, lithics of quartzite, micaceous schist, ?pyrophyllite & ?granite, bent muscovite flakes, silt to very fine sand size zircon & tourmaline
Matrix:	rare stringers of anhedral brown clay near the burrow margins, blocky opaque organic matter
Authigenic minerals:	pervasive pore filling & grain replacing kaolin booklets range in diameter from 5 to 40 microns, scattered pyrite framboids, traces of Fe stained micritic siderite in the kaolin, rare very fine sand size green grains of glaucony with wormy texture
<u>Composition of the mudstone:</u>	
Framework grains:	rare silt size monocrystalline & polycrystalline quartz, corroded K feldspars that lack twinning, lithics of micaceous schist & quartzite, bent fresh muscovite flakes up to 0.12mm length, altered (?chloritised) biotite, accessory tourmaline
Matrix:	abundant anhedral pale to dark brown clay & blocky opaque material (?vitrinite), rare orange coloured stringers (?liptinite)
Authigenic minerals:	pyrite framboids, grain replacing Fe rich micrite, deformed green grains of glaucony with wormy texture
<u>Composition of the fine grained sandstone:</u>	
Framework grains:	monocrystalline quartz, polycrystalline quartz with straight crystal boundaries, up to coarse sand size partially corroded K-feldspar that lacks twinning, fresh feldspar with pericline twinning, lithics of chert, micaceous schist, quartzite & ?pyrophyllite, oxidised grains, straight muscovite flakes, accessory silt size zircon, rutile & fine sand size tourmaline
Matrix:	blocky opaque organic matter, stringers of brown anhedral clay
Authigenic minerals:	grain replacing anhedral Fe rich micrite, pyrite framboids & grain replacing blocky pyrite, grain replacing kaolin booklets up to 50 microns diameter, very fine sand size green grains of glaucony with either wormy or fibrous texture

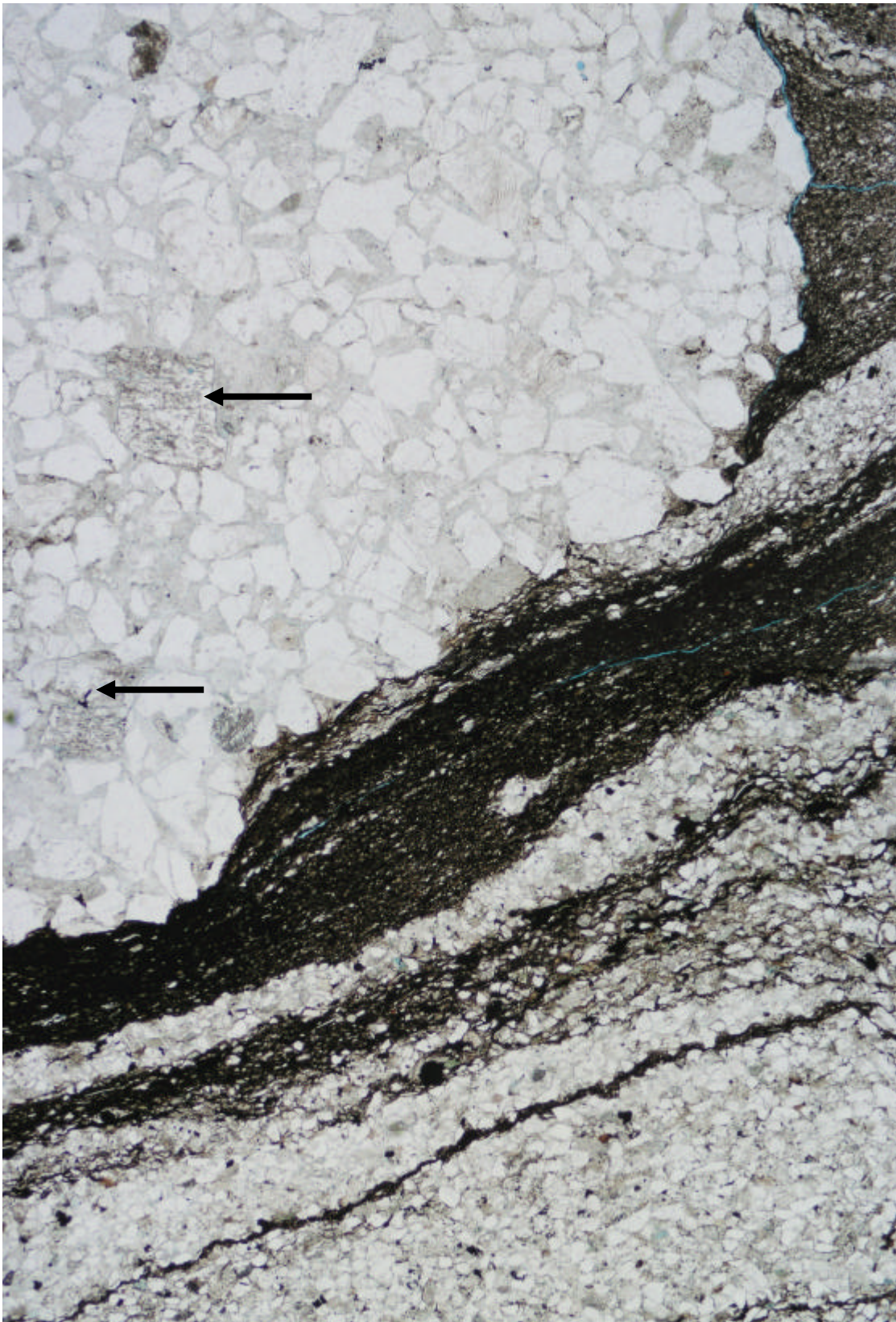


Figure 16a
Erosional contact between the burrow filled with medium grained sand and finer grained laminated sediments. Soft sediment deformation is associated with the burrow. Note the coarse grained partially corroded K-feldspars (arrows) in the burrow. Casino-3, Core plug 9, depth 2006.70m (Driller). Plane light. Horizontal field of view 6.5mm.

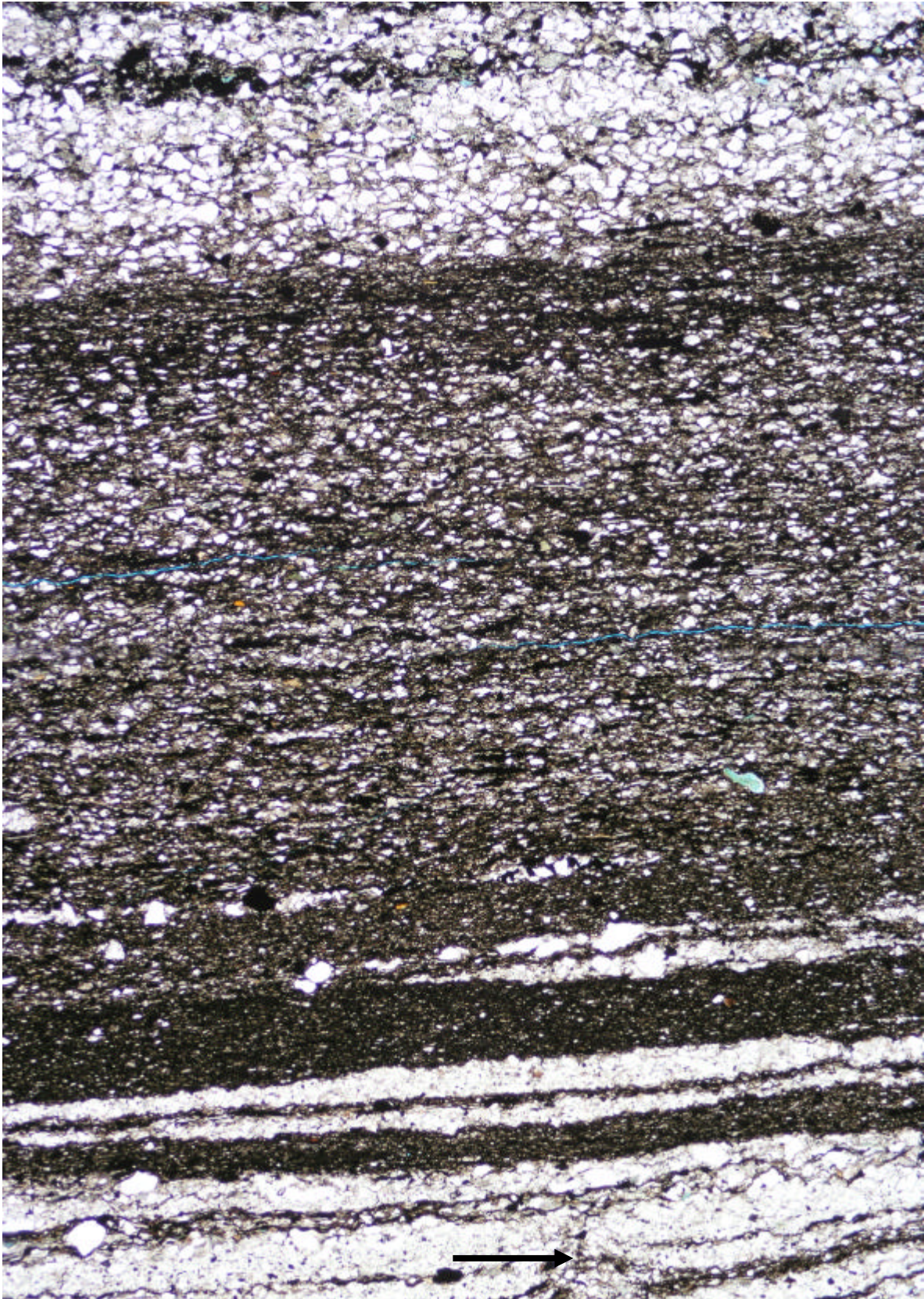


Figure 16b General view illustrating the thin sandy lenses (ripples) trapped in mudstone to form lenticular bedding. Note the disrupted bedding probably due to a water escape structure (arrow). Casino-3, Core plug 9, depth 2006.70m (Driller). Plane light. Horizontal field of view 6.5mm.

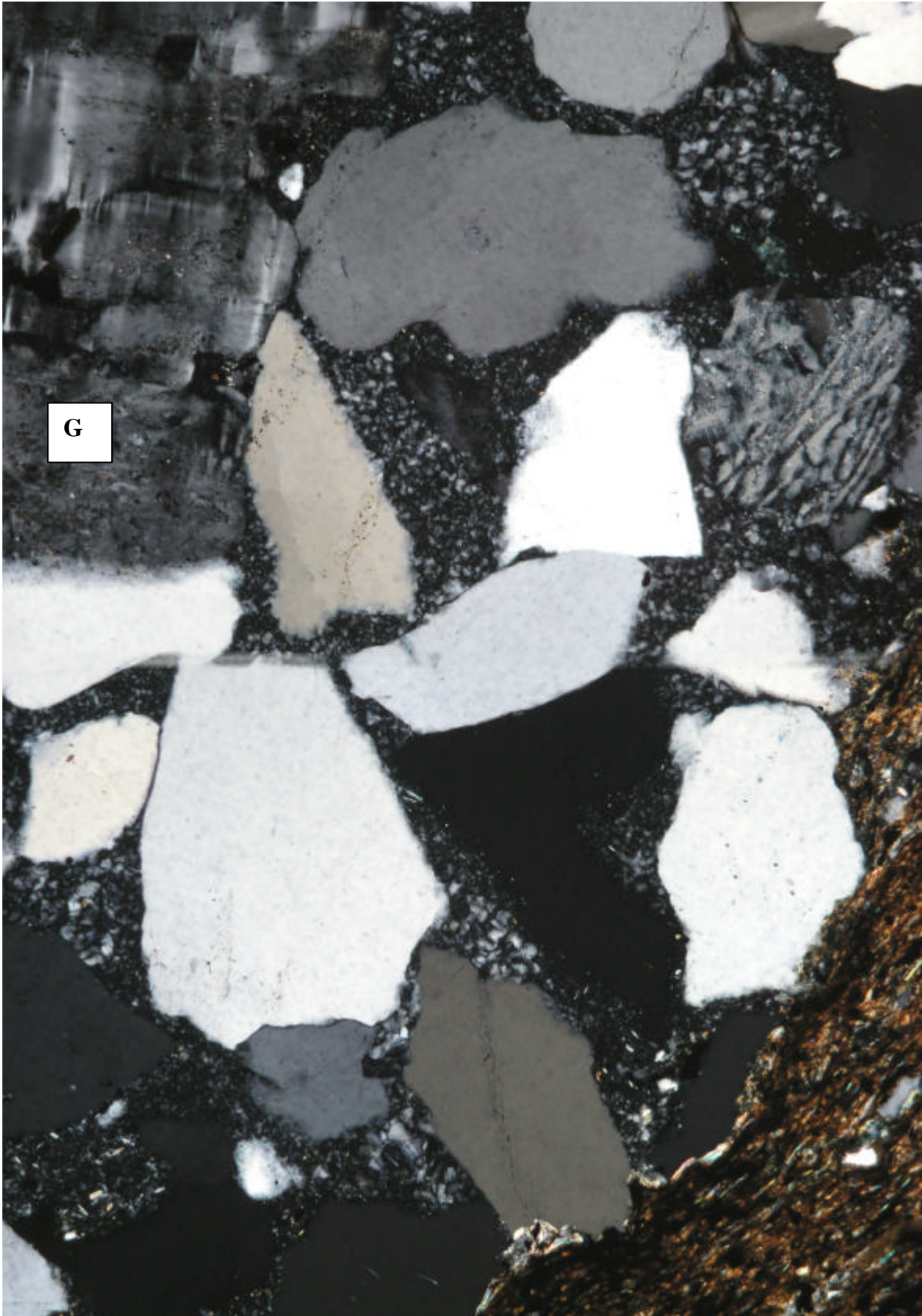


Figure 16c
Enlargement of the contact between the burrow filled with medium grained sand and finer grained laminated sediments. Note the feldspar with granophyric texture (upper RHS) and a possible ?granitic (G) lithic (feldspar with tartan twinning plus quartz) in the burrow. Casino-3, Core plug 9, depth 2006.70m (Driller). Crossed nicols. Horizontal field of view 1.30mm.

4.17 Casino-3, Core plug 5, depth 2005.46m (Driller) Waarre Cb

Rock classification:

Subarkose

Texture:

Sedimentary structures:	grain alignment & changes in grain size indicate the presence of weakly defined bedding
Average grain size:	medium sand (0.43mm)
Range in grain size:	very fine sand to granules
Roundness / sphericity:	subangular to subrounded with low to moderate sphericity
Sorting:	moderate (0.92 ϕ)
Texture:	grain supported
Packing / grain contacts:	open packing / point & tangential grain contacts
Pore types:	primary intergranular pores dominate, rare honeycomb, intragranular and grain size dissolution pores, micropores associated with kaolin

Composition:

Framework grains:	monocrystalline quartz, polycrystalline quartz dominantly with straight crystal boundaries, highly corroded K-feldspars that lack twinning & others with tartan twinning & granophyric texture, lithics of chert (with minor corrosion), siltstone, ?granite, shale, quartzite & micaceous schist, fresh & altered bent muscovite flakes up to 0.5mm in length, accessory very fine to medium sand size tourmaline & very fine sand size zircon
Matrix:	blocky opaque organic matter with cellular structure (?inertinite)
Authigenic minerals:	grain replacing kaolin booklets up to 30 microns in diameter, minor framboids & blocky pyrite replacing grains & filling pores, rare anhedral to subhedral clear spar & dusty micrite replacing grains & filling adjacent pores, irregular prismatic quartz overgrowths

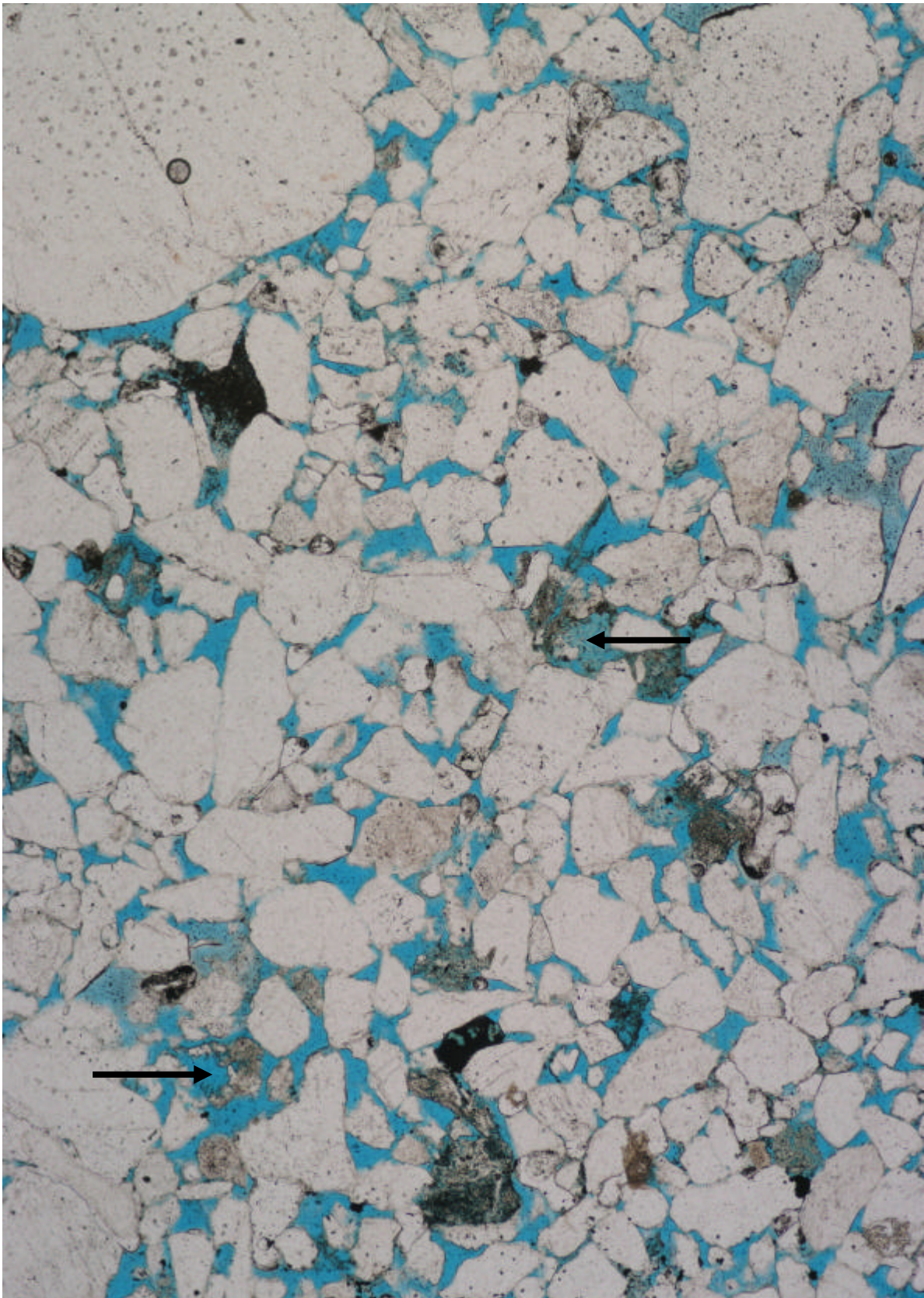


Figure 17 General field of view illustrating the variation in grain size and dominance of primary intergranular pores (blue). Highly corroded feldspars (arrows) are also apparent. Casino-3, Core plug 5, depth 2005.46m (Driller). Plane light. Horizontal field of view 3.25mm.

4.18 Casino-3, MSCT 3, depth 2005.5m (Logger) Waarre Cb

Rock classification:

Subarkose

Texture:

Sedimentary structures:	weakly defined bedding indicated by a change in grain size
Average grain size:	medium sand (0.30mm)
Range in grain size:	very fine to coarse sand
Roundness / sphericity:	subangular to subrounded with low to moderate sphericity
Sorting:	moderately well sorted (0.58 ϕ)
Texture:	grain supported
Packing / grain contacts:	open packing / point & tangential grain contacts
Pore types:	dominantly primary intergranular pores, minor honeycomb & intragranular pores, micropores, rare grain fracturing is probably an artifact of sampling

Composition:

Framework grains:	monocrystalline quartz, polycrystalline quartz with straight crystal boundaries, highly corroded K-feldspars that lack twinning & relatively fresh feldspar with tartan twinning, corroded remnants of granophyric texture, lithics of chert (corroded), ?granite, shale, quartzite & micaceous schist, fresh & altered splayed & bent muscovite flakes up to 0.45mm length, accessory very fine sand size rutile & zircon, silt to very fine sand size tourmaline
Matrix:	blocky opaque organic matter
Authigenic minerals:	prismatic quartz overgrowths, blocky & framboidal pyrite on grain margins & replacing grains, grain replacing kaolin booklets up to 40 microns in diameter rarely fill adjacent pores, one medium sand size green grain with wormy texture typical of glaucony has been fragmented during sampling

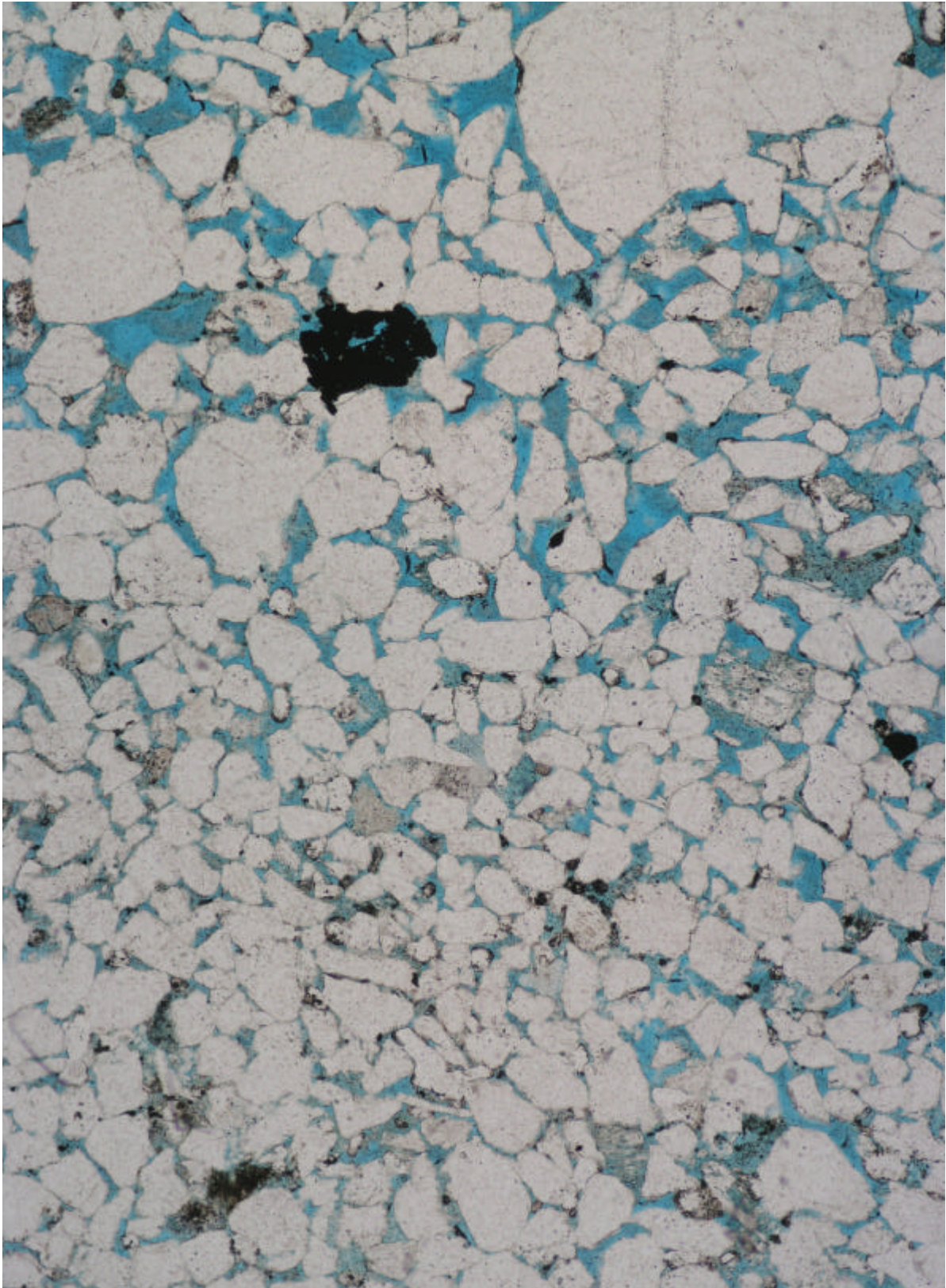


Figure 18 Packing in the finer grained bed is slightly closer than the coarse grained bed. The large blocky opaque material is organic matter. Casino-3, MSCT 3, depth 2005.5m (Logger). Plane light. Horizontal field of view 3.25mm.

4.19 Casino-3, MSCT 2, depth 2002.5m (Logger) Waarre Cb

Rock classification:

Subarkose

Texture:

Sedimentary structures:	weak grain alignment may indicate the orientation of bedding
Average grain size:	fine to medium sand boundary (0.25mm)
Range in grain size:	very fine to medium sand
Roundness / sphericity:	subangular to subrounded with low to moderate sphericity
Sorting:	well sorted (0.44 ϕ)
Texture:	grain supported
Packing / grain contacts:	open packing / point & tangential grain contacts
Pore types:	primary intergranular pores dominant, minor grain size & honeycomb dissolution pores, micropores associated with kaolin

Composition:

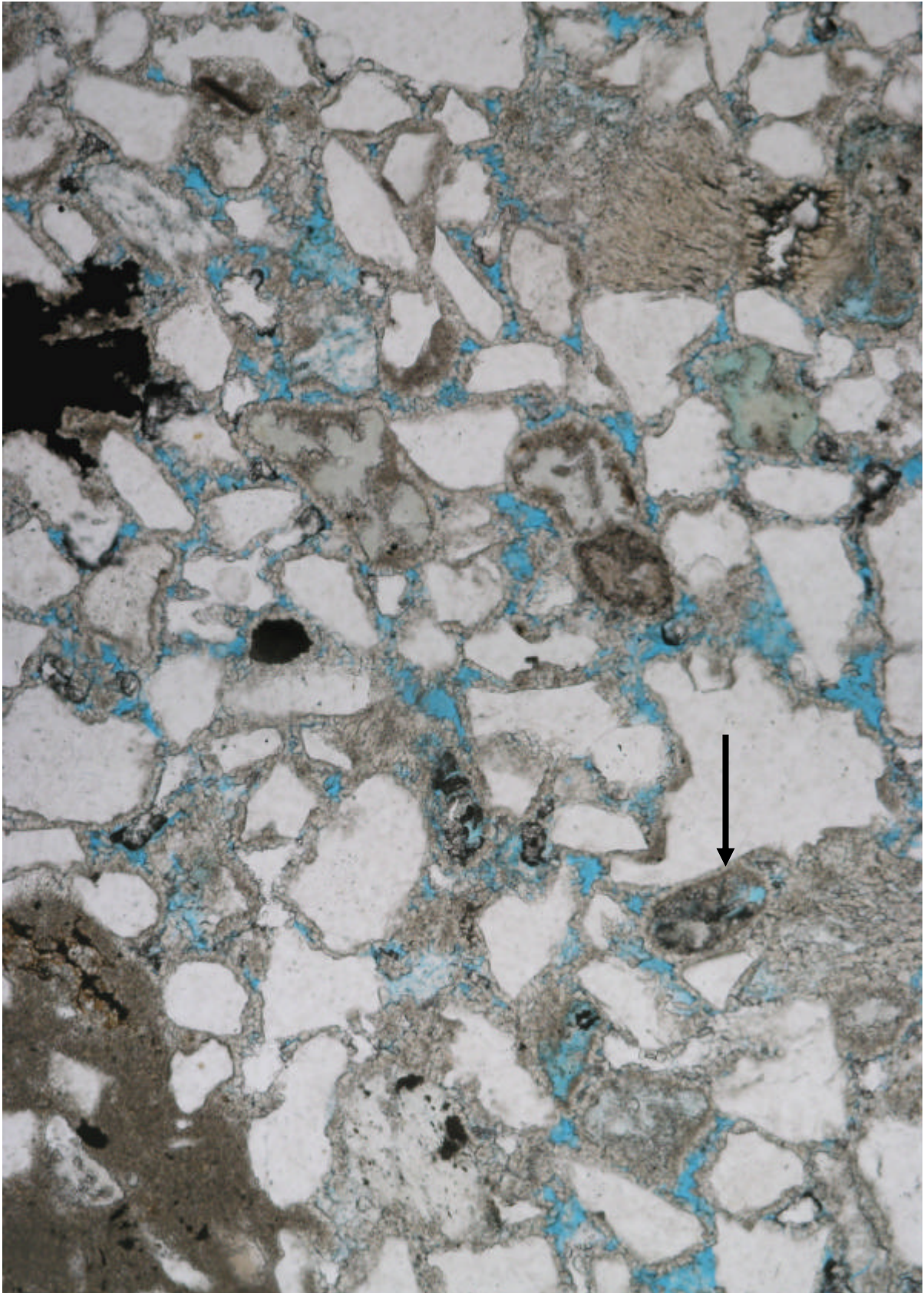
Framework grains:	monocrystalline quartz, polycrystalline quartz with either straight or sutured crystal boundaries, highly corroded K-feldspars lack twinning, remnants of granophyric texture, lithics of chert, shale, micaceous schist & quartzite, the origin of highly altered lithics is unknown, bent muscovite flakes up to 0.35mm in length, accessory very fine to medium sand size tourmaline & very fine sand size zircon & rutile
Authigenic minerals:	prismatic & rhombohedral quartz overgrowths, pore filling & grain replacing kaolin booklets & verms up to 50 microns diameter, minor illite associated with the kaolin, traces of anhedral Fe rich microspar & micrite replacing grains & filling pores, rare pyrite framboids on grain margins, deformed medium sand size green grains with wormy texture typical of glaucony



Figure 19 General field of view illustrating the uniform grain size in this sandstone. Intergranular pores (blue) tend to be elongate suggesting good permeability. Casino-3, MSCT 2, depth 2002.5m (Logger). Plane light. Horizontal field of view 3.25mm.

4.20 Casino-3, MSCT 1, depth 1987.0m (Logger) Waarre Cb

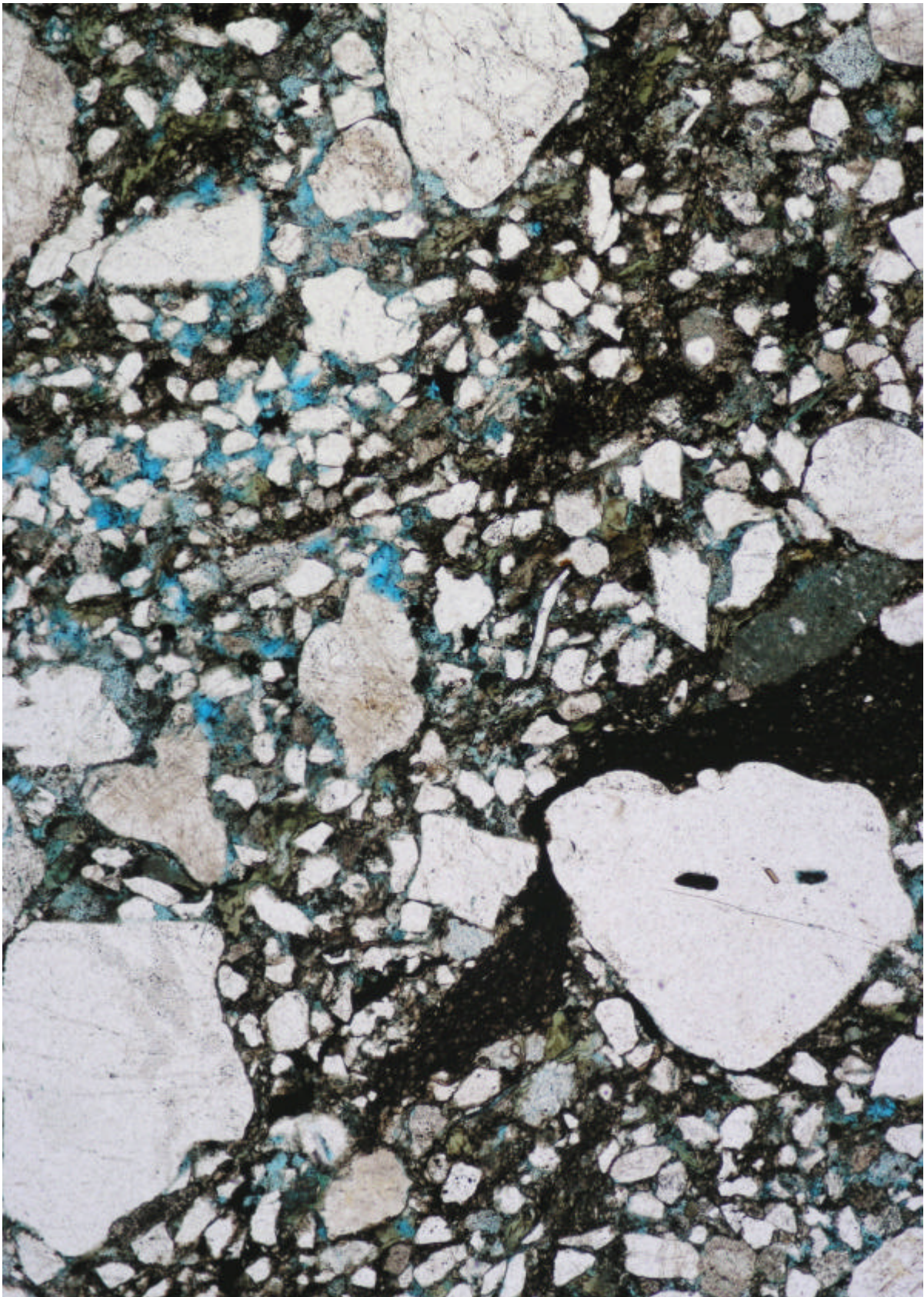
<u>Rock classification:</u>	Carbonate Cemented Subarkose
<u>Texture:</u>	
Sedimentary structures:	cross bedding is outlined by the abundance of organic matter & changes in grain size
Average grain size:	medium sand (0.29mm)
Range in grain size:	very fine to very coarse sand
Roundness / sphericity:	angular to subangular with low sphericity
Sorting:	moderately sorted (0.81 ϕ)
Texture:	cement supported
Packing / grain contacts:	open packing / rare point contacts
Pore types:	primary intergranular pores, grain size & honeycomb dissolution pores, micropores, intergranular pore size & interconnections between pores are limited by circumgranular equant cement
<u>Composition:</u>	
Framework grains:	monocrystalline quartz, polycrystalline quartz with straight crystal boundaries, fresh plagioclase with albite twinning, highly corroded K-feldspars that lack twinning or have tartan twinning are up to coarse sand in size, other K-feldspars with tartan twinning are fresh, lithics of chert, quartzite, micaceous schist & possibly mudstone, highly altered lithics of polycrystalline & monocrystalline quartz & kaolin were probably igneous in origin, bent & splayed altered muscovite flakes up to 0.60mm in length, accessory very fine sand size zircon, rutile & tourmaline
Matrix:	reddish black organic matter with remnants of cellular structure
Authigenic minerals:	equant crystals of scalenohedral Fe rich carbonate spar up to 15 microns in diameter completely rim grains, these rims are suspended around grain size dissolution pores, spar & micrite has also completely replaced grains & partially replaced organic matter, in patches of the section there is a partial micritic rim on framework grains prior to the spar, rare very fine sand size green grains with wormy texture are probably composed of glauconite, pore filling & grain replacing kaolin booklets up to 50 microns diameter, traces of illite associated with the kaolin, blocky & framboidal pyrite has selectively replaced grains after the carbonate

**Figure 20**

General view illustrating the circumgranular cement surrounding framework grains (arrow) & retention of primary intergranular pores. A large patch of micritic carbonate (lower LHS) could represent a lithic since quartz grains are floating in the cement. Opaque material (upper LHS) is pyrite replacing carbonate. Casino-3, MSCT 1, depth 1987.0m (Logger). Plane light. Horizontal field of view 1.30mm.

4.21 Casino-3, MSCT 11, depth 1970.5m (Logger) Flaxman

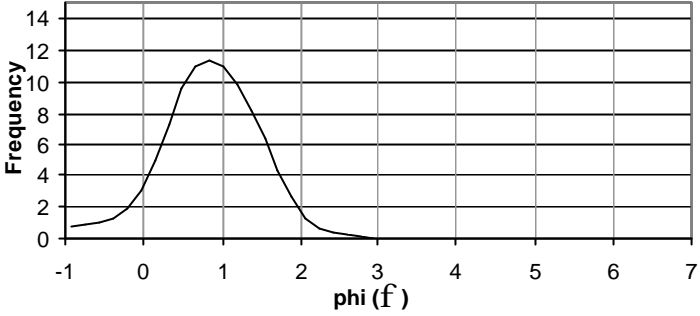
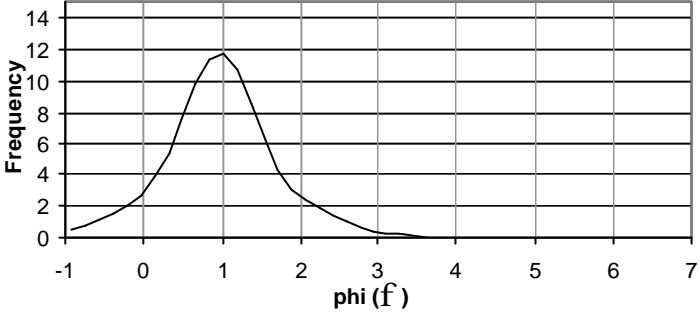
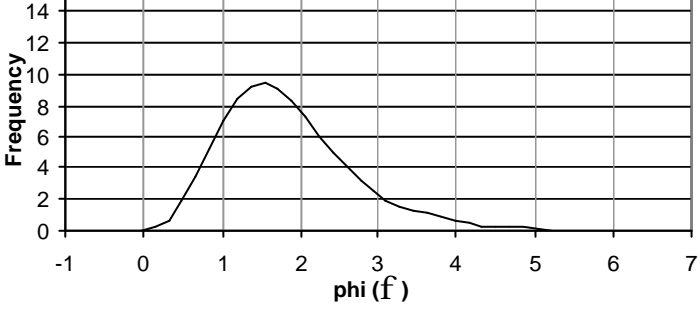
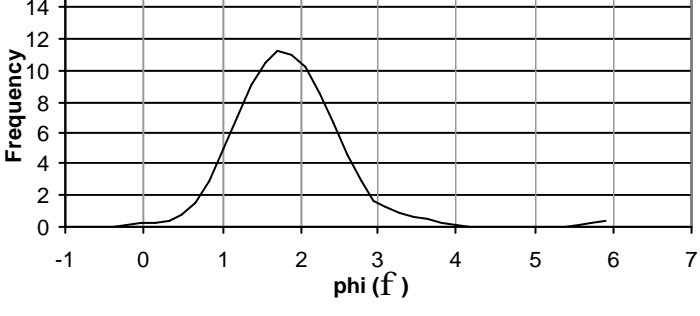
<u>Rock classification:</u>	Carbonate Cemented Sublitharenite
<u>Texture:</u>	
Sedimentary structures:	crenulated clay stringers & very weak grain alignment indicate the orientation of bedding
Average grain size:	medium sand (0.34mm) but grain size distribution is bimodal
Range in grain size:	clay to very coarse sand
Roundness / sphericity:	angular to subrounded with low to moderate sphericity
Sorting:	very poor (2.08 ϕ)
Texture:	grain supported
Packing / grain contacts:	moderately open packing / point & tangential contacts, deformed glaucony
Pore types:	grain size dissolution pores, intragranular & honeycomb pores, micropores associated with kaolin, rare intergranular pores may also be secondary in origin
<u>Composition:</u>	
Framework grains:	monocrystalline quartz, very coarse sand size grains of polycrystalline quartz with straight crystal boundaries, partially corroded plagioclase with albite twinning, K-feldspars that lack twinning or have tartan twinning, other feldspars with granophyric texture, lithics of shale, micaceous schist, quartzite & chert, very coarse sand size highly sericitised & kaolinised lithics may have been igneous, bent & altered muscovite, bent fresh & chloritised biotite up to 0.35mm in length, accessory very fine sand size zircon, tourmaline & sphene
Matrix:	stringers of anhedral brown clay, blocky opaque organic matter (?vitrinite) & stringers of reddish material (?lignite)
Authigenic minerals:	grain replacing kaolin booklets & verms up to 60 microns in diameter, deformed fine to coarse sand size green grains with wormy & fibrous texture typical of glaucony, pervasive anhedral to subhedral single scalenohedral crystals of carbonate spar replacing matrix & framework grains, minor staining indicates the carbonate is Fe rich, blocky spar is pore filling, minor framboidal & blocky pyrite replacing grains

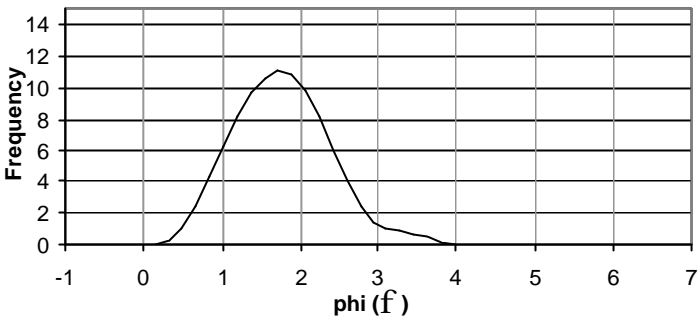
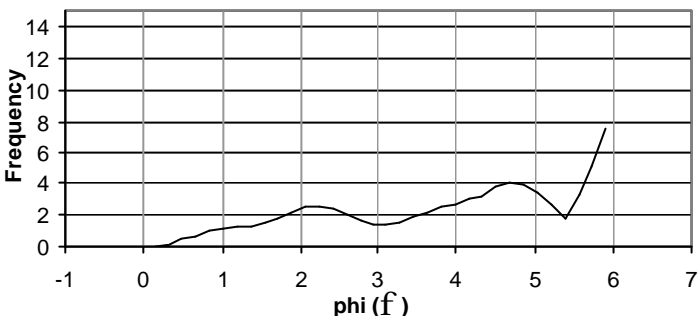
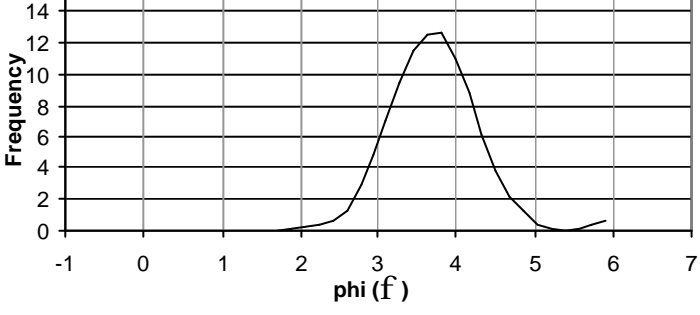
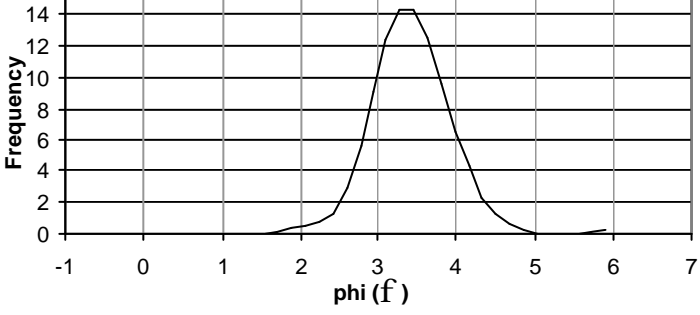
**Figure 21**

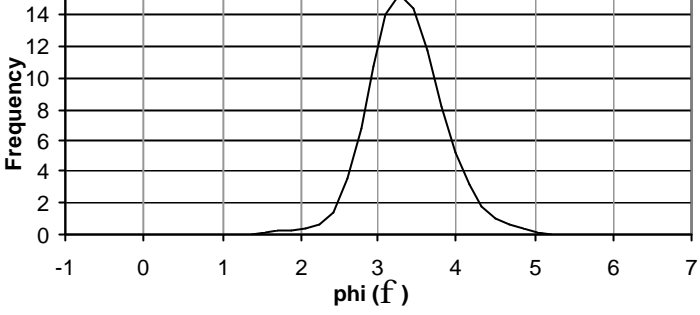
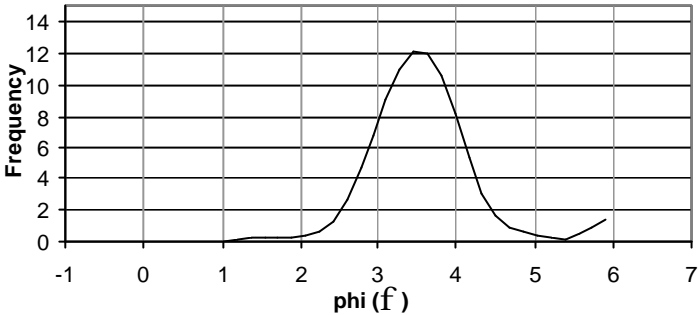
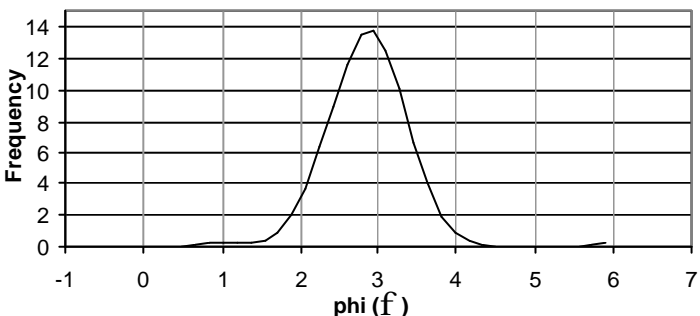
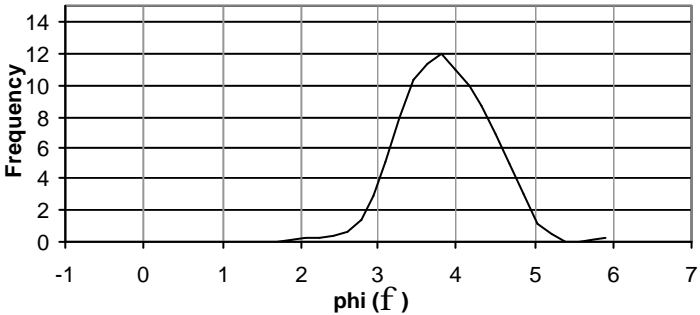
A clay rich laminae (dark brown) and the very poor sorting of this sample are apparent in this field of view. Porosity (blue) has a patchy distribution & is secondary in nature. Casino-3, MSCT 11, depth 1970.5m (Logger). Plane light. Horizontal field of view 3.25mm.

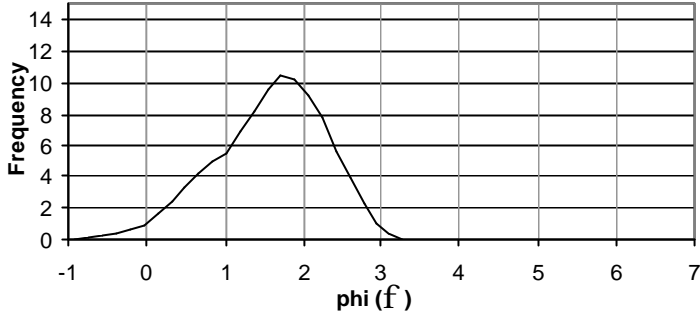
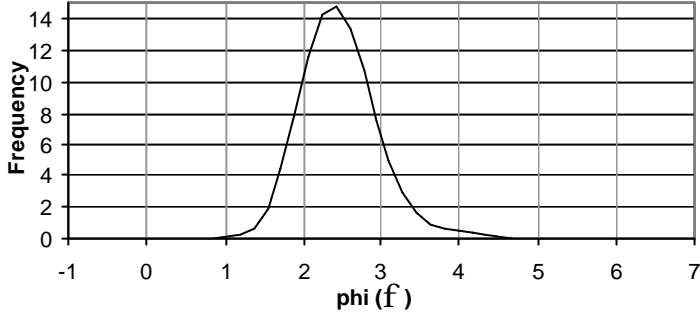
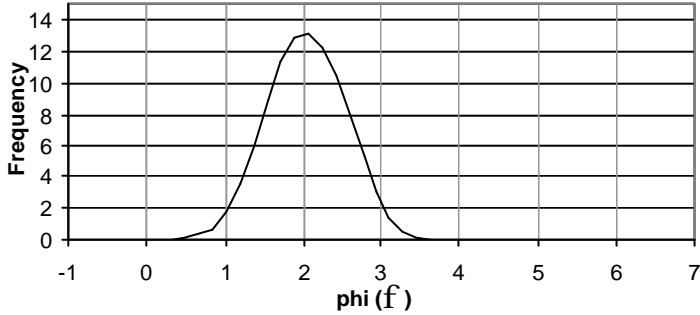
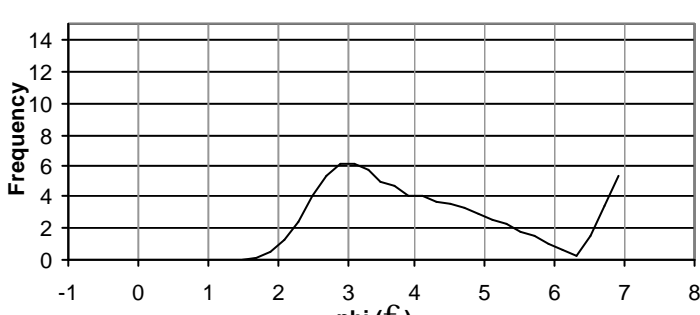
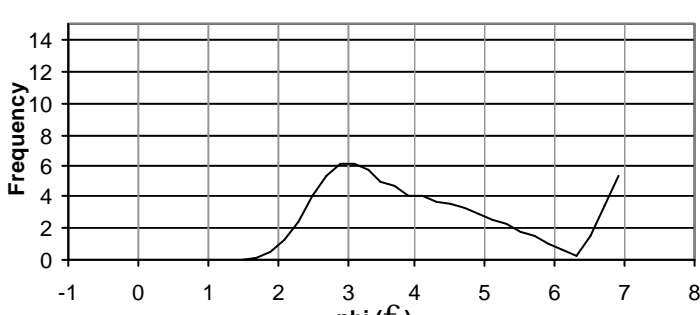
5. GRAIN SIZE ANALYSIS

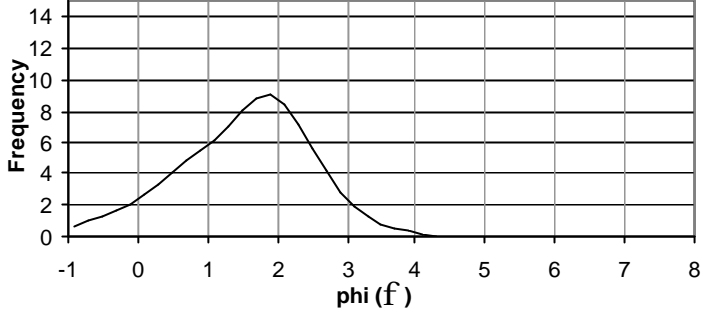
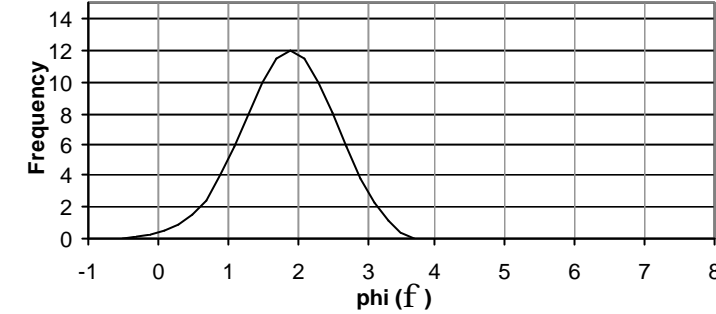
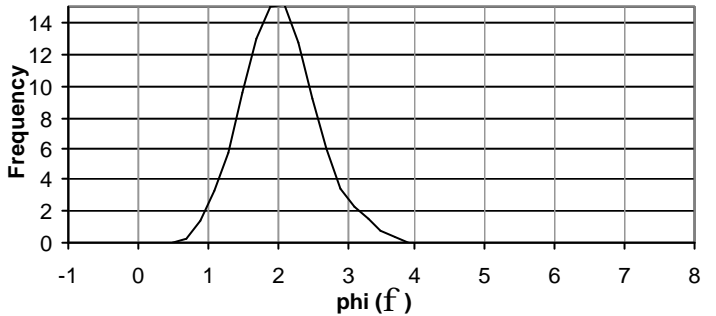
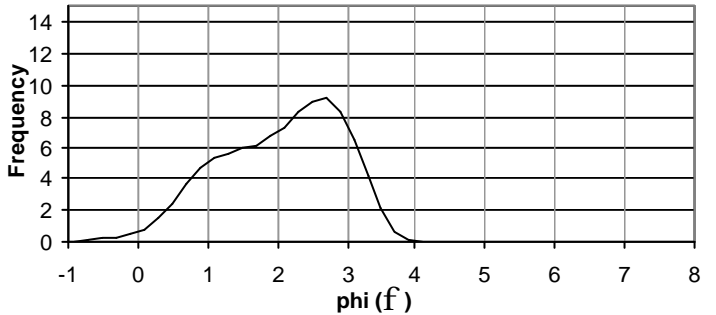
TABLE 3. GRAIN SIZE DATA

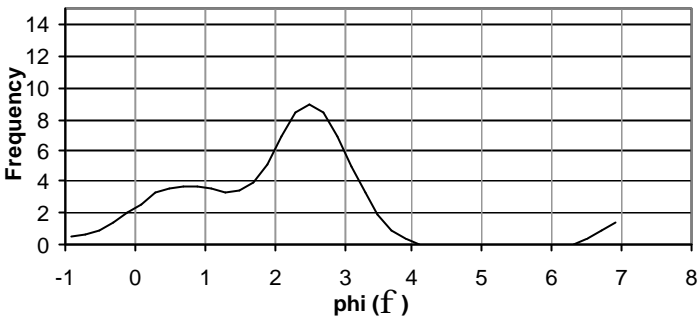
Thin Section Statistics	Frequency Distribution
MSCT: 6	
Depth (m L) 2102.50	
Parameter mm ϕ	
Mean 0.63 0.81 coarse sand	
Mode 0.56 0.83 coarse sand	
Range: min 0.18 2.47 max 2.25 -1.17	
Standard Deviation 0.34 0.61 moderately well sorted	
MSCT: 5	
Depth (m L) 2093.50	
Parameter mm ϕ	
Mean 0.57 0.97 coarse sand	
Mode 0.52 0.96 coarse sand	
Range: min 0.11 3.18 max 1.78 -0.83	
Standard Deviation 0.28 0.67 moderately well sorted	
MSCT: 4	
Depth (m L) 2082.50	
Parameter mm ϕ	
Mean 0.32 1.83 medium sand	
Mode 0.35 1.51 medium sand	
Range: min 0.04 4.64 max 0.68 0.56	
Standard Deviation 0.14 0.80 moderately sorted	
MSCT: 7	
Depth (m L) 2070.50	
Parameter mm ϕ	
Mean 0.30 1.97 medium sand	
Mode 0.29 1.78 medium sand	
Range: min 0.002 8.97 max 0.87 0.20	
Standard Deviation 0.13 1.15 poorly sorted	

Thin Section Statistics			Frequency Distribution	
MSCT: 13				
Depth (m L) 2061.50				
Parameter	mm	ϕ		
Mean	0.31	1.77		
medium sand				
Mode	0.30	1.75		
medium sand				
Range:	min	0.09	3.47	
	max	0.57	0.81	
Standard Deviation	0.11	0.56		
moderately well sorted				
Sample: core chip				
Depth (m D) 2028.50				
Parameter	mm	ϕ		
Mean	0.09	5.43		
very fine sand				
Mode	0.02	5.85		
medium silt				
Range:	min	0.002	8.97	
	max	0.62	0.69	
Standard Deviation	0.13	2.82		
very poorly sorted				
Core plug: 75				
Depth (m D) 2026.49				
Parameter	mm	ϕ		
Mean	0.08	3.86		
very fine sand				
Mode	0.08	3.73		
very fine sand				
Range:	min	0.002	8.97	
	max	0.20	2.32	
Standard Deviation	0.03	1.01		
poorly sorted				
Core plug: 73				
Depth (m D) 2025.90				
Parameter	mm	ϕ		
Mean	0.10	3.48		
very fine sand				
Mode	0.10	3.37		
very fine sand				
Range:	min	0.002	8.97	
	max	0.23	2.12	
Standard Deviation	0.03	0.69		
moderately well sorted				

Thin Section Statistics			Frequency Distribution	
Core plug: 62				
Depth (m D) 2022.60				
Parameter	mm	ϕ		
Mean	0.10	3.37		
	very fine sand			
Mode	0.10	3.31		
	very fine sand			
Range:	min	0.04	4.64	
	max	0.28	1.84	
Standard Deviation	0.03 0.41			
	well sorted			
Core plug: 59				
Depth (m D) 2021.76				
Parameter	mm	ϕ		
Mean	0.09	3.89		
	very fine sand			
Mode	0.09	3.54		
	very fine sand			
Range:	min	0.002	8.97	
	max	0.35	1.51	
Standard Deviation	0.04 1.48			
	poorly sorted			
Core plug: 52				
Depth (m D) 2019.60				
Parameter	mm	ϕ		
Mean	0.14	2.92		
	fine sand			
Mode	0.14	2.87		
	fine sand			
Range:	min	0.002	8.97	
	max	0.50	1.00	
Standard Deviation	0.06 0.75			
	moderately sorted			
Core plug: 41				
Depth (m D) 2016.39				
Parameter	mm	ϕ		
Mean	0.07	3.92		
	very fine sand			
Mode	0.07	3.77		
	very fine sand			
Range:	min	0.002	8.97	
	max	0.22	2.18	
Standard Deviation	0.03 0.70			
	moderately well sorted			

Thin Section Statistics			Frequency Distribution	
Core plug: 31				
Depth (m D) 2013.30				
Parameter	mm	ϕ		
Mean	0.38	1.56		
medium sand				
Mode	0.29	1.77		
medium sand				
Range:	min	0.15	2.74	
	max	1.25	-0.32	
Standard Deviation	0.20	0.66		
moderately well sorted				
Core plug: 20				
Depth (m D) 2009.94				
Parameter	mm	ϕ		
Mean	0.19	2.48		
fine sand				
Mode	0.19	2.36		
fine sand				
Range:	min	0.06	4.06	
	max	0.34	1.56	
Standard Deviation	0.05	0.44		
well sorted				
Core plug: 12				
Depth (m D) 2007.59				
Parameter	mm	ϕ		
Mean	0.26	2.03		
medium sand				
Mode	0.25	2.00		
fine sand				
Range:	min	0.12	3.06	
	max	0.51	0.97	
Standard Deviation	0.08	0.43		
well sorted				
Core plug: 9				
Depth (m D) 2006.70				
Parameter	mm	ϕ		
Mean	0.07	5.13		
medium silt				
Mode	0.12	3.02		
very fine sand				
Range:	min	0.001	9.97	
	max	0.20	2.32	
Standard Deviation	0.06	2.47		
very poorly sorted				

Thin Section Statistics			Frequency Distribution	
Core plug: 5				
Depth (m D) 2005.46				
Parameter	mm	ϕ		
Mean	0.43	1.54		
medium sand				
Mode	0.28	1.84		
medium sand				
Range:	min	0.08	3.64	
	max	2.00	-1.00	
Standard Deviation	0.33	0.92		
moderately sorted				
MSCT: 3				
Depth (m L) 2005.50				
Parameter	mm	ϕ		
Mean	0.30	1.88		
medium sand				
Mode	0.27	1.91		
medium sand				
Range:	min	0.12	3.06	
	max	0.95	0.07	
Standard Deviation	0.13	0.58		
moderately well sorted				
MSCT: 2				
Depth (m L) 2002.50				
Parameter	mm	ϕ		
Mean	0.25	2.04		
fine sand				
Mode	0.25	2.00		
fine sand				
Range:	min	0.10	3.32	
	max	0.46	1.12	
Standard Deviation	0.07	0.44		
well sorted				
MSCT: 1				
Depth (m L) 1987.00				
Parameter	mm	ϕ		
Mean	0.29	2.05		
medium sand				
Mode	0.16	2.62		
fine sand				
Range:	min	0.10	3.32	
	max	1.22	-0.29	
Standard Deviation	0.19	0.81		
moderately sorted				

Thin Section Statistics			Frequency Distribution	
MSCT: 11				
Depth (m L) 1970.50				
Parameter	mm	ϕ		
Mean	0.34	2.37		
	medium sand			
Mode	0.18	2.51		
	fine sand			
Range:	min	0.002	8.97	
	max	1.70	-0.77	
Standard Deviation	0.33	2.08		
	very poorly sorted			



6. X-RAY DIFFRACTION

All X-ray diffraction (XRD) results are summarised in the tables below and the traces from which these results were obtained are presented in Appendix A. Based on the XRD results at least three species of carbonate (siderite, ankerite and calcite) are present in the Waarre Sandstone at Casino-3. Iron rich carbonate described in thin section is comprised of both ankerite and siderite in Unit A, but only siderite in other stratigraphic units. Staining of the thin section from 2022.60m (core plug 62) indicates that the clear calcite spar which fills pores is ferroan. Ankerite and siderite were detected in the Flaxman Formation (MSCT 11). Carbonate cements appear to be most abundant near the base of both Units A and Ca in the Waarre Formation.

TABLE 4 . BULK XRD RESULTS CASINO-3

Sample	Depth m (D/L)	I/M	Kaol	Qtz	Micro	Alb	Cal	Ank	Sid	Pyr	Bar
<i>Strongest peak height in counts</i>											
MSCT 6	2102.5 (L)	-	150	5650	209	-	788	270	207	-	-
MSCT 13	2061.5 (L)	-	181	6895	702	159	171	288	243	-	-
Core chip	2028.5 (D)	131	312	3577	326*	-	-	-	-	39	-
CP 75	2026.49 (D)	188	345	5247	195	114	1142	-	-	-	-
CP 62	2022.60 (D)	135	298	9649	1086	-	1412	-	76	-	-
CP 59	2021.76 (D)	215	566	5810	297	-	-	-	48	-	-
CP 41	2016.39 (D)	182	385	4141	153	-	-	-	1815	83	-
CP 9	2006.70 (D)	315	872	2497	364	-	-	-	183	32	-
MSCT 11	1970.5 (L)	116	387	5189	141	130	-	-	587	-	165

* = sanidine

TABLE 5 . CLAY XRD RESULTS CASINO-3

Sample	Depth m (D/L)	Smec	Chl	Ill	Kaol	Qtz	Micro	Cal	Ank	Sid	Pyr	Bar
<i>Strongest peak height in counts</i>												
MSCT 6	2102.5 (L)	-	-	220	1870	1312	172	668	148	135	-	155
MSCT 13	2061.5 (L)	-	-	251	1288	1856	207	185	253	240	-	-
Core chip	2028.5 (D)	417*	358	581	2330	147	-	-	-	-	121	-
CP 75	2026.49 (D)	230	303	405	1635	1373	212	1284	-	-	-	-
CP 62	2022.60 (D)	189	212	394	3020	1040	183	1036	-	-	-	-
CP 59	2021.76 (D)	217	242	445	3025	1672	208	-	-	-	-	-
CP 41	2016.39 (D)	286*	279	455	2816	1618	195	-	-	593	-	-
CP 9	2006.70 (D)	313*	278	548	2499	1020	153	-	-	299	125	-
MSCT 11	1970.5 (L)	402*	363	476	3152	1644	201	-	161	255	-	210

* = includes montmorillonite

I/M=illite/muscovite, Smec=smectite (montmorillonite, beidellite & saponite), Chl=chlorite, Ill=illite, Kaol=kaolinite, Qtz=quartz, Micro=microcline, Alb=albite, Cal=calcite, Ank=ankerite, Sid=siderite, Pyr=pyrite, Bar=barite

All the XRD results are summarised in the tables above. To facilitate between-sample comparisons of relative abundance for the same mineral, the results in each table are given in counts of peak height. These figures are based on the strongest line for each mineral detected. Caution should be used in assessing relative abundance from these figures since peak height is also significantly affected by factors such as crystal size and crystallinity. For these reasons the figures are even more unreliable when comparing different minerals in the same sample. For example, based on peak height alone carbonate minerals will always appear less abundant than similar proportions of quartz because of differences in crystallinity. Clay minerals will also appear to be less abundant than quartz in a bulk XRD trace because of differences in crystal size. Furthermore, comparison should not be made between peak heights given for bulk samples and those for the clay fractions because results have been influenced by the sampling and preparation methods. XRD will not detect minerals that represent less than approximately 5% of the total rock composition.

Feldspars are dominated by microcline with lesser amounts of albite. In addition, in the core chip from 2028.5m the K-feldspar was identified as sanidine rather than microcline. Quartz is present in all samples and traces of pyrite were noted in selected samples.

In the clay fraction there are variations in the mineralogy between the stratigraphic units. Kaolinite is the most abundant clay mineral in both the Waarre & Flaxman Formations. It is typically highly crystalline and only in Unit A of the Waarre is the kaolin poorly crystalline. Illite was also detected in all samples but it is least abundant in Unit A where it occurs as a discrete mineral (ie it

is not interstratified). Elsewhere, illite is interstratified with very minor amounts of smectite to form illite-smectite. Broadening and asymmetry in the base of the strongest illite peak at 10 Angstroms indicates the presence of smectite. Chlorite is also absent from Unit A. In other stratigraphic units it may be interstratified with trace amounts of smectite as chlorite-smectite. Chlorite peaks are typically broad and this indicates either poor crystallinity or interstratification. Commonly the smectite is present as beidellite or saponite which have a broad peak near 12.5 Angstroms. These peaks are most apparent on the Mg saturated traces. In addition, there are instances where montmorillonite is evident and these appear to be more abundant in the shallower samples. Most of the chlorite-smectite has probably been recorded in thin section descriptions as glaucony (either chlorite &/or glauconite), especially where micas have been replaced.

Barite was noted at the base of Waarre Unit A and in the Flaxman Formation. In the Waarre Sandstone from thin section it appears to be a localised pore filling cement that has replaced kaolin and may have been later partially dissolved. However, it is also possible that the barite is a contaminant from the drilling mud.

7. SCANNING ELECTRON MICROSCOPY

7.1 Casino-3, MSCT 13, depth 2061.5m (Loggers) Waarre Unit A

Reservoir quality in this sandstone is limited by the blockage of pores and pore throats with authigenic cements and clays (Fig. 22a). Typically labile grains are corroded and highly altered and it is possible that minor amounts of the alteration products (especially the very fine kaolin) have been mobilised during sampling further reducing reservoir quality. Micropores are probably the dominant pore type. The highly altered nature of lithics in this sandstone is exemplified by one containing apatite rods, kaolin booklets and fibrous illite (Fig. 22b). The apatite rods have a composition of Ca and P, and a random distribution, although this could be partially the result of sampling. They are hexagonal in cross-section, approximately 1 micron in diameter and 20 microns in length. Given that apatite is a common accessory mineral in all types of igneous rocks it may suggest this was an igneous lithic.

Pore size has been slightly reduced by the presence of quartz overgrowths (Fig. 22c) and feldspar overgrowths (Fig. 22d) but significantly reduced where calcite cements (Fig. 22e) have precipitated. Quartz overgrowths are rare, occurring as both rhombohedra and microcrystalline quartz. Feldspar overgrowths have a composition of Si, Al and K similar to that of the highly corroded cores which have been rimmed. There are at least three phases of carbonate present which can only be differentiated based on their composition. One phase of pore filling spar is calcite and the other is dolomite. Both calcite and dolomite were noted as euhedral rhombohedral spar filling pores and postdating quartz overgrowths. Associated with grain replacing kaolin there is a third phase of carbonate spar. These anhedral to subhedral rhombs and scalenohedra are up to 20 microns in length and composed of siderite (Figs 22f & g). The spar may have precipitated after the kaolin and it contains sufficient Mg where rhombic to be described as high Mg siderite. The irregular habit of some siderite may indicate that it has been partially corroded. Kaolin booklets which have replaced grains are typically subhedral to euhedral pseudo-hexagonal platelets approximately 1 to 5 microns in diameter (Fig. 22g), although examples up to 20 microns were noted. Rarely there is fibrous illite on the margins of grain replacing kaolin (Fig. 22h). This illite appears to be associated with the replaced grains and there is no evidence that authigenic illite bridges pores.

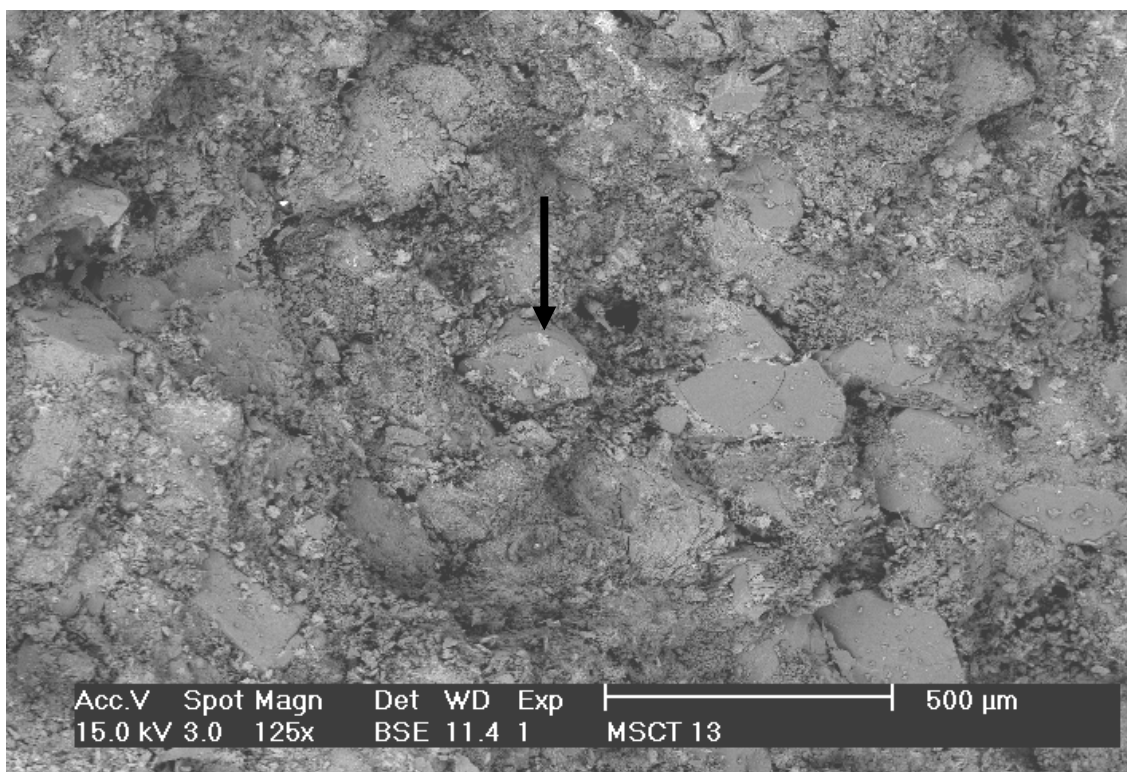


Figure 22a General field of view illustrating the lack of primary intergranular pores due to infilling by very fine grained material. An enlargement of the RHS of the quartz grain marked with an arrow is shown in Figure 22c and the LHS is enlarged in Figure 22f. Backscattered electron photomicrograph. Casino-3, MSCT 13, depth 2061.5m (Loggers). Bar scale 500 microns.

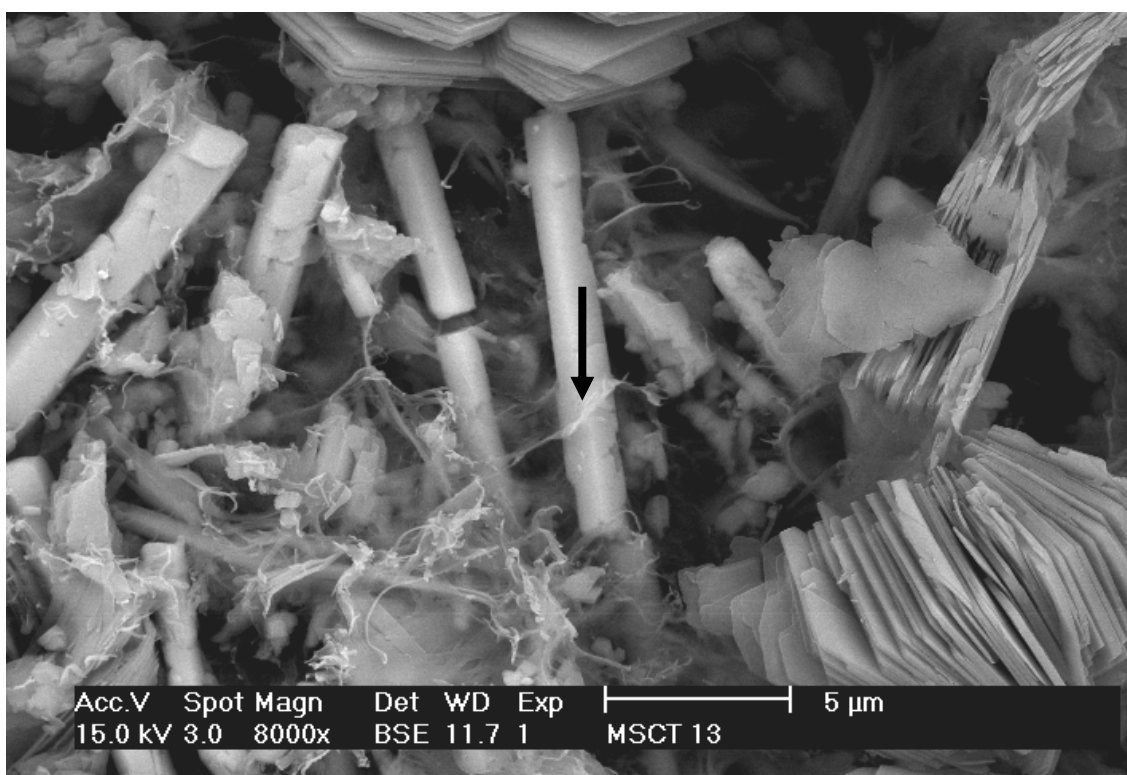


Figure 22b Highly altered igneous lithic with apatite rods partially coated by illite (arrow). Note the kaolin booklets are up to 20 microns in diameter and euhedral. Backscattered electron photomicrograph. Casino-3, MSCT 13, depth 2061.5m (Loggers). Bar scale 5 microns.

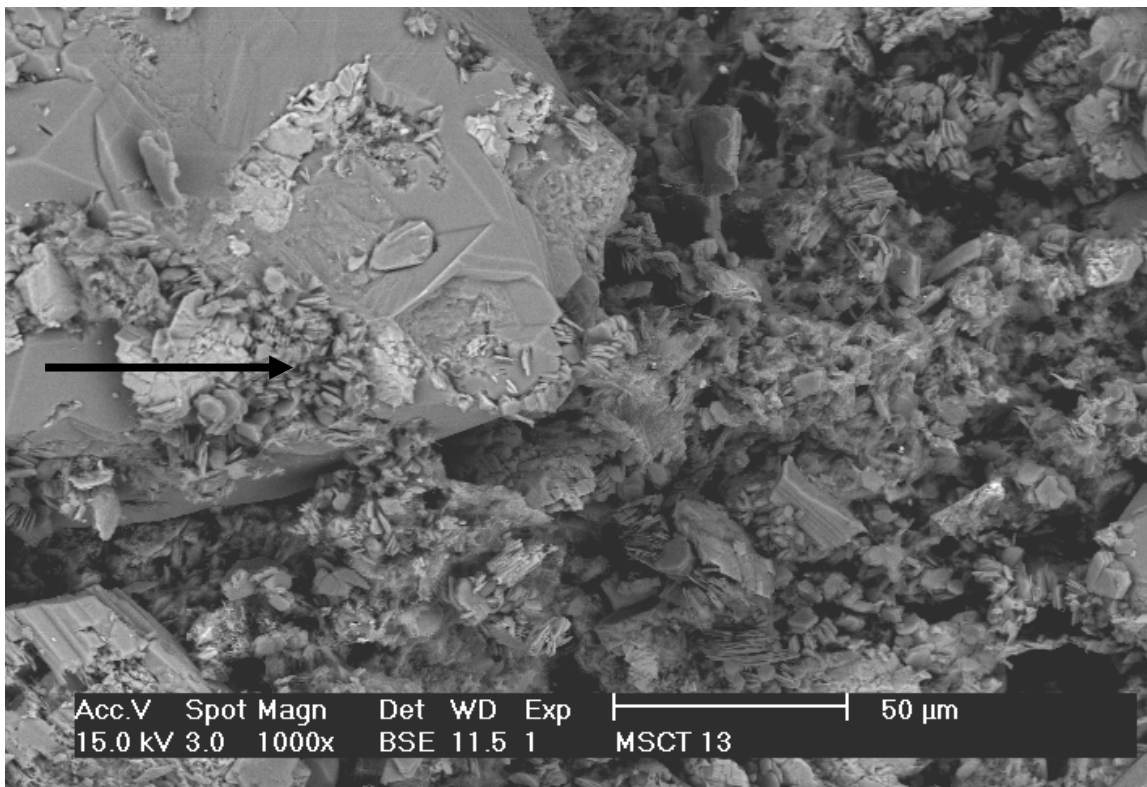


Figure 22c Minor development of quartz overgrowths is indicated by the way kaolin is imbedded in the surface of a quartz grain (arrow). Note the highly corroded nature of the adjacent grain. Backscattered electron photomicrograph. Casino-3, MSCT 13, depth 2061.5m (Loggers). Bar scale 50 microns.

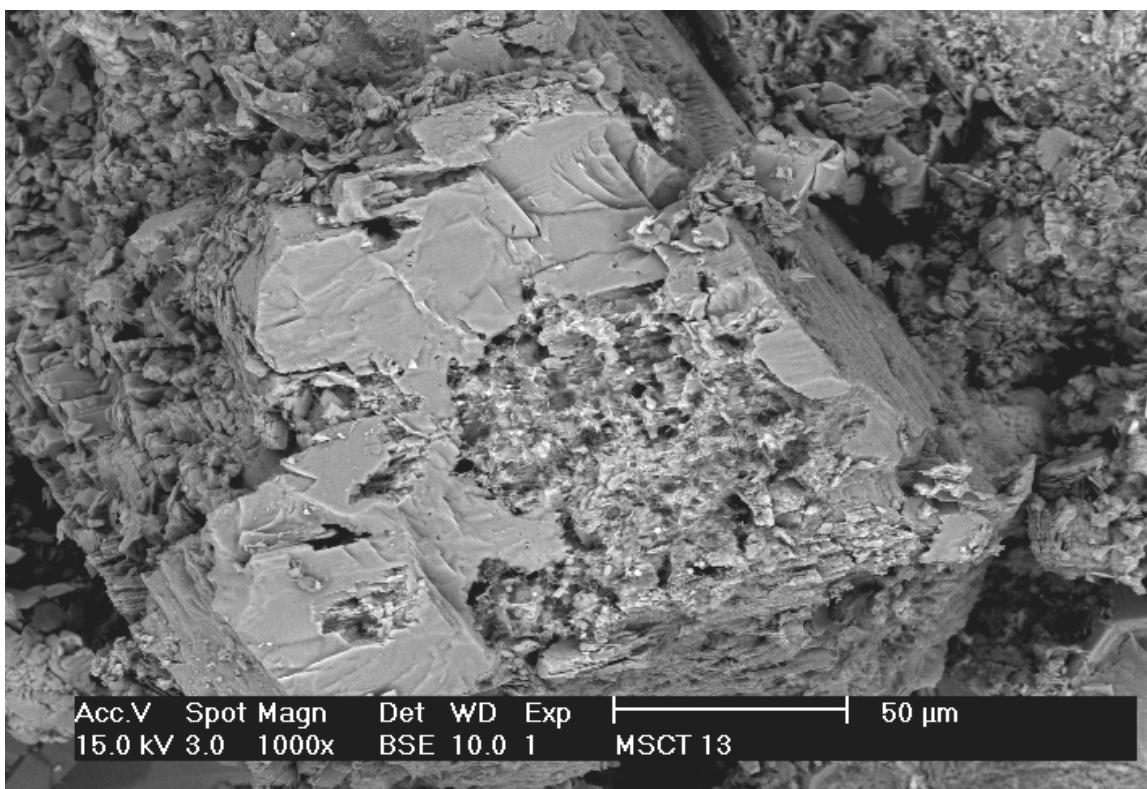


Figure 22d Irregular feldspar overgrowth surrounding a partially corroded detrital core. Backscattered electron photomicrograph. Casino-3, MSCT 13, depth 2061.5m (Loggers). Bar scale 50 microns.

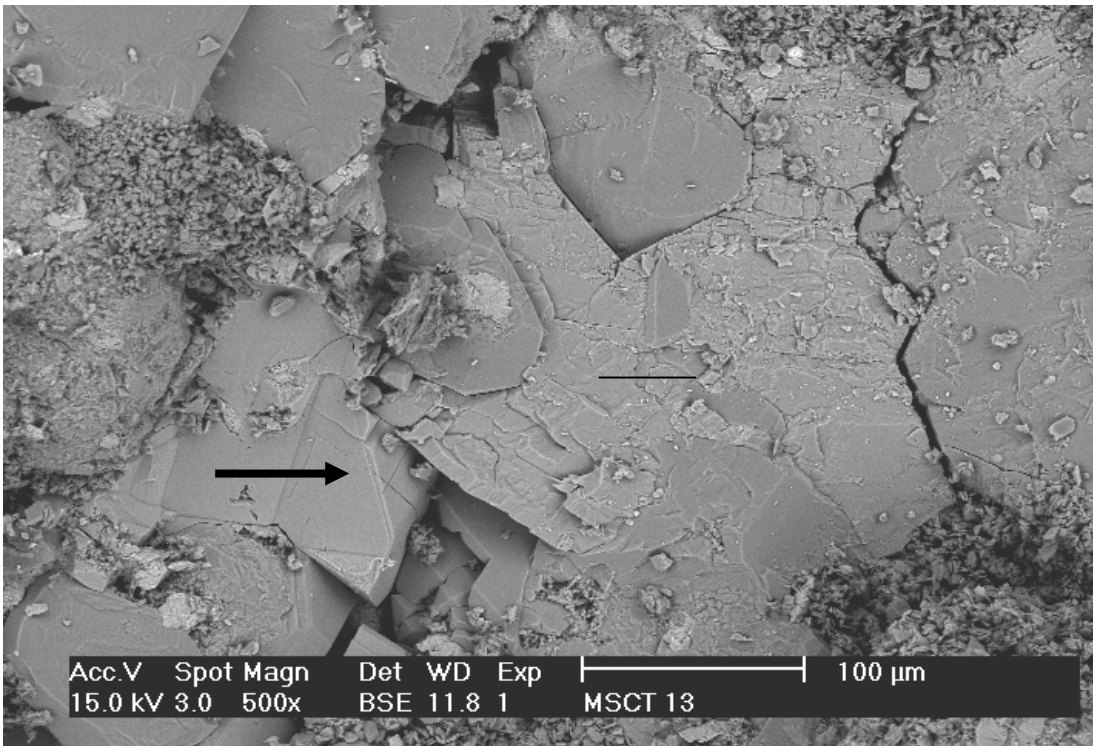
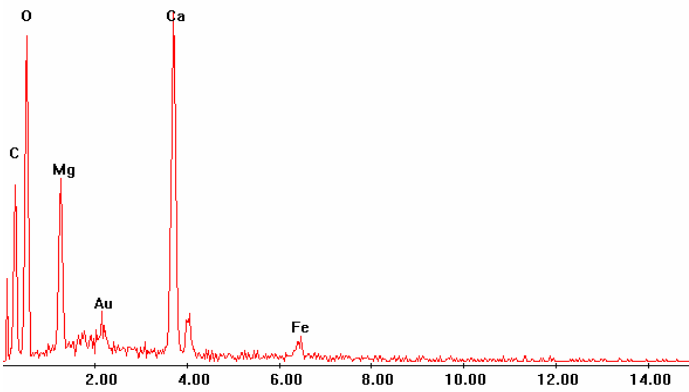
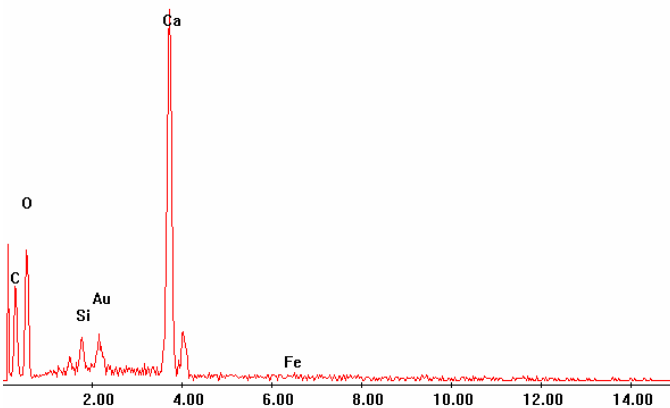


Figure 22e Backscattered electron photomicrograph and associated EDS traces of pore filling euhrhedral, rhombohedral carbonate spar. The small arrow indicates the location of the dolomite EDS analysis and the large arrow is the site of the calcite EDS trace. Note the quartz grains (slightly darker grey) had overgrowths prior to precipitation of the dolomite. Casino-3, MSCT 13, depth 2061.5m (Loggers). Bar scale 100 microns.



EDS trace of dolomite cement. Location indicated in Figure 22e.



EDS trace of calcite cement. Location indicated in Figure 22e.

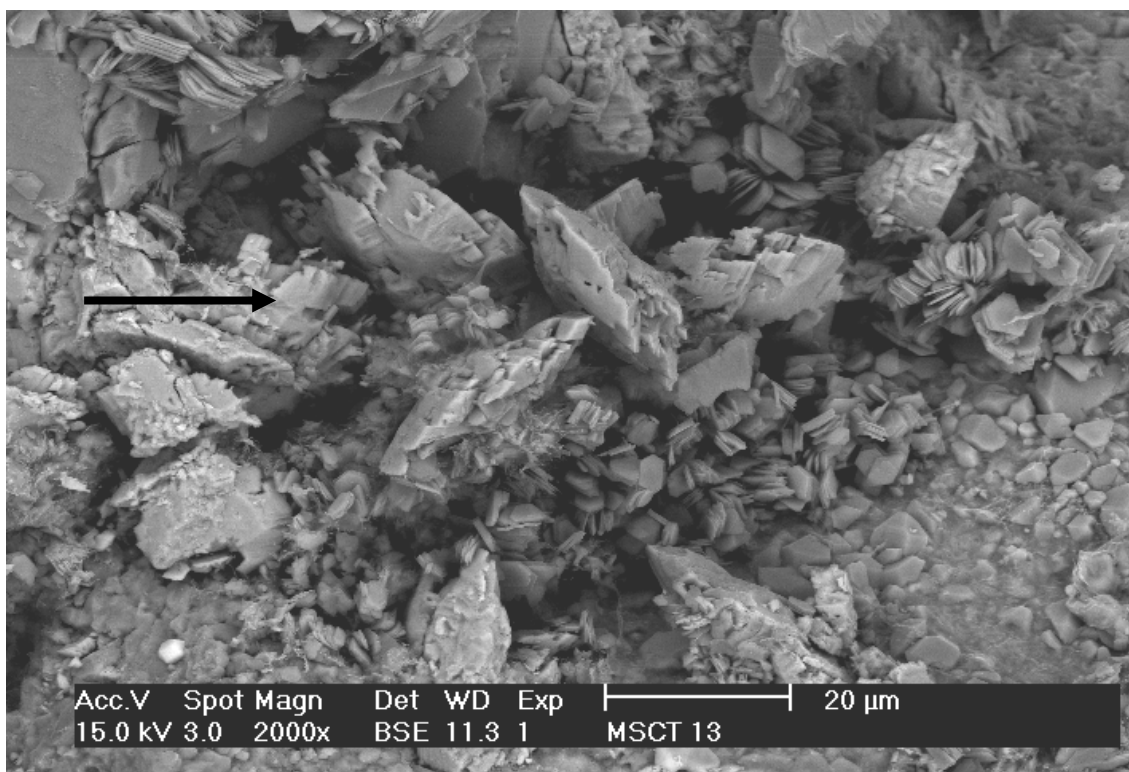


Figure 22f A detrital grain has been replaced by minute kaolin booklets and then irregular high Mg siderite scalenohedra (arrow) precipitated in the kaolin. Note the microcrystalline quartz precipitated on the grain on the RHS. The location of this photomicrograph is shown in Figure 22a. Backscattered electron photomicrograph. Casino-3, MSCT 13, depth 2061.5m (Loggers). Bar scale 20 microns.

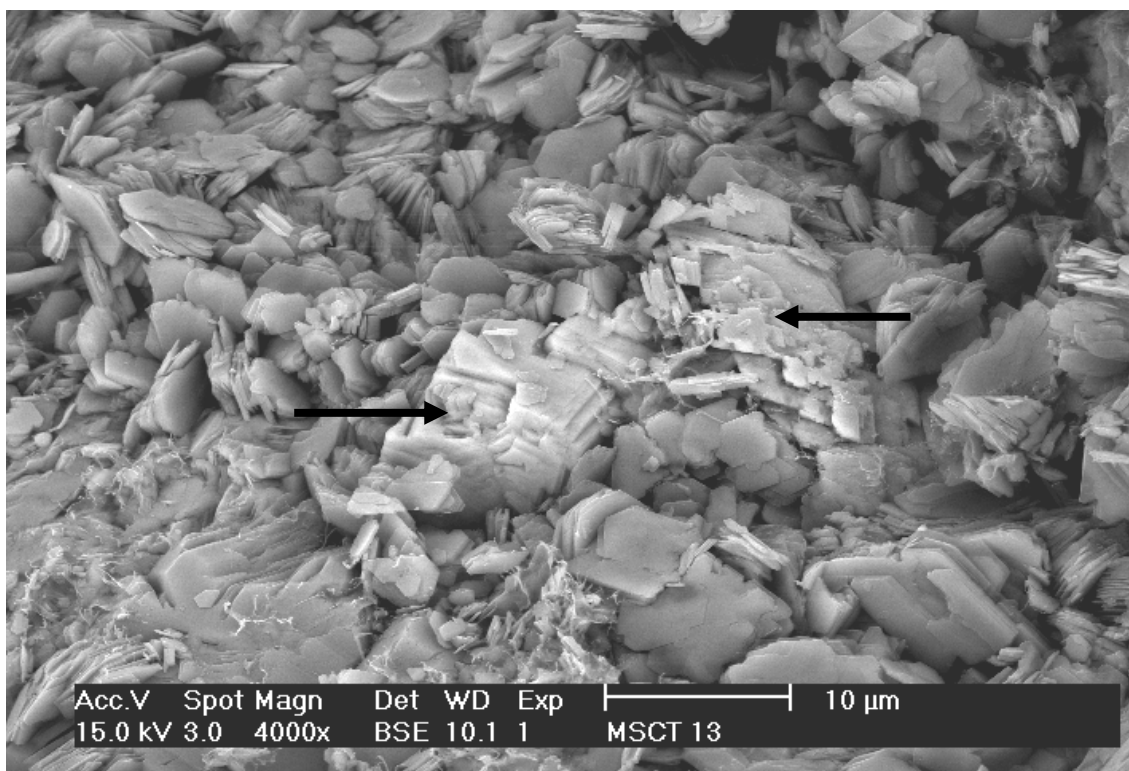


Figure 22g Minute kaolin booklets have replaced this grain followed by high Mg siderite (arrows). Note the variations in carbonate crystal habit, the more anhedral crystal may have been partially dissolved. Backscattered electron photomicrograph. Casino-3, MSCT 13, depth 2061.5m (Loggers). Bar scale 10 microns.

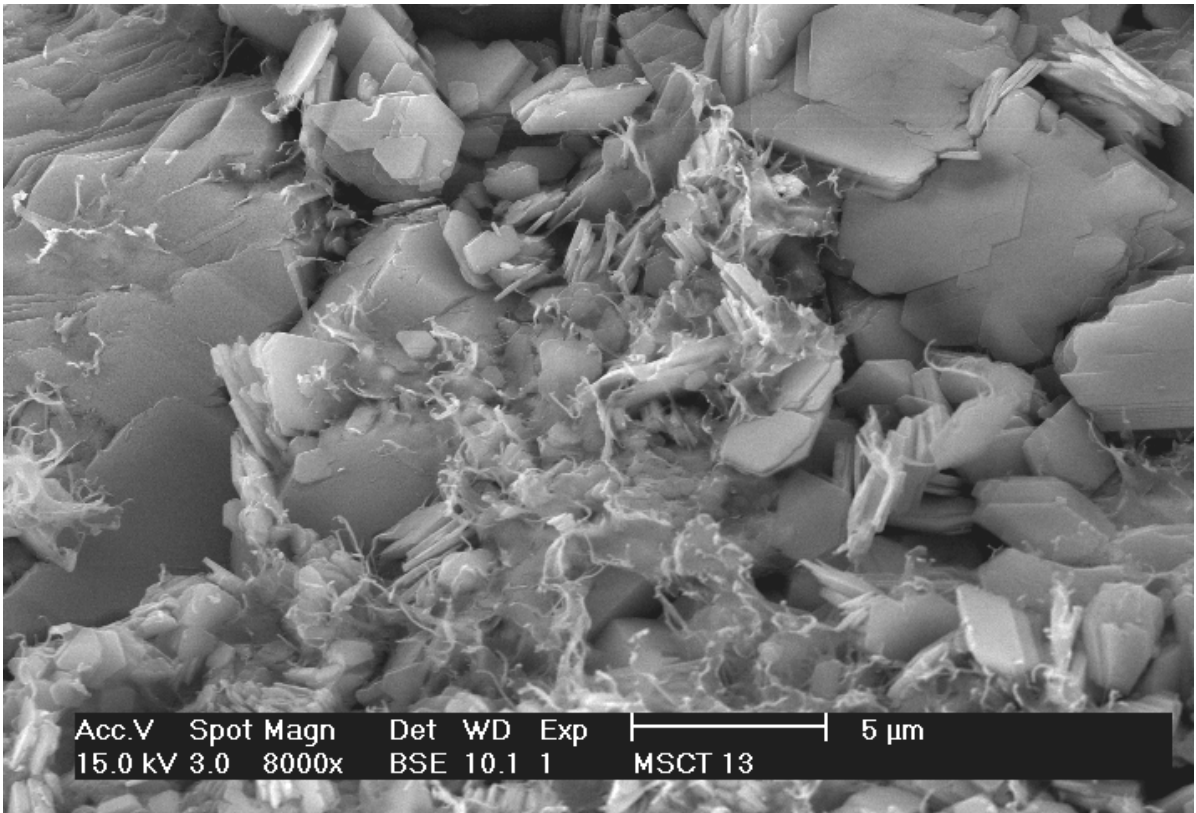


Figure 22h This enlargement of the area immediately below the siderite rhomb in Figure 22g illustrates the presence of minor lettuce-like illite associated with the grain replacing kaolin. Backscattered electron photomicrograph. Casino-3, MSCT 13, depth 2061.5m (Loggers). Bar scale 5 microns.

7.2 Casino-3, Core plug 75, depth 2026.49m (Drillers) Waarre Unit Ca

Framework grains of quartz and K-feldspar were identified in this fine grained sandstone. Reservoir quality is very poor due to the abundance of pore filling calcite spar. Minor fracturing (Fig 23a) and grain plucking was probably the result of sampling. There are secondary dissolution pores and micropores apparent which suggest permeability would be limited.

Detrital clay was recognised from submicron thick platelets aligned tangentially to framework grains (Fig. 23b). This clay has the composition of Si, Al and K which is consistent with the presence of illite. Authigenic clays of kaolin and smectite were also identified. Kaolin occurs as booklets of variable size from approximately 1 to 8 microns in diameter which have replaced grains (Fig. 23c). Typically the booklets are subhedral with ragged edges. They are imbedded in the calcite spar where it fills pores adjacent to kaolin replaced grains. This suggests that calcite postdates the precipitation of kaolin. Calcite spar contains trace amounts of Fe, it forms a blocky cement where it fills primary pores and elsewhere occurs as single rhombohedral crystals up to 10 microns in diameter. The latter were noted within a dissolution pore (Fig. 23d) where remnants of illite-smectite had partially inhibited the calcite (Fig. 23e). Therefore the illite-smectite must have been present prior to the calcite and may have been replacing particular components in the original grain (?lithic).

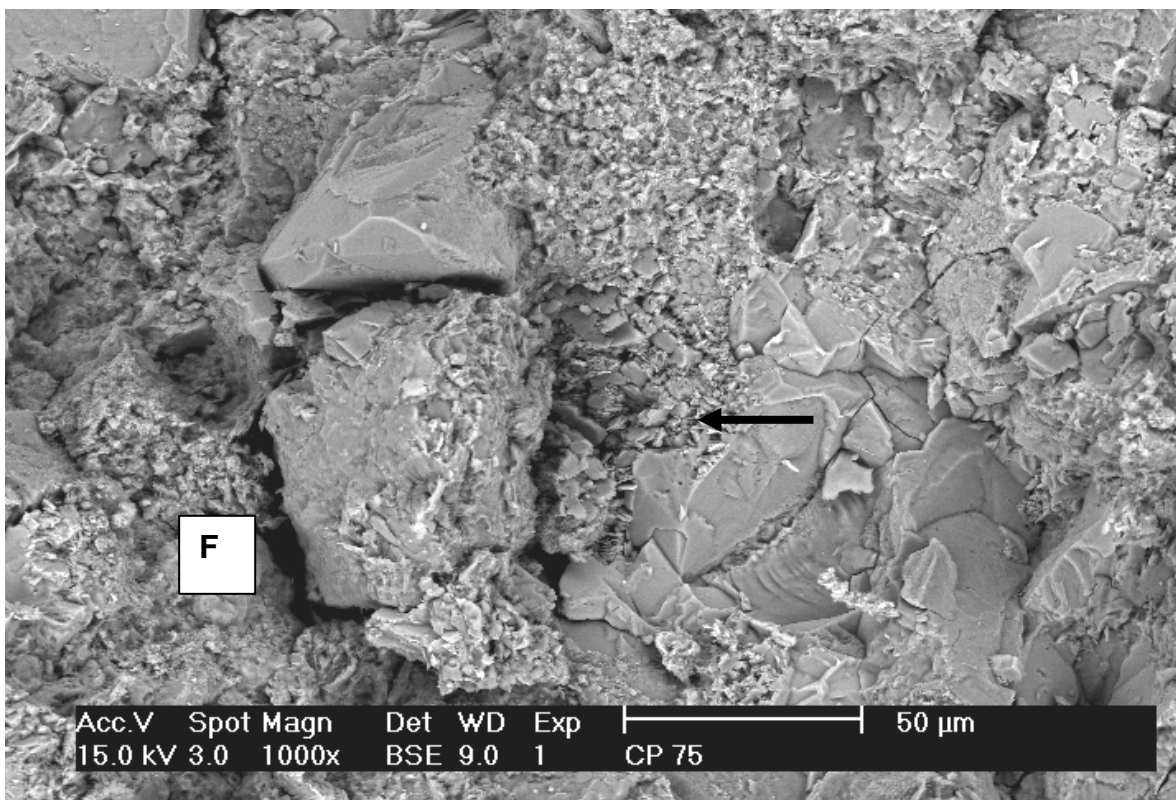


Figure 23a General view illustrating the poor reservoir quality of this sandstone. Minor fracturing (F) around grains was probably the result of sampling. The location of Figure 23c is indicated by the arrow. Backscattered electron photomicrograph. Casino-3, CP 75, depth 2026.49m (Drillers). Bar scale 50 microns.

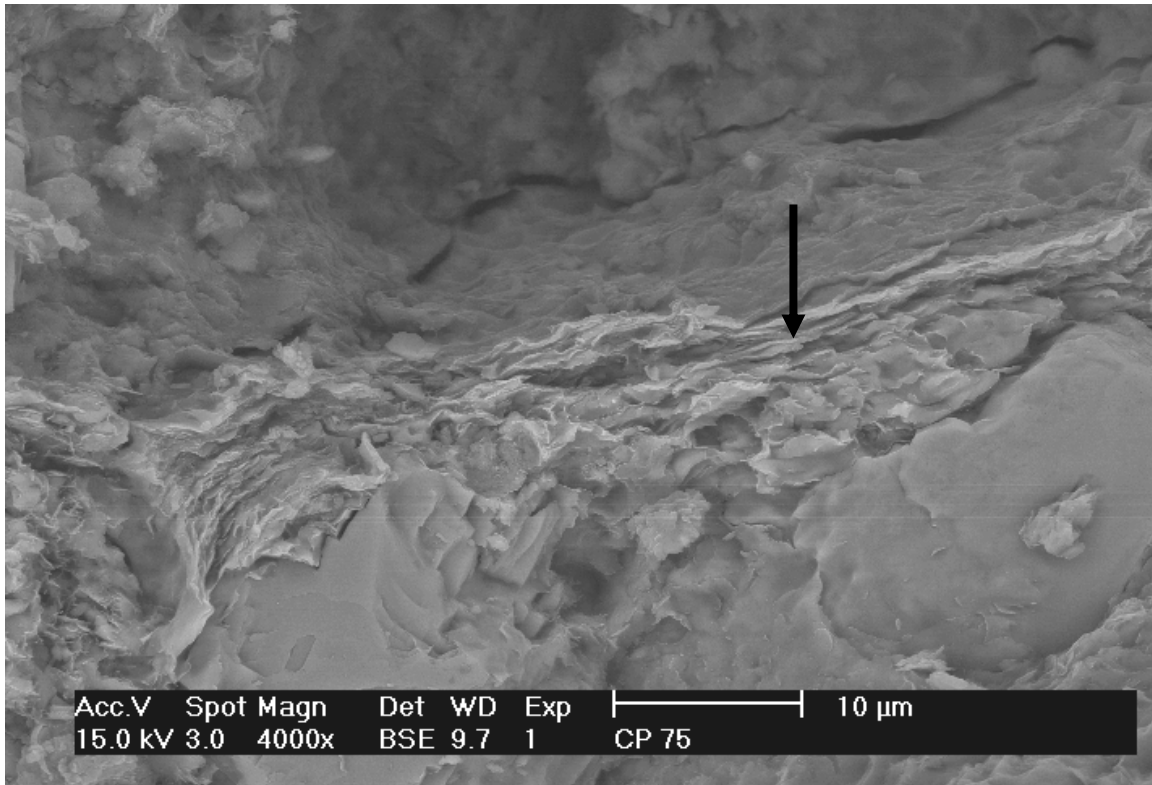
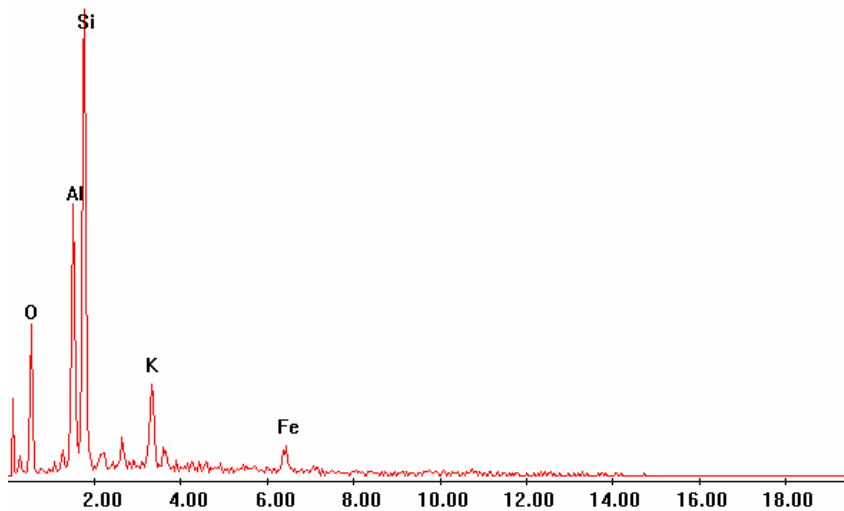


Figure 23b Backscattered electron photomicrograph and associated EDS trace of very thin platelets of detrital clay (arrow) that are aligned tangentially to where a grain was plucked during sampling. The adjacent flat areas are composed of calcite which appears to have replaced grains. Casino-3, CP 75, depth 2026.49m (Drillers). Bar scale 10 microns.



EDS trace of the detrital illite illustrated in Figure 23b.

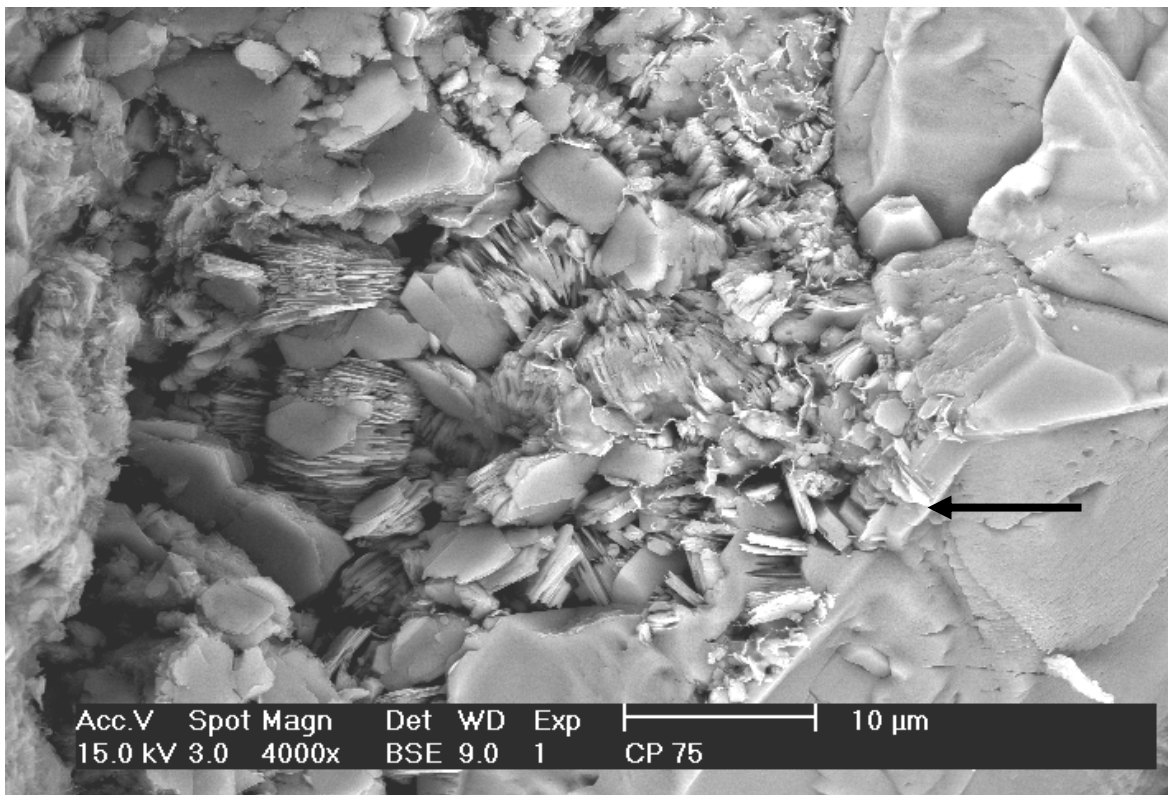


Figure 23c Grain replacing kaolin has been partially engulfed (arrow) when calcite spar precipitated in an adjacent pore. The location of this photomicrograph is illustrated in Figure 23a. Backscattered electron photomicrograph. Casino-3, CP 75, depth 2026.49m (Drillers). Bar scale 10 microns.



Figure 23d Dissolution pore that has been partially filled by calcite crystals (arrow). Backscattered electron photomicrograph. Casino-3, CP 75, depth 2026.49m (Drillers). Bar scale 10 microns.

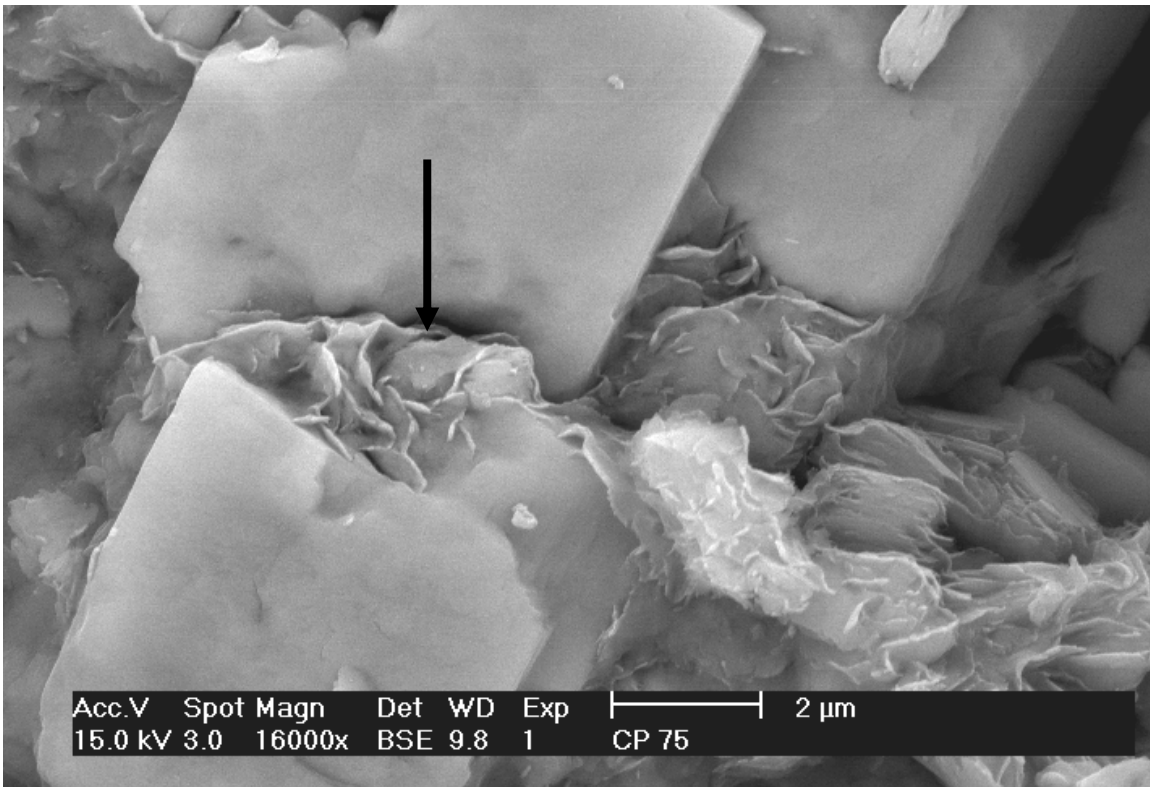
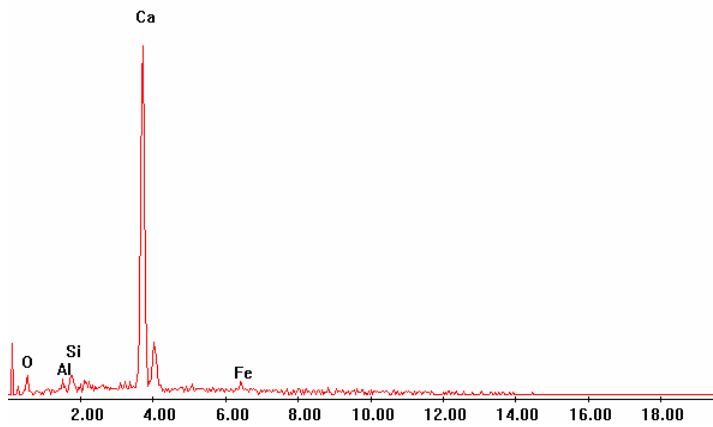
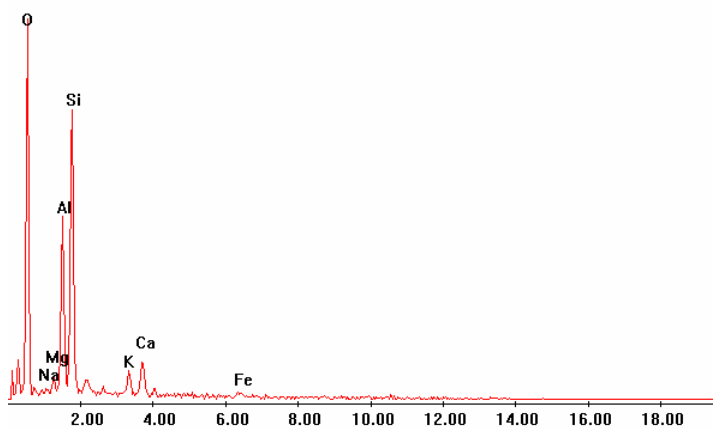


Figure 23e Backscattered electron photomicrograph and associated EDS traces showing an enlargement of the central area in Figure 23d. Calcite crystals have been inhibited by the presence of illite-smectite (arrow). Casino-3, CP 75, depth 2026.49m (Drillers). Bar scale 2 microns.



EDS trace of calcite crystals illustrated in Figure 23e.



EDS trace of interstratified illite-smectite illustrated in Figure 23e.

7.3 Casino-3, Core plug 52, depth 2019.6m (Drillers) Waarre Unit Ca

Reservoir quality in this sandstone should be relatively good because primary intergranular pores have been preserved. These pores are commonly outlined by euhedral quartz overgrowths (Fig. 24a) which have reduced the pore size but minimised the effects of compaction. Porosity has been enhanced by the partial dissolution of K-feldspars (Fig. 24b) and alteration of other feldspars/lithics to illite (Fig. 24c) and other components. Typically the sericitised grains are also partially corroded. Associated with the illite there are traces of more lettuce-like authigenic clay which may indicate the presence of smectite. As noted for previous samples, the smectite is associated with altered grains and does not appear to bridge primary intergranular pores. However, in this example secondary micropores within the altered grains are bridged by the smectite. This distribution of smectite is unlikely to have a major influence on reservoir quality.

Permeability in this sandstone may be reduced by the amount of kaolin which has filled pores and the possibility that it could migrate. Kaolin booklets are typically comprised of subhedral to euhedral pseudo-hexagonal platelets less than 10 microns in diameter (Fig. 24d). Rarely the booklets have a vermiform habit. The kaolin has replaced grains and been squeezed into adjacent pores. Minor amounts of carbonate spar were found where feldspars/lithics had been altered to illite and smectite. The carbonate occurs as euhedral rhombohedra ranging in diameter from 5 to 20 microns (Fig. 24e). EDS analysis indicates a range of compositions for the carbonate from ankerite to ferroan dolomite due to changes in the relative proportions of Mg, Fe and Ca. Ankerite appears to have precipitated prior to the smectite because it is coated by the clay. However, it is possible that the carbonate has simply displaced the smectite as the carbonate crystal developed. Trace amounts of pyrite (Fig. 24f) were noted imbedded in a quartz overgrowth. The minute crystals (less than 1 micron diameter) were probably part of framboids which were destroyed during sampling. The fact that these pyrite crystals are engulfed by authigenic quartz suggests framboidal pyrite precipitated prior to quartz overgrowths.

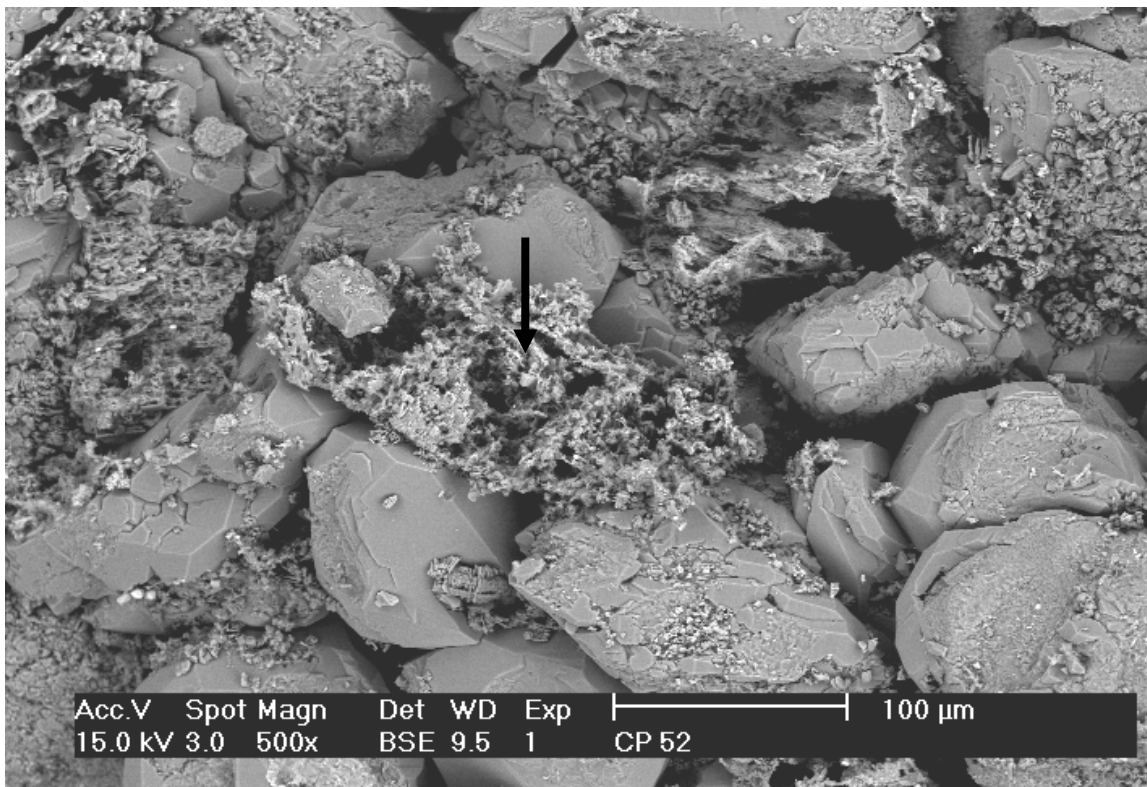


Figure 24a General field of view illustrating the preservation of primary intergranular pores and corroded nature of feldspars. Quartz overgrowths are apparent on the edges of clean pores. The location of Figure 24c is marked with an arrow. Backscattered electron photomicrograph. Casino-3, CP 52, depth 2019.6m (Drillers). Bar scale 100 microns.

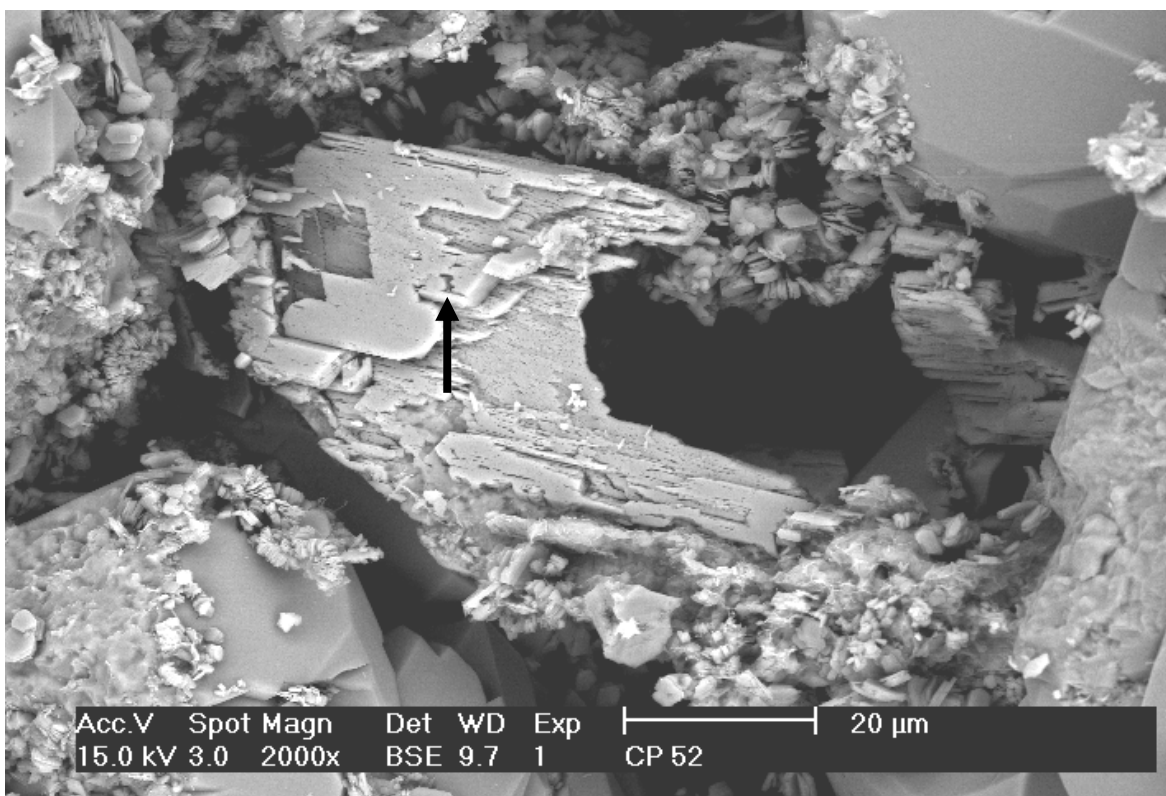


Figure 24b Highly corroded K-feldspar which appears to have an overgrowth (arrow), but this has pitting indicative of dissolution. Backscattered electron photomicrograph. Casino-3, CP 52, depth 2019.6m (Drillers). Bar scale 20 microns.

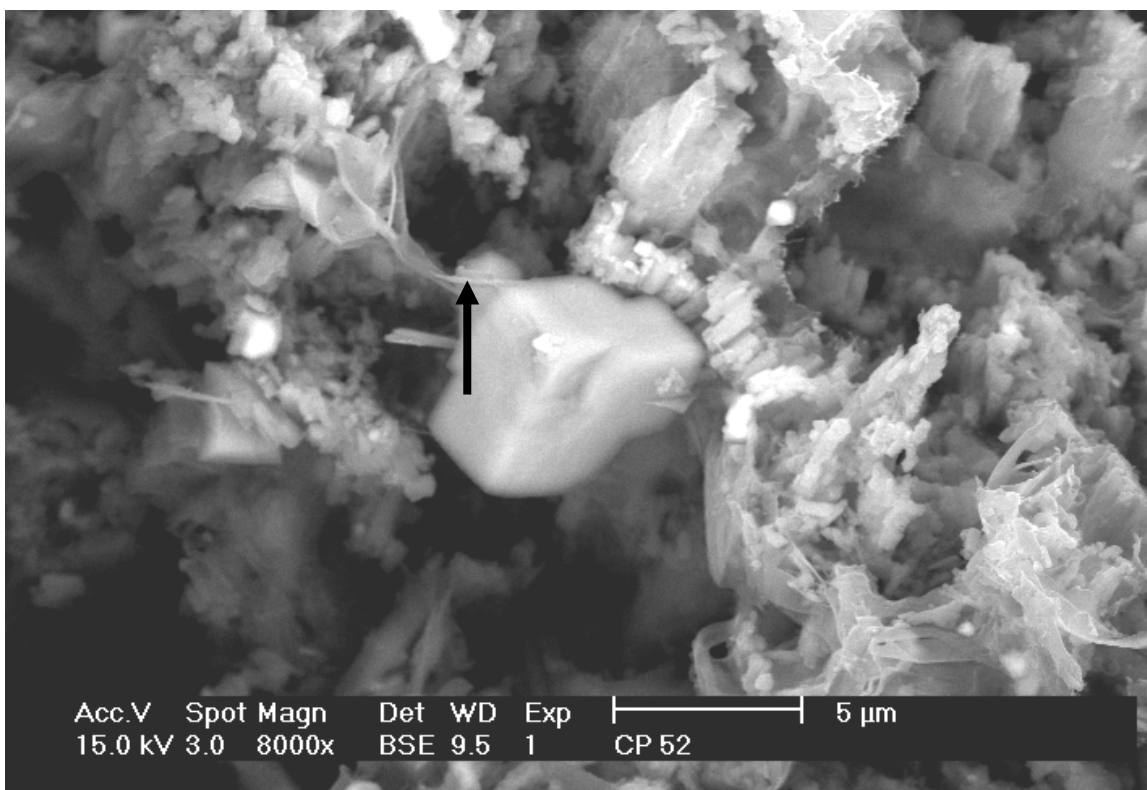
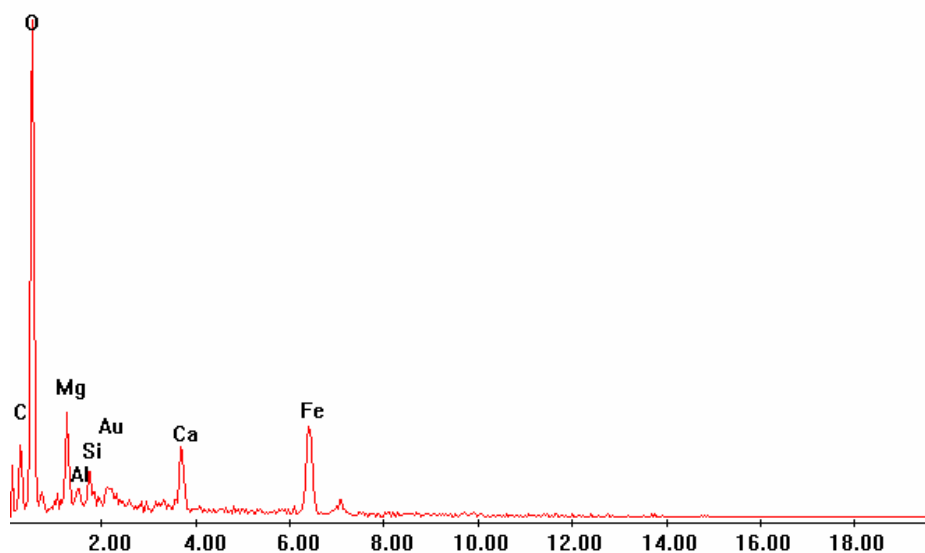


Figure 24c Remnants of corroded and sericitised ?feldspar/lithic includes more lettuce-like smectitic clay (arrow). The latter is bridging a micropore within this highly altered grain. Note the central rhombohedral crystal of ankerite (EDS trace) to which the smectite is attached. Backscattered electron photomicrograph. Casino-3, CP 52, depth 2019.6m (Drillers). Bar scale 5 microns.



EDS trace of ankerite illustrated in Figure 24c.

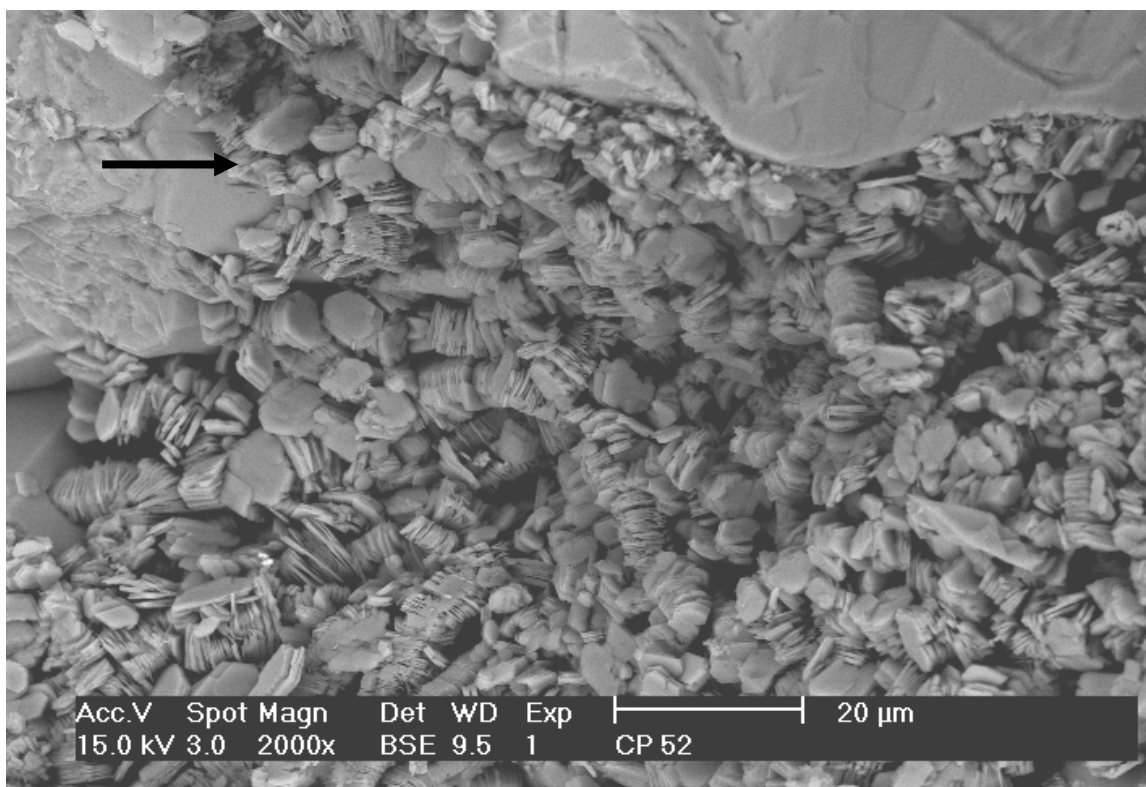


Figure 24d Pore filling and grain replacing kaolin booklets are engulfed by quartz overgrowths on grain margins (arrow). Backscattered electron photomicrograph. Casino-3, CP 52, depth 2019.6m (Drillers). Bar scale 20 microns.

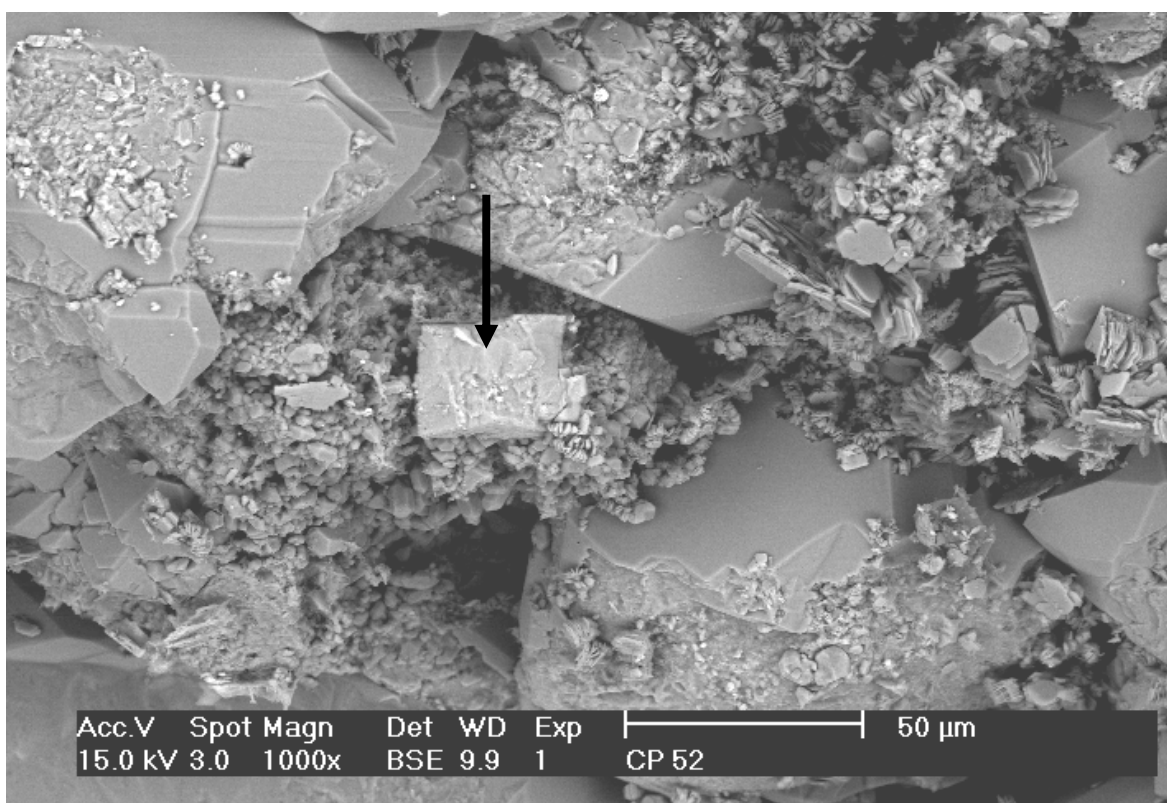
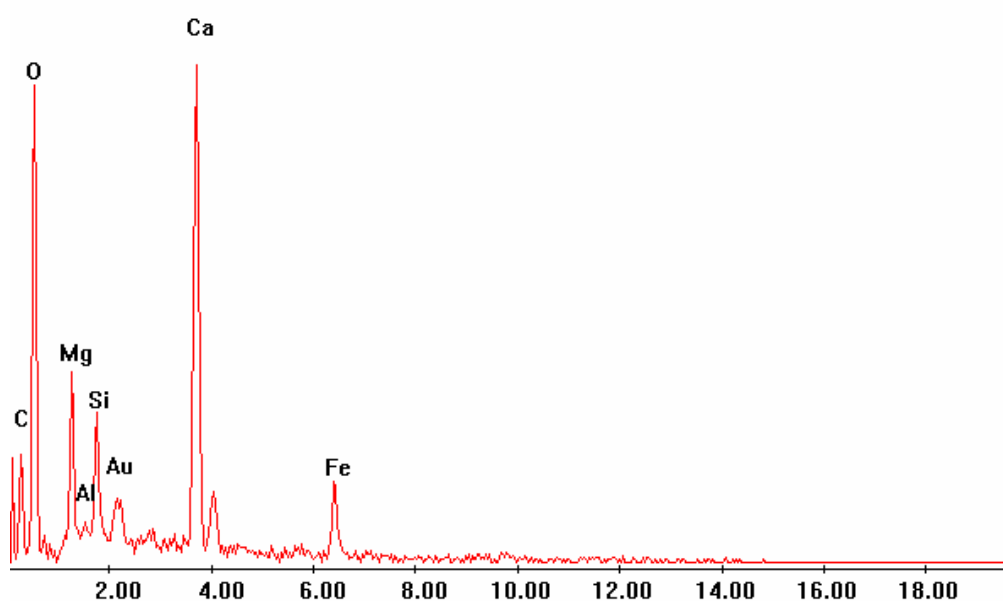


Figure 24e A crystal of dolomite (arrow) has precipitated within a highly altered grain. Note the euhedral quartz overgrowths on surrounding grains and infilling of pores and pore throats by kaolin and corroded material. Backscattered electron photomicrograph. Casino-3, CP 52, depth 2019.6m (Drillers). Bar scale 50 microns.



EDS trace of dolomite illustrated in Figure 24e.

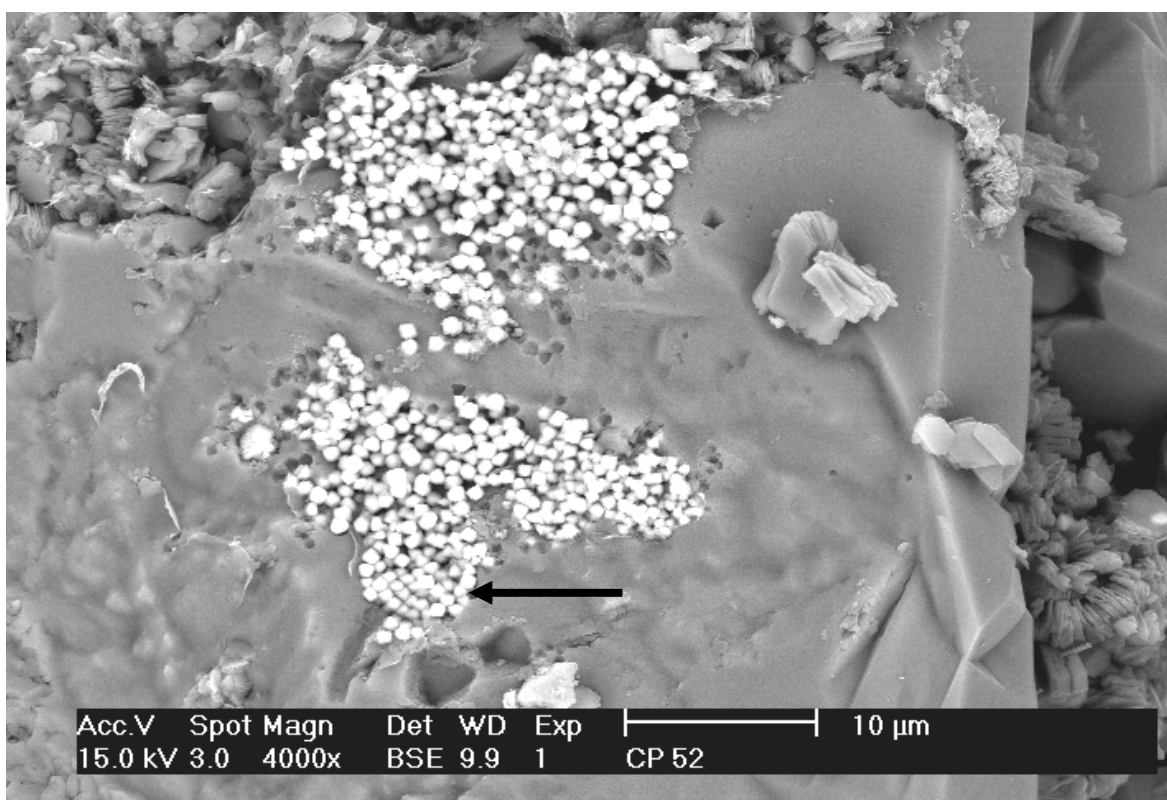


Figure 24f The very bright minute crystals imbedded in this quartz overgrowth are comprised of pyrite. The rounded arrangement of crystals (arrow) suggests these were framboids of pyrite. Backscattered electron photomicrograph. Casino-3, CP 52, depth 2019.6m (Drillers). Bar scale 10 microns.

7.4 Casino-3, Core plug 41, depth 2016.39m (Drillers) Waarre Unit Ca

Reservoir quality was limited by the abundance of siderite cement in this sandstone. There are rare dissolution pores and micropores within highly altered grains. EDS analysis of the siderite indicates the presence of Mg and Ca in addition to the dominance of Fe which indicates chemical substitution of some Fe⁺². Typically the siderite can be recognised as anhedral to subhedral blocky pore filling and grain replacing cement (Fig. 25a). Blocky pyrite has also filled pores in isolated patches and partially replaced grains.

It was very difficult to recognise individual grains on the surface of this sample due to extensive alteration of grains and abundance of cement. Highly altered grains are commonly a mixture of anhedral kaolin booklets, microcrystalline quartz and illite-smectite (Figs. 25b & c). Kaolin booklets are typically 2 to 8 microns in diameter. The microcrystalline quartz is less than 1 micron in diameter. Lettuce-like illite-smectite coats the other components in these grains and could be an alteration product of micas. In addition, there were rare examples of euhedral crystals the composition of which suggest the presence of rutile and possibly staurolite (Figs 25d & 25e). Both these minerals are common in metamorphic schists and gneisses and may indicate that a high percentage of the altered grains were metamorphic lithics.

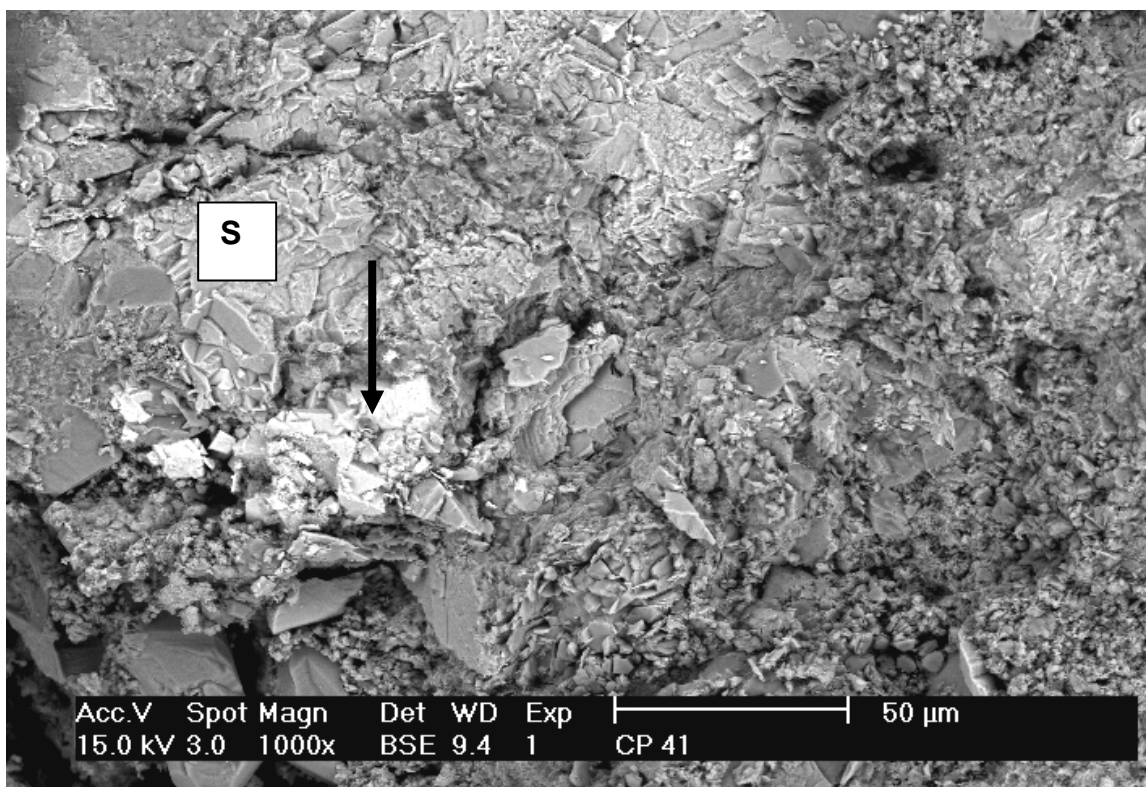


Figure 25a In backscattered mode it is possible to distinguish areas of siderite cement (S) from very bright pyrite cement (arrow) and other more siliceous material. Note the lack of reservoir quality. Backscattered electron photomicrograph. Casino-3, CP 41, depth 2016.39m (Drillers). Bar scale 50 microns.

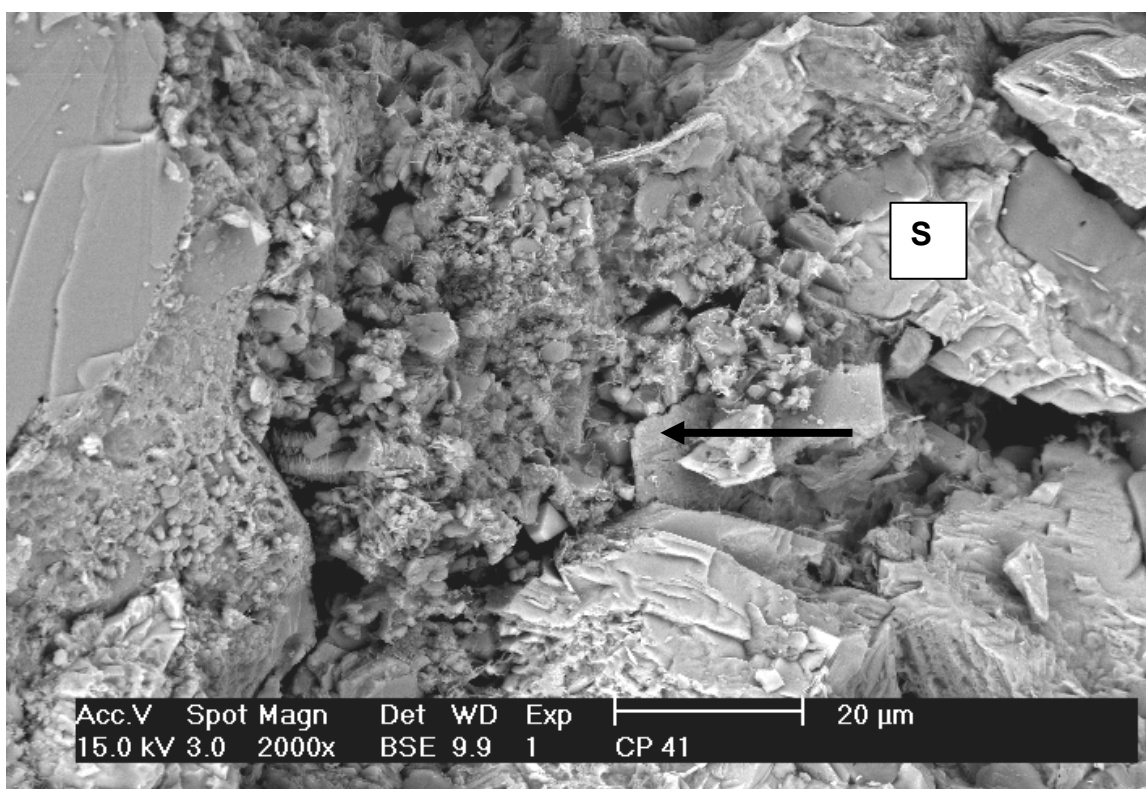


Figure 25b A highly altered grain can be recognised surrounded by light grey siderite cement (S) and quartz (darker grey). The location of Figure 25c is indicated by the arrow. Backscattered electron photomicrograph. Casino-3, CP 41, depth 2016.39m (Drillers). Bar scale 20 microns.

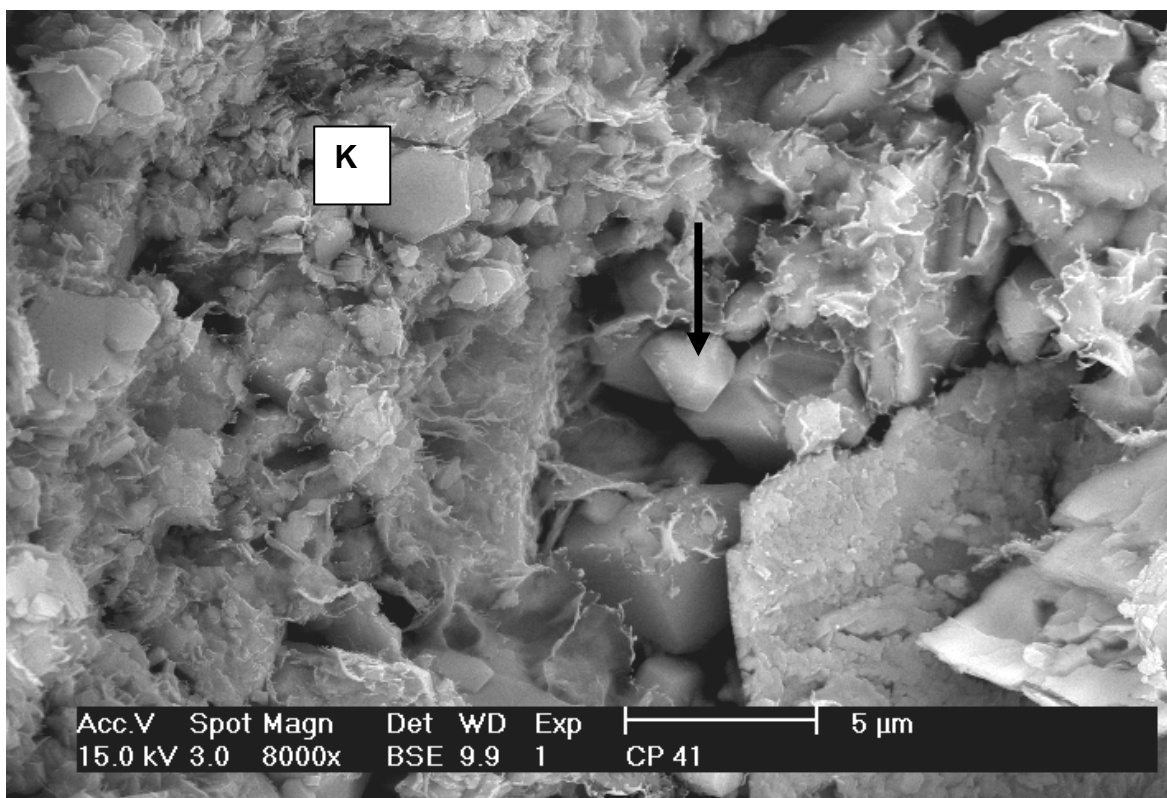
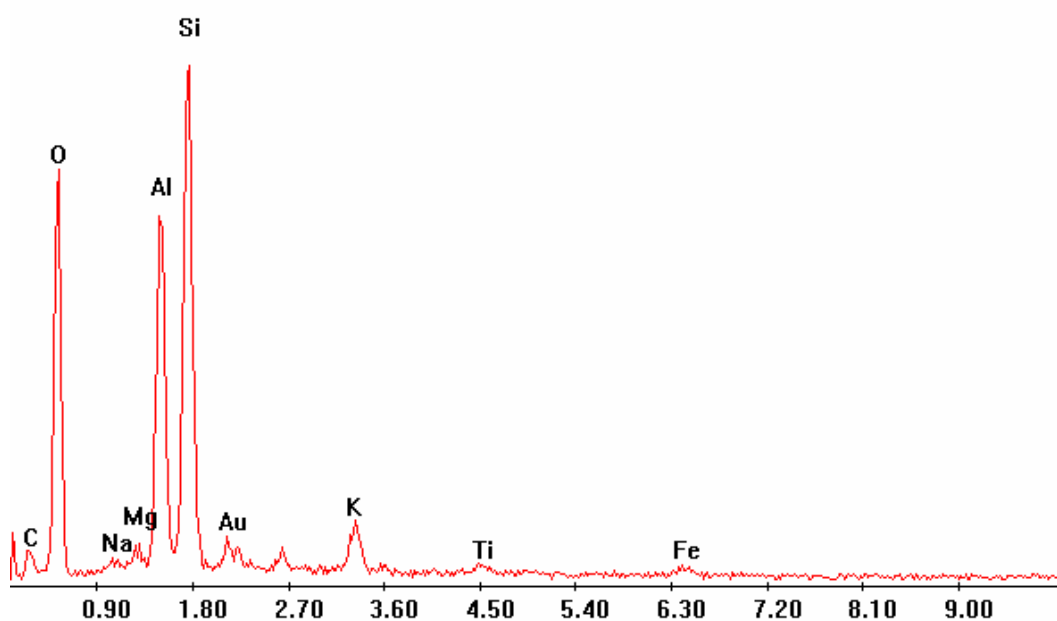


Figure 25c Enlargement of Figure 25b illustrating the composition of this highly altered grain. There are pseudo-hexagonal kaolin booklets (K), microcrystalline quartz (arrow) and lettuce-like smectite apparent. Backscattered electron photomicrograph. Casino-3, CP 41, depth 2016.39m (Drillers). Bar scale 5 microns.



EDS trace of the smectite in Figure 25c includes K which may indicate this is interstratified illite-smectite.

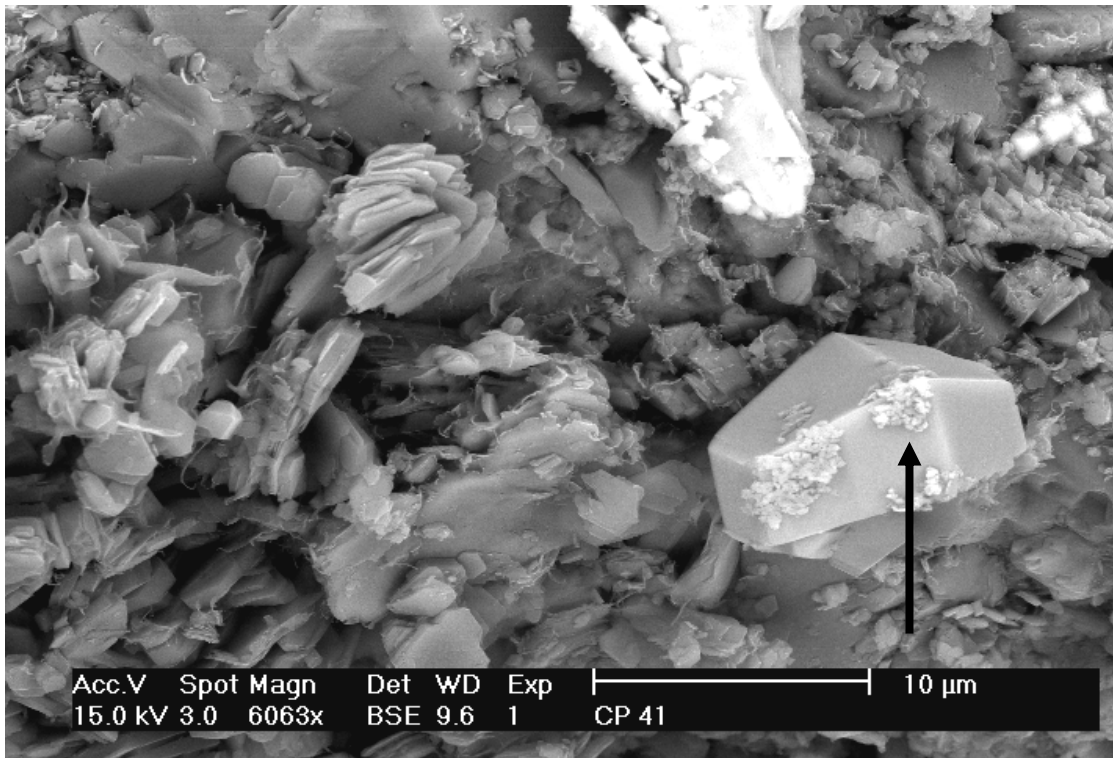


Figure 25d Another altered grain with kaolin booklets, minor illite flakes, very bright pyrite and a euhedral crystal (arrow) which has a composition of Ti. The composition suggests this crystal is rutile. Backscattered electron photomicrograph. Casino-3, CP 41, depth 2016.39m (Drillers). Bar scale 10 microns.

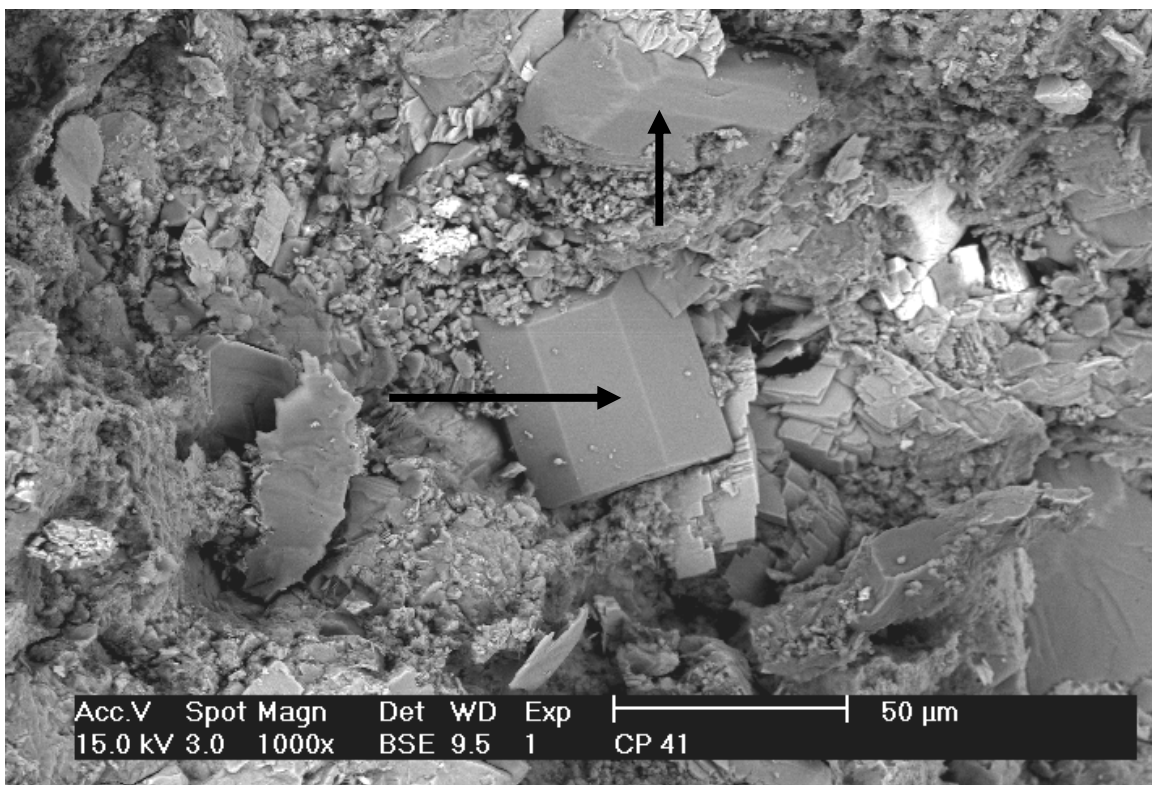
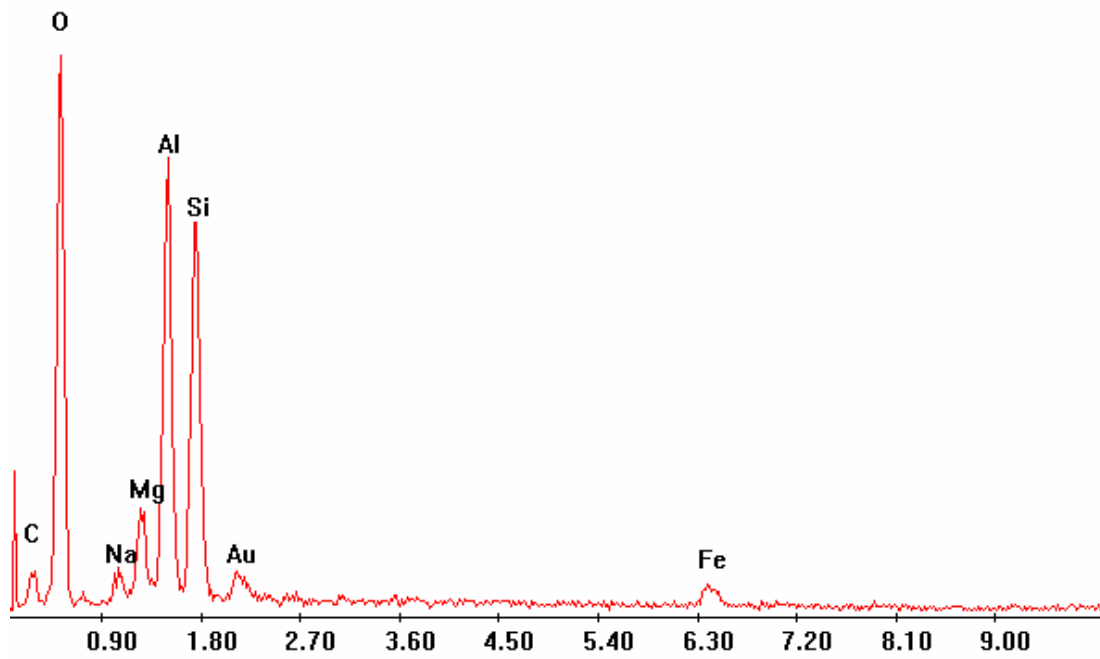


Figure 25e Again this highly altered grain contains euhedral crystals (arrows) the composition of which might indicate the presence of staurolite. On the RHS of the central crystal there is minor siderite cement and the other very bright areas are composed of pyrite. Backscattered electron photomicrograph. Casino-3, CP 41, depth 2016.39m (Drillers). Bar scale 50 microns.



EDS trace of the staurolite illustrated in Figure 25e.

7.5 Casino-3, Core plug 5, depth 2005.46m (Drillers) Waarre Unit Cb

Reservoir quality in this sandstone should be good because primary intergranular pores have been preserved (Fig. 26a). The elongate nature of these pores indicates that permeability has not been restricted and this would explain why there are traces of drilling mud throughout the sample. In all instances where the drilling mud contamination was analysed it was composed of sylvite (KCl). Typically intergranular pores have angular outlines due to the presence of euhedral quartz overgrowths which in places are incipient (Fig. 26b). The relative lack of labile grains in this sample has ensured that quartz overgrowths could precipitate. Porosity has been enhanced by the partial dissolution of K-feldspars to form honeycomb pores, but this would not significantly improve permeability. Feldspars have also been altered to kaolin and these booklets are commonly imbedded in the quartz overgrowths. Kaolin may have reduced permeability where it appears to have migrated (Fig. 26c). Alternatively this damage was caused during sample preparation for the SEM. The only other authigenic mineral identified was siderite which has precipitated within an altered grain (Fig. 26d). Siderite occurs as subhedral to euhedral scalenohedra up to 50 microns in length. EDS of the siderite detected the presence of Fe, Mg and Ca similar to the composition of siderite in Core plug 41.

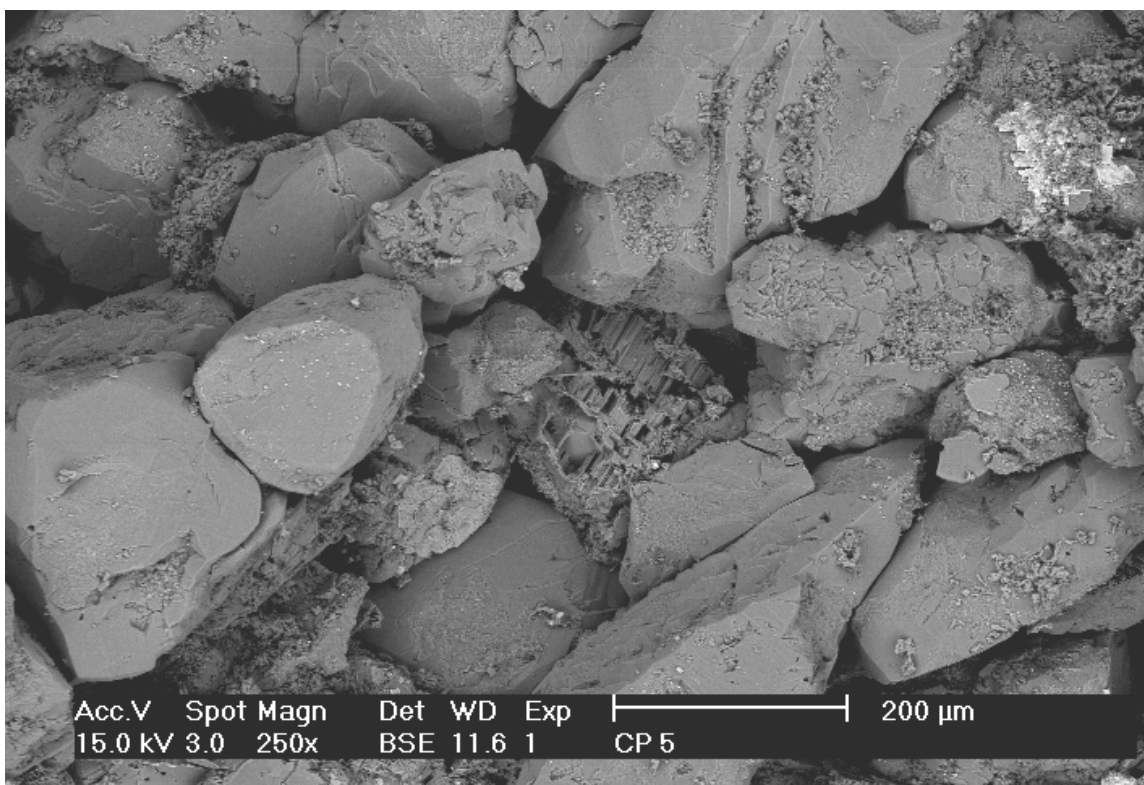


Figure 26a General view illustrating the excellent preservation of primary intergranular pores. Note the central grain of partially dissolved K-feldspar and the speckled bright patch of sylvite. Backscattered electron photomicrograph. Casino-3, CP 5, depth 2005.46m (Drillers). Bar scale 200 microns.

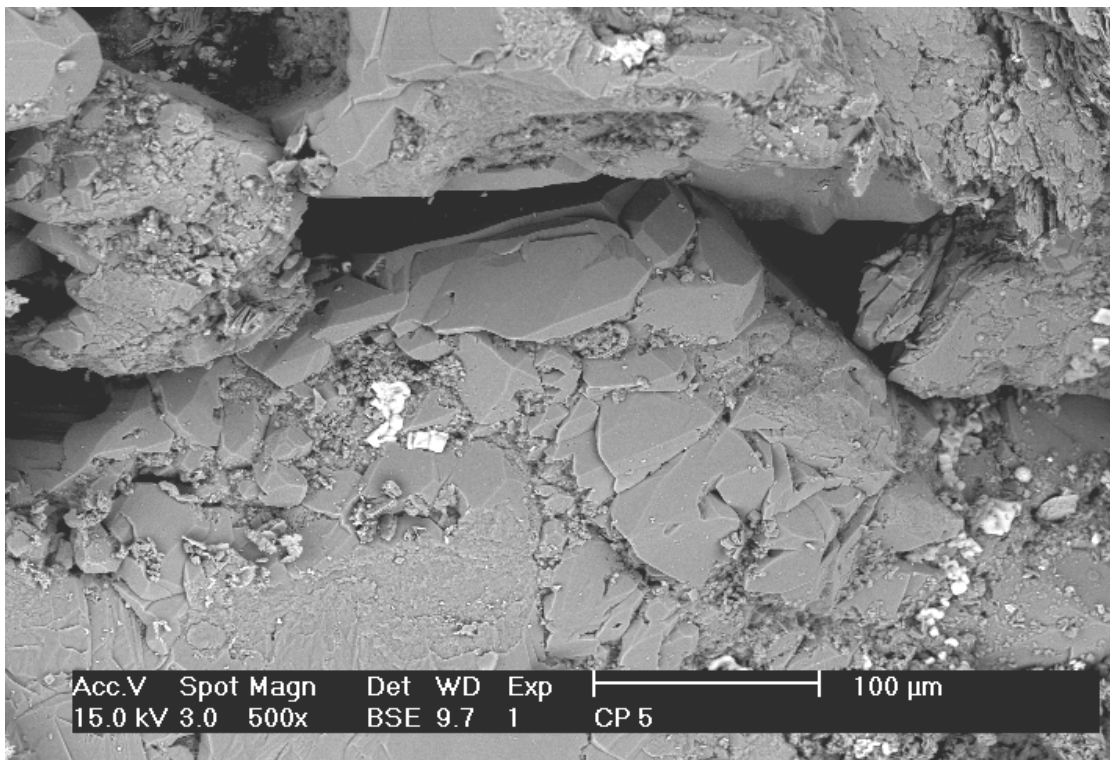


Figure 26b The quartz overgrowth on this central grain is comprised of multiple coalescing smaller euhedral to subhedral crystals. Kaolin booklets are trapped between the overgrowths and there are very bright specks of sylvite on the surface. Backscattered electron photomicrograph. Casino-3, CP 5, depth 2005.46m (Drillers). Bar scale 100 microns.

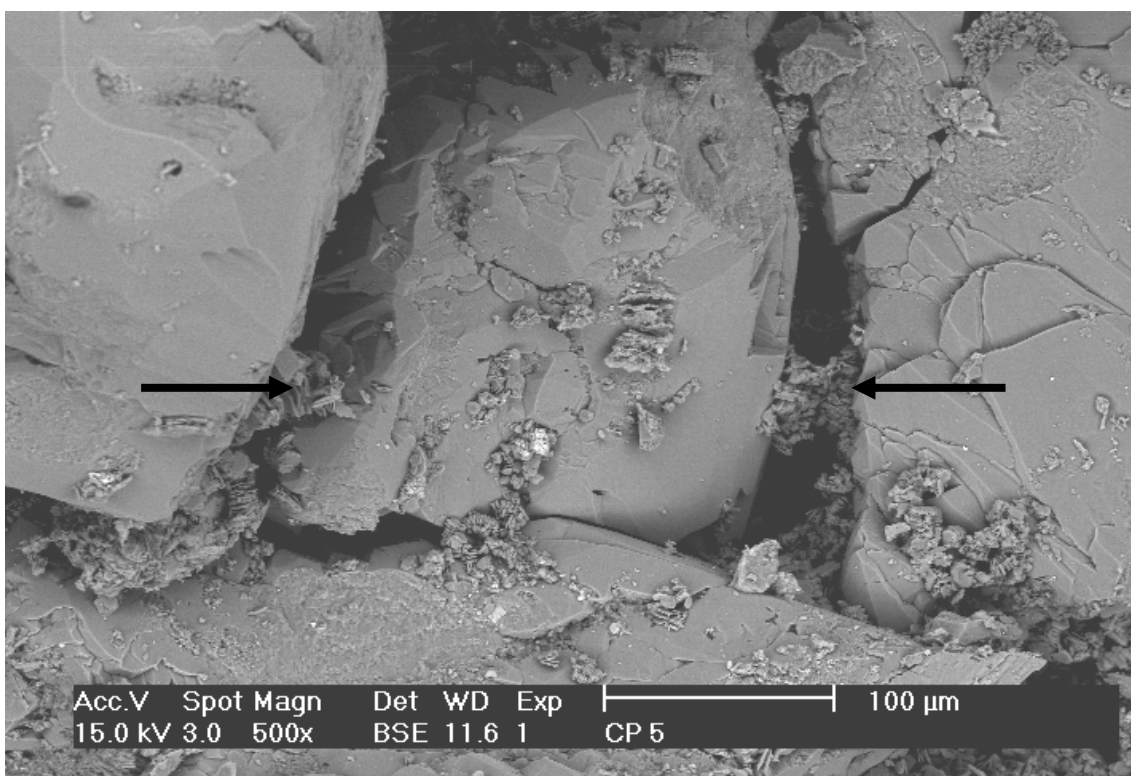


Figure 26c Kaolin (arrows) appears to have migrated into the pores either side of a quartz grain. Alternatively, this damage was caused during sample preparation. Backscattered electron photomicrograph. Casino-3, CP 5, depth 2005.46m (Drillers). Bar scale 100 microns.

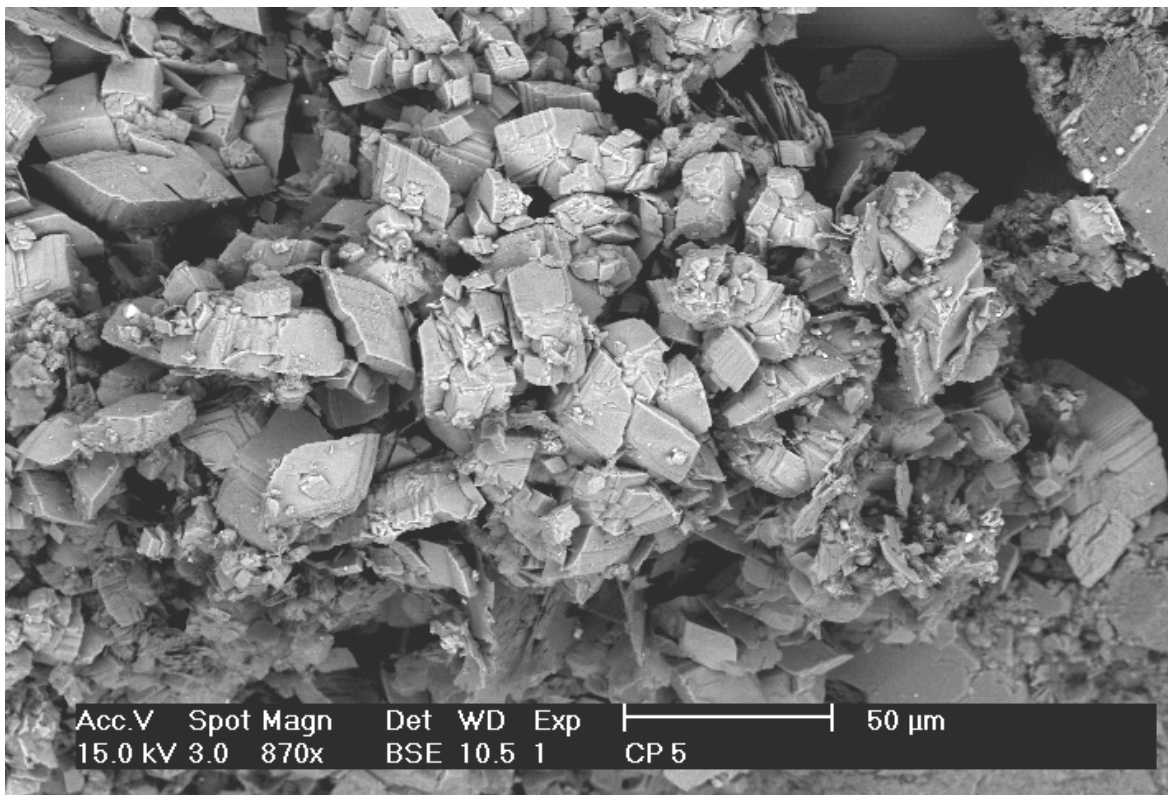
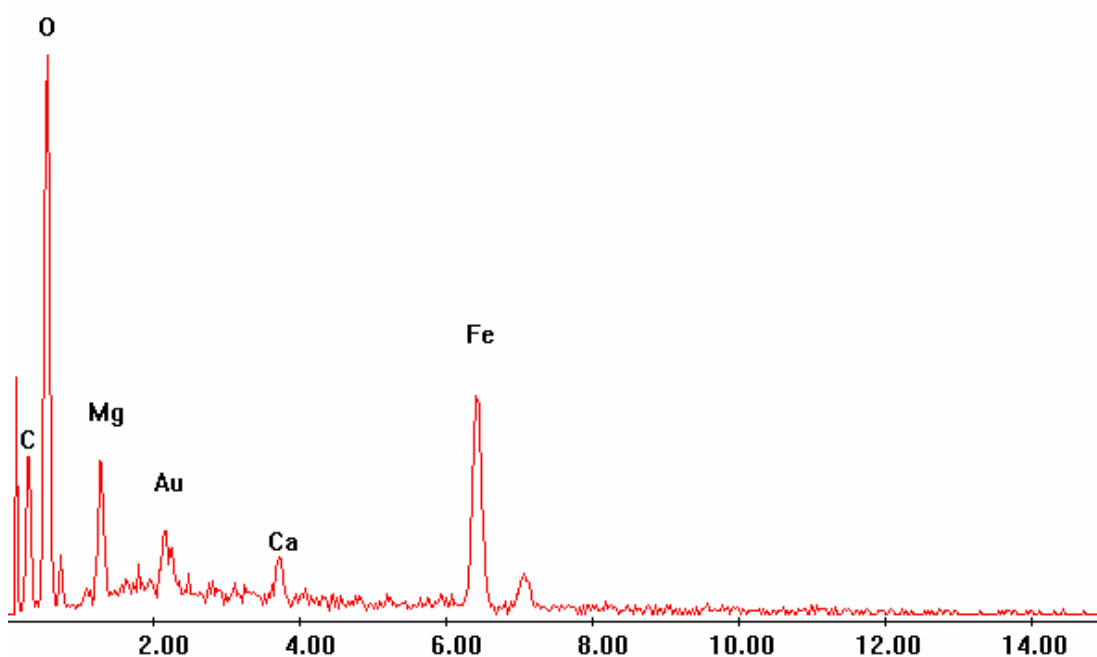


Figure 26d Siderite scalenohedra have precipitated in a highly altered labile grain. Kaolin is the main component of the altered grain. Backscattered electron photomicrograph. Casino-3, CP 5, depth 2005.46m (Drillers). Bar scale 50 microns.



EDS trace of high Mg siderite illustrated in Figure 26d.

8. DISCUSSION

All references to depths used in this discussion and the associated diagrams are corrected log depths (Table 1). Stratigraphic subdivisions for Casino-1, -2 and -3 were correct as of 13th January 2004 (*pers comm* M. Zwigulis). Formation tops had been modified since the petrology study on samples from Casino-1 and Casino-2 (Phillips, 2003).

8.1 Lithology & texture

a. Casino-3

Waarre Formation sandstones studied from Unit A are comprised of medium to coarse grained, poor to moderately well sorted, texturally submature sublitharenites and feldspathic litharenites (Fig. 27a). The basal samples (MSCTs 6, 5, 4) are carbonate cemented lithologies. It is possible that if the composition of grains replaced by carbonates was known for MSCTs 6 and 5 that these sediments would originally have been litharenites or possibly feldspathic litharenites. Grain size distributions are unimodal and symmetrical, although there is a slight tendency to positive skewness in the medium grained sands. Grain shape is typically angular to subangular with low to moderate sphericity. Grains are slightly more angular in shallower feldspathic litharenites. Grain alignment, variations in grain size and lithic content indicates the presence of planar bedding in the sandstones. Bioturbation is apparent in the feldspathic litharenite of MSCT 4 and an incipient siderite nodule has formed in MSCT 13.

Sandstones from Unit Ca in Casino-3 are comprised of very fine to medium grained, poor to well sorted, sublitharenites and subarkoses (Fig. 27a). The shallowest sample (core plug 9) is an interlaminated mudstone and very fine grained sandstone, and the basal sample (core chip at 2032.5m) is a very fine grained, poorly sorted greywacke. Three of the very fine grained sublitharenites are carbonate cemented (CPs 75, 62 & 41). Grain size distributions for the sandstones are unimodal and symmetrical with only slight negative skewness apparent in core plug 31. In contrast, the grain size distribution for the greywacke is polymodal and negative skewed, and the interbedded mudstone-sandstone is bimodal and positive skewed. Grain shape ranges from angular to subrounded with low to moderate sphericity. Planar laminae that are 1 to 3mm in thickness are common in the finer grained sandstones. Bioturbation of these sediments is apparent from the presence of burrows disrupting laminae. Ripples, flaser bedding, lenticular bedding, dewatering structures and a burrow are apparent in the interlaminated mudstone and very fine grained sandstone of core plug 9. Medium grained subarkoses (CPs 31 & 12) near the top of the sequence have evidence of cross bedding and bioturbation is absent.

The four samples from Unit Cb at Casino-3 are comprised of medium grained, moderately to well sorted, texturally mature, subarkoses (Fig. 27a). Negative skewness is apparent in the grain size distributions of core plug 5 and MSCT 1. Other samples have unimodal and symmetrical grain size distributions. Grain shape is angular to subrounded with low to moderate sphericity in MSCT 1 and subangular to subrounded in the other samples. Bedding is poorly defined by weak grain alignment and changes in grain size. Cross bedding is outlined by the abundance of organic matter and changes in grain size in the moderately sorted subarkose of MSCT 1.

Sediments studied from the Flaxman Formation in Casino-3 (MSCT 11) are comprised of a medium grained, very poorly sorted, texturally submature carbonate cemented sublitharenite. Grain size distribution is almost bimodal and negatively skewed. One peak occurs near the middle of the fine sand classification and the other is in the medium to coarse sand grain size. Grain shape is angular to subrounded with low to moderate sphericity and planar bedding is evident.

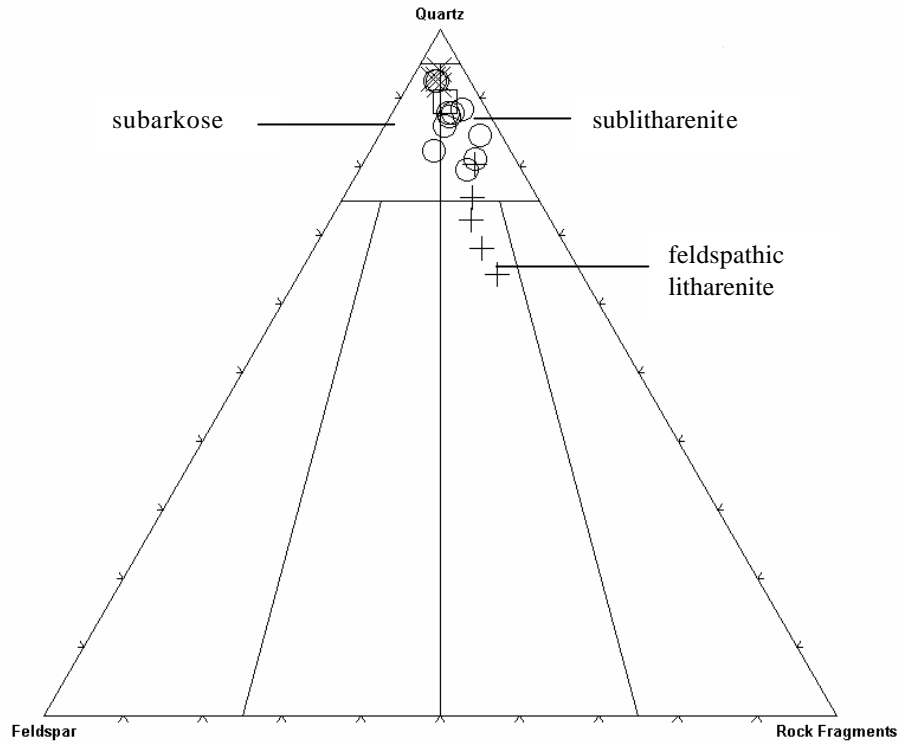


Figure 27a. Folk Sandstone Classification for samples from Casino-3.
 + Waarre A O Waarre Ca X Waarre Cb Flaxman

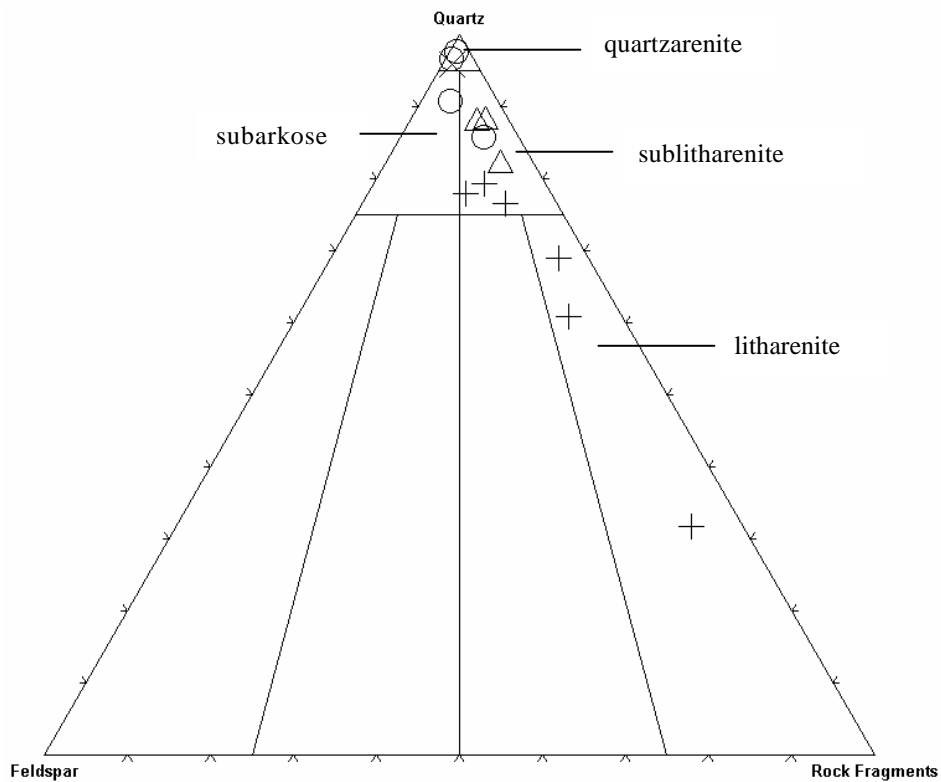


Figure 27b. Folk Sandstone Classification for samples from Casino-1 & -2
 Casino-2 + Waarre A O Waarre Ca X Waarre Cb Casino-1 < Waarre A
 Data from Phillips (2003), note that some values used were visual estimates of composition not point counts.

b. Comparison with Casino-1 & -2

Unit A samples from Casino-1 and -2 were described as fine to medium grained, well to poorly sorted sublitharenites and litharenites (Phillips, 2003). It is clear from comparison of Figures 27a and 27b that the litharenites at Casino-3 contain less lithics than those from Casino-2. Typically grain size distributions in Casino-1 and -2 were unimodal and symmetrical with only one sample displaying positive skewness (Swc 15, 1857.0m Casino-2). Sandstones from Casino-3 have a similar grain size distribution with positive skewness only apparent in MSCT 4. Average grain size at Casino-1 and -2 in Unit A was finer (range 0.15 to 0.40mm) than Casino-3 (range 0.30 to 0.63mm).

Greywackes from the base of Unit Ca are lithologically very similar in Casino-3 and -2. Grain shape is angular to subangular with low sphericity in both samples. However, grain size distributions show a positive skew in Casino-2 and a very irregular negative skew in Casino-3. Lenticular bedding is apparent in Casino-2 and bioturbated laminae at Casino-3. Sandstones from Unit Ca are restricted to subarkoses and sublitharenites at Casino-3 whilst quartzarenites are also evident at Casino-2. These quartzarenites are coarser grained than any of the samples studied from Casino-3 but this may be an artifact of the sampling rather than a significant difference between the wells. Grain shapes tend to be more angular at Casino-2 and grain size distributions are positive skewed. In contrast the grain shapes from Casino-3 are more rounded and where skewness is apparent it is negative. Bioturbation appears to be more pronounced in the finer grained sediments from Casino-3.

Only one sample was studied from Unit Cb at Casino-2 therefore any comparison with the sandstones from Casino-3 is probably artificial. However, the sand at Casino-2 is coarser grained, more quartz rich, has more angular grain shape and a positive grain size distribution. Sediments from Casino-3 are finer grained, contain more feldspars relative to lithics, have more rounded grain shape and grain size distributions are negative skewed. Only MSCT 1 has similar grain shape to that of the sample from Casino-2.

8.2 Detrital mineralogy & sediment provenance

a. Casino-3

Waarre Unit A sediment was dominantly derived from an igneous/metamorphic terrane (Figs 28a & b). The relative abundance of metamorphic lithics suggests that more sediment was eroded from this source. Evidence for interpretation of this igneous/metamorphic sediment provenance is provided by:

- the presence of polycrystalline quartz with either straight or sutured crystal boundaries,
- both K-feldspars and plagioclase,
- metamorphic lithics of shale, micaceous schist, quartzite and possibly pyrophyllite,
- igneous lithics of volcanic (glass & rhyolite) and plutonic (granite & feldspar with granophyric texture) nature, and
- accessory minerals of tourmaline, zircon and rare rutile.

Sedimentary lithics in Unit A of chert and chalcedony could have been reworked from older sedimentary sequences and the mudstone and siltstone lithics may have been reworked from within Unit A. There is a broad increase in feldspar content from the deepest to shallowest samples (Fig. 28b) of Unit A. Metamorphic lithics over the same depths also increase and this may suggest that the metamorphic terrane supplied the feldspars. Perhaps this increase in feldspars and metamorphic lithics is indicative of slight uplift in the metamorphic terrane during deposition of Unit A. An alternative explanation might be that the calcite cement at the base of Unit A has selectively replaced feldspars and metamorphic lithics. Originally these labile grains were more abundant and the apparent trends are therefore not indicative of any change in sediment provenance.

Overall in Waarre Unit Ca there is a broad decrease in polycrystalline quartz, feldspars and lithics from the base to the top of the unit (Figs 28a & b). This trend may indicate a lack of tectonic movement during deposition of Unit Ca. Metamorphic lithics remain more abundant than igneous or sedimentary lithics throughout the unit and this suggests a similar sediment provenance to that of

Unit A. Decline in the abundance of polycrystalline quartz and total absence of volcanic lithics in Unit Ca does indicate changes compared to Unit A.

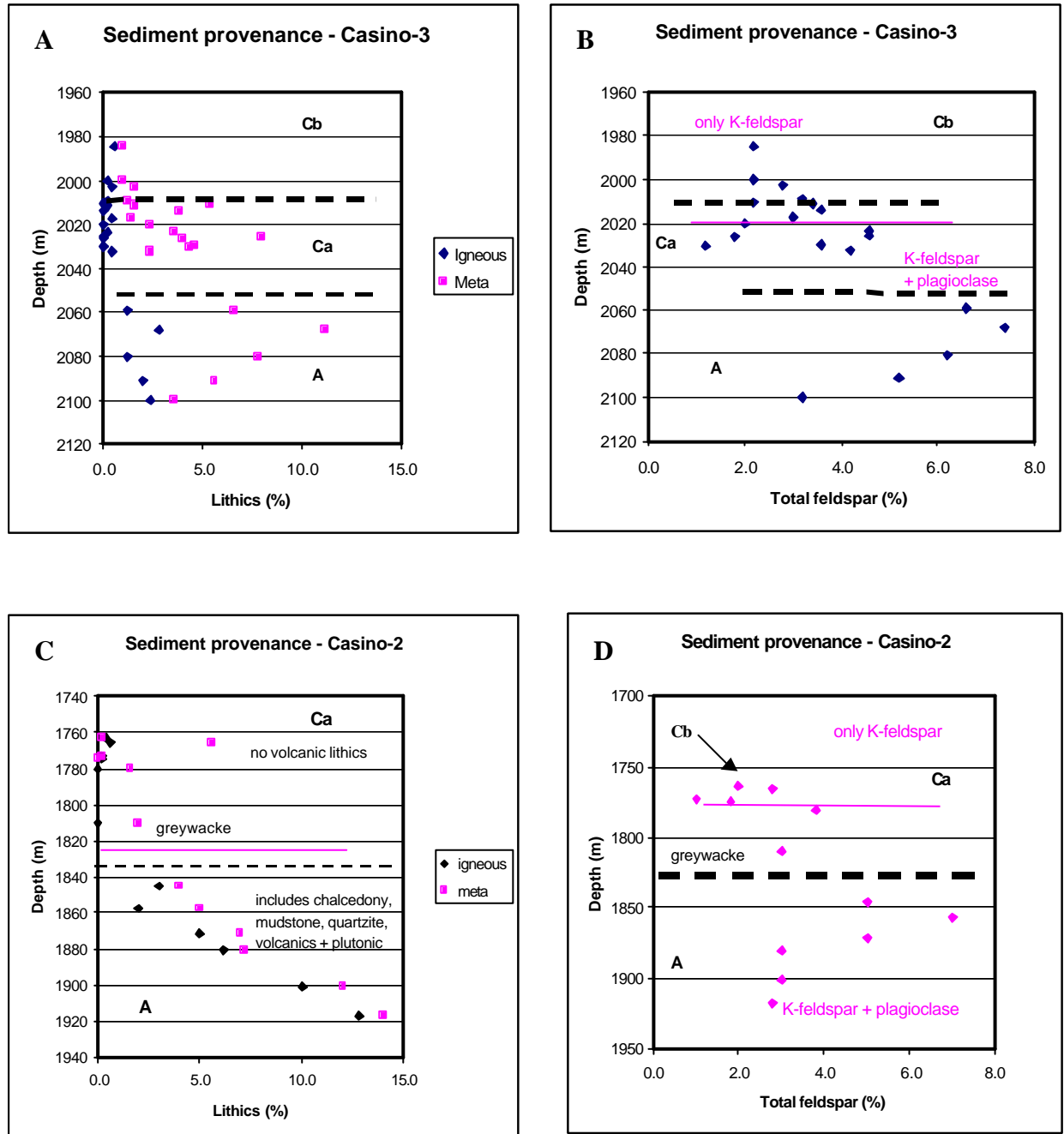


Figure 28 Comparison of sediment provenance for the Waarre Formation at Casino-3 (this report) and Casino-2 (Phillips, 2003). Note that Casino-2 data includes visual estimates of crushed sidewall cores that may not be accurate.

Furthermore, increased rutile content may suggest that the metamorphic terrane was even more important than the igneous as a source of sediment for Unit Ca. A subtle change in sediment provenance may also be apparent in the middle of Unit Ca. From Core plug 31 upward where the sediment becomes coarser there is no plagioclase or chalcedony present.

Trends identified in Waarre Unit Ca are continued into Unit Cb. Feldspar and lithic abundance continues to decline. Feldspars are restricted to the more stable K-feldspars except in MSCT 1 where plagioclase was also identified. Lithics continue to be dominated by metamorphic

fragments of shale, micaceous schist and quartzite and the metamorphic sediment provenance is confirmed by the accessory mineral suite. Volcanic lithics and chalcedony are absent from Unit Cb. Highly altered granitic fragments and feldspars with granophyric texture suggest the plutonic terrane continued to provide minor sediment during deposition of Unit Cb. K-feldspars are up to coarse sand in size in MSCT 1 and these feldspars plus the plagioclase could be attributed to a slight change in sediment provenance at this time. There is no evidence of a change in sediment provenance between MSCT 1 of Unit Cb and MSCT 11 of the Flaxman Formation.

Throughout deposition of the Waarre Sandstone at Casino-3 sediment was dominantly derived from Palaeozoic basement which included both metamorphic and igneous rocks. Basement would have been exposed on both the King Island High to the east of Casino-3 and in the Delamerian/Lachlan Fold Belts to the north at the beginning of the Turonian (Geary *et al*, 2001). Basement was probably uplifted during or prior to deposition of Unit A as suggested by the high feldspar and lithic contents. After this time the volcanics associated with the igneous terrane were no longer a source of sediment. It is possible that the volcanics were reworked from the Late Jurassic Coleraine Volcanics exposed when the Otway Ranges to the east or the Merino Uplift to the north-west was uplifted in the Turonian (Geary *et al*, 2001). When the Shipwreck Trough developed the Otway Ranges source would have been cut off from the Casino Field. This is one possible explanation for the lack of volcanics in Waarre Units Ca and Cb. If the source was the Merino Uplift then it would be anticipated that rare volcanics might still be present in Units Ca and Cb. The exact timing of development of the Shipwreck Trough in the Late Cretaceous would have determined when sediment ceased to reach the Casino Field from the east.

b. Comparison with Casino-1 & -2

Sediment in Unit A from all three wells appears to have been derived dominantly from a metamorphic terrane with significant input from an igneous (volcanic and plutonic) source. Metamorphic lithics are always more abundant than igneous lithics and volcanic lithics are specifically restricted to Unit A. The number of volcanic lithics at the base of Unit A in Casino-2 is much higher (13%) than Casino-3 (2.4%). This fact might be consistent with Casino-2 being closer to the volcanic source during initial deposition of Unit A. Alternatively these lithics may have been concentrated in the slightly finer grained sediments of Casino-2 because of their different hydraulic response. An increase in feldspar content towards the top of Unit A is apparent in sediments from both Casino-2 and -3 (Figs 28b & d). However, this trend does not correspond to an increase in metamorphic lithics in Casino-2 as it did at Casino-3. Therefore uplift of a metamorphic terrane was probably not the source of feldspars. The feldspar trend may be an artifact of preservation as suggested earlier, since calcite cements have selectively replaced feldspars and these cements are most abundant near the base of this unit. No trend is apparent from the three sidewall cores at Casino-1 where feldspar percentages are significantly lower (2-3%). High percentages of polycrystalline quartz in Unit A at Casino-3 (average 9.3%) compared to Casino-2 (average 3.3%) and Casino-1 (average 0.5%) might be an artifact of the sampling methods. In the sidewall cores from Casino-2 and -1, polycrystalline quartz may be crushed and therefore visual estimates are low.

The broad trend of declining numbers of feldspars and lithics in Unit Ca continues into Unit Cb across the Casino Field. At Casino-2 there is no chalcedony in Unit Ca or Cb, whereas at Casino-3 it is present in the base of Unit Ca (up to Core plug 59). Furthermore there is evidence of trace amounts of plagioclase in the base of Unit Ca at Casino-3 which was not evident at Casino-2. The significance of these apparent differences is difficult to assess because of the possibility that sampling of coarser sands at Casino-2 has biased the data set.

8.3 Depositional environments

Lemon (2002 & 2003) has provided a comprehensive assessment of depositional environments based on core logging at Casino-3 and -2. No attempt has been made to duplicate that work in this study. Comments re Waarre units Ca and Cb are restricted to additional information available from the petrology study.

a. Casino-3

Partridge (1997) suggested that diverse marine microplankton indicate deposition at the base of the Waarre Formation was characterised by a transgression which flooded the basin. Petrology samples from Unit A at Casino-3 should therefore reflect this transgression. Coarse grain size, moderate sorting and bedding at the base of Unit A indicates that moderately high energy hydraulic regimes operated during deposition. Grain size distributions in the overlying medium grained sands display slight positive skewness (MSCTs 4 & 13) which might be interpreted as evidence of a fluvial rather than beach influence (Tucker, 2001). These medium grained samples all contain minor amounts of early siderite cement and organic matter which could confirm the terrestrial location. In MSCT 13 there is evidence of an incipient siderite nodule. However, trace amounts of fine sand size glaucony with wormy texture typical of glauconite in MSCT 7 and the presence of framboidal pyrite in most samples suggests a marine influence. In summary these indicators may reflect a marginal marine depositional setting, possibly an estuary. Channels leading into the estuary and shallow sand bars could have either coarsening or fining upwards log characteristics similar to those displayed in Unit A at Casino-3. The fact that grain size distributions are unimodal rather than bimodal may reflect a wave rather than tide dominated estuary. Orientation of the estuary would have been determined by the timing of development of the Shipwreck Trough and the associated faults on the Mussel Platform.

The regressive sequence of Units Ca and Cb is well documented by Lemon (2003). The basal core chip from Unit Ca (2032.5m) contains 4.2% glauconite which confirms the marine depositional environment of this greywacke. Laminated and bioturbated fine grained offshore storm deposits (CPs 75, 73, 62 & 59) all contain minor amounts of chlorite replacing micas (1.8 to 6.6%) rather than glauconite. Similar chloritic grains are also evident in the overlying sediments (CPs 52 & 41) which were described as nearer shore. Development of siderite nodules in core plug 41 and the higher percentage of oxidised grains in this sample are consistent with deposition nearer to shore and possible exposure. Many of the unidentified oxidised grains throughout this interval could be reworked glauconite. Cross bedding is apparent in the coarser grained sediments assigned to the interval of tidal channels (CPs 31, 20 & 12). There are still rare grains of glauconite and chlorite, and traces of siderite to suggest a marginal marine setting. The grain size distribution of core plug 31 is negative skewed which can be interpreted as evidence of a beach rather than fluvial sand. At the top of Unit Ca there is an interval of interlaminated mudstone and very fine grained sandstone (CP 9) which Lemon (2003) assigned to a lagoon based on the restricted trace fossil assemblage. It is also possible that rather than a lagoon this interval represents a tidal flat. Flaser and lenticular bedding apparent in thin section indicate fluctuations in sediment supply and flow strength that are common on a tidal flat (Tucker, 2001). Dewatering structures suggest the sediment was supersaturated with fluid when deposited. Grain size distribution is bimodal consistent with the tidal influence and there is a high percentage of organic matter present. Infilling of the burrow in this very fine laminated sediment by medium grained sand indicates that deposition occurred near to a much higher energy sequence. The composition of the angular to subrounded sand which fills the burrow is very similar to that of core plug 12 and includes very fine sand size grains of glauconite. Perhaps a tidal channel migrated across the tidal flat and organisms burrowed from the channel bottom into the underlying muddy sediments. If CP 9 was deposited on a tidal flat then this muddy unit might be laterally more continuous than a lagoon. However, in either setting there were probably migrating tidal channels that eroded into the underlying laminated sediments thus reducing the chances that this muddy interval forms a continuous seal between Units Ca and Cb.

Lemon (2003) assigned the core in Unit Cb to a sequence of fluvial channels based on the poorer sorting, more angular grains and coally matter. There is evidence from the petrology study which included 3 MSCT samples (3, 2 & 1) above the core that the depositional environment was not

wholly fluvial. Rare very fine to medium sand size grains of glauconite suggests a more marginal marine setting. Furthermore, grain shape is typically subangular to subrounded and therefore not as angular as the underlying tidal deposits. Only the carbonate cemented subarkose of MSCT 1 has angular to subangular grains. This particular sample also contains trace amounts of plagioclase which was not identified in any other sample from Unit Cb and may suggest a slightly different sediment provenance. The distinctive equant circumgranular cement in MSCT 1 is probably composed of dusty calcite rather than siderite as suggested in the thin section description. Crystal habit of the carbonate indicates that it precipitated in a meteoric phreatic regime (Tucker, 1988). Minor micritic rims that predate the circumgranular cement are common in marine phreatic environments. These successive carbonate cements might suggest that the sands were originally deposited as an interwave sand and then became part of a beach. Grain size distribution in this sample is negative skewed which supports the beach interpretation. The gamma ray log displays a fining upwards sequence that may indicate this was the beginning of a transgressive sequence and not a continuation of underlying fluvial or deltaic channels.

Framboidal pyrite and minor glaucony in the muddy sublitharenite of MSCT 11 from the Flaxman Formation are thought to be indicative of a marine depositional environment. Deposition occurred rapidly from high energy currents resulting in very poor sorting and a range in grain size from clay to very coarse sand. Organic matter in the muddy laminae accumulated during quieter periods. There are a number of possible settings in which this sediment could have accumulated including slumping on a delta front or as a result of turbidity currents.

b. Comparison with Casino-1 & -2

Sedimentary structures were not well preserved in the crushed sidewall cores from Unit A at Casino-1 and -2 making identification of depositional environments very difficult. Muddy laminae and bedding outlined by organic matter indicate fluctuations in the hydraulic regime. Identification of thick cutinite in Casino-1 (Swc 12) may reflect deposition in close proximity to land plants. Typically the sediments from Casino-2 and -1 are better sorted, finer grained and have more rounded grain shapes than those recorded for Casino-3. This might indicate more reworking of sediments and/or a quieter hydraulic regime than Casino-3. Glauconite was not apparent in any of the samples from Casino-2 but there were trace amounts in the three samples from Casino-1. This fact combined with trace amounts of framboidal pyrite would confirm a marginal marine depositional environment for the Casino Field. At the base of Unit A in Casino-2 (Swc 7) there are oxidised rims on grains and unidentified oxidised grains which suggest that this fine grained sediment was exposed. Perhaps a sand bar at the estuary mouth was emergent for a short period prior to the transgression. None of the samples at Casino-3 show evidence of this exposure but this may be a sampling artifact. Comparison of the wireline logs at Casino-2 and -3 in Unit A show a series of stacked fining and coarsening upward units. Muddy intervals between the sands are thicker at Casino-2 suggesting a location more marginal to the main channel system. Casino-3 was probably closer to the channel axis and this would explain the coarser grain size and more angular nature of grains. Higher percentages of organic matter and a very thick basal muddy interval at Casino-1 might indicate a location further away from the main estuary channels adjacent to a marsh. The only indication of deepening water depths is the presence of trace amounts of glauconite in the shallowest samples of Casino-3 and Casino-1. Lemon (2003) has suggested that faulting on the Mussel Platform influenced the distribution of sediment in the upper part of Waarre Unit A. If this interpretation is correct then the estuary was oriented approximately east-west and flowed into the Shipwreck Trough. This hypothesis re orientation suggests that throughout deposition of the Waarre Formation sediment provenance was always controlled by the east-west faults on the Mussel Platform. Therefore a change in the direction from which sediment was derived must have occurred further back along the transport path to explain why there are no volcanic lithics in Units Ca and Cb.

At the base of Unit Ca in Casino-2 (Swc 21, 1810m) there is an interbedded greywacke and mudstone with ripples and possible lenticular bedding. It was suggested previously (Phillips, 2002) that this sample could be representative of a prodelta deposit because of the sedimentary structures and high percentage of glauconite present (7%). Presumably the greywacke (2032.5m) from the base of Casino-3 core which is lithologically very similar and has 4.2% glauconite, had a similar depositional environment. This interpretation would be consistent with the deltaic

sedimentation recognised elsewhere on the Mussel Platform (Geary, *et al*, 2001) in the Upper Waarre Formation. Overlying these muddy sediments are the offshore storm deposits recognised from core by Lemon (2002 & 2003). No additional information can be provided regarding this interval based on comparison of petrology results from Casino-2 and -3. Tidal channel deposits in Casino-2 (CPs 25 & 30) have bimodal grain size distributions that are positive skewed (?fluvial) and lack glauconite. In contrast, the tidal channel deposits from Casino-3 are unimodal and more negatively skewed similar to a beach sand and there are traces of glauconite. Similarly the sample from Unit Cb in Casino-2 with a positively skewed grain size distribution is more clearly fluvial in origin than the negatively skewed sands in Casino-3. These observations could indicate a slightly more marine setting for Casino-3 than Casino-2 during deposition of the channel sequences in Units Ca and Cb.

8.4 Authigenic mineralogy & diagenetic alteration

a. Casino-3

All stratigraphic units from Casino-3 contain trace to minor amounts of glauconite, siderite and framboidal pyrite which probably relate to the depositional environments. Typically glauconite forms at the sediment-water interface on continental shelves between 100 and 500m (Weaver, 1989) when sedimentation rates are low. Hence glauconite identified in muddy sediments from Casino-3 (ie core chip from 2032.5m) is more likely to be *in situ* and that in sandy sediments has probably been reworked. Glauconite forms by the replacement of precursor minerals, fossils and pellets when pH is near 8, Eh is slightly reducing due to abundant organic matter and there is sufficient Fe present. The dark green colour of the glauconite at Casino-3 indicates that it was a mature form, probably with high K₂O values. As glauconite reaches maturity the texture changes from wormy to a more fibrous habit which makes it hard to distinguish from chlorite replacing a mica. It is possible that at least some of the chlorite described from CPs 75, 73, 62, 59, 52 & 41 was mature glauconite. The poorly crystalline nature of glauconite means that it does not respond well to X-ray diffraction. This fact combined with the relatively low percentages (~1-4%) even in the muddy sediments at Casino-3, would explain why glauconite was not detected from XRD. It is common for glauconite grains to also contain minor amounts of smectite (Weaver, 1989). The latter was identified in Casino-3 samples and may also be present in altered lithics as seen in the SEM.

Framboidal pyrite commonly forms soon after burial in marine depositional environments when conditions are reducing and Fe has been liberated from iron oxides/hydroxides on clays and organic matter (Tucker, 2001). Sulphide is derived mainly from bacterial reduction of sulphate dissolved in the sea water. Concentrations of dissolved sulphate are generally much higher in sea water than fresh water hence pyrite is rare in nonmarine sediments. Only trace amounts of pyrite (less than 1%) were noted in Waarre Units A and Cb, compared to minor amounts (up to 5%) in Waarre Ca. This may indicate a stronger marine influence during deposition of the Waarre Ca sediments which is consistent with the depositional environments hypothesised by Lemon (2003). Rounded pyrite nodules up to 0.6mm in diameter that may have formed when fecal pellets were replaced were noted in CP 75. Blocky pyrite may be either early or late diagenetic in origin. Late blocky pyrite forms during bacterial reduction of reservoir bitumen.

Siderite is more common in fresh water than sea water because it requires low sulphide activity and high carbonate activity to precipitate. Siderite can be found in marine sediments that have been exposed to meteoric waters during a hiatus in sedimentation and/or where freshwater plumes move offshore in aquifers after storms (Thyne & Gwinn, 1994). Cement stratigraphy indicates that micritic siderite and single scalenohedral crystals of siderite that have replaced grains (micas and lithics) and partially filled pores were early diagenetic cements, especially in Unit A. The shallowest samples from Unit A (MSCTs 4, 7 & 13) have relatively high concentrations of siderite (9-10%) and an incipient nodule was described in MSCT 13. The latter might be a burrow filled with sediment and micritic siderite. Micrite, in contrast to spar, forms when there is very rapid precipitation and multiple sites for nucleation. It is possible that the burrow allowed meteoric waters to reach deeper into the sediment and thus initiate siderite precipitation by diluting the sulphate content of the marine pore waters. If this explanation for a higher siderite content in the

shallowest samples from Unit A is correct it may suggest that the depositional environment was periodically influenced by meteoric waters in the upper part of the section. If a transgression was in progress as hypothesised by Partridge (1997) for the basal Waarre Formation then water depths should be deepening and becoming more marine, not the reverse. It is possible that the increase of siderite abundance, regardless of the transgression, could be explained by minor uplift on the Mussel Platform at this time. Thus water depths would have become shallower and thus more influenced by meteoric waters despite the regional transgression.

In Unit Ca most siderite is present as anhedral spar reflecting slower rates of precipitation. There are only minor amounts of siderite in the storm deposits (1.6-3.4%) probably because of the higher dissolved sulphate content of marine pore waters. Precipitation of siderite was probably only possible when storm deposits acted as offshore palaeoaquifers that were flushed by meteoric waters during storms or low tides. Oxidation of glaucony grains and possibly lithics would also have occurred at this time. Very high concentrations of anhedral sparry siderite (33.2%) in CP 41 of Unit Ca (Fig. 29b), which has been assigned to a storm deposit nearer to shore by Lemon (2003), requires a different interpretation. Again burrowing is apparent and siderite nodules have precipitated in the burrow. Nodule cores are micritic and may have replaced fecal pellets. Partial rims of spar on the nodules are columnar in habit which probably reflects a mixed meteoric/marine phreatic depositional environment. It is possible that the siderite precipitated soon after burial when tidal channels were deposited in the overlying sequence and pore waters became fresher. Dissolved sulphate levels in the porewaters would have been reduced and this initiated siderite precipitation. If this hypothesis is correct then there could be siderite cements elsewhere in sands immediately below the thick sequence of stacked tidal channels in Unit Ca.

Trace amounts of anhedral micritic and microsparry siderite were recorded in samples from the upper part of Unit Ca and the lower section of Unit Cb. Siderite in these samples is interpreted as an early diagenetic mineral which has dominantly replaced grains rather than filled pores. This observation may indicate that both Fe and carbonate were not in high enough concentrations in the pore waters to favour precipitation of siderite. Only where a detrital grain had sufficient Fe did replacement occur. This hypothesis is consistent with the higher percentages of grain replacing anhedral to subhedral siderite noted in CP 9 (3.4%) from Unit Ca and MSCT 11 (14.8%) from the Flaxman Formation. Both these samples have significant clay matrix in which the siderite has precipitated. Fe oxides attached to the clays were the most likely source of Fe for this siderite. Lack of siderite in the greywacke core chip from Unit Ca (2032.5m) can be attributed to the totally marine depositional environment of this sample which would have high dissolved sulphate levels thus inhibiting siderite precipitation.

Micritic and equant circumgranular cements identified in MSCT 1 at the top of Unit Ca are also indicative of depositional environments and reflect early diagenesis. As discussed in the section on depositional environments these cements are thought to indicate that sediment was deposited in a marine phreatic zone and then became part of a meteoric phreatic setting. It is possible that at least some of the grains removed by dissolution from this sample were fossils.

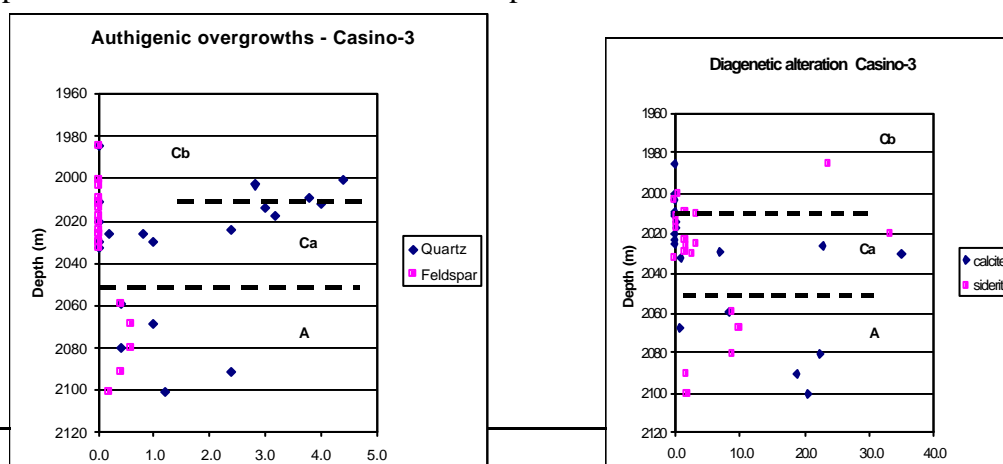
It is commonly believed that kaolin forms in continental settings when meteoric waters flush sediments soon after burial. Alternatively, if the sediment is marine then either a phase of uplift and exposure is invoked, or the decomposition of organic matter sets up a low pH (Tucker, 2001). Kaolin forms when pH is between 4 and 7, and K^+ activity is low and the necessary ions have been supplied by the dissolution/alteration of feldspars and/or micas. Kaolin was identified as kaolinite from X-ray diffraction. Kaolinite has replaced grains in all samples (range 0.4 to 4.8%) from Casino-3. Where micas have been replaced the booklets and verms are up to 100 microns in diameter. Elsewhere the booklets are commonly 1 to 25 microns in diameter and minor compaction has squeezed the kaolinite into adjacent intergranular pores. Only in the burrow fill of CP 9 does kaolinite appear to have precipitated from solution into all available pores. Fresh water associated with the overlying channel system must have flushed the burrow to produce this abundance of kaolinite. Decomposition of organic matter in the muddy sediments of CP 9 may also have contributed to a low pH.

It was clearly illustrated in the SEM study that scalenohedral siderite has precipitated within patches of grain replacing kaolinite. This relationship suggests that the formation of kaolinite was a relatively early diagenetic event prior to siderite precipitation. Furthermore it was noted that kaolinite has been engulfed by quartz overgrowths and this might suggest kaolin had already formed when the quartz precipitated. Slightly higher amounts of kaolinite in Waarre Unit A can probably be attributed to the higher detrital feldspar content of this interval. Trace amounts of illite associated with grain replacing kaolin may have formed as pore fluids became neutral to alkaline after kaolin had precipitated. If K^+ , Si and Al were still available then illite would have formed.

Although quartz overgrowths probably postdate the alteration of feldspars and micas to kaolinite, this cement was sufficiently early to minimise mechanical compaction in the cleaner sands. Quartz overgrowths were identified in all stratigraphic units (Fig. 29a) except the Flaxman Formation. The latter is not surprising given the abundance of detrital clay in this sample (MSCT 11) which would have inhibited silicification. Other samples within the Waarre Formation with high percentages of clay also lack quartz overgrowths. There is a broad increase in silicification from Waarre Unit Ca into Unit Cb in the channel facies (Fig. 29a) which was probably controlled by the number of lithics (Fig. 30). Detrital lithics inhibit the sites available for silicification. The subarkose (MSCT 1) at the top of Unit Cb lacks quartz overgrowths because of an early carbonate cement. Silica was probably derived from several sources for the development of quartz overgrowths including the excess released when feldspars were altered to kaolin (Bjorlykke, 1988) and due to dissolution of detrital quartz at mica/clay contacts during mechanical compaction (Bjorkum *et al*, 1998) as indicated in CP 59.

Feldspar overgrowths are restricted to Waarre Unit A (Fig. 29a), they occur on corroded detrital grains and are composed of K-feldspar that lacks twinning. Timing of formation has not been ascertained but it did occur after a phase of feldspar dissolution. Alkaline pore waters with sufficient K, Si and Al would favour feldspar overgrowth development. These same conditions are required for illite precipitation. Elsewhere an association between feldspar overgrowths, illite and volcanic lithics has been noted (De Ros *et al*, 1994). Volcanic lithics are restricted to Waarre Unit A and it is possible that weathering of these lithics provided the elements necessary for K-feldspar overgrowths. When the sediment was flushed by meteoric waters soon after burial some feldspars and micas were altered to kaolinite, whilst others may have been completely dissolved to produce grain size dissolution pores. Feldspars from a volcanic source would have been relatively more unstable and hence more likely to dissolve. But as pore waters became more alkaline, and unstable volcanic lithics and glass altered to smectite, K activity increased so that both illite and feldspar overgrowths would have formed. It would appear that the degree of supersaturation of pore waters with K, Si and Al was relatively low because large K-feldspar crystals grew as overgrowths (Fig. 22d) rather than numerous fine crystals which would characterise rapid crystallization.

Another authigenic cement restricted to the base of Waarre Unit A (MSCTs 6 & 5) is pore filling and kaolin replacing blocky barite (2.6-3%). Cement relationships indicate that the barite precipitated after the quartz overgrowths and kaolin, and possibly before the calcite. Therefore this was not a primary cement related to the depositional environment because it postdates feldspar and mica alteration. There are two possible mechanisms via which barite could have



precipitated in the coarse grained carbonate cemented sublitharenites but evidence for either of these sources is not considered conclusive. Firstly, barite could have precipitated from the drilling mud and thus represents a contaminant. However, invasion by drilling mud seems unlikely because permeability was probably poor due to the lack of primary intergranular pores in these samples. Typically when barite does precipitate from drilling mud it forms bladed crystals that bridge pores and this was not the case in Unit A. It is possible that the drilling mud was more heavily weighted with barite when drilling commenced and this explains its concentration at the base of Unit A. The second mechanism that could have introduced barite would require the migration of hot saline fluids from elsewhere in the basin. Solubility of barite in water is very slight but heating and the presence of chlorides does increase solubility. Migration of these saline fluids could have been related to structuring and rifting during the break-up of Australia and the Antarctic. This hypothesis assumes that there was a salt deposit somewhere in the Paleozoic basement, or the Otway Group to source the brine. Further work beyond the scope of this study would be required to ascertain the validity of this hypothesis.

Figure 29 Abundance of authigenic cements in the Waarre Formation at Casino-3 (this report) and -2 (Phillips, 2003). Note that Casino-2 data includes visual estimates of crushed sidewall cores that may not be accurate.

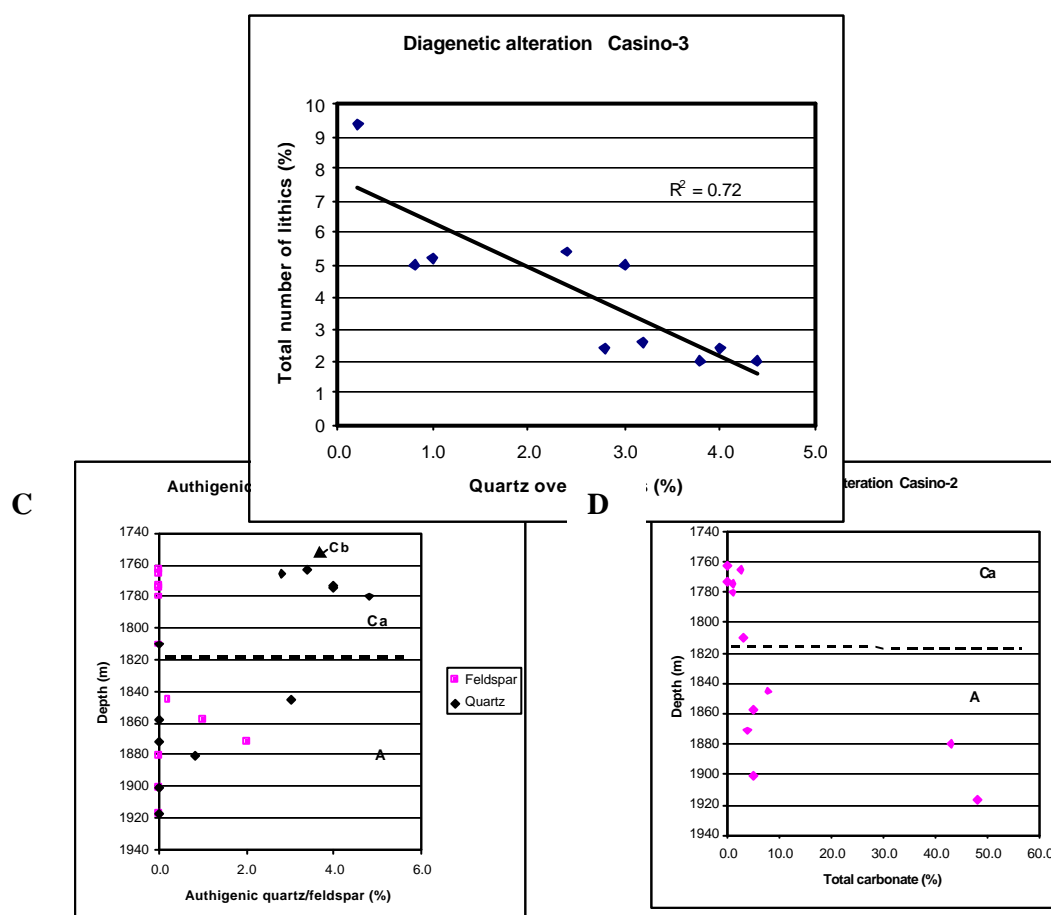


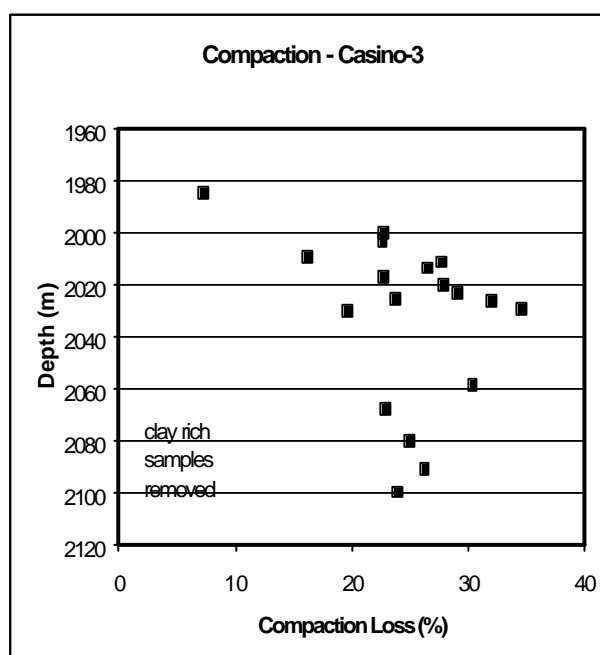
Figure 30. Control of detrital mineralogy on the development of quartz overgrowths in Waarre Units Ca and Cb for samples that do not have high percentages of detrital clay nor carbonate cements.

Calcite and ankerite/dolomite cements in Casino-3 are comprised of poikilotopic twinned subhedral to euhedral blocky spar that are indicative of late diagenetic burial cements. Pore filling calcite contains trace amounts of Fe and is therefore slightly ferroan, it forms a pervasive cement at the base of Unit A (MSCTs 6, 5 & 4) and at selected intervals near the base of Unit Ca (CP 75 & 62) as illustrated in Figure 29b. Where calcite has replaced grains it commonly lacks iron. Associated with the calcite there are minor amounts of both ankerite and dolomite. XRD results suggest that ankerite is more abundant than dolomite and has been described in thin section as Fe rich spar. Dolomite was only identified in the SEM study after EDS analyses and would appear to be ferroan dolomite that might form a continuous substitution with the ankerite. Fe and Mg in

both the dolomite and ankerite could have been derived from the earlier siderite cements. EDS analyses of the siderite indicated variable concentrations of Mg. Precipitation of these late diagenetic carbonate cements would have occurred when pore fluids were alkaline, Eh was reducing and carbonate activity was high. CO₂ could have been released from organic matter in the sediments during maturation or prior to decarboxylation and hydrocarbon migration. Those samples with high percentages of calcite cement do not contain plagioclase, but it is preserved in other sediments from Unit A and the base of Unit Ca where there is only minor calcite cement. It is possible that plagioclase dissolution provided the source of calcium necessary for calcite precipitation.

All samples show evidence of minor mechanical compaction and this is most pronounced in those samples that lack significant early cement or have a high percentage of detrital clay. In Unit A where there are calcite cements at the base of the unit the loss of porosity due to compaction is approximately 25%. Similar values were calculated for samples from Unit Ca which have carbonate cements and also for those samples which lack calcite cement (Fig. 31). These observations indicate that compaction occurred before the introduction of calcite cements. MSCT 1 from the top of Unit Cb has the lowest compaction loss value of all the sandstones at Casino-3. This lack of compaction is not just due to shallower depth of burial but the fact that the cement in this subarkose was related to the depositional environment and therefore very early. Mechanical compaction would have been inhibited by the cement. There is no statistically significant relationship between depth and compaction loss at Casino-3 but a very vague trend can be visualised. Porosity loss due to compaction does appear to increase with depth. Within Units Cb and Ca this trend is slightly more pronounced ($r^2 = 0.51$) but it could be an artifact of the finer grain size and more muddy nature of sediments near the base of Unit Ca.

Dissolution of labile grains to produce grain size and honeycomb pores is also apparent in most samples. The highest number of dissolution pores occur in Unit A and the base of Unit Ca where there are the highest number of labile grains (feldspars and lithics). This phase of dissolution probably occurred during early diagenesis when meteoric waters flushed sediments. Siderite cement in CP 41 above the gas-water contact appears to be highly corroded and it is possible



that this dissolution occurred later in the diagenetic sequence when hydrocarbons migrated into Waarre Unit Ca.

Figure 31. Loss of porosity due to compaction with depth in Casino-3 for the Waarre Formation. Compaction loss was calculated using the method of Lundegard (1992).

The complete paragenetic sequence identified from Casino-3 is summarised in Figure 32 below. Not all samples have evidence of each event as discussed above. A high percentage of the authigenic minerals were relatively early diagenetic forming in response to depositional environments and flushing by meteoric waters soon after burial. Diagenetic zonation may have been partially controlled by the detrital mineralogy and sediment provenance. Volcanic lithics and plagioclase feldspars may have influenced the distribution of feldspar overgrowths and late calcite cement.

Event	Diagenetic Stage		
	Early	Middle	Late
glauconite	---		
pyrite	---		----
kaolin	----		
dissolution/oxidation	----		----
siderite	----	-----	
quartz		----	
feldspar		----	
illite/smectite		----	
compaction	-----		
calcite/ferroan calcite	----		-----
ankerite/dolomite			----
hydrocarbons			----

Figure 32. Paragenetic sequence for samples from Casino-3

b. Comparison with Casino-1 & -2

The paragenetic sequence based on the relationships seen in MSCT and core samples from Casino-3 is consistent with previous results from Casino-1 and -2 (Phillips, 2003). At the base of Unit A in Casino-2 and -3 there are significant late diagenetic calcite cements and feldspar overgrowths are restricted to Unit A (Fig. 29). Quartz overgrowths are less abundant in Unit A than Ca probably because of the higher percentage of lithics in Unit A which inhibited silicification. Samples from Casino-2 show an increase in silicification over a 20m depth interval within Units Ca & Cb. This trend is the reverse of that observed at Casino-3 (compare Figs 29a & c). Silicification is commonly thought to increase with depth because of higher temperatures enhancing dissolution at grain-clay contacts. However, this trend is unlikely to be observed over a 20m interval because temperature would not change significantly and therefore it is probably an artifact of the small number of samples from Casino-2.

Late diagenetic carbonate cements also occur at the base of Unit Ca in Casino-3 but were not evident in Casino-2 from the petrology study. However, Lemon (2002) noted a poikilotopic ?dolomite cement from core logging in medium to coarse grained cross bedded sands within the gas pay zone at approximately 1765.5m. Given this location it is possible that the cement was partially corroded during hydrocarbon migration developing minor secondary porosity similar to that of CP 41 in Casino-3. Exactly what has controlled the distribution of these cemented intervals is not clear but they are probably not laterally continuous across the Casino Field. Distribution of cements controlled by depositional environments might be laterally continuous but these carbonates are late diagenetic. Precipitation might have occurred where a localised source of Ca was available.

Subtle differences in diagenesis between the wells include the oxidation of grains and rims at the base of Unit A in Casino-2 (Swc 7) and the zonation apparent in a siderite nodule in the same sample. These features are probably related to the depositional environment and therefore were not recognised at Casino-3. Similarly the very early equant circumgranular cement in MSCT 1 at Casino-3 is not apparent in the other wells because a beach facies has not been studied from Casino-1 or Casino-2.

8.5 Reservoir quality

a. Casino-3

Pore types in the Waarre Formation at Casino-3 are both primary and secondary in nature. Primary intergranular pores are commonly angular in outline due to the presence of a rim of authigenic quartz and where elongate are probably interconnected. Secondary dissolution pores are grain sized, honeycomb where feldspars have been partially corroded and intragranular due to the dissolution of labile grains in lithics. It is possible that fossils have been dissolved to form secondary pores in MSCT 1. Typically fractures seen in thin section were identified as artifacts because they are developed parallel to bedding. Microporosity was estimated from the relative abundance of kaolinite. In the SEM it is apparent that these pores between booklets and verms may contribute to total porosity but may not represent effective porosity. In rare instances where kaolinite booklets have a very fine crystal size (1-5 microns) there is the possibility of migration during production. Figure 33 illustrates the distribution of these various pore types in each stratigraphic unit of the Waarre Formation. In Unit A there is a high percentage of dissolution pores, in contrast

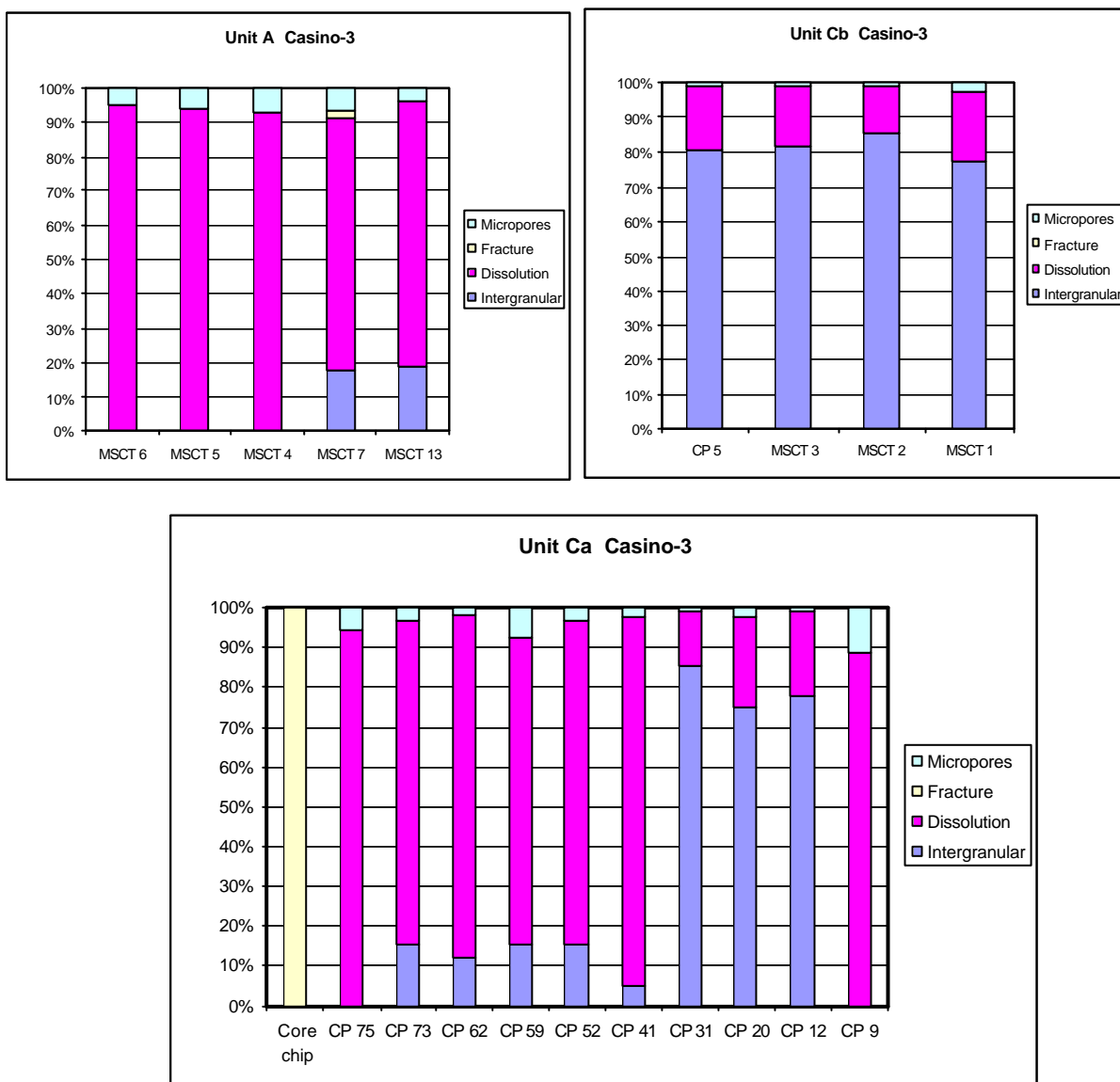


Figure 33. Relative percentages of different pore types in the Waarre Formation at Casino-3.

to Unit Cb which is dominated by primary intergranular pores. Unit Ca has a mixture of samples that have either high percentages of dissolution pores or a high proportion of primary intergranular pores. The Flaxman Formation (MSCT 11) sample is dominated by secondary dissolution pores with trace amounts of intergranular and microporosity.

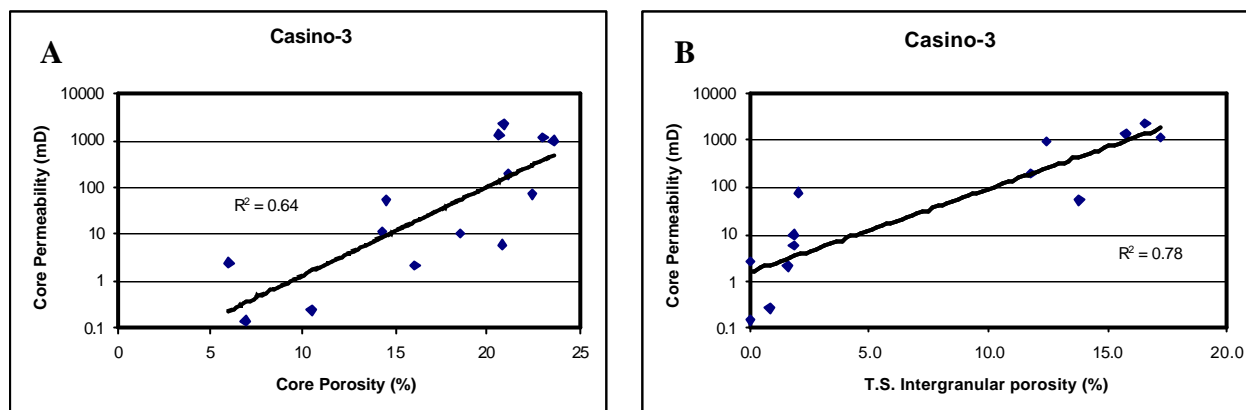


Figure 34. Relationships between core permeability and porosity measured in routine core analysis (A) and from thin section estimates of intergranular porosity (B) in the Waarre Formation at Casino-3.

Porosity is typically considered a function of depth (pressure, temperature and time) and rock composition (grain size, sorting, packing, detrital and authigenic mineralogy). Permeability can be controlled by porosity and rock composition. In these siliciclastics confined to the Waarre Formation the influences of pressure, temperature and time can all be considered a function of depth. Estimates of porosity loss due to compaction (Fig. 31) do show a very vague relationship to depth.

Measurements of core porosity and permeability in Casino-3 show only a moderate ($r^2 = 0.64$) relationship (Fig. 34a) suggesting that both parameters may not be controlled by exactly the same factors. A series of univariate analyses were performed to test certain parameters as the controls of reservoir quality in Casino-3. Core permeability measurements show a strong correlation ($r^2=0.78$) with the identification of intergranular porosity in thin section (Fig. 34b). Therefore intergranular porosity and not rock composition probably controlled permeability. This is not surprising given that secondary dissolution pores are unlikely to be interconnected and hence contribute to effective porosity. Permeability was not influenced by sorting ($r^2 = 0.22$) but grain size ($r^2 = 0.74$) in Units Ca and Cb may have been important. Similarly core porosity was not strongly influenced by sorting ($r^2=0.53$) but estimates of thin section porosity were controlled by grain size ($r^2=0.75$) in Units Ca & Cb (Fig. 35). Grain size in both Units Ca and Cb would have been related to the hydraulic regimes of particular depositional environments. Finer grain sizes are associated with the storm deposits and coarser grain sizes with the channel sequences. Storm deposits have a relatively high percentage of dissolution pores compared to the intergranular pores which dominate the channel sands (Fig. 33). Therefore despite the statistics it is possible that the type of pores preserved are more important than grain size as a control of reservoir quality. In Unit A grain size is not an important influence on reservoir quality and most of the pores are secondary dissolution pores.

To ascertain the influence of detrital mineralogy on reservoir quality cross plots of porosity and permeability against the total number of lithics and ductile grains (metamorphic lithics, micas plus glaucony grains) were constructed for the Waarre Formation from Casino-3. These correlations do not show a strong control of detrital mineralogy on reservoir quality. Permeability is slightly influenced by the number of ductile grains ($r^2=0.57$) and to a lesser extent the total number of lithics ($r^2=0.49$) but porosity is not controlled by the number of lithics ($r^2 = 0.27$) and only weakly by the ductile grain content ($r^2=0.58$). Based on these results it can be assumed that the reactive clays of illite-smectite and chlorite-smectite which concentrate in altered lithics and grains of glaucony, did not have a major impact on permeability.

Precipitation of authigenic minerals in pores is a more obvious control of porosity, especially where carbonate cements have developed. Porosity estimated from thin section has a correlation coefficient of $r^2=0.49$ (Fig. 36) when all the pore filling authigenic minerals are combined (ie carbonate, quartz, feldspar, barite, kaolin plus pyrite). This correlation improves to $r^2=0.70$ (which would be more the anticipated value) if MSCT 1 is removed from the data set. This subarkose has a very early equant circumgranular cement which minimised compaction and helped the

retention of primary porosity rather than reducing it. Carbonate cements in general and even more specifically pore filling carbonate had a very limited control on porosity (Fig. 36b). Clearly these cements are of localised importance but do not have a general control on reservoir quality.

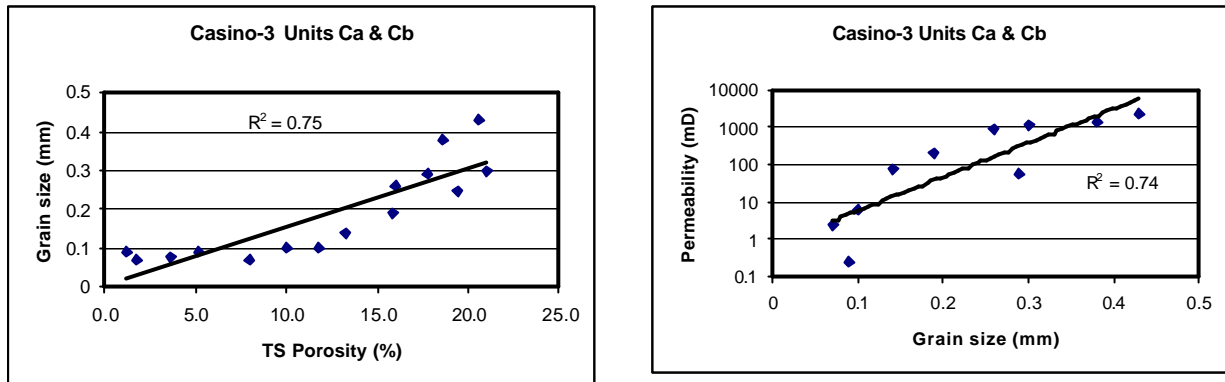


Figure 35 Cross plots illustrating the strong correlation between grain size and both porosity and permeability in Waarre Units Ca & Cb at Casino-3.

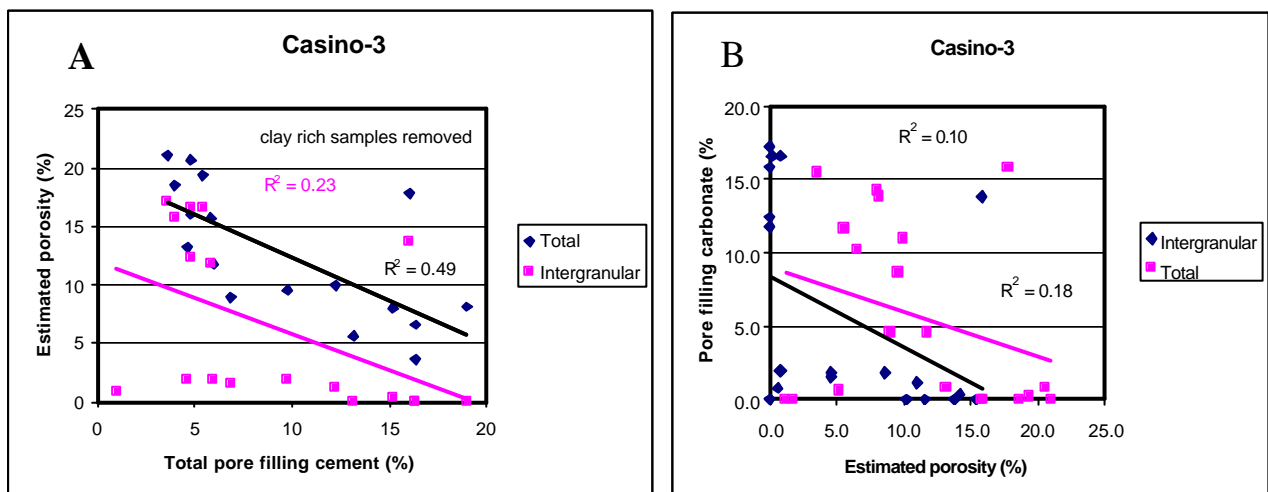


Figure 36 Cross plots showing the influence of pore filling authigenic minerals on porosity in the Waarre Formation at Casino-3. Graph **A** is all the minerals combined and graph **B** is only the pore filling carbonate.

In all stratigraphic units of the Waarre Formation from Casino-3 very strong correlations exist between intergranular pores and the percentage of quartz and feldspar overgrowths (Fig. 37). These early cements minimised compaction and preserved reservoir quality. For Unit A the correlation coefficient is $r^2=1.0$, in Unit Ca $r^2=0.81$ and in Unit Cb the value is $r^2=0.75$. It has already been established from the discussion of diagenesis that feldspar overgrowths are restricted to Unit A because elements for their precipitation were probably derived from volcanic lithics. Quartz overgrowths are better developed in the cleaner sands of Units Ca and Cb where there are minimum numbers of lithics (Fig. 30).

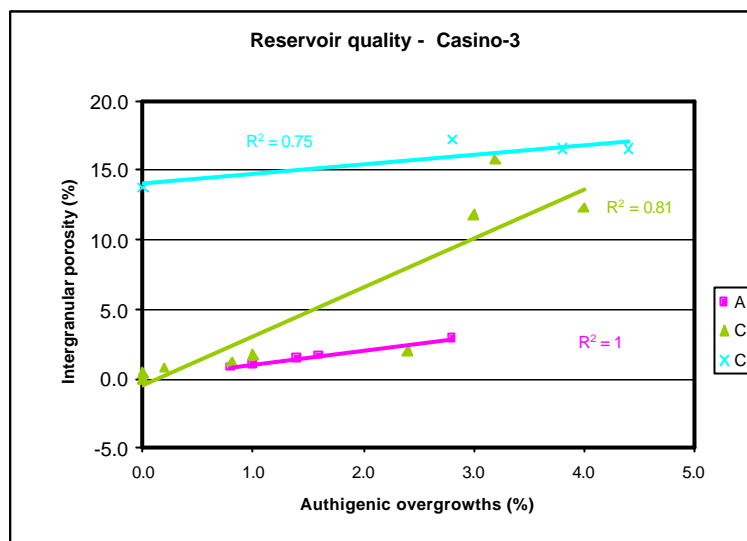


Figure 37. Cross plot illustrating the relationships between primary intergranular pores and feldspar plus quartz overgrowths for each stratigraphic unit of the Waarre Formation at Casino-3.

b. Comparison with Casino-1 & -2

Primary intergranular pores may be better preserved in the Waarre Formation at Casino-1 and -2 than are apparent at Casino-3. However, it is difficult to know to what extent this observation is an artifact of the difference in sample types between wells. In Unit A from Casino-1 and -2 there appear to be a higher percentage of primary intergranular pores (average 3.8%) than at Casino-3 (average 0.7%) but dissolution pores remain dominant across the field. In Unit Ca from Casino-2 there are also a higher percentage of primary pore types (average 16.3%) than the mixture of dissolution (average 5.9%) and primary (average 5.1%) noted from Casino-3.

Depth (as a measure of pressure, temperature and time) has a greater influence on porosity in Casino-2, than Casino-3 (Fig. 38). This greater decline in porosity might be a function of the larger depth interval studied at Casino-2. If samples were taken from a similar depth range in Casino-3 they might show the same trend.

In terms of the control of rock composition (grain size, sorting, packing, detrital and authigenic mineralogy) on porosity there are a number of similarities across the field. Overall porosity was very weakly influenced by grain size ($r^2=0.48$) in Casino-1 and -2 but there is no relationship with sorting ($r^2=0.01$). These observations are consistent with the results from Casino-3. Detrital mineralogy as reflected by the total number of lithics has a very weak correlation ($r^2=0.33$) with porosity in Casino-1 and -2 similar to that reported from Casino-3. Of the authigenic minerals the strongest correlation is noted between the abundance of feldspar and quartz overgrowths and total estimated porosity (compare Figs. 37 & 39). At Casino-1 and -2 it was possible to identify this trend ($r^2=0.84$) using total estimated porosity rather than primary intergranular porosity because there are a higher proportion of intergranular pores in all stratigraphic units at Casino-1 and -2. This trend is apparent in all stratigraphic units across the Casino Field and is thought to be the prime control of reservoir quality. Furthermore, it is highly likely that permeability has been controlled by intergranular porosity not rock composition.

Reservoir quality in the Casino Field has been retained where early authigenic overgrowths of quartz and feldspar provided a rigid framework to limit mechanical compaction. This preservation of primary intergranular pores strongly influenced the retention of permeability. Development of quartz overgrowths was limited where there are abundant lithics in Unit A and feldspar overgrowths may be restricted to this Unit by the distribution of volcanic lithics. Quartz overgrowths are better developed in the cleaner and coarser grained sands of Units Ca and Cb. Therefore the detrital mineralogy determined the authigenic mineralogy which in turn influenced the

preservation of primary intergranular pores. Based on these observations reservoir quality should be consistent across the field. Localised cements of carbonate have reduced porosity but do not appear to have a major influence on the overall reservoir quality.

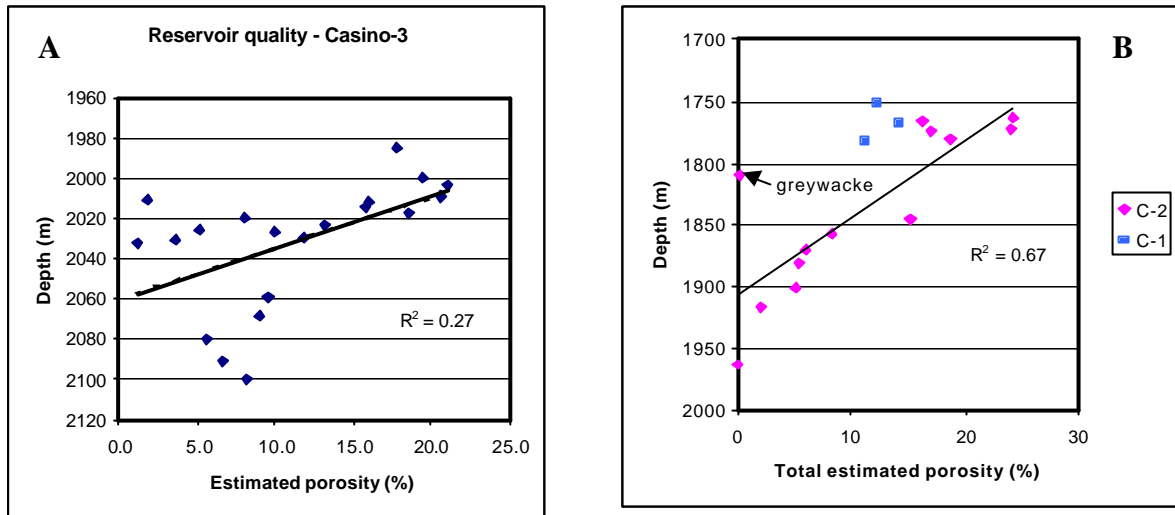


Figure 38. Cross plots of depth versus thin section estimates of porosity for the Waarre Formation in Casino-3 (A), Casino-2 and -1 (B). Note that data for Casino-1 & -2 (Phillips, 2003) is a mixture of point counts & visual estimates.

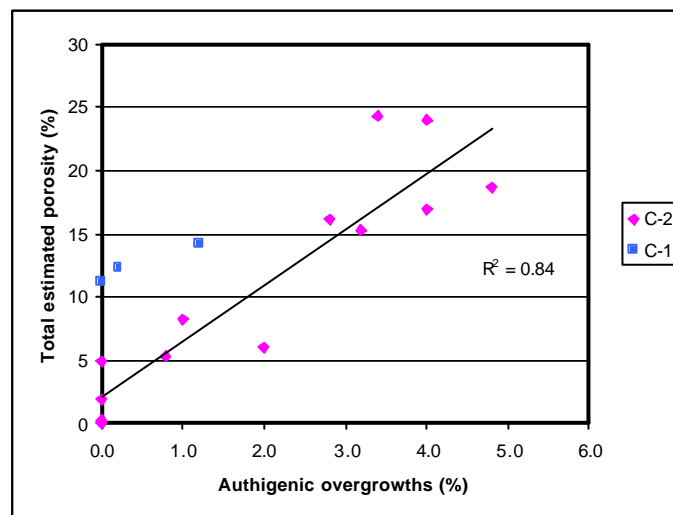


Figure 39. Cross plot illustrating the control of feldspar and quartz overgrowths on porosity in the Waarre Formation at Casino-2 and -1. Note that this data (Phillips, 2003) is a mixture of point counts & visual estimates.

9. CONCLUSIONS

1. Litharenites and sublitharenites from Waarre Unit A at Casino-3 are slightly coarser grained, they contain less lithics, and grains are more angular than Unit A sediments in Casino-2 and -1. Sediment was dominantly derived from both a metamorphic and igneous (volcanic and plutonic) terrane. Deposition occurred in a marginal marine setting, possibly a wave dominated estuary. Casino-3 was probably located closer to the channel axis than Casino-2, and Casino-1 may be juxtaposed to a marsh.
2. A significant change in sediment provenance and depositional environments is apparent in the regressive Waarre Unit Ca. Sandstones vary from very fine to coarse grained sublitharenites, subarkoses and quartzarenites. Volcanic lithics are absent and there is a decline in the number of both feldspars (particularly plagioclase) and lithics. Depositional environments could range from prodelta muds at the base, through storm deposits to tidal channels and flats/ lagoons at the top of the sequence. There are indications that Casino-3 was located closer to the marine influence than Casino-2 at this time.
3. Laminated sands and muds deposited in lagoons/ tidal flats that occur between Units Ca and Cb probably do not form a continuous seal. Migrating tidal channels may have intermittently eroded into this unit.
4. Medium to coarse grained subarkoses and quartzarenites from Waarre Unit Cb show a continuation of the trend in declining feldspar and lithic contents that was apparent in Unit Ca. Volcanic lithics and chalcedony are absent, and relatively mineralogically stable metamorphic lithics and K-feldspars are dominant. Casino-2 was more strongly fluvial influenced than Casino-3 where a possible beach facies occurs at the top of the sequence.
5. Diagenetic alteration in the Waarre Formation was typically early and related to depositional environments and flushing by meteoric waters. Feldspar overgrowths are restricted to Unit A probably because of the influence of volcanic lithics. Localised late diagenetic ferroan calcite cements at the base of Unit A and Unit Ca in Casino-3 may be related to the distribution of plagioclase as a source of calcium.
6. Primary intergranular porosity in the Waarre Formation is preserved where early development of quartz and feldspar overgrowths provided a rigid framework to minimise mechanical compaction. Quartz overgrowths are better developed in the cleaner sands where there are less lithics in Units Ca and Cb. Therefore detrital mineralogy determined the distribution of authigenic minerals which are the prime control of porosity. Permeability was controlled by the preservation of intergranular porosity, not rock composition. Early equant circumgranular carbonate cement in the beach facies of Unit Cb also minimised mechanical compaction. Late ferroan calcite cements had a detrimental but localised influence on reservoir quality and are unlikely to be laterally continuous across the field. Reactive clay minerals that are confined to altered lithics and grains of glaucony, do not appear to have a significant influence on permeability.
7. The medium grained, very poorly sorted sublitharenite studied from the Flaxman Formation at Casino-3 was deposited very rapidly in a marine setting, possibly from a turbidity current or as a slump on a delta front. Sediment provenance was very similar to that in Unit Cb. Reservoir quality is unlikely to be good due to the abundance of detrital clay and siderite cement.

10. GLOSSARY

Boehm lamellae

Parallel trails of vacuoles in quartz that are thought to form during deformation (metamorphism) of grains.

Framboid

A cluster of pyrite crystals with a spheroidal outline.

Glaucony

A term used to describe green minerals without any genetic connotations. If the green minerals can be identified, a specific mineral name is given.

Glaucinite

An Fe-rich dioctahedral illite. The term is also used to refer to a family of Fe-rich dioctahedral clays with varying ratios of expanded (smectite) and non-expanded layers.

Granophyric Texture

A variety of micrographic intergrowth of quartz and alkali feldspar that is either crudely radiate or is less regular than micrographic texture.

Honeycomb Porosity

Secondary porosity produced by the corrosion (etching) of detrital grains.

Hydrocarbon envelope

Solid bitumen surrounding a mineral containing radioactive elements. Radiation causes polymerisation of hydrocarbon chains within oil that rims grains.

Micrographic Intergrowth

A regular intergrowth of two minerals.

Microporosity

Porosity directly associated with clay minerals.

nd

Abbreviation meaning not detected.

Neomorphism

All transformations between a mineral and the same mineral, or another of the same general composition.

Poikilotopic

A sedimentary textural term denoting a single crystal of carbonate enclosing more than one framework grain.

Vacuole

Gas or liquid filled inclusion.



11. REFERENCES

- ADAMS, A.E., W.S. MACKENZIE & C. GUILFORD (1984) *Atlas of sedimentary rocks under the microscope*. Longman Scientific & Technical, 104p.
- BJORKUM, P.A., E.H. OELKERS, P.H. NADEAU, O. WALDERHAUG & W.M. MURPHY (1998) Porosity prediction in quartzose sandstones as a function of time, temperature, depth, stylolite frequency and hydrocarbon saturation. *American Association of Petroleum Geologists Bulletin*, 82, 4, pp. 637-648.
- BJORLYKKE, K (1988) Sandstone diagenesis in relation to preservation, destruction and creation of porosity. In CHILINGARIAN, G.V. & K.H. WOLF (eds) *Diagenesis, I, Developments in Sedimentology*, 41, pp. 555-588.
- DE ROS, L.F., G.N.C. SGARBI & S. MORAD (1994) Multiple authigenesis of K-feldspar in sandstones: evidence from the Cretaceous Areado Formation, Sao Francisco Basin, Central Brazil. *Journal of Sedimentary Research*, A64, 4, pp. 778-787.
- FOLK, R.L. (1974) *Petrology of sedimentary rocks*. Hemphill, 182p.
- GEARY, G.C., A.E. CONSTANTINE & I.S.A REID (2001) New perspectives on structural style and petroleum prospectivity, offshore Eastern Otway Basin. In HILL, K.C. & BERNECKER, T (Eds) *Eastern Australasian Basins Symposium, A Refocused Energy Perspective for the Future*, Petroleum Exploration Society of Australia, Special Publication, pp. 507-517.
- HARRELL, J. (1984) A visual comparator for degree of sorting in thin and plane sections. *Journal of Sedimentary Petrology*. 54, pp. 646-650.
- LEMON, N. (2002) *Casino-2, Core logging report*. Internal report for Santos Ltd.
- LEMON, N. (2003) *Casino-3, Core logging report and interpretation of controls on sedimentation during deposition of the Waarre Ca unit*. Internal report for Santos Ltd.
- LUNDEGARD, P.D. (1992) Sandstone porosity loss - a "big picture" view of the importance of compaction. *Journal of Sedimentary Petrology*, 62, pp. 250-260.
- PARTRIDGE, A. (1997) New Upper Cretaceous Palynology of the Sherbrook Group, Otway Basin. Victorian Supplement, *PESA News*, April/May, p9.
- PETTIJOHN, F.J., P.E. POTTER & R. SIEVER (1987) *Sand and sandstone*. Springer-Verlag, New York, 553p.
- PHILLIPS, S.E. (2003) *Petrology Report of Casino-1 & Casino-2, Otway Basin (VIC/P 44)*. Confidential report written for Santos Ltd by PGPC, 81p.
- STANTON, P.T. & M.D. WILSON (1994) Measurement of independent variables - composition. In M.D. WILSON (Ed) *Reservoir quality assessment and prediction in clastic rocks. SEPM Short Course 30*, 432p.
- TERRY R.D. & G.V. CHILINGAR (1955) Summary of "Concerning some additional aids in studying sedimentary formations" by M.S. Shrestor. *Journal of Sedimentary Petrology*, 25, pp. 229-234.
- THYNE, G.D. & C.J. GWINN (1994) Evidence for a paleoaquifer from early diagenetic siderite of the Cardium Formation, Alberta, Canada. *Journal of Sedimentary Research*, A64, 4, pp. 726-732.

TUCKER, M. (1988) *Techniques in sedimentology*. Blackwell Scientific, 394p.

TUCKER, M.E. (2001) *Sedimentary petrology, an introduction to the origin of sedimentary rocks*. (3rd Ed) Blackwell Scientific, 262p.

WEAVER, C.E. (1989) Clays, muds and shales. *Developments in Sedimentology* 44, Elsevier, 819p.



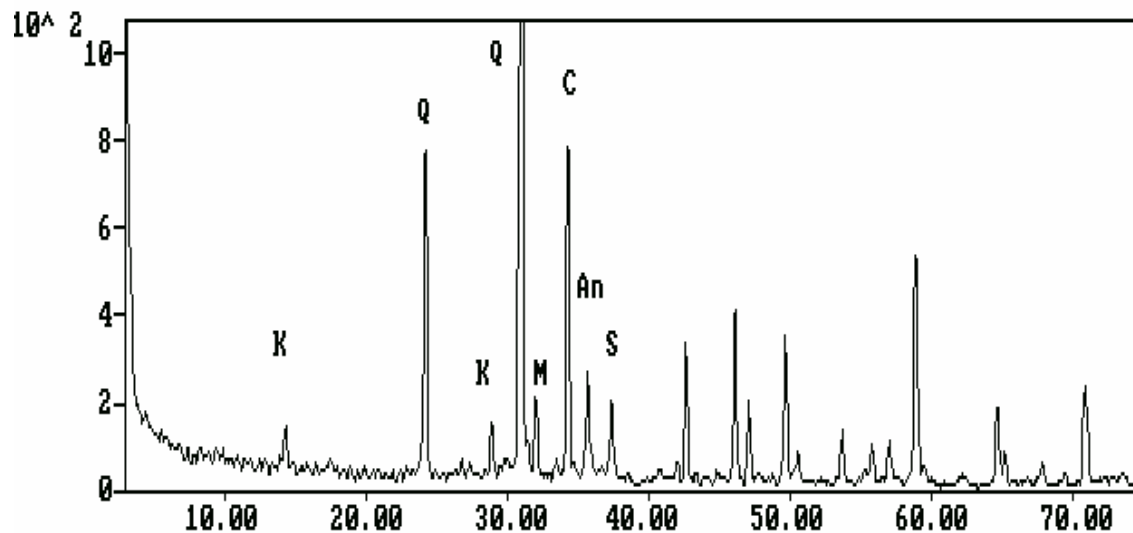
12. APPENDIX A

XRD TRACES

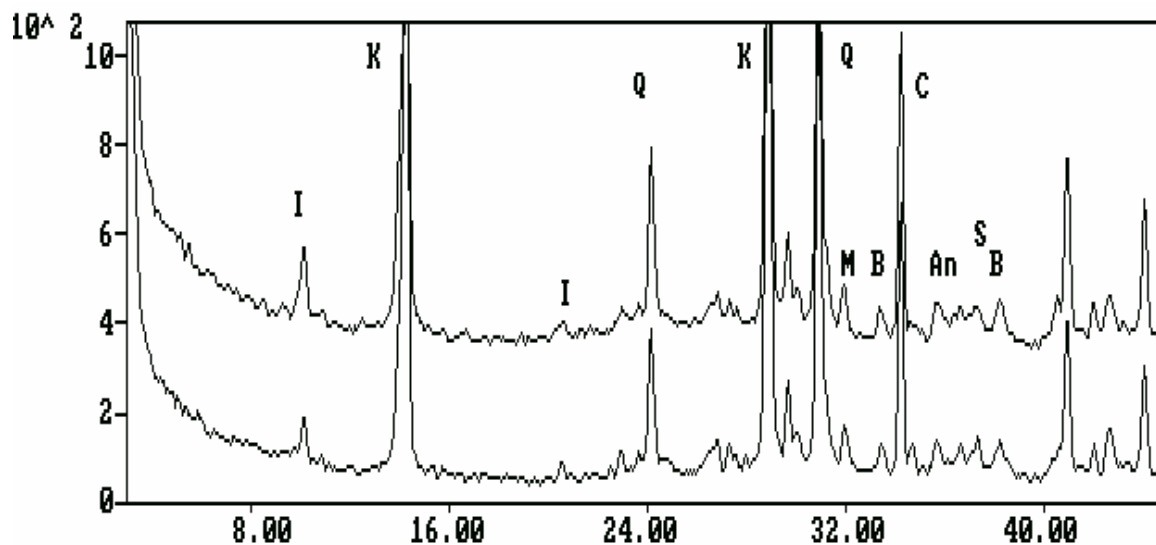
Only the strongest peaks for each mineral identified have been labeled on the XRD traces. The horizontal axis on each trace is in degrees two theta and the vertical axis is in counts of peak height. For the clay fraction both Mg saturated and Mg plus glycerol traces have been included to demonstrate movements in the peaks that aided identification of smectite. The fact that peaks did move in response to glycerol indicates the presence of smectite rather than vermiculite. The following abbreviations have been used on the XRD traces:

A = albite
An = ankerite
B = barite
C = calcite
Ch = chlorite
I/M = illite or muscovite
K = kaolinite
M = microcline
P = pyrite
Q = quartz
S = siderite
Sa = sanidine
Sm = smectite

Sample: CASINO-3, MSCT 6, depth 2102.5m (Logger).

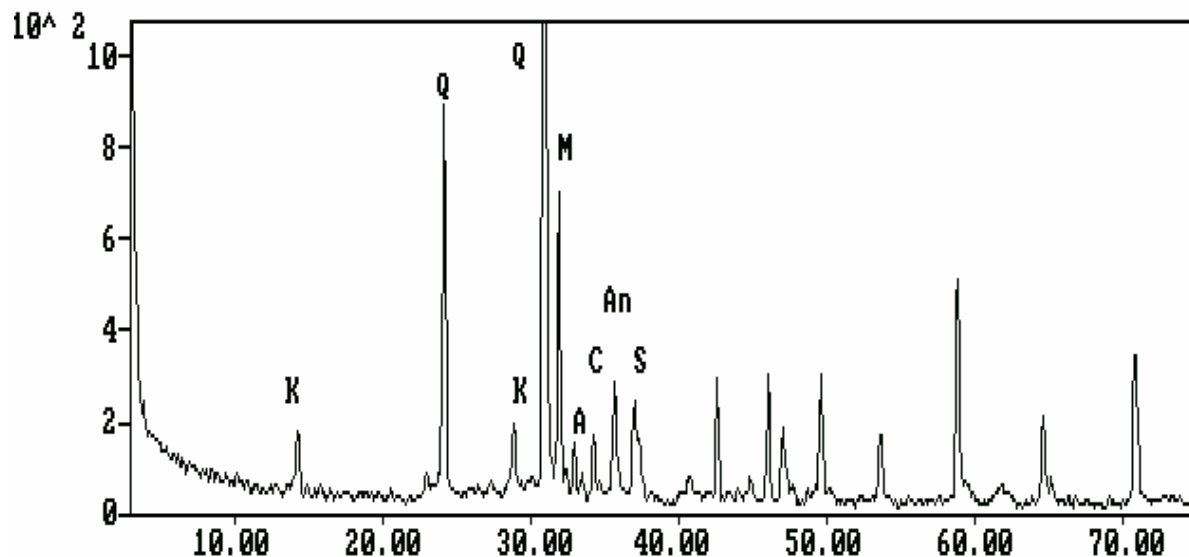


Bulk XRD trace.

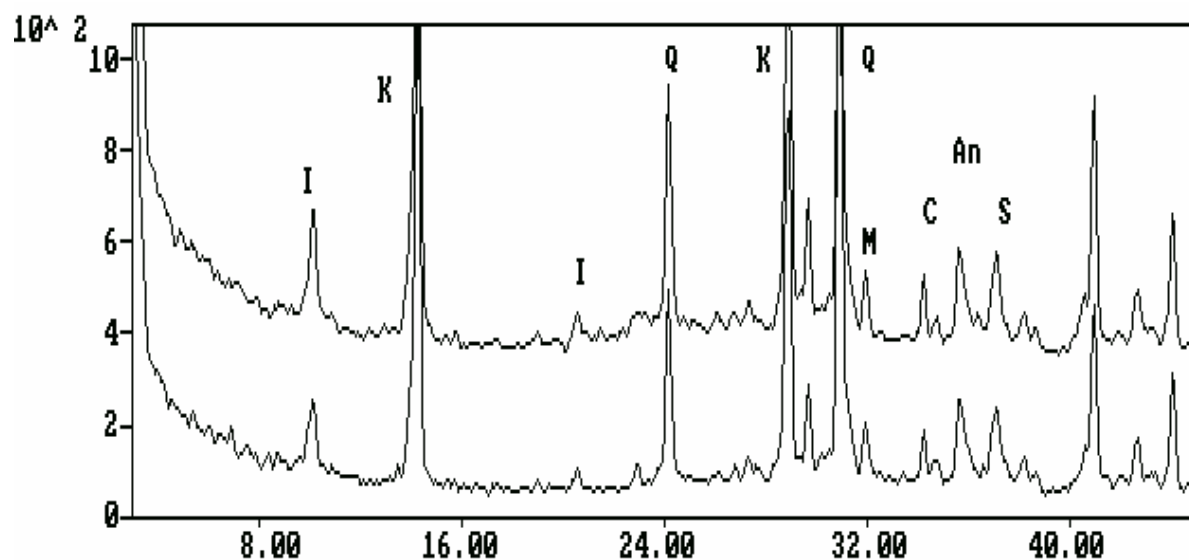


Clay XRD traces. (Lower trace is Mg saturated and air dried. Upper trace is Mg and glycerol saturated and air dried.)

Sample: CASINO-3, MSCT 13, depth 2061.5m (Logger).

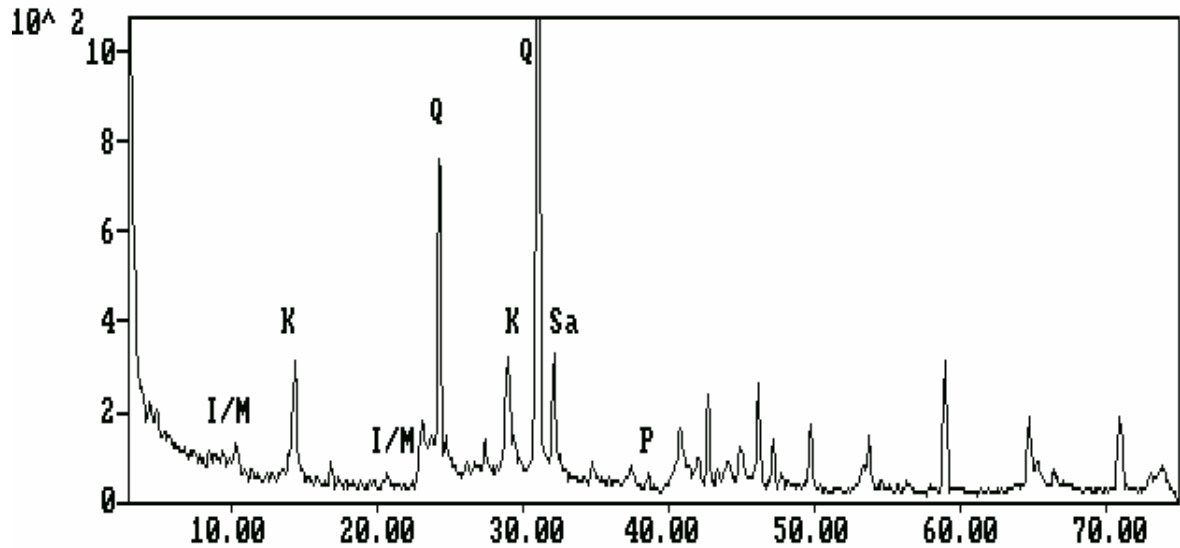


Bulk XRD trace.

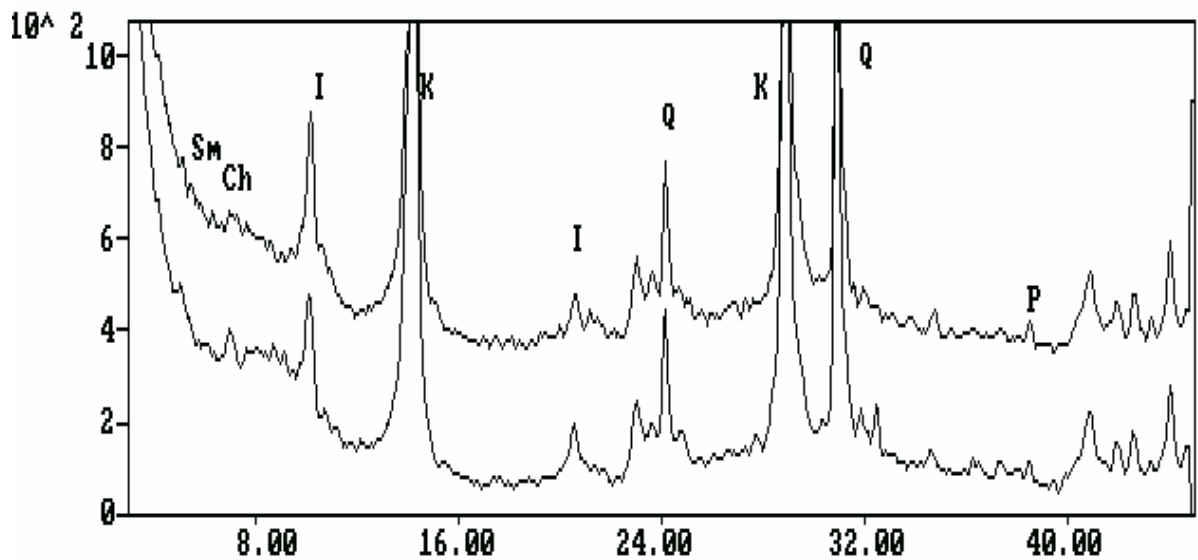


Clay XRD traces. (Lower trace is Mg saturated and air dried. Upper trace is Mg and glycerol saturated and air dried.)

Sample: CASINO-3, Core chip, depth 2028.5m (Driller).

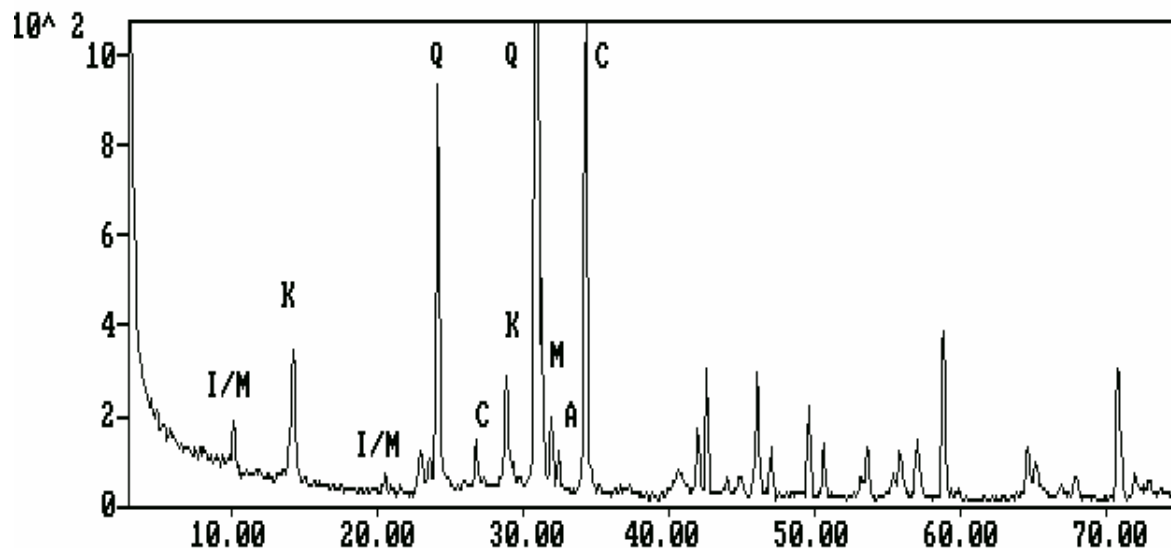


Bulk XRD trace.

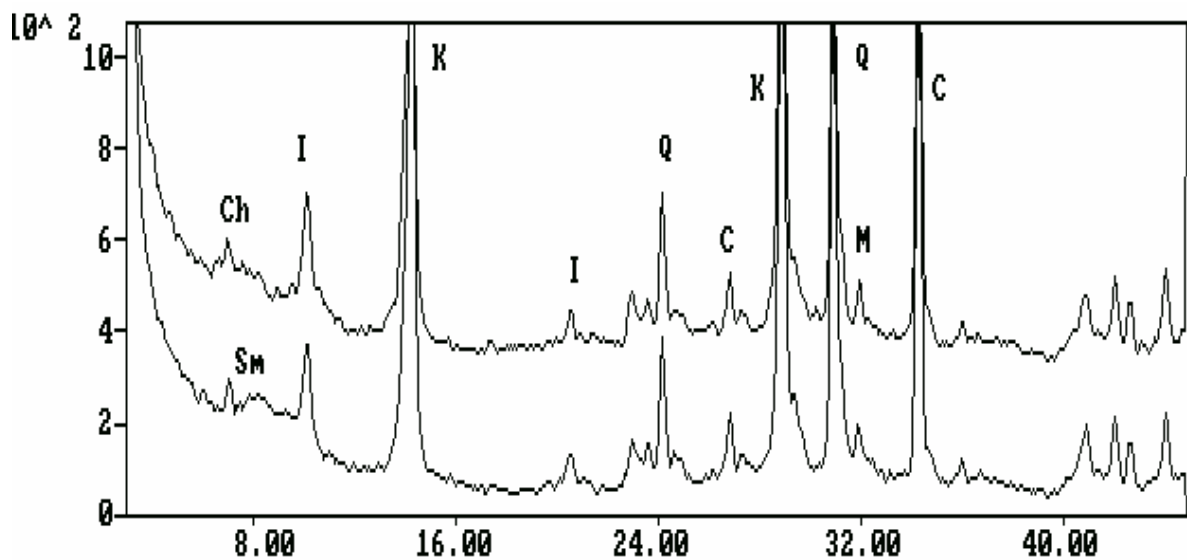


Clay XRD traces. (Lower trace is Mg saturated and air dried. Upper trace is Mg and glycerol saturated and air dried.)

Sample: CASINO-3, Core plug 75, depth 2026.49m (Driller).

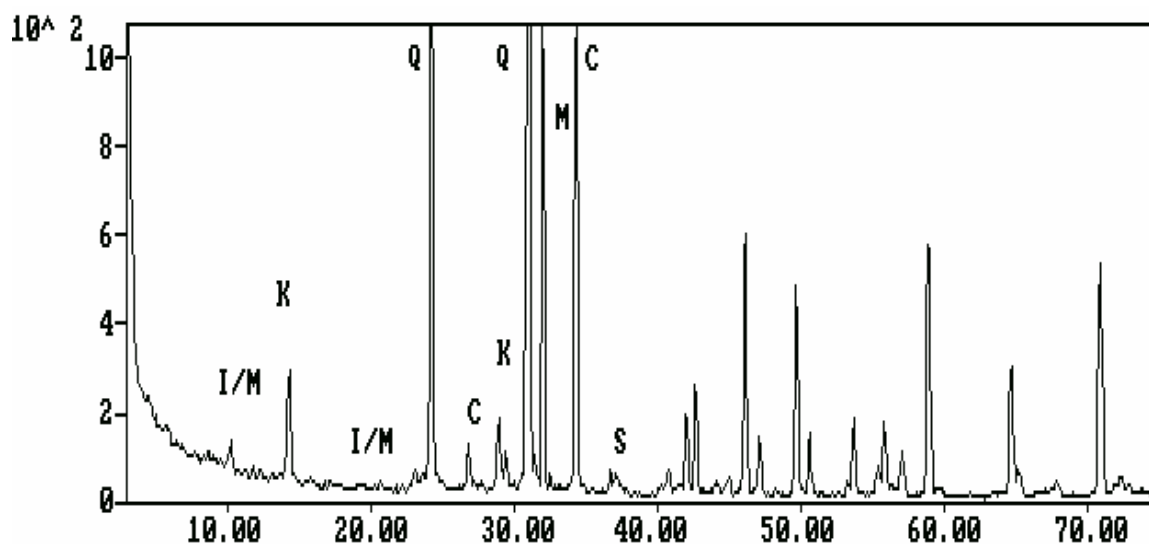


Bulk XRD trace.

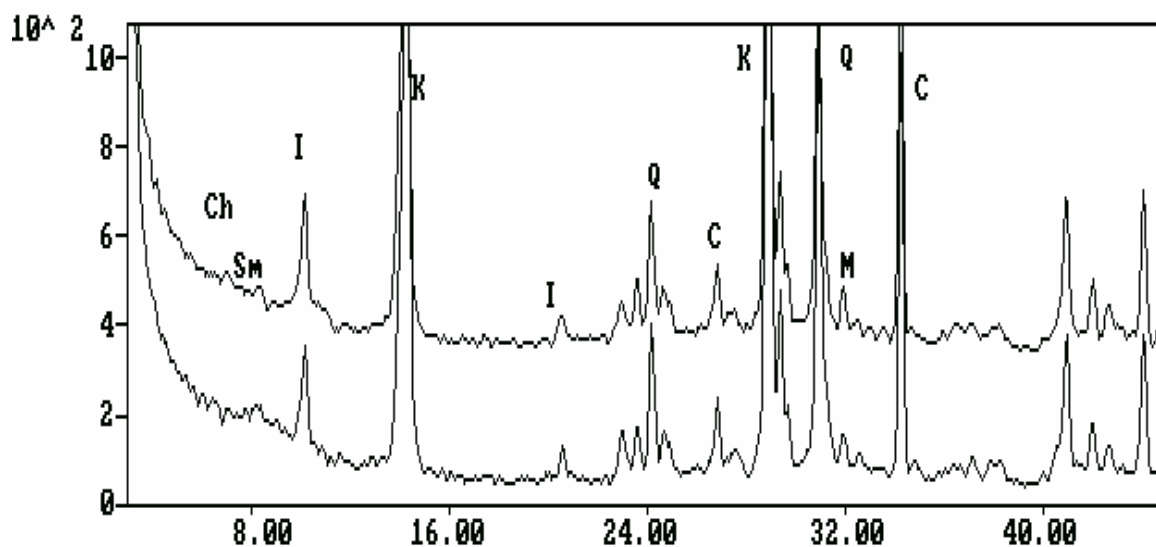


Clay XRD traces. (Lower trace is Mg saturated and air dried. Upper trace is Mg and glycerol saturated and air dried.)

Sample: CASINO-3, Core plug 62, depth 2022.60m (Driller).

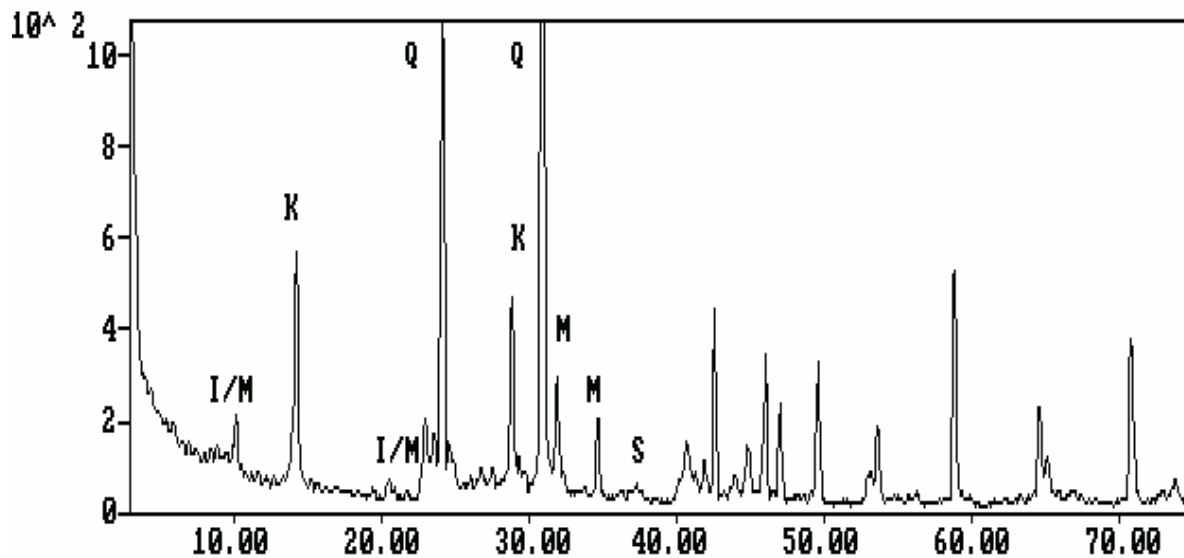


Bulk XRD trace.

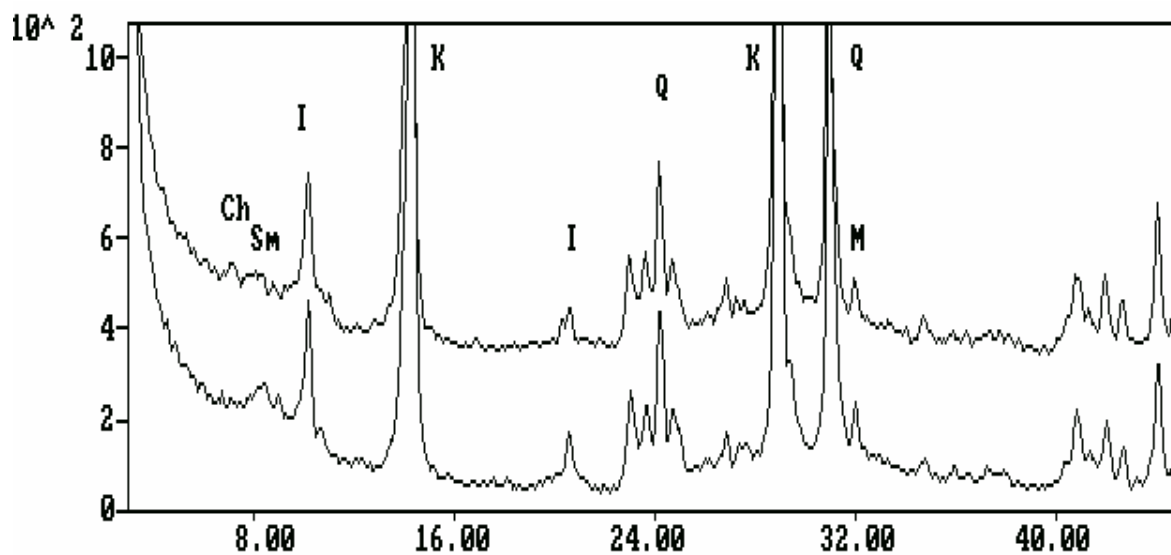


Clay XRD traces. (Lower trace is Mg saturated and air dried. Upper trace is Mg and glycerol saturated and air dried.)

Sample: CASINO-3, Core plug 59, depth 2021.76m (Driller).

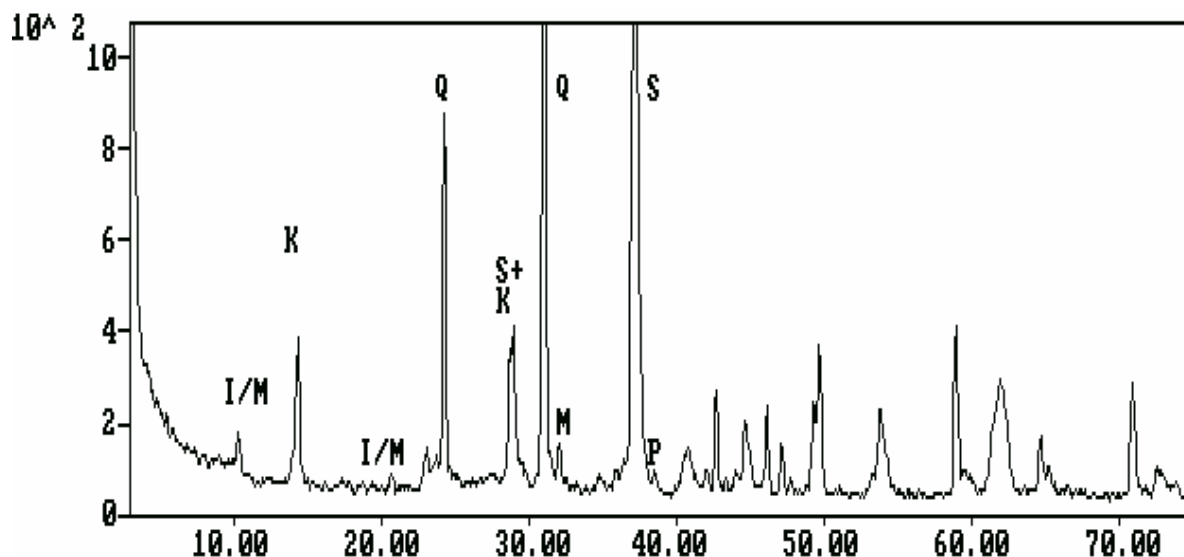


Bulk XRD trace.

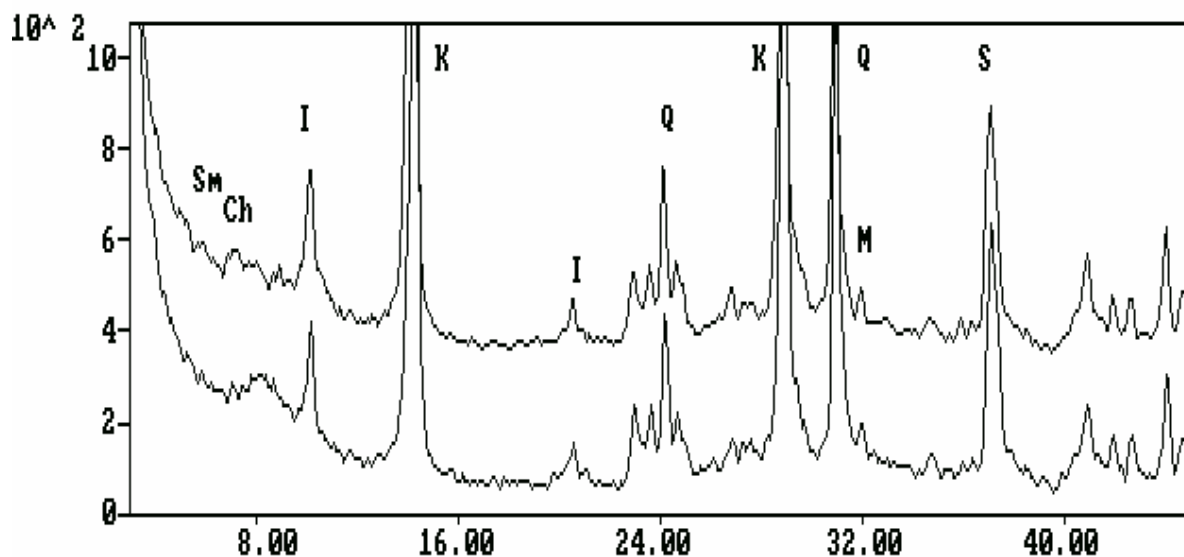


Clay XRD traces. (Lower trace is Mg saturated and air dried. Upper trace is Mg and glycerol saturated and air dried.)

Sample: CASINO-3, Core plug 41, depth 2016.39m (Driller).

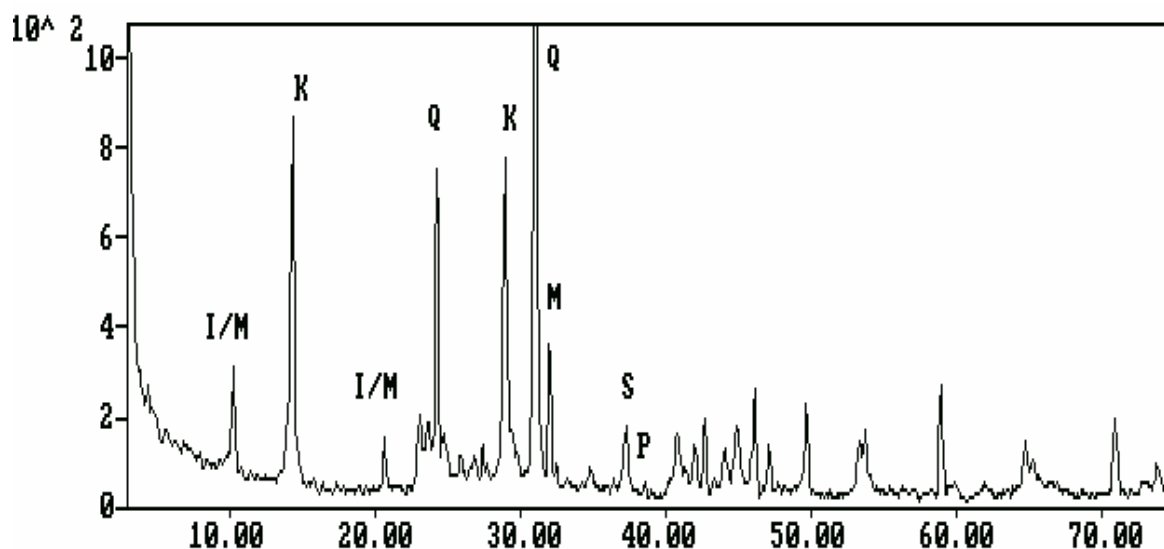


Bulk XRD trace.

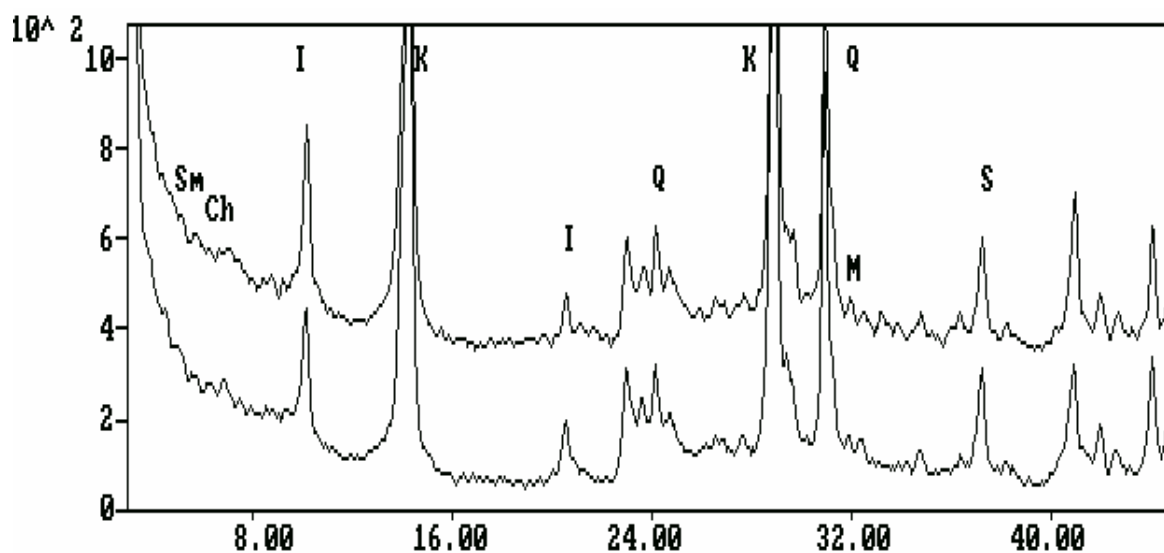


Clay XRD traces. (Lower trace is Mg saturated and air dried. Upper trace is Mg and glycerol saturated and air dried.)

Sample: CASINO-3, Core plug 9, depth 2006.70m (Driller).

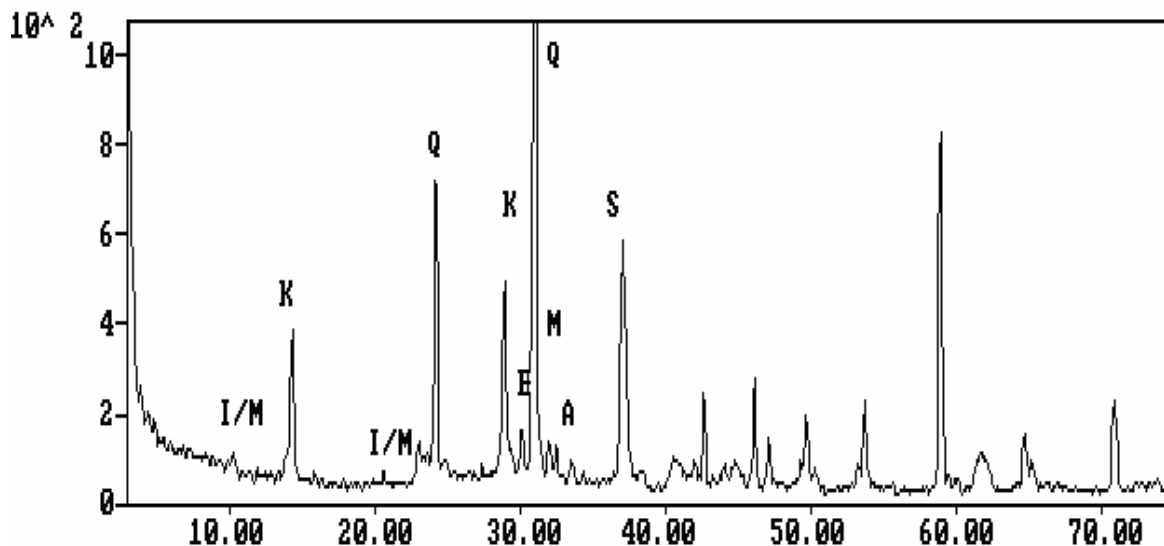


Bulk XRD trace.

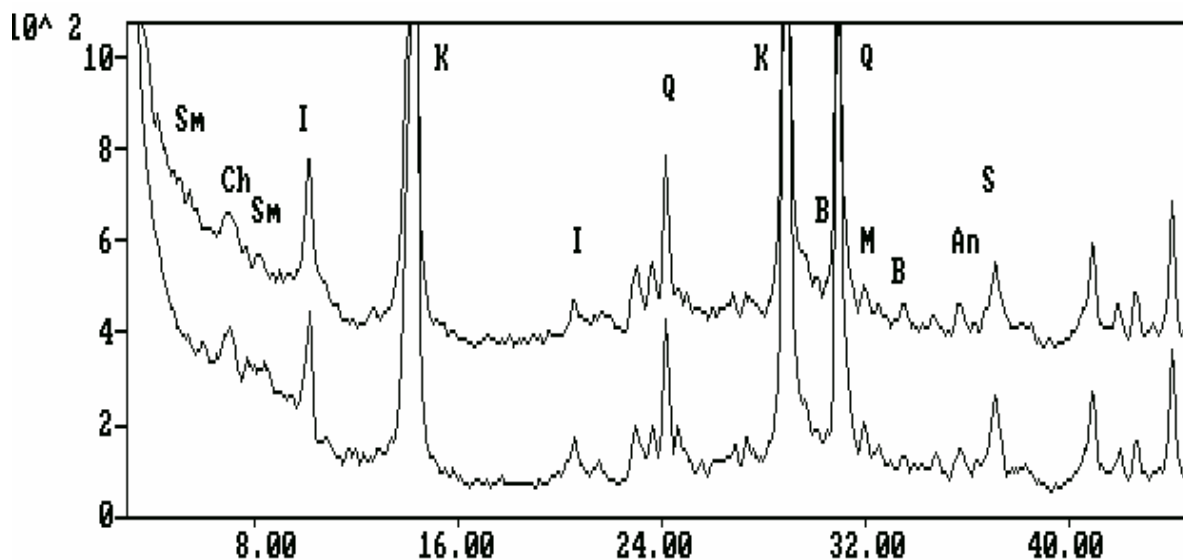


Clay XRD traces. (Lower trace is Mg saturated and air dried. Upper trace is Mg and glycerol saturated and air dried.)

Sample: CASINO-3, MSCT 11, depth 1970.5m (Logger).



Bulk XRD trace.



Clay XRD traces. (Lower trace is Mg saturated and air dried. Upper trace is Mg and glycerol saturated and air dried.)

APPENDIX VI : PALYNOLOGY REPORT

The Palynology Report is presented overleaf.

**SANTOS PALYNOLOGY SECTION
EXPLORATION SERVICES DEPARTMENT**

Palynology Report No. 2001/33

Author: G. WOOD & R.HELBY

Approved by: G.WOOD

PALYNOLOGICAL REPORT NO. 2003/33
PALYNOSTRATIGRAPHICAL ANALYSIS

CASINO -3 WELL

Santos Ltd
A.C.N. 007 550 923

Circulation: Geology Operations, Team Leader, EIC, Palynology Files

Introduction

The palynological content of ten conventional core samples, twenty sidewall core samples and sixteen cuttings samples from Santos Casino-3, were examined.

The palynostratigraphic results are presented in on Table 1.

G. Wood & R. Helby

Santos

Study: . Casino-3

Author: G. Wood & R. Helby

PALYNOSTRATIGRAPHICAL DATA

Table 1

Report No. 2003/33

Page 1 of 13

SAMPLE	DEPTH (M)	PALYNOSTRATIGRAPHICAL UNIT (Age)	INFERRED STRATIGRAPHICAL UNIT	REWORKED ELEMENTS		PRESER VATION	YIELD	DIVER SITY	REMARKS
				%	AGE				
SWC30	1165.0	<i>Isabelidinium korojonense</i> (mid to late Campanian)	Timboon Ss	X	Perm.	Fair-good	Mod.	High	Moderate diversity, but numerically restricted, dinocyst suite with <i>Isabelidinium pellucidum</i> , <i>Chatangiella micracantha</i> , <i>Manumiella</i> sp. cf. <i>M. druggii</i> and <i>Odontochitina indigena</i> . Very diverse spore-pollen suite with <i>Gambierina rudata</i> , <i>Lactoropollenites</i> sp., <i>Nothofagidites</i> spp. and <i>Tricolporites lilliei</i> . Shallow shelf.
SWC29	1259.0	<i>Isabelidinium korojonense</i> (mid to late Campanian)	Timboon Ss	1	Perm.	Fair-good	Mod.	High	Moderate diversity, but restricted, dinocyst suite with <i>Isabelidinium pellucidum</i> , <i>Chatangiella micracantha</i> , <i>Manumiella</i> sp. cf. <i>M. druggii</i> and <i>Spinidinium</i> sp. cf. <i>S. spinulosum</i> . Acritarchs prominent including <i>Nummus</i> sp. (9%) and <i>Paralecaniella</i> sp. (3%). Very diverse spore-pollen suite with <i>Forcipites sabulosus</i> , <i>Gambierina rudata</i> , <i>Nothofagidites</i> spp. and <i>Tricolporites lilliei</i> . Shallow shelf.
SWC28	1408.0	<i>Xenikoon australis</i> (early to mid Campanian)	Paaratte Formation	X	Perm.	Fair-good	Mod.	High	Restricted (1% of total palynomorphs), low diversity dinocyst suite with <i>Xenikoon australis</i> , <i>Gillinia hymenophora</i> and <i>Palaeohystrichophora infusorioides</i> . Diverse spore-pollen suite with <i>Gambierina rudata</i> , <i>Nothofagidites</i> spp. and <i>Peninsulapollis gillii</i> . Shallow shelf.
SWC27	1509.0	<i>Xenikoon australis</i> (early to mid Campanian)	Paaratte Formation	1	Perm.	Fair-good	Mod.	High	Relatively rich (18%) but low diversity dinocyst suite dominated by <i>Xenikoon australis</i> with <i>Nelsoniella aceras</i> and <i>N. semireticulata</i> . Diverse spore-pollen suite with <i>Clavifera vultuosus</i> , <i>Forcipites sabulosus</i> , <i>G. rudata</i> , <i>Nothofagidites</i> spp. and <i>P. gillii</i> . Shallow shelf.

Santos

Study: . Casino-3

Author: G. Wood & R. Helby

PALYNOSTRATIGRAPHICAL DATA

Table 1

Report No. 2003/33

Page 2 of 13

SAMPLE	DEPTH (M)	PALYNOSTRATIGRAPHICAL UNIT (Age)	INFERRED STRATIGRAPHICAL UNIT	REWORKED ELEMENTS		PRESER VATION	YIELD	DIVER SITY	REMARKS
				%	AGE				
SWC26	1528.5	<i>Xenikoon australis</i> (early to mid Campanian)	Paaratte Formation	1	Perm.	Fair-good	Mod.	High	Restricted (4%), low diversity dinocyst suite with <i>Xenikoon australis</i> and <i>Palaeohystrichophora infusorioides</i> . Diverse spore-pollen suite with <i>Camarozonosporites bullatus</i> , <i>Clavifera vultuosus</i> , <i>Forcipites sabulosus</i> , <i>Lactoropollenites</i> sp <i>Nothofagidites</i> spp., <i>Peninsulapollis gillii</i> and <i>Tricolporites apoxyexinus</i> . Shallow shelf.
SWC25	1557.0	<i>Xenikoon australis</i> (early to mid Campanian)	Paaratte Formation	X	Perm.	Poor-good	Mod.	High	Rich (28%), moderate diversity dinocyst suite dominated by <i>Xenikoon australis</i> . Diverse spore-pollen suite with <i>Clavifera vultuosus</i> , <i>Forcipites sabulosus</i> , <i>Nothofagidites</i> spp. and <i>Tricolpites confessus</i> . Shallow shelf.
SWC24	1582.5	<i>Xenikoon australis</i> (early to mid Campanian)	Paaratte Formation	X	Perm.	Fair-good	Mod.	High	Fairly rich (18%), moderate diversity dinocyst suite dominated by <i>Xenikoon australis</i> , <i>Nelsoniella aceras</i> and frequent <i>N. tuberculata</i> . Diverse spore-pollen suite with <i>Camarozonosporites bullatus</i> , <i>Forcipites sabulosus</i> , <i>Nothofagidites</i> spp. and <i>Peninsulapollis gillii</i> . Shallow shelf.
SWC23	1607.5	<i>Xenikoon australis</i> (early to mid Campanian)	Paaratte Formation	1	Perm.	Fair-good	Mod.	High	Rich (30%), moderate diversity dinocyst suite dominated by <i>Xenikoon australis</i> with <i>Nelsoniella aceras</i> and <i>N. tuberculata</i> . Diverse spore-pollen suite with <i>Clavifera vultuosus</i> , <i>Forcipites sabulosus</i> and <i>Peninsulapollis gillii</i> . Shallow shelf.

Santos

Study: . Casino-3

Author: G. Wood & R. Helby

PALYNOSTRATIGRAPHICAL DATA

Table 1

Report No. 2003/33

Page 3 of 13

SAMPLE	DEPTH (M)	PALYNOSTRATIGRAPHICAL UNIT (Age)	INFERRED STRATIGRAPHICAL UNIT	REWORKED ELEMENTS		PRESER VATION	YIELD	DIVER SITY	REMARKS
				%	AGE				
SWC22	1623.5	<i>Xenikoon australis</i> (early to mid Campanian)	Paaratte Formation	1	Perm.	Fair-good	Mod.	High	Low diversity dinocyst suite with <i>Xenikoon australis</i> , <i>Nelsoniella aceras</i> , <i>Areosphaeridium suggestium</i> and frequent (8%) <i>Heterosphaeridium</i> spp. Diverse spore-pollen suite with <i>Nothofagidites senectus</i> and <i>Tricolporites apoxyexinus</i> . Shallow shelf.
SWC21	1660.0	<i>Xenikoon australis</i> (early to mid Campanian)	Paaratte Formation	2	Perm.	Fair-good	Mod.	High	Restricted, low diversity dinocyst suite with <i>Xenikoon australis</i> , <i>Nelsoniella tuberculata</i> and frequent (4%) <i>Heterosphaeridium</i> spp. Diverse spore-pollen suite not well characterized with <i>Australopollis obscuris</i> (3%) and prominent <i>Proteacidites</i> spp (12%). Shallow shelf.
SWC20	1705.5	<i>Xenikoon australis</i> (early to mid Campanian)	Paaratte Formation	X	Perm.	Fair-good	Mod.	High	Restricted, low diversity dinocyst suite with <i>Xenikoon australis</i> , <i>Nelsoniella tuberculata</i> and rare <i>Heterosphaeridium</i> spp. Diverse spore-pollen suite <i>Lactoropollenites</i> sp., <i>Nothofagidites senectus</i> and prominent <i>Proteacidites</i> spp (10%). Shallow shelf.
CUTT	1764	<i>Xenikoon australis</i> (early to mid Campanian)	Paaratte Formation	X	Perm.	Fair-good	Mod.	High	Restricted, low diversity dinocyst suite with <i>Xenikoon australis</i> , <i>Odontochitina porifera</i> and frequent <i>Heterosphaeridium</i> spp. Diverse spore-pollen suite, not well characterized, with <i>Australopollis obscuris</i> (3%) and prominent <i>Proteacidites</i> spp (12%). Shallow shelf.

Santos

Study: . Casino-3

Author: G. Wood & R. Helby

PALYNOSTRATIGRAPHICAL DATA

Table 1

Report No. 2003/33

Page 4 of 13

SAMPLE	DEPTH (M)	PALYNOSTRATIGRAPHICAL UNIT (Age)	INFERRED STRATIGRAPHICAL UNIT	REWORKED ELEMENTS		PRESER VATION	YIELD	DIVER SITY	REMARKS
				%	AGE				
CUTT	1800	Nelsoniella aceras (early Campanian)	Skull Ck Mudstone to Paaratte Formation	1	Perm.	Fair-good	Mod.	High	Restricted, low diversity dinocyst suite with <i>Nelsoniella aceras</i> , <i>N. tuberculata</i> , <i>Odontochitina porifera</i> and relatively 3% frequent <i>Heterosphaeridium</i> spp. Diverse spore-pollen suite, not well characterized, with <i>Australopollis obscuris</i> (4%) and frequent <i>Proteacidites</i> spp (9%). Shallow shelf.
CUTT	1857	Nelsoniella aceras (early Campanian)	Skull Ck Mudstone to Paaratte Formation	-	-	Fair-good	Mod.	High	Moderate diversity dinocyst suite with <i>Isabelidinium</i> cretaceum, <i>Nelsoniella aceras</i> , <i>Odontochitina porifera</i> , <i>Trithyrodinium vermiculatum</i> and <i>Xenikoon australis</i> (caved ?). Diverse spore-pollen suite includes <i>Clavifera vultuosus</i> , <i>Nothofagidites senectus</i> , <i>Proteacidites</i> spp. (3%) and <i>Tetracolporites reticulatus</i> (caved ?). Shallow shelf.
CUTT	1863	Isabelidinium rotundatum (Late Santonian – early Campanian)	Nullawarre Gnsd/ Skull Creek Mdst	1	Perm.	Fair-good	Mod.	High	Relatively rich (36%), moderately diverse, dinocyst suite with <i>I. rotundatum</i> , <i>Hexagonifera glabra</i> , <i>Nelsoniella aceras</i> , <i>Occisucysta septata</i> , <i>Odontochitina porifera</i> and prominent <i>Trithyrodinium vermiculatum</i> . The spore-pollen suite is not well characterized (<i>Proteacidites</i> spp. 5%). Shelfal marine.
CUTT	1878	Isabelidinium rotundatum (Late Santonian – early Campanian)	Nullawarre Gnsd/ Skull Creek Mdst	-	-	Fair-good	Mod.	High	Relatively rich (37%), moderately diverse, dinocyst suite with frequent <i>I. rotundatum</i> , <i>Hexagonifera glabra</i> , <i>Occisucysta septata</i> , <i>Odontochitina porifera</i> and <i>Trithyrodinium vermiculatum</i> . <i>Nelsoniella aceras</i> and <i>Xenikoon australis</i> present, possibly caved. The spore-pollen suite not well characterized. Shelfal marine.

Santos

Study: . Casino-3

Author: G. Wood & R. Helby

PALYNOSTRATIGRAPHICAL DATA

Table 1

Report No. 2003/33

Page 5 of 13

SAMPLE	DEPTH (M)	PALYNOSTRATIGRAPHICAL UNIT (Age)	INFERRED STRATIGRAPHICAL UNIT	REWORKED ELEMENTS		PRESER VATION	YIELD	DIVER SITY	REMARKS
				%	AGE				
CUTT	1896	Isabelidinium rotundatum (Late Santonian – early Campanian)	Nullawarre Gnsd/ Skull Creek Mdst	2	Perm.	Fair-good	Mod.	High	Rich (53%), diverse, dinocyst suite with <i>Isabelidinium cretaceum</i> , <i>I. rotundatum</i> , <i>Hexagonifera glabra</i> , <i>Occisucysta septata</i> , <i>Odontochitina wannabe</i> and <i>Trithyrodinium vermiculatum</i> . <i>Nelsoniella aceras</i> and <i>Xenikoon australis</i> present, but considered caved. Shelfal marine.
CUTT	1932	<i>Isabelidinium cretaceum</i> Late Santonian	Belfast Mudstone C	-	Perm.	Fair-good	Mod.	High	Relatively rich (37%), moderately diverse, dinocyst suite with <i>Isabelidinium cretaceum</i> , <i>I. rotundatum</i> , <i>Amphidiadema denticulata</i> , <i>Hexagonifera glabra</i> , <i>Odontochitina porifera</i> , <i>O. wannabe</i> and <i>Trithyrodinium vermiculatum</i> . <i>Nelsoniella aceras</i> and <i>Xenikoon australis</i> present, but considered caved. The spore-pollen suite is not well characterized. Shelfal marine.
CUTT	1932	<i>Isabelidinium cretaceum</i> Late Santonian	Belfast Mudstone C	-	Perm.	Poor-fair	Mod.	High	Relatively rich (31%), moderately diverse, dinocyst suite with <i>Isabelidinium cretaceum</i> , <i>Amphidiadema denticulata</i> , <i>Hexagonifera glabra</i> , <i>Occisucysta septata</i> , <i>Odontochitina porifera</i> , <i>O. wannabe</i> and <i>Trithyrodinium vermiculatum</i> . <i>Isabelidinium rotundatum</i> , <i>Nelsoniella aceras</i> and <i>Xenikoon australis</i> present, but considered caved. The spore-pollen suite is not well characterized. Shelfal marine.
CUTT	1943	<i>Odontochitina porifera</i> (?) Early to mid Santonian	Belfast Mudstone B (?)	-	Perm.	Poor-fair	Mod.	High	Moderately diverse dinocyst suite (17% total palynomorphs) with <i>Isabelidinium</i> spp., including <i>I. rectangularare</i> (?), “frequent” <i>Odontochitina porifera</i> and tentative <i>I. balmei</i> , <i>Trithyrodinium marshalli</i> . Spore-pollen suite includes <i>Tricolporites apoxyxinus</i> . Near-shore.

Santos

Study: . Casino-3

Author: G. Wood & R. Helby

PALYNOSTRATIGRAPHICAL DATA

Table 1

Report No. 2003/33

Page 6 of 13

SAMPLE	DEPTH (M)	PALYNOSTRATIGRAPHICAL UNIT (Age)	INFERRED STRATIGRAPHICAL UNIT	REWORKED ELEMENTS		PRESER VATION	YIELD	DIVER SITY	REMARKS
				%	AGE				
SWC16	1951.0	<i>Lower Valensiella griphus</i> (Turonian)	Lower Flaxman Fm	1	Perm.	Poor-fair	Mod.	High	Restricted (5%), moderately diverse, dinocyst suite with "frequent" <i>Valensiella griphus</i> , "frequent" <i>Chlamydothorea</i> sp., <i>Isabelidium balmei</i> and <i>Kiokansium polypes</i> . Spore-pollen suite not well defined. Near-shore.
SWC15	1958.5	<i>Lower Valensiella griphus</i> (Turonian)	Lower Flaxman Fm	1	Perm.	Poor-fair	Mod.	High	Fairly restricted (12%), moderately diverse, dinocyst suite with "common" <i>Valensiella griphus</i> , <i>Isabelidium</i> sp., <i>Kiokansium polypes</i> and "frequent" <i>Odontochitina costata</i> (s.l.). <i>Amosopollis cruciformis</i> common (11%). Spore-pollen suite not well defined. Near-shore.
SWC13	1969.0	<i>Lower Valensiella griphus to upper Isabelidium evexus</i> (Turonian)	Lower Flaxman Fm to Waarre SS - Cb	1	Perm.	Poor-fair	Mod.	High	Relatively rich (39%), moderate diversity dinocyst suite with <i>Cribroperidinium edwardsii</i> , <i>Kiokansium polypes</i> , <i>Palaeohystrichophora infusorioides</i> and dominated by <i>Heterosphaeridium</i> spp. (26% total palynomorphs). <i>Amosopollis cruciformis</i> common (12%). Spore-pollen suite not well defined. Near-shore.
SWC12	1974.5	<i>Lower Valensiella griphus to upper Isabelidium evexus</i> (Turonian)	Lower Flaxman Fm to Waarre SS - Cb	-	-	Poor-fair	Mod.	High	Moderate diversity dinocyst suite with <i>Cribroperidinium edwardsii</i> , <i>Exochosphaeridium</i> spp., <i>Isabelidium</i> spp., <i>Kiokansium polypes</i> , <i>Tanyosphaeridium salpinx</i> and frequent <i>Heterosphaeridium</i> spp. <i>Amosopollis cruciformis</i> frequent (6%). Spore-pollen suite not well defined. Near-shore.

Santos

Study: . Casino-3

Author: G. Wood & R. Helby

PALYNOSTRATIGRAPHICAL DATA

Table 1

Report No. 2003/33

Page 7 of 13

SAMPLE	DEPTH (M)	PALYNOSTRATIGRAPHICAL UNIT (Age)	INFERRED STRATIGRAPHICAL UNIT	REWORKED ELEMENTS		PRESER VATION	YIELD	DIVER SITY	REMARKS
				%	AGE				
SWC10	1980.0	Lower Valensiella griphus to upper Isabelidium evexus (Turonian)	Lower Flaxman Fm	1	Perm.	Poor-fair	Mod.	High	Relatively rich (39%), moderate diversity dinocyst suite with frequent <i>Apteodinium</i> sp. (JGG), <i>Cribopteridinium edwardsii</i> , <i>Kiokansium polypes</i> , <i>Spinidium</i> sp. A and dominated by <i>Heterosphaeridium</i> spp. (22% total palynomorphs). <i>Amosopollis cruciformis</i> frequent (8%). Spore-pollen suite not well defined. Near-shore.
CUTT	1992	Kiokansium polypes (undiff.) (Turonian)	Waarre Ss - Cb	1	Perm.	Poor-fair	Mod.	High	Fairly restricted (10%), low diversity dinocyst suite with <i>Apteodinium</i> sp. (JGG), <i>Circulodinium "distinctum"</i> , <i>Oligosphaeridium pulcherrimum</i> and <i>Xiphophoridium alatum</i> . <i>Heterosphaeridium</i> spp. frequent (6%). Spore-pollen suite includes <i>Appendicisporites</i> spp. and <i>Australopollis obscuris</i> . Near-shore.
CUTT	1995	Kiokansium polypes (undiff.) (Turonian)	Waarre Ss - Cb	2	Perm.	Poor-fair	Mod.	High	Restricted (<10%), moderate diversity dinocyst suite with <i>Apteodinium</i> sp. (JGG), <i>Circulodinium "distinctum"</i> , <i>Exochosphaeridium</i> spp., <i>Kiokansium polypes</i> , <i>Oligosphaeridium</i> spp. and <i>Palaeoperidinium cretaceum</i> . <i>Heterosphaeridium</i> spp. frequent (<4%). Caving from Belfast Mdst evidenced by <i>Isabelidium cretaceum</i> and <i>Trithyrodinium vermiculatum</i> . Spore-pollen suite not well defined. Near-shore.

Santos

Study: . Casino-3

Author: G. Wood & R. Helby

PALYNOSTRATIGRAPHICAL DATA

Table 1

Report No. 2003/33

Page 8 of 13

SAMPLE	DEPTH (M)	PALYNOSTRATIGRAPHICAL UNIT (Age)	INFERRED STRATIGRAPHICAL UNIT	REWORKED ELEMENTS		PRESER VATION	YIELD	DIVER SITY	REMARKS
				%	AGE				
CUTT	1995	Kiokansium polypes (<i>undiff.</i>) (<i>Turonian</i>)	Waarre Ss - Cb	2	Perm.	Poor-fair	Mod.	High	Restricted (<10%), moderate diversity dinocyst suite with <i>Apteodinium</i> sp. (JGG), <i>Circulodinium</i> "distinctum", <i>Exochosphaeridium</i> spp., <i>Kiokansium polypes</i> , <i>Oligosphaeridium</i> spp. and <i>Palaeoperidinium cretaceum</i> . <i>Heterosphaeridium</i> spp. frequent (<4%). <i>Isabelidinium evexus</i> plexus not recorded. Caving from Belfast Mdst evidenced by <i>Isabelidinium cretaceum</i> and <i>Trithyrodinium vermiculatum</i> . Spore-pollen suite not well defined. Near-shore.
CUTT	1998	Kiokansium polypes (<i>undiff.</i>) (<i>Turonian</i>)	Waarre Ss - Cb	2	Perm.	Poor-fair	Low	High	Moderate diversity dinocyst suite with <i>Kiokansium polypes</i> , <i>Oligosphaeridium</i> spp. and <i>Palaeoperidinium cretaceum</i> . <i>Isabelidinium evexus</i> plexus not recorded. Caving from Belfast Mdst to Paaratte Formation prominent. Near-shore.
SWC6	2000.5	Isabelidinium evexus (<i>undiff.</i>) (<i>Turonian</i>)	Waarre Ss – Ca/Cb	-	-	Poor-good	Low	High	Moderate diversity dinocyst suite (19% total palynomorphs) with <i>Isabelidinium evexus</i> (?), <i>Kiokansium polypes</i> , <i>Palaeohystrichophora infusorioides</i> and <i>Palaeoperidinium cretaceum</i> . <i>Heterosphaeridium</i> spp. frequent (<5%). Spore-pollen suite not well defined, but includes <i>Laevigatosporites musa</i> . Near-shore.
CUTT	2001	Kiokansium polypes (<i>undiff.</i>) (<i>Turonian</i>)	Waarre Ss - Cb	1	Perm.	Poor-fair	Mod.	High	Very restricted in-situ dinocyst suite with substantial Flaxman Formation to Paaratte Formation caving. Dominated by <i>Heterosphaeridium</i> spp. (11%). Near-shore.

Santos

Study: . Casino-3

Author: G. Wood & R. Helby

PALYNOSTRATIGRAPHICAL DATA

Table 1

Report No. 2003/33

Page 9 of 13

SAMPLE	DEPTH (M)	PALYNOSTRATIGRAPHICAL UNIT (Age)	INFERRED STRATIGRAPHICAL UNIT	REWORKED ELEMENTS		PRESER VATION	YIELD	DIVER SITY	REMARKS
				%	AGE				
SWC5	2004.0	Isabelidinium evexus (undiff.) (Turonian)	Waarre Ss – Ca/Cb	-	-	Poor-fair	Low	High	Moderate diversity dinocyst suite (17% of total palynomorphs) including <i>Isabelidinium evexus</i> with <i>Apteodinium</i> sp. (JGG), <i>Cribroperidinium edwardsii</i> , <i>Kiokansium polyopes</i> , <i>Oligosphaeridium</i> spp. and <i>Palaeoperidinium cretaceum</i> . Algal cysts prominent (10% including <i>Amosopollis cruciformis</i> , <i>Nummus</i> spp. and <i>Palambages</i> sp.). Near-shore.
FHC	2010.6	Isabelidinium evexus (undiff.) (Turonian)	Waarre Ss – Ca/Cb	1	Perm.	Poor-fair	Low	High	Moderately diverse spore-pollen suite with “frequent” <i>Appendicisporites</i> spp., and “frequent” <i>Verrucosporites admirabilis</i> . <i>Laevigatosporites musa</i> and <i>Hoegisporis trinalis</i> not recorded. Very restricted microplankton suite (<2%) with rare <i>Exochosphaeridium</i> spp. and <i>Heterosphaeridium</i> spp. <i>Amosopollis</i> nor recorded. Fringing marine.
FHC	2011.0	Heterosphaeridium acme (Turonian)	Waarre Ss – Ca	3 1	Perm. Triassic	Poor-fair	Low	High	Low diversity dinocyst suite (17% total palynomorphs) including <i>Apteodinium</i> sp. (JGG), <i>Kiokansium polyopes</i> , <i>Odontochitina costata (s.l.)</i> , <i>Oligosphaeridium</i> spp. and <i>Subtilisphaera</i> sp. <i>Heterosphaeridium</i> spp. dominate (11%). <i>Amosopollis</i> not recorded. Near-shore.

Santos

Study: . Casino-3

Author: G. Wood & R. Helby

PALYNOSTRATIGRAPHICAL DATA

Table 1

Report No. 2003/33

Page 10 of 13

SAMPLE	DEPTH (M)	PALYNOSTRATIGRAPHICAL UNIT (Age)	INFERRED STRATIGRAPHICAL UNIT	REWORKED ELEMENTS		PRESER VATION	YIELD	DIVER SITY	REMARKS
				%	AGE				
FHC	2013.7	Heterosphaeridium acme (Turonian)	Waarre Ss – Ca	1	Perm.	Poor-fair	Low	High	Restricted (7% of total palynomorphs), low diversity dinocyst suite including <i>Kiokansium polypes</i> , <i>Oligosphaeridium</i> spp. and <i>Palaeoperidinium cretaceum</i> (?). <i>Heterosphaeridium</i> spp. dominate (5%). <i>Amosopollis</i> not recorded. Spore-pollen suite includes <i>Appendicisporites tricornitatus</i> , <i>Hoegisporis trinalis</i> , <i>Laevigatosporites musa</i> and frequent <i>Verrucosisporites admirabilis</i> . Near-shore.
FHC	2014.2	Heterosphaeridium acme (Turonian)	Waarre Ss – Ca	1	Perm.	Poor-fair	Low	High	Rich, moderately diverse dinocyst suite including <i>Cribroperidinium</i> spp., <i>Cyclonephelium compactum</i> , frequent <i>Kiokansium polypes</i> , <i>Oligosphaeridium</i> spp. and frequent <i>Palaeoperidinium cretaceum</i> . <i>Heterosphaeridium</i> spp. dominate (27%). <i>Amosopollis</i> not recorded. Spore-pollen suite includes <i>Appendicisporites distocarinatus</i> , <i>Hoegisporis trinalis</i> and <i>Verrucosisporites admirabilis</i> . Near-shore.
FHC	2021.1	Heterosphaeridium acme (Turonian)	Waarre Ss – Ca	-	-	Poor-fair	Mod.	High	Rich, moderately diverse dinocyst suite including <i>Apteodinium</i> sp. (JGG), <i>Cribroperidinium edwardsii</i> , <i>Kiokansium polypes</i> , common <i>Oligosphaeridium</i> spp. and <i>Palaeoperidinium cretaceum</i> . <i>Heterosphaeridium</i> spp. totally dominate (56%). <i>Amosopollis</i> not recorded. Spore-pollen suite includes <i>Hoegisporis trinalis</i> , <i>Laevigatosporites musa</i> and <i>Verrucosisporites admirabilis</i> . Near-shore.

Santos

Study: . Casino-3

Author: G. Wood & R. Helby

PALYNOSTRATIGRAPHICAL DATA

Table 1

Report No. 2003/33

Page 11 of 13

SAMPLE	DEPTH (M)	PALYNOSTRATIGRAPHICAL UNIT (Age)	INFERRED STRATIGRAPHICAL UNIT	REWORKED ELEMENTS		PRESER VATION	YIELD	DIVER SITY	REMARKS
				%	AGE				
FHC	2027.15	Heterosphaeridium acme (Turonian)	Waarre Ss – Ca	1	Perm.	Poor-fair	Mod	High	Moderate diversity dinocyst suite (18% total palynomorphs) including <i>Apteodinium</i> sp. (JGG), <i>Cyclonephelium compactum</i> , frequent <i>Kiokansium polypes</i> , frequent <i>Oligosphaeridium</i> spp. and <i>Palaeoperidinium cretaceum</i> . <i>Heterosphaeridium</i> common (9%). <i>Amosopollis</i> not recorded. Near-shore.
FHC	2027.3	Heterosphaeridium acme (Turonian)	Waarre Ss – Ca	-	-	Poor-fair	Mod.	High	Rich (39%), moderately diverse, dinocyst suite including <i>Apteodinium</i> sp. (JGG), <i>Cyclonephelium membraniphorum</i> , “frequent” <i>Kiokansium polypes</i> and common <i>Oligosphaeridium</i> spp. <i>Heterosphaeridium</i> dominates (25%). <i>Amosopollis</i> not recorded. Spore-pollen suite includes <i>Appendicisporites</i> spp., <i>Hoegisporis trinalis</i> and <i>Laevigatosporites musa</i> . Near-shore.
FHC	2027.5	Heterosphaeridium acme (Turonian)	Waarre Ss – Ca	-	-	Poor-fair	Low	High	Rich (62%)but low diversity dinocyst suite with frequent <i>Kiokansium polypes</i> and common <i>Oligosphaeridium</i> spp. <i>Heterosphaeridium</i> dominates (44%). <i>Amosopollis</i> not recorded. Spore-pollen suite includes <i>Appendicisporites</i> spp., <i>Hoegisporis trinalis</i> , <i>Laevigatosporites musa</i> and “frequent” <i>Verrucosisporites admirabilis</i> . Near-shore.

Santos

Study: . Casino-3

Author: G. Wood & R. Helby

PALYNOSTRATIGRAPHICAL DATA

Table 1

Report No. 2003/33

Page 12 of 13

SAMPLE	DEPTH (M)	PALYNOSTRATIGRAPHICAL UNIT (Age)	INFERRED STRATIGRAPHICAL UNIT	REWORKED ELEMENTS		PRESER VATION	YIELD	DIVER SITY	REMARKS
				%	AGE				
FHC	2028	Heterosphaeridium acme (Turonian)	Waarre Ss – Ca	1	Perm.	Poor-fair	Mod	High	Rich (60%), moderately diverse, dinocyst suite including “frequent” <i>Kiokansium polypes</i> , particularly prominent <i>Oligosphaeridium</i> spp. and <i>Palaeoperidinium cretaceum</i> . <i>Heterosphaeridium</i> dominates (38%). <i>Amosopollis</i> not recorded. Spore-pollen suite not well characterized. Near-shore.
FHC	2032.25	Heterosphaeridium acme (Turonian)	Waarre Ss – Ca	-	-	Poor-fair	Mod.	High	Rich (62%), low diversity, dinocyst suite with <i>Chlamydophorella nyei</i> , <i>Kiokansium polypes</i> , <i>Oligosphaeridium</i> spp., <i>Palaeohystrichophora infusorioides</i> and <i>Palaeoperidinium cretaceum</i> ., <i>Heterosphaeridium</i> totally dominates (71%). <i>Amosopollis</i> not recorded. Spore-pollen suite not well characterized. Near-shore.
SWC3	2050	Cribooperidinium edwardsii (Turonian)	Waarre Ss – Ca	-	-	Poor-fair	Mod.	High	Relatively rich (15%), moderately diverse, dinocyst suite including <i>Chlamydophorella nyei</i> , <i>Cyclonephelium compactum</i> , <i>Isabelidium</i> spp., <i>Kiokansium polypes</i> and frequent <i>Oligosphaeridium</i> spp. <i>Cribooperidinium</i> spp. particularly prominent (8%). Spore-pollen suite includes <i>Appendicisporites tricornitatus</i> , <i>Hoegisporis trinalis</i> , <i>Laevigatosporites musa</i> (?). Near-shore.
CUTT	2103	Kiokansium polypes (undiff.) (Turonian)	Waarre Ss - A	1	Perm.	Poor-fair	Low	High	Heavily contaminated by caving from Belfast Mudstone to Paaratte Formation. Zone assignment tentative - based on occurrence of <i>Kiokansium polypes</i> . Spore-pollen suite lacks diagnostic species.

Santos

Study: . Casino-3

Author: G. Wood & R. Helby

PALYNOSTRATIGRAPHICAL DATA

Table 1

Report No. 2003/33

Page 13 of 13

SAMPLE	DEPTH (M)	PALYNOSTRATIGRAPHICAL UNIT (Age)	INFERRED STRATIGRAPHICAL UNIT	REWORKED ELEMENTS		PRESER VATION	YIELD	DIVER SITY	REMARKS
				%	AGE				
CUTT	2106	Phyllocladidites mawsonii (<i>undiff.</i>) (Turonian)	Waarre Ss - A	3	Perm.	Poor-fair	Low	High	Heavily contaminated by caving from Belfast Mudstone to Paaratte Formation. Zone assignment tentative - based on occurrence of <i>Appendicisporites distocarinatus</i> . Other diagnostic species were not observed.

APPENDIX VII : DRILL STEM TEST ANALYSIS REPORT

Santos

CASINO GAS FIELD DEVELOPMENT

CASINO-3 DRILL STEM TEST ANALYSIS REPORT

APPROVAL

TITLE	NAME	SIGNATURE	DATE
Staff Reservoir Engineer	Andries Steyn	AS	25/02/04

DATE	REV	REASON FOR ISSUE	AUTHOR	CHECKED	APPROVED
25/02/04	0	Casino-3 DST Analysis Report	AS	IGP	IGP



1 Executive Summary

The Casino-3 delineation well was drilled and tested during November 2003. The primary objective of the well was to establish the free water level to facilitate an accurate estimation of the original gas in-place (OGIP). The primary gas-bearing Waarre C objective was intersected at 1956.8 m SS and a free water level was successfully established at 1999 m SS. Geophysical logs revealed high quality reservoir sandstone and a test was proposed.

The Waarre C_b interval was perforated from 1981.6 - 1990.6 m SS (9 metres) underbalanced with high shot density guns. The conventional gas test comprised an initial flow and build-up. This was followed by a clean-up period and a build-up to stabilise the well. The main multi-rate flow period comprised three flows through increasing choke sizes. This was followed by a final build-up. Fluid samples were obtained from the separator and pressure transient data was acquired by downhole electronic gauges. The test was performed using Schlumberger test tools with a 9 5/8" permanent packer run on 4½" PH6 tubing. The test was technically sound and no major problems were experienced. The following rates were measured during the DST:

Period	Choke (Inches)	Q _{gas} (MMscf/d)	Q _{Cond} (stb/d)	Q _{Water} (bwpd)	CGR (stb/MMscf)	WHP (psia)	BHP (psia)
Clean-up flow	64/64	44.93	-	-	-	1839	2722
Second BU	-	-	-	-	-	-	2862
Multi rate flow 1	36/64	19.54	4.0	5.8	0.20	2382	2830
Multi rate flow 2	48/64	27.41	9.0	11.3	0.33	2216	2797
Multi rate flow 3	64/64	44.51	21.0	27.7	0.47	1863	2729
Final BU	-	-	-	-	-	-	2859

Pressure transient behaviour revealed the entire gas-bearing interval contributing to flow and not only the perforated interval. The following basic reservoir parameters were estimated through pressure transient analysis:

Initial reservoir pressure, p _i	2870.43 psia at 1983.6 m SS
Average permeability, k	445 md
Permeability thickness product, kh	41 000 md.ft (h = 92.2 feet)
Total skin, S' (1 st multi-rate period)	17.4
Total skin, S' (2 nd multi-rate period)	27.5 (unreliable data point)
Total skin, S' (3 rd multi-rate period)	37.1
Mechanical skin, S _M	1.9
Non-Darcy coefficient, D	0.000768 1/(Mscf/day)

The measured rate of 27.41 MMscf/day for the second multi-rate flow period appears to be incorrect since the flow period could not be matched at all during the full test history match routine, nor could the derived total skin value be used during multi-rate transient analysis.

Early-time pressure transient response was modelled to a dual-layer system, which is consistent with the layering revealed through geophysical logging. The possible response from a third layer was not modelled. Late-time pressure behaviour was modelled to two intersecting faults. Although the non-uniqueness of the modelling is acknowledged, an attempt was made throughout the analysis to be consistent with geophysical mapping and layering as revealed by drilling and logging results. The full test sequence history was matched to two boundaries or faults between 500 feet and 1600 feet respectively away from the wellbore.

A wellbore hydraulics exercise was performed in order to quantify the additional pressure drop experienced in the tubing due to the fact that the pressure gauges were placed some 25.72 metres above the bottom of the test string. This additional pressure drop from the gauge depth to the bottom of the tubing is established as non-linear or non-Darcy skin. The purpose of the wellbore hydraulics exercise was to back-out the additional pressure drop to refine the non-Darcy D-factor for use in reservoir simulation. Results are presented in the table below:

Comment	1st Flow	3rd flow
Total skin including additional Δp due to presence of test string	17.4	37.1
Non-Darcy coefficient including additional Δp due to test string	0.0007682	1/(Mscf/day)
Total skin with additional Δp due to test string backed out	12.1	23.7
Non-Darcy coefficient with additional Δp due to test string backed out	0.0004687	1/(Mscf/day)

Table of Contents

1	EXECUTIVE SUMMARY	1
2	INTRODUCTION	6
3	TEST STRING OVERVIEW	7
4	DATA ACQUISITION	9
5	SEQUENCE OF EVENTS	11
6	WELL PARAMETERS AND ROCK PROPERTIES	13
7	RESERVOIR FLUID SAMPLING AND PROPERTIES	14
8	TEST INTERPRETATION	16
8.1	Test overview	16
8.2	Initial build-up	16
8.3	Clean-up period	17
8.4	Second build-up	17
8.5	Multi-rate transient analysis	17
8.6	Final build-up	18
8.7	Full test sequence history match	18
8.8	Analysis model	18
9	WELL DELIVERABILITY AND WELLBORE HYDRAULICS	21
10	REFERENCES	23
11	APPENDICES	24

List of Figures

Figure 1:	Location map	6
Figure 2:	Log interpretation and perforated interval	6
Figure 3:	Seal assembly and test string configuration	7
Figure 4:	TCP string diagram	7
Figure 5:	Difference between gauges 1728 & 2850	10
Figure 6:	Difference between gauges 1728 & 3818	10
Figure 7:	Difference between gauges 2850 & 3818	10
Figure 8:	List of samples collected during the test	14
Figure 9:	Pressure/Viscosity/Z-factor relationship	14
Figure 10:	Pressure/Viscosity/ C_t relationship	14
Figure 11:	Pressure/ $m(p)$ (pseudo pressure) relationship	14
Figure 12:	Test temperature profile	15
Figure 13:	Horner plot with temperature extrapolation	15
Figure 14:	Entire dataset recorded by gauge 3818 during DST 1	16
Figure 15:	Full test overview	16
Figure 16:	Log-log plot of initial build-up	16
Figure 17:	Horner plot of initial build-up	16
Figure 18:	Pressure data of the Casino complex	17
Figure 19:	Log-log plot of second build-up	17
Figure 20:	Superposition plot of second build-up	17
Figure 21:	Log-log plot of three multi-rate flow periods	17
Figure 22:	Radial flow plot of three multi-rate flow periods	17
Figure 23:	Radial flow plot with rate dependency backed out	17
Figure 24:	Total skin versus flow rate plot	17
Figure 25:	Log-log plot of final build-up	18
Figure 26:	Semi-log plot of final build-up	18
Figure 27:	Full test sequence history match using homogeneous model	18
Figure 28:	Late-time pressure behaviour match using final build-up	18
Figure 29:	Early-time and late-time match using final build-up	18
Figure 30:	Full test sequence history match to model	19
Figure 31:	Full test sequence history match to model with adjusted second flow rate	19
Figure 32:	Inflow performance curve	21
Figure 33:	First flow data point before matching	21
Figure 34:	First flow data point matched with Petroleum Experts 3 correlation	21
Figure 35:	Third data point before matching	21
Figure 36:	Third flow data point matched with Petroleum Experts 3 correlation	21
Figure 37:	DST 1 pressure drop through the tubing	22
Figure 38:	Skin versus flow rate plot with additional pressure drop backed out	22

List of Tables

Table 1: Detailed TCP information	7
Table 2: Surface testing equipment	8
Table 3: Gauge programming and location	9
Table 4: Surface data acquisition	10
Table 5: Summary of flow and shut-in periods	11
Table 6: Well parameters and reservoir rock properties	13
Table 7: Reservoir fluid composition	14
Table 8: Reservoir fluid properties	15
Table 9: Test overview	16
Table 10: Model parameters	20
Table 11: Wellbore hydraulics results	22
Table 12: Total skin and D-factors comparison	22

List of Appendices

Appendix 1: Sequence of events

2 Introduction

The Casino Gas Field is located in approximately 70 metres water depth in the Otway Basin in permit VIC/P44 offshore Victoria, Australia as shown on the location map, Figure 1. The current permit holders are Santos Ltd (50% and Operator), AWE Group (25%) and Mitsui Group (25%).

The field was discovered by the Casino-1 exploration well drilled by the Ocean Bounty during August/September 2002. The well encountered the primary target Waarre Sandstone at 1718 metres SS and a full logging suite revealed a total of 21.5 metres of gas pay in the Waarre "A" section - the so called "Older Sand". The gas-water contact (GWC) for the Older Sand was not intersected at the well. The well was plugged and abandoned, as per program, without coring or testing.

The Casino-2 well was drilled as an immediate appraisal well during September and October 2002 by the Ocean Bounty rig. The well targeted the "Younger Waarre Cb/Ca" sand as well as the "Older Sand" already intersected at Casino-1. A total of 30 metres of good quality gas-bearing sandstone was intersected in the Waarre "Cb/Ca", however, the GWC was not intersected. Casino-2 also intersected the Waarre "A" sand and established the GWC. A core was cut through the Waarre Cb/Ca. The well was not tested and was plugged and abandoned as per program.

The Casino-3 delineation well, drilled during November 2003 by the Ocean Epoch, was designed primarily to intersect the GWC in the Waarre Cb/Ca sand in order to determine the Gas-in place and therefore project development viability. The well intersected gas bearing sands in the Waarre Cb/Ca reservoir at a depth of 1956.8 m SS. Casino-3 successfully appraised the field and demonstrate the presence of an approximate vertical gas column of 300 metres in the Younger Sand with a GWC at 1996 m SS. A 27 metre core was cut through the main reservoir section and a full logging suite was run including mechanical sidewall cores in the Older Sand.

The primary Waarre Cb/Ca reservoir was drill-stem tested with 9.0 metres of perforations from 1979.0 to 1988.0 m SS. The log interpretation and perforated interval are presented in Figure 2. The primary technical test objectives were as follow:

- Determine reservoir properties kh, skin and productivity index.
- Demonstrate well deliverability and inflow performance.
- Determine non Darcy skin required for dynamic modelling.
- Acquire representative reservoir fluid samples for PVT analysis.

Secondary technical test objectives were:

- Trace analysis for H₂, H₂S, and mercaptan-sulphur required for GSA.
- Confirmation of initial reservoir pressure as determined from MDT data.
- Monitor sand production.
- Determine radius of investigation and identify boundaries if any.
- Acquire optimum pressure transient data to calibrate numerical model.

3 Test String Overview

Equipment load-out, program preparation and well test supervision was performed by AWT. Schlumberger provided the DST string including the perforating guns, surface testing equipment, surface and downhole data acquisition and slickline services. Halliburton provided pumping, nitrogen and cementing services while Weatherford provided tubing rental services. Oilphase provided sampling services and BHI provided drilling fluids.

The test string was run on 4½" PH6 L80 15.5 lb tubing with ID = 3.83". The test was performed using a 9 5/8" permanent packer set on Schlumberger electric line. Downhole flow control was achieved using an annulus operated PCT valve as the primary valve for opening and closing the well. Circulating valves were also annulus operated. The DST string with 3 3/8" tubing conveyed perforating guns was conveyed on the packer locator and stung through the 4" permanent packer seal bore extension.

The firing system was a dual HDF/TCF hydraulically actuated firing head; the TCF is slickline retrievable in the event of a misfire. Gauges were located in a gauge carrier above the PCT valve with gauges ported below the ball. A Sentries 3 sub-surface safety valve was installed to provide the shut and unlatch capability at the BOP. A lubricator valve was installed approximately 30 metres below the drill floor to provide an additional tubing barrier and allow for loading of PLT string and through tubing perforating guns if required. A schematic of the seal assembly and the test string configuration is presented in Figure 3. The TCP string diagram is shown in Figure 4 and the detail TCP information in Table 1. A study comparing conventional 4½" TCP guns against 3 3/8" TCP guns with deep penetrations showed that the 3 3/8" guns were the preferred choice especially in view of the fact that 3 3/8" guns could be utilised for both primary and contingency perforating. (Attach appendix?? 61 pages).

Perforation interval	2004.0 - 2013 m MDRT
Perforation date	8 November 2003
Gun System	Schlumberger Powerjet TCP
Gun Size	3 3/8" HSD (86 mm)
Shot density	6 spf
Phasing	60 degrees
Charge type	34JL UJ
Explosive type	PJ 3406 HMX charges
Avg entrance hole size	0.28047 inches
Avg formation penetration	13.319 inches

Table 1: Detailed TCP information

After scraping the casing around the packer setting region, the well was circulated to a 1.11 SG (9.33 ppg) KCl brine before running in with the CBL logging string and DST string. Prior to perforating the well, a diesel cushion was circulated down to the MCCV circulating valve to achieve an underbalance of approximately 465 psi. The diesel density was 0.84 SG (7.0 ppg).

Standard Schlumberger surface equipment comprised the following (Table 2):

Surface equipment	Nominal size	Design pressure
Flowhead	3"	10 000 psi
ESD valve	3"	10 000 psi
Choke manifold	3"	10 000 psi
Steam exchanger	3"	5 000 psi
Horizontal separator	42" x 10'	1440 psi
Oil manifold	3"	1440 psi
Surge tank	2 x 50 bbl capacity	150 psi
Transfer pump	Positive displacement type	100 psi (outlet P)
Burners	18 000 bbl/day	-

Table 2: Surface testing equipment

4 Data Acquisition

Downhole pressure and temperature were acquired by Schlumberger UNIGAGE-CQG™ (WCQR) pressure/temperature crystal quartz gauge sensors located in the DGA gauge carrier above the PCT ball valve, ported below the valve. The measuring point was at 1967.73 m MDRT for all gauges. Gauge specifications are as follows:

Temperature rating:	177° C
Pressure rating:	16 000 psi
Maximum OD:	1.2"
Make-up length:	71.2"
Shock environment (TCP):	Class 6
Service:	H ₂ S
Standard memory size:	256 kbyte (100 000 data sets) 1 Mbyte (400 000 data sets) optional
Battery autonomy:	18 - 50 days (3 - 9 month battery available)

Measurement performances for the WCQR gauges are as follows:

Calibration ranges:	1000 - 15000 psi
Pressure accuracy:	±1 to 2.5 psi
Pressure resolution:	0.01 psi at 1-sec scan, <0.005 psi at 5-sec scan
First week stability:	0.2 psi (decreasing with time)
Long term stability:	1.5 to 2.0 psi over 6 months
Temperature accuracy:	±0.5° C
Temperature resolution:	0.01° C

A total of four WCQR gauges were employed for the Casino-3 DST, all of them located in the same gauge carrier. All four gauges functioned successfully. Small sampling intervals were selected due to the high anticipated formation permeability. No surface read-out was acquired, although the option was available for these types of gauges. Table 3 summarises the gauge programming and location.

Gauge number	Capacity	Sampling	Location
WCQR # 1728	120 kbyte	4 secs fixed	DGA gauge carrier - tubing pressure
WCQR # 2850	120 kbyte	4 secs fixed	DGA gauge carrier - tubing pressure
WCQR # 3818	440 kbyte	1 second fixed	DGA gauge carrier - tubing pressure
WCQR # 2855	120 kbyte	15 secs fixed	DGA gauge carrier - annulus pressure

Table 3: Gauge programming and location

ASCII files containing data from all the gauges were imported into PanSystem™ test analysis software for data validation and pressure transient analysis. Difference in the absolute pressure readings for the 3 gauges recording tubing pressure was in general less than 0.5 psi. This is illustrated in the following figures:

Figure 5: Difference between gauges 1728 & 2850

Figure 6: Difference between gauges 1728 & 3818

Figure 7: Difference between gauges 2850 & 3818

Sudden changes in pressure at rate changes create spikes in the difference curves in Figures 6 & 7. This effect is due to very small time shifts, since the sampling periods for the gauges were different.

Surface data was acquired electronically through a Unix-operated "Smart Software" system, run on a PC. It comprised the following:

- Surface Testing Acquisition Network STAN-A.
- Surface Testing Front End STAF-AB.
- Delta 10k psi surface pressure sensors STPS-C at the wellhead.
- Frode Pederson surface temperature sensors STTS-A & STTS-B at the wellhead.
- Floco pulse transmitter SFNT-A at the separator.
- Rotron pulse transmitter SRNT-A at the separator.
- Honeywell differential pressure measurement 400" H₂O - separator.
- Absolute pressure measurement STPS-A/B, separator static pressure sensor.
- Frode Pederson surface temperature sensors STTS-A & STTS-B at the separator.

Data Type	Acquisition frequency
Wellhead	
Pressure and temperature	15 minutes initially 30 minutes stabilised
BS&W	15 minutes initially 30 minutes stabilised
H ₂ S and CO ₂ content	15 minutes initially 30 minutes stabilised
Choke/changes/opening and shutting the well take the above readings	Every 2 minutes for 15 minutes then 15 minutes initially 30 minutes stabilised
Separator	
Pressure and temperature	15 minutes initially 30 minutes stabilised
Oil/gas flow rate variables	15 minutes initially 30 minutes stabilised
Physical properties	30 minutes
Shrinkage	60 minutes
H ₂ S and CO ₂ content	30 minutes
Meter calibration	3 times per flow rate

Table 4: Surface data acquisition

5 Sequence of Events

The detailed sequence of events can be found in Appendix I. After displacing the string content to diesel to achieve an underbalance, the annulus pressure was increased to 1500 psi to open the PCT ball valve. The annulus pressure was then further increased to 4000 psi to detonate the TCP guns. A strong positive indication of detonation was observed at 06:02 on the morning of 8 November 2003.

The well was first opened at 06:03 on 8 November 2003 for the initial flow period with duration of 10 minutes. A total of 14 bbl of diesel was displaced to the surge tank during the initial flow period. The PCT valve was then closed at 06:13 for the initial build-up period of 2.00 hours.

The well was re-opened for the clean-up period at 08:14 on a small adjustable choke. Minor problems were experienced with hydrates and the flow was diverted through the steam exchanger. The well was shut in at surface at 08:53 to allow re-ignition of pilot lights at the burner. The adjustable choke was increased gradually and first gas appeared at surface at 09:20. Throughout the flow period, the BS&W was monitored together with other flow parameters. When the BS&W was sufficiently low and flow parameters stable, flow was diverted through the separator at 12:54 on 8 November 2003 on a fixed 1" choke. Contingency PVT samples were collected at the separator. The well was shut-in at the PCT valve at 15:45 for the second build-up period.

A multi-rate flow period followed the second build-up period. The well was flowed through increasing choke sizes of 36/64^{ths}, 48/64^{ths} and 64/64^{ths} of an inch through the separator. During these flow periods, reservoir fluid samples were collected at the separator and the well-stream was analysed for Hg and sulphur content. All other flow parameters were monitored and recorded by a surface acquisition system.

Period	Choke (Inches)	Duration (Hours)	Q _{gas} (MMscf/d)	Q _{Cond} (stb/d)	Q _{Water} (bwpd)	CGR (stb/MMscf)	WHP (psia)	BHP (psia)
Initial Flow	24/64	0.167	-	-	-	-	593	2849
Initial BU	-	2.017	-	-	-	-	-	2864
Clean-up flow	64/64	7.517	44.93	-	-	-	1839	2722
Second BU	-	5.167	-	-	-	-	-	2862
Multi rate flow 1	36/64	6.667	19.54	4.0	5.8	0.20	2382	2830
Multi rate flow 2	48/64	5.867	27.41	9.0	11.3	0.33	2216	2797
Multi rate flow 3	64/64	6.217	44.51	21.0	27.7	0.47	1863	2729
Final BU	-	10.450	-	-	-	-	-	2859

Table 5: Summary of flow and shut-in periods

The well kill procedure was implemented as per program following the end of the final build-up. The annulus pressure was increased to open the PCT valve. Ten barrels of 9.3 ppg KCl brine, followed by 10 barrels of CaCO₃ LCM (lost circulation material) was pumped down the test string followed by KCl brine at 9.5 barrels/min. After bull-heading some of the brine into

the formation, the PCT valve was cycled into the hold-open position and the test string was un-stung from the packer. The content of the string was reverse circulated to surface followed by more circulation the normal way around until the gas levels were acceptable. The test string was then pulled to surface and the pressure gauges recovered. The well was plugged and abandoned as per program.

6 Well Parameters and Rock Properties

The well was completed with a cemented 9 5/8" casing in a 12¼" open-hole section. Cement bond logs revealed a good cement bond across the zone of interest. Raw geophysical logs and interpreted logs are presented in Figure 2 which also shows the perforated interval.

Well parameters and reservoir rock properties are listed in Table 6.

Primary target formation	Waarre Cb/Ca sandstone
Reference elevation	26 metres above LAT
Well geometry	Vertical
Driller's TD	2071.33 m PBTD RT
Well type	Delineation well
Casing size (OD)	9 5/8 inches
Casing ID	8.681 inches
Perforation Interval	2004 - 2013 m MDRT
Underbalance	465 psi
Wellbore Radius (r_w), feet	0.510417 feet
Tubing ID	3.83 inches
Tubing OD	4½ inches
Hole Size	12¼ inches
Porosity	0.211 (fraction)
Formation Thickness (h)	92.2 feet
Average Water Saturation (S_w)	0.4 (fraction)
Rock Compressibility (c_f), 1/psi	3.5667 e -06 1/psi
Water Compressibility (c_w), 1/psi	3.06 e-06 1/psi

Table 6: Well parameters and reservoir rock properties

7 Reservoir Fluid Sampling and Properties

Reservoir fluid and other samples were collected at the test separator during the clean-up and main flow periods. A list of samples collected during the test can be seen in Figure 8.

The Casino reservoir fluid is a sweet, dry gas with a condensate-gas ratio of approximately 0.3 - 0.5 bbl/MMscf. Pressurised gas PVT samples collected at the separator have been analysed for composition, the results are presented in Table 7 (compositional analysis up to C₂₀⁺ available in PVT report).

Component	Separator Liquid Composition (mole%)	Separator Gas Composition (mole%)	Reservoir Fluid Composition (mole%)
H ₂ S	0.00	0.00	0.00
CO ₂	0.41	0.89	0.89
N ₂	0.20	2.02	2.02
C ₁	19.13	94.41	94.34
C ₂	1.49	1.91	1.91
C ₃	1.12	0.45	0.45
iC ₄	0.43	0.08	0.08
nC ₄	0.51	0.07	0.07
iC ₅	0.29	0.02	0.02
nC ₅	0.17	0.01	0.01
C ₆	2.16	0.03	0.03
C ₇	8.77	0.05	0.06
C ₈	6.33	0.04	0.05
C ₉	9.2	0.02	0.03
C ₁₀	10.91	0.00	0.01
C ₁₁	9.25	0.00	0.01
C ₁₂ ⁺	29.63	0.00	0.02
Total	100.00	100.00	100.00

Table 7: Reservoir fluid composition

Since the fluid type is a dry gas, fluid properties were derived using the gas composition including CO₂ and N₂. From the compositional data, the gas gravity and critical pressure and temperature were calculated and the Z-factor is computed using the Schmidt-Wenzel equation of state (EOS). The gas viscosity is calculated using the correlation of Carr et al. The following tables are presented graphically:

- Figure 9: Pressure/Viscosity/Z-factor relationship
- Figure 10: Pressure/Viscosity/C_t relationship
- Figure 11: Pressure/m(p) (pseudo pressure) relationship

The pressure draw-down during flow periods are small as a result from the high permeability. It can be seen from the m(p)/pressure relationship that all pressure transients during the test are within the linear section of the relationship. Nevertheless, m(p) pseudo pressure was used throughout during the test analysis.

In general, during a gas test, downhole temperature drops during flow periods (Dual Thompson effect) and increase during shut-in periods. The inverse is true for the Casino-3 DST, probably due to the observed small pressure draw-downs during flow periods. The Dual Thompson effect is related to the expansion of gas during larger pressure draw-downs, and is probably negligible in the case of the Casino-3 DST. The temperature profile is presented in Figure 12. The static reservoir temperature was determined by plotting the final build-up temperature against a Horner function and extrapolating to infinity. Results can be seen on Figure 13. Other reservoir fluid properties used in the test analysis are presented in Table 8.

Initial Reservoir Pressure (p_i)	2870.43 psia @ 2006 m MDRT
Static reservoir temperature	193.4° F @ 2006 m MDRT
Molecular Weight of Reservoir Fluid	118.5 lbmole
Gross/Net Heating Value of Reservoir Fluid	1018/918 BTU/scf
Molecular Weight of C_{12}^+	299.14 lbmole
Density of C_{12}^+	0.8707 g/cm ³
API of C_6^+ @ 60° F	47.13 deg API
B_g at p_i	0.00580398 rcf/scf
μ_{gas} at p_i	0.0187828 centipoise
Z at p_i	0.907776
C_g at p_i	3.2350e-04 1/psi
C_w at p_i	3.1264e-06 1/psi
C_f at p_i	3.5667e-06 1/psi
C_t at p_i	1.9891e-04 1/psi
Gas Gravity	0.592 (air = 1)
ρ_{gas} @ standard conditions	0.04517 lb/ft ³
ρ_{gas} @ reservoir conditions	7.747 lb/ft ³
Gas Fluid Pressure Gradient @ reservoir	0.0538 psi/ft
Wobbe Index	46.1

Table 8: Reservoir fluid properties

Analysis for trace metals and sulphur revealed the presence of 80 ppb of mercury and 70 - 80 mg/kg sulphur (ASTM D5453). Vanadium and nickel were also present at a low concentration of approximately 1 mg/kg.

8 Test Interpretation

8.1 Test overview

Data acquired from gauge number 3818, set at a one second fixed sampling rate, was used for the test analysis. While the other two gauges acquired good data at four second fixed sampling intervals, the data density recorded by gauge 3818 following rate changes are much higher. Early-time data following a rate change is often critical in test interpretation. Figure 14 presents the entire dataset recorded by gauge 3818 during DST 1.

The test overview is presented in Figure 15. The well was opened up gradually during the clean-up period which was sub-divided into 6 transients. Rates for the clean-up transients have been estimated based on the BHP, except for the final transient which was measured at the separator.

Transient	Duration (Hours)	Final BHP (psia)	Gas Rate (MMscf/d)	Comments
1	0.131945	2863.699951	0	Data start
2	0.317655	2861.214111	20	Initial flow period
3	2.309763	2863.73291	0	Initial BU period
4	4.33405	2838.875	17	Clean-up 1
5	5.58622	2822.043945	20.5	Clean-up 2
6	6.3619	2798.947998	26.5	Clean-up 3
7	7.09926	2769.284912	35.5	Clean-up 4
8	7.598021	2739.751953	42.3	Clean-up 6
9	9.837768	2721.731934	44.9	Clean-up 6
10	15.92757	2861.772949	0	Second BU period
11	22.6173	2830.035889	19.54	Multi rate 1
12	28.5831	2797.053955	27.5	Multi-rate 2
13	34.84304	2727.738037	44.51	Multi-rate 3
14	43.89433	2858.644043	0	Final BU period

Table 9: Test overview

Data for each of the transients was reduced using a data reduction algorithm in PanSystem (resample to n points per log cycle). A small smoothing constant of 0.05 window span was used to improve the signal to noise ratio. The smoothing algorithm is a local linear estimator based on nearest neighbours. Further data editing involved elimination of noisy data peaks and individual data points, especially near rate changes, but ensuring that the overall pressure trend is honoured.

8.2 Initial build-up

The purpose of the initial build-up is to get an estimate of the initial reservoir pressure from the Horner extrapolated P^* and compare the result with wireline pressure data (MDT). The data is not good enough to make a reliable estimate of reservoir properties. Figure 16 is a log-log plot of the initial build-up. Although wellbore storage and radial flow can be recognised, no interpretation was performed on the initial build-up. Figure 17 is a Horner plot of the initial build-up yielding an extrapolated pressure (p_i) of 2863.7 psia at gauge depth.

The gauge measuring point is at 1967.73 m MDRT and the mid perforation depth at 2006.00 m MDRT. This resulted in a correction of 6.73 psia using a gas pressure gradient of 0.0536 psi/ft derived from PVT analysis. The final estimated value for p_i is 2870.43 psia at 2006 m MDRT. The DST derived value for p_i compares favourable with the MDT data acquired in the Casino-3 well (Figure 18) and is approximately 0.7 psi higher than the MDT data point acquired at the same level.

8.3 Clean-up period

No transient analysis was performed on the clean-up period.

8.4 Second build-up

The second build-up followed the clean-up period. The log-log plot (Figure 19) shows very little wellbore storage which is consistent with the high permeability and the downhole closure. A radial flow period for the total system can be identified at approximately 0.1 hours elapsed time. The semi-log plot, Figure 20, uses a superposition time function and pseudo pressure. The semi-log straight line through the radial flow section gives the following results:

- k = 449 md
- kh = 41400 md.ft ($h = 92.2$ feet)
- Total skin = 39.1
- Δp_{skin} = 117 psi

8.5 Multi-rate transient analysis

This analysis is aimed at determining the mechanical skin and non-Darcy skin factors. Following the second build-up, the well was flowed at three different rates through increasing choke sizes. The flow-after-flow gas test is a conventional approach in highly permeable formations. Figure 21 is a log-log plot of the three sequential flow periods. Identification of flow regimes is hardly possible on this plot, however, it should be kept in mind that these are all draw-down periods where the production rate is probably varying during flow periods.

On the radial flow plot, Figure 22, the estimated permeability from build-up analysis was imposed by adjusting the semi-log straight lines through the flow data until a permeability of approximately 440 md was achieved. The permeability derived from build-up analysis is likely to be more reliable. Figure 23 is a similar radial flow plot of the three sequential flow periods, but with the rate dependency backed out. In theory, all three lines should lie on top of each other with the rate dependency corrected for. This is indeed the case for the first and third flow period, but not for the second flow period. This is a very important observation and a strong case to suggest that the gas rate measurement at the separator is incorrect for the second flow period. This possible error in rate measurement will become more evident as the test analysis progress. Figure 24 is the total skin versus flow rate plot. The total skin value for the second flow period was ignored when fitting a line through the data points. Consideration of the middle data point would result in extrapolation to an unrealistic negative

mechanical skin, which would again support some inconsistency (like the possible incorrect rate measurement). The skin versus flow-rate plot yielded the following results:

- Mechanical skin = 1.9
- Non-Darcy D factor = 0.000768 1/(Mscf/day)

8.6 Final build-up

Radial flow can be clearly identified from the log-log plot (Figure 25) while wellbore storage is again poorly developed due to the downhole shut-in. Late time effects are evident after about 1.0 hour elapsed time, but these will be dealt with later in this report. The semi-log plot is presented in Figure 26. A late-time upward curvature can clearly be seen on the semi-log plot, indicating the influence of outer boundaries. The following reservoir parameters were estimated from the semi-log straight line through the radial flow period:

- k = 445 md
- kh = 41000 md.ft ($h = 92.2$ feet)
- Total skin = 35.4
- $?p_{skin}$ = 107 psi

The results are similar to the interpreted results from the second build-up. There is a reduction in total skin from 39.1 to 35.4, possibly an indication of the well cleaning up.

8.7 Full test sequence history match

Figure 27 is a full test sequence history match using a radial homogeneous flow model and an infinitely acting boundary model. Although the pressure match with the initial build-up is good, the second and final build-up does not match the homogeneous model and it is clear that some boundary conditions and reservoir heterogeneity need to be introduced to obtain an improved history match. Another observation is that the second flow of the multi-rate flow period shows a poor pressure match. This again supports the possibility of an incorrect gas rate measurement.

8.8 Analysis model

History matching the DST pressure profile to a reservoir model was done in two steps. Firstly the late time behaviour was matched to an outer boundary model consisting of two linear no-flow intersecting faults. The final build-up was matched to two boundaries or faults between 500 feet and 1600 feet respectively away from the wellbore. This history match is shown in Figure 28 and a good match was obtained.

To match the early time pressure behaviour, a "dual permeability" model was found to yield the best match. In reality, the model can best be described as a "two-layer" model where the first layer is the actual perforated Waarre Cb interval and the second layer probably the Waarre Ca interval immediately below the Waarre Cb and separated by the thin shale from the Waarre Cb. MDT data clearly revealed that the Waarre Cb and Ca are hydraulically the same system. The pressure history match with the described model is shown in Figure 29.

The early time dip on the derivative is interpreted as the response of the perforated interval only. The second dip in the derivative could be the transient response of the Waarre Ca directly below the perforated Waarre Cb. There was however no attempt to match this second dip to a model. Thereafter, the derivative stabilises and shows a horizontal flat section from about 0.07 to 1.0 hours elapsed time. This flat section is interpreted to be the total system behaviour with $h = 92.2$ feet, the entire gas-bearing interval, including the lower quality Waarre Cb interval above the perforated interval. The basic reservoir properties, permeability and skin, were estimated from this radial flow section.

The dual-layer model has two distinct layers with horizontal radial flow in both layers. Only one layer is open to the wellbore and the second layer cross-flows vertically into the producing layer. The parameters describing a dual-layer system are defined as follows:

- κ (Kappa): This is the flow capacity ratio and describes the ratio of permeability-thickness in a dual layer system. The parameter is calculated by:

$$\mathbf{k} = \frac{k_1 h_1}{(k_1 h_1 + k_2 h_2)}$$

Where "1" denotes the perforated layer. In the model, $\kappa = 0.99$, which means that the kh of the perforated Waarre Cb is dominating the production, as expected.

- λ (Lambda): This is the inter-porosity flow coefficient/matrix-fracture exchange. The common range is 10^{-4} to 10^{-8} . For a dual layer reservoir with flow between layer 2 and layer 1, λ is calculated as:

$$\mathbf{l} = \frac{T_{Eff} r_w^2}{(k_1 h_1 + k_2 h_2)}$$

Where "1" denotes the perforated layer, "2" denotes the unperforated layer and T_{Eff} is the effective vertical conductivity. T_{Eff} is estimated using knowledge of vertical permeability and layer thickness.

- ω (Omega): This is the storativity ratio/capacity contrast ($0 < \omega < 1$). This parameter takes into account the capacity contrast that exists between the two layers. The closer the value of ω is to 1, the later the onset of the transition. The storativity in a dual layer system is calculated from:

$$\mathbf{w} = \frac{(fhC_t)_1}{[(fhC_t)_1 + (fhC_t)_2]}$$

Where "1" denotes the perforated layer and "2" the unperforated layer. The value of $\omega = 0.15$ in the model, meaning a very early onset of the transition.

The full test history match is presented in Figure 30. A good match is obtained between the observed pressure transient and the selected model, except for the clean-up period where rates have been estimated and except for the second flow of the multi-rate flow period where an incorrect rate measurement is suspected. If the flow rate for the second flow period is changed to 31.5 MMscf/day (approximately the rate that should have been measured), then a very good full test history match is obtained. This match is presented in Figure 31. Table 10 summarises the parameters used to obtain the model match.

Flow model:	Dual-layer
Outer boundary model:	Two intersecting faults at 60°
Compressibility:	Constant
Wellbore storage coefficient (C_s):	0.007 bbl/psi
Permeability (k):	440 md
Permeability thickness product (kh):	41 000 md.ft
Mechanical skin (S):	1.9
Reservoir thickness (h):	92.2 feet
?:	0.15
?:	0.99
?:	0.0014
Non-Darcy coefficient (D):	0.0007682 1/(Mscf/day)
Linear no-flow boundary 1:	1000 feet
Linear no-flow boundary 2:	1600 feet
Initial reservoir pressure (p_i):	2863.7 psia

Table 10: Model parameters

It is important to acknowledge that the suggested model is non-unique and that the same pressure transient behaviour may be matched to an alternative model, or by adjusting existing model parameters. Nevertheless, geophysical logs and seismic mapping supports the proposed model.

9 Well Deliverability and Wellbore Hydraulics

The objective of performing well deliverability and wellbore hydraulics were two fold. Firstly to calibrate the inflow curve using the three data points obtained from the multi-rate flow period. The Petroleum Experts™ software was used to generate the inflow performance curve. The Multirate C and n correlation was used to generate the well inflow performance curve. This correlation fits the backpressure equation to the test data, requiring the input of reservoir pressure and temperature. It determines the coefficients of the backpressure equation that best fits the measured flowing bottom-hole pressure. The inflow curve is presented in Figure 32.

Secondly, the outflow relationship was generated in order to quantify the additional pressure drop experienced in the tubing due to the fact that the pressure gauges were placed some 25.72 metres above the bottom of the test string (the perforated pup joint). Ideally, the gauges should be placed adjacent to, or as close as possible, to the perforations. This is not always practical, and in the case of Casino-3, the gauges were placed in a gauge carrier immediately above the ball valve with ports below the ball. The additional pressure drop from the gauge depth to the bottom of the tubing is established as non-linear or non-Darcy skin. The purpose of the wellbore hydraulics exercise was to back-out the additional pressure drop to refine the non-Darcy D-factor for use in reservoir simulation. This exercise was performed using the following steps:

1. Input valid PVT data and calculate PVT tables where necessary.
2. Input downhole equipment. This function was performed with care to ensure the input of exact ID's and depths for all the test tools, the 4½ PH6 tubing and the casing. This will ensure the correct pressure drop calculations through different ID's.
3. Input geothermal gradient, average heat capacity and tubing roughness.
4. Compare typical tubing correlations available in the industry to the first flow (36/64") and the third flow (64/64") of the multi-rate flow period.
 - Figure 33 shows the first-flow data point before matching. The data point is closest to the Petroleum Experts 3 and Duns and Ros Modified correlations.
 - Figure 34 shows the first-flow data point matched to the Petroleum Experts 3 correlation with matching parameters 1.15 and 0.98 respectively. The match obtained is good and the pressure drops through the 4½" tubing, the test tools and the casing can be distinguished clearly.
 - Figure 35 shows the third-flow data point before matching. Again, the data point is closest to the Petroleum Experts 3 and Duns and Ros Modified correlations.
 - Figure 36 shows the data point matched to the Petroleum Experts 3 correlation. Although the match with Duns and Ros Original is slightly better, the matching parameters for the Petroleum Experts 3 correlation of 1.16 and 0.95 is superior and this correlation will be used.

Using the matched correlations, the additional pressure drop caused by the fact that the gauges were employed 25.72 metres above the bottom of the tubing may be backed-out. The pressures measured at the gauge, bottom of the tubing and mid perforation depth

respectively, are presented in Figure 37. Table 11 summarises the results obtained from the wellbore hydraulics exercise.

Comment	1st Flow	3rd flow
Pressure drop from gauge depth to bottom of string	11.66 psi	42.92 psi
Pressure drop from bottom of string to mid perforation depth	2.59 psi	2.55 psi
Additional non-linear Δp due to gauges in tubing	6.33 psi	37.6 psi
Actual measured BHF at gauge depth	2830.04 psia	2727.74 psia
Expected BHFP at gauge depth if tubing effect is backed out	2836.37 psia	2765.34 psia

Table 11: Wellbore hydraulics results

The final step is to re-calculate the total skin factors and the associated non-Darcy flow coefficient with the adjusted flowing pressure as described above. This was performed in PanSystem and the plot can be seen in Figure 38. Table 12 compares the calculated total skin factors and D-factors before and after the additional pressure drop was backed out.

Comment	1st Flow	3rd flow
Total skin including additional Δp due to presence of test string	17.4	37.1
Non-Darcy coefficient including additional Δp due to test string	0.0007682	1/(Mscf/day)
Total skin with additional Δp due to test string backed out	12.1	23.7
Non-Darcy coefficient with additional Δp due to test string backed out	0.0004687	1/(Mscf/day)

Table 12: Total skin and D-factors comparison

10 References

1. Schlumberger Well Testing Report, Casino-3, DST # 1. Report number 2003 017, 8 November 2003.
2. EPS PanSystem 3.0a user guide.
3. Well Testing Interpretation Methods. Bourdarot, G. Editions Technip, 1998.
4. PROSPER IPM 3.5 user guide. Petroleum Experts Limited.

11 Appendices

Date	Time	Elapsed Time	Events
06-Nov-03	00:00	06-Nov-03	
06-Nov-03	02:00	02:00	3-Nov-03 sample 1.01 mud from mud pits taken at 10:00 32,000 ppm Cl.
06-Nov-03	02:35	02:35	Picked up flowhead to rig floor.
06-Nov-03	04:15	04:15	Laid out flowhead with tail pipe to pipe deck.
06-Nov-03	05:30	05:30	Laid out Sentree to pipe deck.
06-Nov-03	06:00	06:00	Commenced rig up wireline for GR-CCL-CBL-VDL-Junk billy run
06-Nov-03	07:45	07:45	RIH with wireline string.
06-Nov-03	08:00	08:00	POOH due to tool string would pass through wear bushing.
06-Nov-03	08:25	08:25	Removed gauge ring 8 3/8" from Junk billy.
06-Nov-03	08:30	08:30	RIH with wireline string.
06-Nov-03	12:30	12:30	Wireline tools at surface.
06-Nov-03	13:00	13:00	Finished rig down of wireline tools.
06-Nov-03	13:30	13:30	0.0 Set 9 5/8" Model S permanent Seal bore packer into RT.
06-Nov-03	14:04	14:04	1.1 Connected wireline setting tool to packer.
06-Nov-03	14:40	14:40	1.7 RIH with wireline GR-CCL-CPST-packer string.
06-Nov-03	17:20	17:20	4.3 Set packer at 1977.56m MDRT.
06-Nov-03	18:30	18:30	5.5 Finished rig down of wireline equipment.
06-Nov-03	19:30	19:30	6.5 Held JSA on rig floor for running of TCP guns and BHA.
06-Nov-03	19:45	19:45	6.8 Picked up TCP guns to rig floor.
06-Nov-03	20:26	20:26	7.4 Picked up TFTV and seal assembly.
06-Nov-03	20:42	20:42	7.7 Picked up PCT and Gauge carrier.
06-Nov-03	21:40	21:40	8.7 Picked up 1 joint of 3 1/2" PH6 tubing.
06-Nov-03	21:47	21:47	8.8 Picked up MCVL.
06-Nov-03	22:10	22:10	9.2 Picked up 1 joint of 3 1/2" PH6 tubing.
06-Nov-03	22:17	22:17	9.3 Picked up SHORT.
06-Nov-03	22:40	22:40	9.7 Picked up crossover from 3 1/2" to 4 1/2" PH6
06-Nov-03	22:43	22:43	9.7 Picked up 1 stand of 4 1/2" PH6 tubing.
06-Nov-03	22:50	22:50	9.8 Commenced rig up for pressure testing BHA.
06-Nov-03	23:11	23:11	10.2 Commenced pressure test of BHA to 4500 psi
06-Nov-03	23:26	23:26	10.4 Good test to 4500psi.
06-Nov-03	23:50	23:50	10.8 Pressure tested booms found leak.
07-Nov-03	00:00	07-Nov-03	11.0
07-Nov-03	00:15	00:15	11.3 Continued to RIH with 4 1/2" PH6 tubing.
07-Nov-03	06:08	06:08	17.1 Commenced pressure test of string to 4500 psi
07-Nov-03	06:36	06:36	17.6 Good test to 4500psi.
07-Nov-03	06:40	06:40	17.7 Connected drill pipe to string.
07-Nov-03	06:55	06:55	17.9 Laid out a 1 joint of drill pipe for better height control on space out.
07-Nov-03	07:10	07:10	18.2 TCP guns in seal bore assembly.
07-Nov-03	07:23	07:23	18.4 String stab into packer assembly.
07-Nov-03	07:30	07:30	18.5 Closed LPR and UPR
07-Nov-03	07:35	07:35	18.6 Opened LPR and UPR.
07-Nov-03	07:40	07:40	18.7 POOH.
07-Nov-03	08:00	08:00	19.0 Run back into hole due to poor ram indication on drill pipe.

07-Nov-03	09:05	09:05	20.1	Sit down on packer with 20000 lbs.
07-Nov-03	09:06	09:06	20.1	Closed LPR and MPR
07-Nov-03	09:14	09:14	20.2	Opened LPR and MPR.
07-Nov-03	09:15	09:15	20.3	POOH.
07-Nov-03	10:09	10:09	21.2	Connected two 4 1/2" PH6 pup joints to string 2.38m 2.37m.
07-Nov-03	10:55	10:55	21.9	Held toolbox meeting rig floor prior to connecting Sentree to string.
07-Nov-03	11:00	11:00	22.0	Picked up Sentree to rig floor.
07-Nov-03	11:05	11:05	22.1	Connected SenTree to test string.
07-Nov-03	11:20	11:20	22.3	Connected umbilical to SenTree.
07-Nov-03	11:30	11:30	22.5	Commenced function testing SenTree panel Line A for 5 mins.
07-Nov-03	11:35	11:35	22.6	Commenced function testing SenTree panel Line B for 5 mins.
07-Nov-03	11:41	11:41	22.7	Function tested line C for unlatching 14 secs to unlatch.
07-Nov-03	11:45	11:45	22.8	Opened ball and flapper on SenTree.
07-Nov-03	13:20	13:20	24.3	Connected lubricator valve to Test string. Function ball.
07-Nov-03	13:50	13:50	24.8	Changed bails.
07-Nov-03	14:40	14:40	25.7	Picked up Flow Head to rig floor.
07-Nov-03	14:45	14:45	25.8	Commenced rig up of Kill line coflexip hose.
07-Nov-03	16:00	16:00	27.0	Commenced rig up of Flow line coflexip hose.
07-Nov-03	16:30	16:30	27.5	Sample 1.02 brine from mud pits.
07-Nov-03	17:08	17:08	28.1	Opened Flow Wing Valve prior to flushing lines.
07-Nov-03	17:14	17:14	28.2	Commenced flushing lines with water to burners against TFTV prior to pressure testing.
07-Nov-03	17:15	17:15	28.3	ESD malfunction.
07-Nov-03	17:30	17:30	28.5	ESD operational, re-commenced flushing lines to burners.
07-Nov-03	17:35	17:35	28.6	Closed choke manifold and kill wing valve prior to pressure testing Kill line to 4500psi.
07-Nov-03	18:11	18:11	29.2	Good test to 4500psi.
07-Nov-03	18:12	18:12	29.2	Opened kill wing valve
07-Nov-03	18:15	18:15	29.3	Commenced pressure testing Flow line against Choke manifold and TFTV to 4500psi.
07-Nov-03	18:40	18:40	29.7	Good test to 4500psi.
07-Nov-03	18:42	18:42	29.7	Closed SSTT and bled off pressure to 500psi to monitor for returns.
07-Nov-03	18:59	18:59	30.0	Pressured to 4500psi to equalise
07-Nov-03	19:24	19:24	30.4	Bled off pressure above lubricator valve to 500 psi to monitor for returns.
07-Nov-03	19:43	19:43	30.7	Pressured back to 4500psi to equalise, opened lubricator valve.
07-Nov-03	20:37	20:37	31.6	Pressured annulus to 1500psi to lock open TFTV and shear PORT.
07-Nov-03	20:40	20:40	31.7	Bled off tubing pressure at choke manifold.
07-Nov-03	20:51	20:51	31.9	Confirmed TFTV locked open and by-pass closed. Bled annulus pressure.
07-Nov-03	20:53	20:53	31.9	Pressured annulus to 1500psi to unlock PCT.
07-Nov-03	20:56	20:56	31.9	Bled off annulus pressure to zero.
07-Nov-03	21:17	21:17	32.3	Commenced floco oil meter factor.
07-Nov-03	22:30	22:30	33.5	Completed meter factor.
08-Nov-03	00:00	08-Nov-03	35.0	

08-Nov-03	00:25	00:25	35.4	Held JSA on rig floor for displacing string with diesel cushion.
08-Nov-03	00:39	00:39	35.7	Applied 500 psi to annulus.
08-Nov-03	00:42	00:42	35.7	Commenced cycling MCCV, pressured tubing to 1500psi and bled off at choke manifold.
08-Nov-03	00:51	00:51	35.9	Confirmed MCCV open (2 cycles). Closed choke manifold.
08-Nov-03	01:00	01:00	36.0	Commenced diesel displacement.
08-Nov-03	03:20	03:20	38.3	Finished displacing diesel cushion. 88bbls pumped.
08-Nov-03	03:32	03:32	38.5	Pressure bled off at choke manifold.
08-Nov-03	03:33	03:33	38.6	Commenced pumping 10bbls of diesel to surge tank.
08-Nov-03	03:50	03:50	38.8	Finished pumping diesel. 11bbls diesel, 4 bbls water.
08-Nov-03	04:00	04:00	39.0	Closed choke manifold.
08-Nov-03	04:15	04:15	39.3	Held JSA on the rig floor prior to starting well test program.
08-Nov-03	05:00	05:00	40.0	Increased recording rate of WHP and CSGP to 1sec prior to perforating well.
08-Nov-03	05:35	05:35	40.6	Held JSA on the rig floor prior to perforating the well.
08-Nov-03	05:44	05:44	40.7	Pressured annulus to 1500psi to open the PCT.
08-Nov-03	05:45	05:45	40.8	Pressured tubing to 4000 psi.
08-Nov-03	05:53	05:53	40.9	Pressure bled off at choke manifold to set HDF firing head.
08-Nov-03	06:02	06:02	41.0	Good indication guns fired.
08-Nov-03	06:03	06:03	41.1	Opened well on 16/64" adjustable choke to surge tank. (Initial Flow Period)
08-Nov-03	06:06	06:06	41.1	Increased to 20/64" adjustable choke.
08-Nov-03	06:07	06:07	41.1	Increased to 24/64" adjustable choke.
08-Nov-03	06:12	06:12	41.2	14 bbls return to Surge tank.
08-Nov-03	06:13	06:13	41.2	Shut in well at PCT and choke manifold for initial build up. (Initial Shut-In Period)
08-Nov-03	08:13	08:13	43.2	Pressured up annulus to 1500psi to open PCT.
08-Nov-03	08:14	08:14	43.2	Opened well on 16/64" adjustable choke to surge tank. (Clean-up Flow Period)
08-Nov-03	08:22	08:22	43.4	Increased to 20/64" adjustable choke.
08-Nov-03	08:30	08:30	43.5	Diverted flow from Surge tank to Burner.
08-Nov-03	08:32	08:32	43.5	Increased to 24/64" adjustable choke.
08-Nov-03	08:37	08:37	43.6	BSW 100% diesel.
08-Nov-03	08:38	08:38	43.6	Commenced methanol injection at upstream data header.
08-Nov-03	08:44	08:44	43.7	Bled down annulus pressure 1250 psi
08-Nov-03	08:48	08:48	43.8	Increased to 32/64" adjustable choke.
08-Nov-03	08:51	08:51	43.9	Diverted flow through steam exchanger.
08-Nov-03	08:53	08:53	43.9	Shut in well at choke manifold due pilot lights on burner went out.
08-Nov-03	09:09	09:09	44.2	Commenced pumping from surge tank to burner.
08-Nov-03	09:15	09:15	44.3	Opened well on 16/64" adjustable choke to burner
08-Nov-03	09:16	09:16	44.3	Increased to 20/64" adjustable choke.
08-Nov-03	09:19	09:19	44.3	Increased to 24/64" adjustable choke.
08-Nov-03	09:20	09:20	44.3	Diverted flow through steam exchanger. Gas at surface
08-Nov-03	09:21	09:21	44.3	Increased to 28/64" adjustable choke.
08-Nov-03	09:29	09:29	44.5	Increased to 32/64" adjustable choke.
08-Nov-03	09:33	09:33	44.6	Exercised choke.
08-Nov-03	09:36	09:36	44.6	Increased to 36/64" adjustable choke.
08-Nov-03	09:46	09:46	44.8	BSW 95%

08-Nov-03	09:49	09:49	44.8	Exercised choke.
08-Nov-03	10:15	10:15	45.3	Increased to 40/64" adjustable choke.
08-Nov-03	10:22	10:22	45.4	Bled off annulus pressure to 1300
08-Nov-03	10:45	10:45	45.8	Increased to 44/64" adjustable choke.
08-Nov-03	10:49	10:49	45.8	Exercised choke.
08-Nov-03	10:51	10:51	45.8	Increased to 42/64" adjustable choke.
08-Nov-03	10:56	10:56	45.9	Bled off annulus pressure to 1300.
08-Nov-03	11:06	11:06	46.1	Opened steam exchanger bypass by a couple of turns to reduce unstable WHDCP.
08-Nov-03	11:18	11:18	46.3	Closed steam exchanger bypass.
08-Nov-03	11:30	11:30	46.5	Increased to 44/64" adjustable choke.
08-Nov-03	11:38	11:38	46.6	Bled off annulus pressure to 1300.
08-Nov-03	12:17	12:17	47.3	Bled off annulus pressure to 1300.
08-Nov-03	12:22	12:22	47.4	Increased to 52/64" adjustable choke.
08-Nov-03	12:37	12:37	47.6	Finished pumping methanol to data header.
08-Nov-03	12:54	12:54	47.9	Opened inlet valve to separator.
08-Nov-03	13:01	13:01	48.0	Increased to 58/64" adjustable choke.
08-Nov-03	13:34	13:34	48.6	Diverted flow from adjustable choke 58/64" to fix choke 64/64".
08-Nov-03	13:40	13:40	48.7	Bypass steam exchanger.
08-Nov-03	14:03	14:03	49.1	Bled off annulus pressure to 1300.
08-Nov-03	14:14	14:14	49.2	Lowered 4" orifice plate.
08-Nov-03	15:00	15:00	50.0	Sample 1.03 water from water sight glass on separator.
08-Nov-03	15:10	15:10	50.2	Commenced samples 1.04 & 1.05; PVT condensate (bottle 7597-MA), & PVT gas (bottle 5072A).
08-Nov-03	15:35	15:35	50.6	Finished taking samples 1.04 & 1.05.
08-Nov-03	15:44	15:44	50.7	Lifted orifice plate.
08-Nov-03	15:45	15:45	50.8	Shut in well at PCT and choke manifold for build up 2. (Build Up Period #2)
08-Nov-03	15:46	15:46	50.8	Closed choke manifold.
08-Nov-03	17:03	17:03	52.1	Opened SSV and PWV on FH after repairs to ESD panel.
08-Nov-03	21:00	21:00	56.0	Annulus during shut was topped up.
08-Nov-03	21:30	21:30	56.5	Held JSA on rig floor for Multi-flow period prior to opening well.
08-Nov-03	21:36	21:36	56.6	Started methanol injection into data header, 60gallons/day.
08-Nov-03	21:48	21:48	56.8	Pressured annulus to 1500 psi to open PCT.
08-Nov-03	21:55	21:55	56.9	Opened well on 36/64" adjustable choke to gas flare. (Multi Flow Period #1)
08-Nov-03	21:57	21:57	57.0	Diverted flow through steam exchanger.
08-Nov-03	22:09	22:09	57.2	Bled annulus to 1300psi.
08-Nov-03	22:29	22:29	57.5	Switched flow through 36/64" fixed choke.
08-Nov-03	22:38	22:38	57.6	CO2 = 0.3%, H2S = 0ppm
08-Nov-03	22:46	22:46	57.8	Bled annulus to 1300psi.
08-Nov-03	23:00	23:00	58.0	Diverted flow through separator on 36/64" fixed choke.
08-Nov-03	23:12	23:12	58.2	Lowered 3" orifice plate.
08-Nov-03	23:26	23:26	58.4	Bled annulus to 1300psi.
08-Nov-03	23:30	23:30	58.5	Stopped methanol injection into data header.
09-Nov-03	00:00	09-Nov-03	59.0	
09-Nov-03	00:57	00:57	60.0	Bled annulus to 1400psi.
09-Nov-03	02:49	02:49	61.8	Bled annulus to 1400psi.
09-Nov-03	03:35	03:35	62.6	Commenced samples 1.06 & 1.07, PVT condensate (bottle 6808-MA) & PVT gas (bottle 42106).

09-Nov-03	03:58	03:58	63.0	Finished taking samples 1.06 & 1.07.
09-Nov-03	04:30	04:30	63.5	Raised 3" orifice plate.
09-Nov-03	04:30	04:30	63.5	Commenced sample 1.08, dead condensate sample.
09-Nov-03	04:33	04:33	63.6	Switched flow through 40/64" adjustable choke.
09-Nov-03	04:34	04:34	63.6	Bled annulus to 1200psi.
09-Nov-03	04:35	04:35	63.6	Finished taking sample 1.08.
09-Nov-03	04:41	04:41	63.7	Increased to 48/64" adjustable choke.
09-Nov-03	04:43	04:43	63.7	Switched flow through 48/64" fixed choke. (Multi Flow Period #2)
09-Nov-03	04:51	04:51	63.8	Lowered 3.25" orifice plate.
09-Nov-03	04:52	04:52	63.9	Raised 3.25" orifice plate.
09-Nov-03	04:59	04:59	64.0	Lowered 3.75" orifice plate.
09-Nov-03	09:32	09:32	68.5	Commenced sample 1.09, PVT gas (bottle 1657A).
09-Nov-03	09:58	09:58	69.0	Finished taking sample 1.09.
09-Nov-03	10:31	10:31	69.5	Raised orifice plate.
09-Nov-03	10:32	10:32	69.5	Switched flow through 48/64" adjustable choke.
09-Nov-03	10:33	10:33	69.6	Increased to 64/64" adjustable choke.
09-Nov-03	10:38	10:38	69.6	Switched flow through 64/64" fixed choke. (Multirate Flow Period #3)
09-Nov-03	10:40	10:40	69.7	Lowered 4" orifice plate.
09-Nov-03	10:44	10:44	69.7	Bypass steam exchanger.
09-Nov-03	11:36	11:36	70.6	Bled annulus to 1300psi.
09-Nov-03	12:30	12:30	71.5	Finished taking sample 1.11 1 It drum from water sight glass on separator.
09-Nov-03	14:35	14:35	73.6	Finished taking sample 1.12 20 It drum from water line.
09-Nov-03	15:15	15:15	74.3	Commenced samples 1.13 & 1.14, PVT condensate (bottle 7276-MA) & PVT gas (bottle A2633).
09-Nov-03	15:37	15:37	74.6	Finished taking samples 1.13 & 1.14.
09-Nov-03	16:46	16:46	75.8	Shut in well at PCT and choke manifold for build up 3. (Build Up Period #3)
09-Nov-03	16:47	16:47	75.8	Closed choke manifold.
09-Nov-03	17:00	17:00	76.0	Finished taking sample 1.15 20 It drum from water sight glass on separator.
09-Nov-03	17:10	17:10	76.2	Finished taking sample 1.16 1 It drum from water line.
09-Nov-03	17:12	17:12	76.2	Finished taking sample 1.17 1 It drum from water line.
09-Nov-03	17:13	17:13	76.2	Finished taking sample 1.18 1 It drum from water sight glass on separator.
09-Nov-03	17:14	17:14	76.2	Finished taking sample 1.19 1 It drum from water sight glass on separator.
09-Nov-03	19:00	19:00	78.0	Emptied separator fluids into the surge tank to calculate BSW for Multi Flow Period.
09-Nov-03	19:35	19:35	78.6	BSW = 57% water. Condensate = 10.91bbbls, water = 14.43bbbls.
09-Nov-03	19:45	19:45	78.8	Commenced pumping out of surge tank to starboard flare.
09-Nov-03	20:00	20:00	79.0	Finished pumping, contents of surge tank empty.
10-Nov-03	02:30	02:30	85.5	Held JSA on rig floor prior to killing the well.
10-Nov-03	03:08	03:08	86.1	Opened kill wing valve.
10-Nov-03	03:13	03:13	86.2	Applied 1500psi to annulus to open the PCT.
10-Nov-03	03:16	03:16	86.3	Good indication PCT opened.
10-Nov-03	03:17	03:17	86.3	Commenced bullheading brine into formation at 10bbbls/min.
10-Nov-03	03:35	03:35	86.6	Commenced flow check. 101.8bbbls brine pumped.
10-Nov-03	03:49	03:49	86.8	Bled off tubing pressure at choke manifold.

10-Nov-03	03:52	03:52	86.9	Closed choke manifold.
10-Nov-03	04:08	04:08	87.1	Opened choke manifold to starboard burner while reverse circulating tubing volume.
10-Nov-03	04:12	04:12	87.2	Closed choke manifold.
10-Nov-03	04:14	04:14	87.2	Commenced cycling PCT to lock open position.
10-Nov-03	04:18	04:18	87.3	Opened LPR
10-Nov-03	04:19	04:19	87.3	Opened choke manifold.
10-Nov-03	04:20	04:20	87.3	Picked up string by 8 m.
10-Nov-03	04:30	04:30	87.5	Closed LPR
10-Nov-03	04:43	04:43	87.7	Commenced cycling PCT into hold open.
10-Nov-03	05:25	05:25	88.4	PCT in hold open.
10-Nov-03	05:52	05:52	88.9	Finished reversing from annulus to burner.
10-Nov-03	05:56	05:56	88.9	Commenced flushing across the flow head.
10-Nov-03	06:08	06:08	89.1	Finished flushing surface equipment.
10-Nov-03	06:12	06:12	89.2	Commenced reverse circulation
10-Nov-03	08:13	08:13	91.2	Finished reverse circulation. 130 bbls pump
10-Nov-03	08:30	08:30	91.5	Good inflow test.
10-Nov-03	08:33	08:33	91.5	Commenced circulation
10-Nov-03	09:21	09:21	92.3	Finished circulation.
10-Nov-03	09:28	09:28	92.5	Pressure up annulus to cycle SHORT
10-Nov-03	09:31	09:31	92.5	Bled off pressure to annulus.
10-Nov-03	09:27	09:27	92.5	Stung back into packer for cycling SHORT
10-Nov-03	09:29	09:29	92.5	Closed LPR
10-Nov-03	09:33	09:33	92.6	Opened LPR.
10-Nov-03	09:35	09:35	92.6	Lifted string out of packer.
10-Nov-03	09:45	09:45	92.8	STAN system turn off.

ENCLOSURE I : COMPOSITE LOG (1:500 SCALE)

ENCLOSURE II : DEPTH STRUCTURE MAP

ENCLOSURE III : STRATIGRAPHIC CROSS SECTION

ENCLOSURE IV : LOG INTERPRETATION ANALOGUE PLOT